JOHANNES GUTENBERG
UNIVERSITÄT MAINZ

JG|U

Novel Strategies for the Synthesis and Transformation of Nitrogen-Containing Molecules

Dissertation
for the degree of "Doctor of Natural Sciences"
in the doctoral subject chemistry

at the Faculty of Chemistry, Pharmaceutical Sciences,
Geography and Geosciences
of the Johannes Gutenberg University Mainz

Marlene Arnold
Born in [redacted]

Mainz, March 2025

1. Examiner: [redacted]
2. Examiner: [redacted]

Day of the oral exam: [redacted]

Acknowledgements

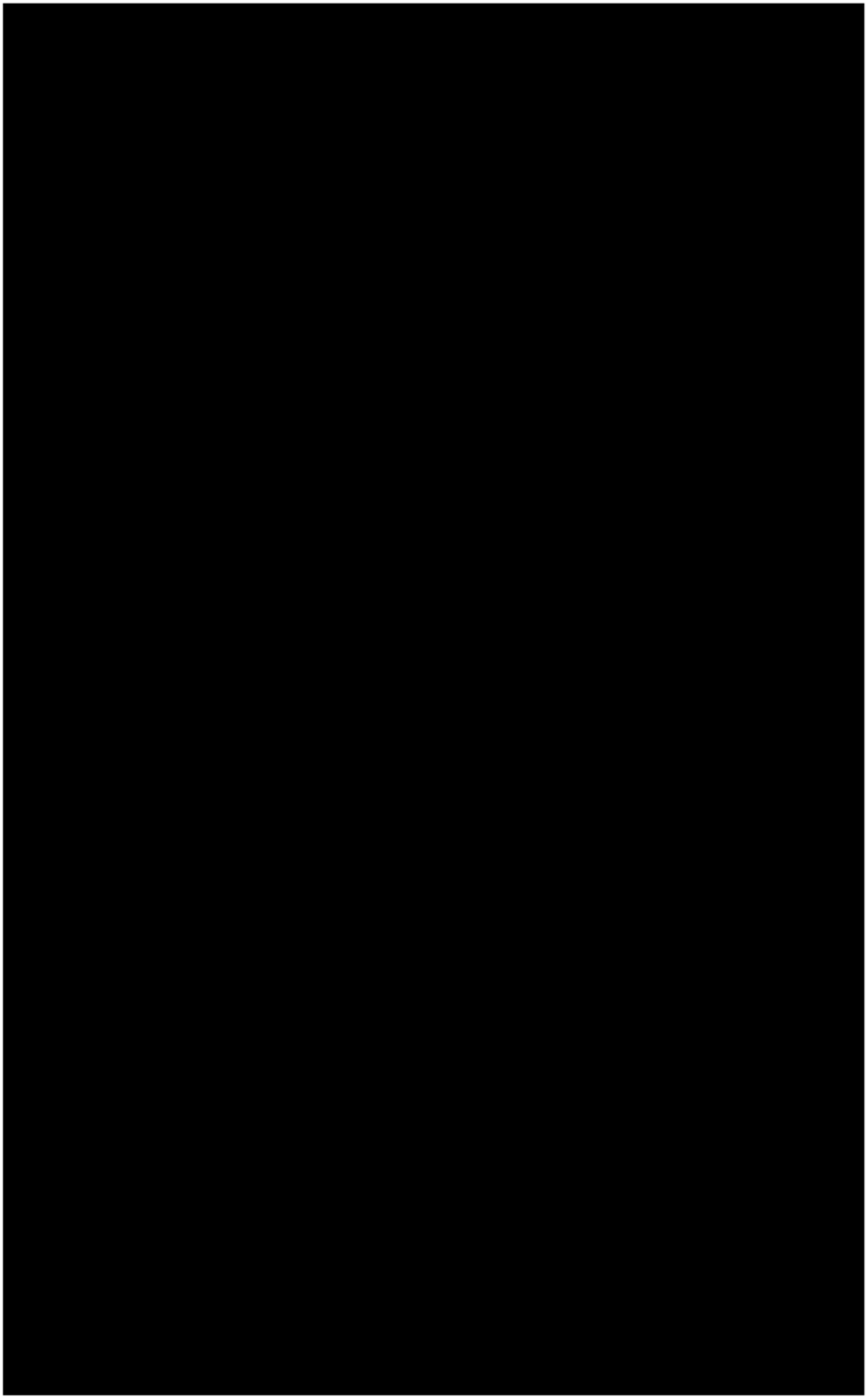

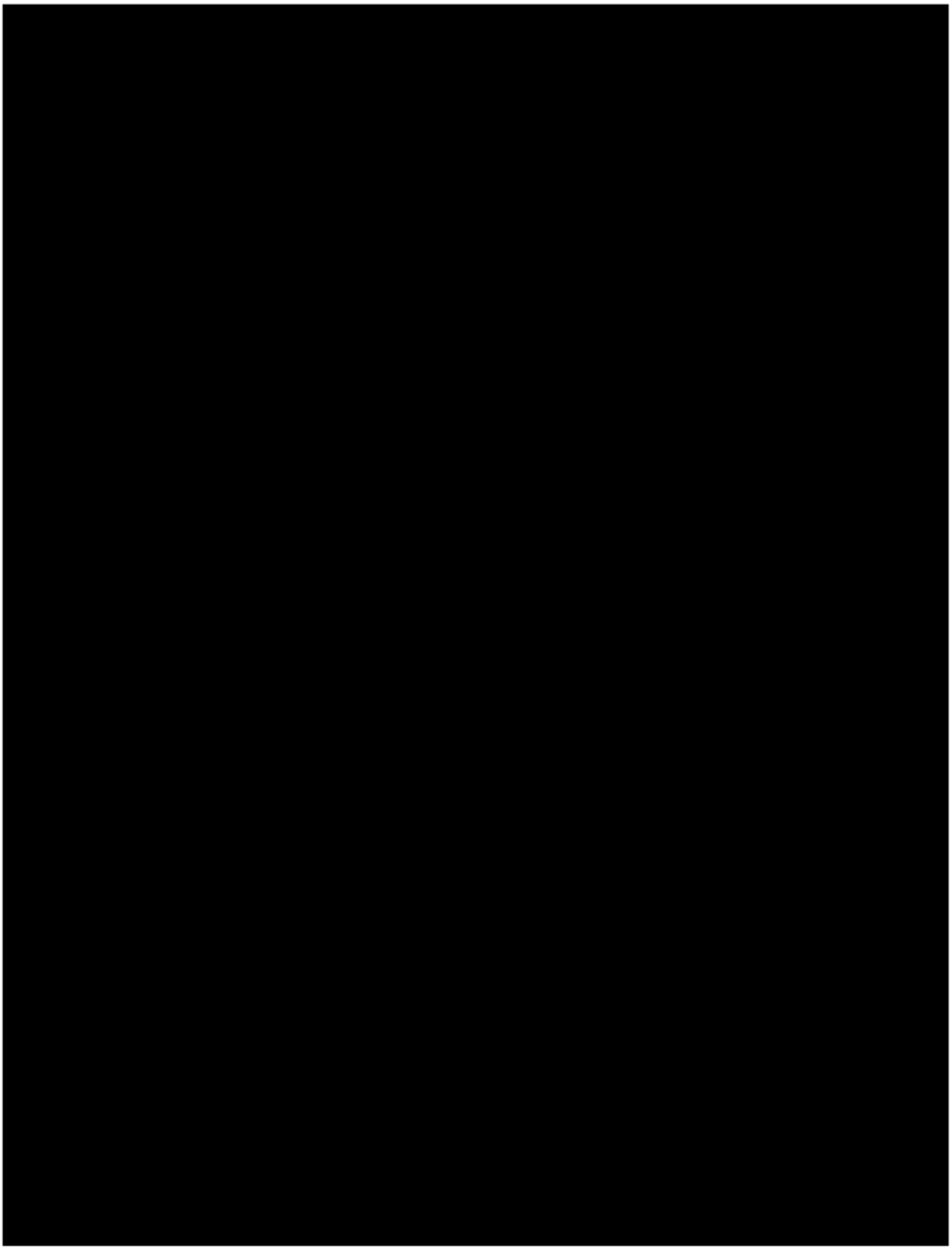

Table of contents

Summary

Over the course of this work, novel strategies for the synthesis and transformation of nitrogen-containing molecules were investigated.

In the first research project, a selective nitrogen insertion methodology for the synthesis of γ-lactams from cyclobutanones was explored. Analogies between an aza-*Baeyer-Villiger* reaction and the corresponding oxygen insertion were identified in terms of regioselectivity and stereospecificity. Consecutively, the mild nature and synthetic applicability of the protocol was demonstrated by exploration of a substrate scope including the transformation of α-substituted cyclobutanones and the gram scale synthesis of 4-phenylpyrrolidin-2-one.

During the second research project, a catalytic asymmetric nitrogen incorporation approach was developed based on the previous studies. Chiral phosphoric acids were identified to effectively catalyse the asymmetric condensation between 3-substituted cyclobutanones and amine reagents. The influence of amine substitution and the effect of varying solvents and temperature on the selectivity of the reaction were investigated. Several previously unknown axially chiral cyclobutanone oxime esters were accessed in good enantioselectivities and yields. Application of the developed protocol enabled transformation of substrates bearing versatile aryl and alkyl substituents. Additionally, the reaction of substrates with varying ring sizes, such as cyclopentanones and cyclohexanones, was successfully performed.

Following on these results, novel strategies for the conversion of axial-to-point chirality by transformation of the previously formed oxime esters were provided in a third research project. Stereospecific chirality transfer enabled the synthesis of point chiral γ-lactams *via Lewis* acid-induced ring-expansion rearrangement of axially chiral cyclobutanone oxime esters. Furthermore, the usability of the nitrogen-containing molecules in ring-opening and ring-contraction reactions to obtain chiral nitriles was evaluated. An interesting base-induced rearrangement resulting in the formation of chiral cyclopropane nitriles was discovered. Fine-tuning of the reaction parameters facilitated the highly selective access to *cis*- and *trans*-diastereoisomers. Combination with the previously developed asymmetric condensation approach achieved the stereodivergent synthesis of all four cyclopropane isomers from simple cyclobutanone precursors in a one-pot protocol. Finally, the synthetic utility of the developed methodology was highlighted by the formal synthesis of an FDA-approved drug candidate.

Zusammenfassung

Im Rahmen dieser Arbeit wurden neuartige Strategien für die Synthese und Umwandlung von stickstoffhaltigen Molekülen untersucht.

Im ersten Forschungsprojekt wurde eine selektive Stickstoffinsertion für die Synthese von γ-Lactamen aus Cyclobutanonen erforscht. Es wurden Parallelen zwischen einer Aza-*Baeyer-Villiger*-Reaktion und der analogen Sauerstoffinsertion in Bezug auf Regioselektivität und Stereospezifität festgestellt. Anschließend wurde die synthetische Anwendbarkeit des Protokolls durch die Betrachtung einer Substratauswahl demonstriert. Die Untersuchung umfasste sowohl die Umwandlung von α-substituierten Cyclobutanonen als auch die Synthese von 4-Phenylpyrrolidin-2-on im Gramm-Maßstab.

Im Rahmen des zweiten Forschungsprojekts wurde aufbauend auf die vorangegangene Studie ein katalytischer Ansatz zur asymmetrischen Stickstoffinkorporation entwickelt. Es wurden chirale Phosphorsäuren identifiziert, die die asymmetrische Kondensation zwischen 3-substituierten Cyclobutanonen und Aminreagenzien wirksam katalysieren. Der Einfluss der Aminsubstitution und die Auswirkung unterschiedlicher Lösungsmittel und Temperaturen auf die Selektivität der Reaktion wurden untersucht. Mehrere bisher unbekannte, axial chirale Cyclobutanonoximester wurden in guter Enantioselektivität und Ausbeute zugänglich gemacht. Die Anwendung des entwickelten Protokolls ermöglichte die Umsetzung von Substraten mit vielseitigen Aryl- und Alkylsubstituenten. Zudem wurde die Reaktion von Substraten mit unterschiedlichen Ringgrößen, wie Cyclopentanonen und Cyclohexanonen, erfolgreich durchgeführt.

Daran anknüpfend wurden in einem dritten Forschungsprojekt neue Strategien für die Umwandlung von axialer Chiralität in Punktchiralität unter Verwendung der zuvor gebildeten Oximester entwickelt. Der stereospezifische Transfer der Chiralität ermöglichte die Synthese punkt chiraler γ-Lactame durch *Lewis*-Säure-induzierte Ringerweiterungs-Umlagerung von axial chiralen Cyclobutanonoximestern. Außerdem wurde die Verwendbarkeit der stickstoffhaltigen Moleküle in Ringöffnungs- und Ringverkleinerungsreaktionen zur Gewinnung chiraler Nitrile untersucht. Es wurde eine interessante baseninduzierte Umlagerung entdeckt, die zur Bildung von chiralen Cyclopropannitrilen führt. Die Anpassung der Reaktionsparameter ermöglichte den selektiven Zugang zu *cis*- und *trans*-Diastereoisomeren. In Kombination mit der zuvor entwickelten Methode zur asymmetrischen Kondensation gelang die stereodivergente Synthese aller vier Cyclopropan-Isomere aus einfachen Cyclobutanon-Vorläufern in einem Eintopf-Protokoll. Abschließend wurde der synthetische Nutzen der entwickelten Methode durch die formale Synthese eines zugelassenen Arzneimittelkandidaten hervorgehoben.

Publication

Parts of this work have been published in peer reviewed journals:

- Stereospecific nitrogen insertion using amino diphenylphosphinates: an Aza-Baeyer–Villiger rearrangement
  M. Ong, M. Arnold, A. W. Walz, J. M. Wahl,*
  Org. Lett. **2022**, *24*, 6171–6175.
  *corresponding author
- Synthesis of 4-phenylpyrrolidin-2-one *via* an Aza-Baeyer-Villiger rearrangement
  M. Ong,# M. Arnold,# J. M. Wahl,*
  Org. Synth. **2023**, *100*, 347-360.
  #authors contributed equally to this work
  *corresponding author
- Nitrogen insertion *via* asymmetric condensation and chirality transfer: a stereodivergent entry to cyanocyclopropanes
  M. Arnold, J. Hammes, M. Ong, C. Mück-Lichtenfeld, J. M. Wahl,*
  manuscript submitted.
  *corresponding author

Presentations

Parts of this work have been presented at the following scientific conferences/workshops:

- Thinking out of the ring. Present and future of small cyclic compounds; Lorentz Center Leiden, The Netherlands; 05/2024
  Synthesis and application of axially chiral cyclobutanone oxime esters for the preparation of chiral cyclopropanes (poster presentation)
- Hochschule trifft Industrie, Switzerland; 09/2024
  Synthesis and application of axially chiral cyclobutanone oxime esters (oral presentation)

Declaration of the work of others included herein

Over the course of the research projects entailed in this thesis, other individuals contributed to the work described herein. Below, a detailed overview of the contributions of each collaborator can be found.

Contributions to the first research project were made by [redacted] and [redacted] during the optimisation of the reaction conditions. Additionally, [redacted] provided amine reagent **2.59** and was involved in the synthesis of lactam **2.49** by preparation of cyclobutanone **2.8** and reproduction of the gram scale reaction. The results presented herein correspond to the independent data obtained in this work.

As part of the second project, [redacted] conducted the first experiment of the asymmetric condensation reaction, while further optimisation and development of reaction conditions were part of this work. [redacted] prepared cyclobutanone **2.8**, which was further purified as part of this work. The reaction of **3.41** and **3.42** in a racemic and enantioselective fashion was performed as part of this work, but [redacted] isolated the racemic samples and determined the enantiomeric ratio. Racemic oxime ester **3.53** was prepared by [redacted] and [redacted] performed to the synthesis of racemic samples of the molecules **3.46** to **3.48**, **3.50** to **3.52**, **3.54** and **3.57**. Additionally, synthesis of enantioenriched oxime ester **3.52** was conducted by [redacted]. Enantioselective synthesis of oxime ester **3.47** was performed by [redacted]. Development of separation conditions for all racemic samples and determination of the enantiomeric ratio of enantioenriched oxime esters using chiral HPLC was part of this work. [redacted] performed the calculations for the mechanistic proposal. The X-ray measurement and structure refinement of samples from the molecules (*R*)-**3.41** and (*R*)-**3.42** was performed by [redacted].

In the third project, [redacted] und [redacted] contributed to the synthesis of cyclobutanone **4.71** by optimisation of the synthesis for intermediate **5.13**. Final synthesis of cyclobutanone **4.71** starting from **4.70** was performed as part of this work. The X-ray measurement and structure refinement of a sample from the molecule (1*S*,2*R*)-**4.49** was performed by [redacted].

Index of abbreviation

AcOH	acetic acid
Ad	adamantyl
BAr_F	tetrakis [3,5-bis(trifluoromethyl)phenyl]borate
$BF_3{\cdot}OEt_2$	boron trifluoride diethyl etherate
BINAP	2,2'-(diphenylphosphino)-1,1'-binaphthyl
Boc	*tert*-butyloxycarbonyl
Bz	benzoyl
CAN	cerium ammonium nitrate
CH_2Cl_2	dichloromethane
cod	cyclooctadiene
dba	dibenzylideneacetone
DCC	*N*,*N*'-dicyclohexalcarbodiimide
DCE	1,2-dichloroethane
DFT	density functional theory
DMF	dimethylformamide
DMSO	dimethyl sulfoxide
dppb	1,4-bis(diphenylphosphino)butane
DPPH	*O*-(diphenylphosphinyl)hydroxylamine
dppp	1,3-bis(diphenylphosphino)propane
dr	diatereomeric ratio
dtbby	2,6-di-*tert*-butylpyridine
er	enantiomeric ratio
es	enantiospecifity
Et_2O	diethyl ether
EtOAc	ethyl acetate
EtOH	ethanol
FDA	Food and Drug Administration
glyme	dimethoxyethane
HFIP	1,1,1,3,3,3-hexafluoroisopropanol
HMDS	hexamethyldisilazide
LDA	lithiumdiisopropylamide
LG	leaving group , leaving group
LiTMP	lithiumtetramethylpiperidine
*m*CPBA	*meta*-chlorobenzoic acid
MeCN	acetonitirle
Mes	mesitylene
MS	molecular sieves
MsOH	methanesulfonic acid
n-$HexN_3$	*n*-hexyl azide
OA	oxidative addition
PhCl	chlorobenzene
PMB	*para*-methoxybenzyl
ppy	2-phenylpyridine
p-TsOH	*para*-toluene sulfonic acid
rr	regioisomeric ratio
SET	single electron transfer
Tf_2O	trifluoromethanesulfonic anhydride
TFA	trifluoroacetic acid
THF	tetrahydrofuran

1 Introduction

Synthetic organic chemistry has contributed to the enhancement of human health and the quality of life by influencing a manifold of different fields.[1] In particular, the ability to design and synthesise small molecules with specific biological activities has had a profound impact on medicine. Thus, modern drug discovery enabled the development of life-saving drugs with therapeutic effects against various medical conditions including infectious diseases, cancer, cardiovascular disorders, and neurological conditions.[2] Advancements in synthetic methodologies therefore continue to drive progress in medicinal chemistry by offering new avenues for optimising the selectivity and safety profiles of medicinal drugs.[3] From the broad spectrum of available therapeutics, small molecule drugs, characterised by their relatively low molecular weight, offer several advantages over biologics, such as oral bioavailability, and cost-effective large-scale production.[4] Therefore, continuously increasing the chemical space and establishing more efficient and sustainable synthetic routes, is an essential topic of ongoing research for organic chemists.[5]

1.1 Nitrogen-containing pharmaceuticals

Heteroatoms and heterocyclic scaffolds are frequently present as the common core in a plethora of active pharmaceuticals and natural products.[6] In 2019, the group of *Njardarson* published a comprehensive analysis of 367 drugs, which are approved by the U.S. Food and Drug Administration (FDA). The study revealed that 58% of the drug candidates contained nitrogen heterocycles. Especially noteworthy is the increasing prevalence in recent small molecule drug discovery.[7] Beyond heterocyclic scaffolds, nitrogen-based functional groups, such as amines, amides and nitriles, are present in even more biologically active compounds.[8] The significant interest in nitrogen-containing pharmaceuticals stems from their enhanced binding affinity, metabolic stability and solubility compared to similar structures without nitrogen scaffolds.[9]

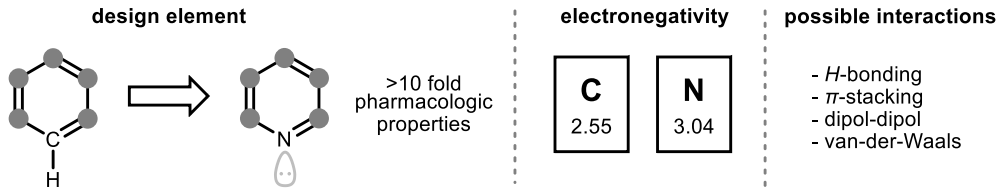

Figure 1. Overview of enhanced properties of nitrogen-containing drugs.[10,11]

As a design element in biomedical research, replacing a *CH* group with nitrogen in aromatic structures can lead to at least a tenfold improvement of pharmacological parameters (Figure 1).[10] These distinct characteristics are attributed to the increased electronegativity of nitrogen, which facilitates intra- and intermolecular electrostatic and orbital interactions, thus enhancing the binding

properties to enzymes and receptors.[12] As a result, small molecules containing nitrogen have found plentiful applications in diverse therapeutic fields, and the continuous development of synthetic strategies remains a major research priority in organic synthesis.[13] In the realm of synthetic chemistry, traditional methodologies employed for the incorporation of nitrogen into molecular frameworks include amide formation, electrophilic amination, transition-metal-catalysed coupling and reductive amination reactions.[14] However, traditional approaches often face challenges related to selectivity, functional group tolerance, and the need for multistep sequences.[15] The ability to perform chemical transformations in a concise and chemospecific fashion is certainly essential in the refinement of lead compounds during the late stage of a synthetic sequence. Fine-tuning of drug structures enables enhancement of pharmacokinetic properties and reduces side effects. Therefore, it is essential to facilitate late-stage functionalisation of a molecules' structure by modification of functional groups or even the alteration of the backbone structure.[16]

1.2 Molecular strain in organic synthesis

While offering significant time and cost savings, the development of mild and selective methods to build and tolerate molecular complexity is of great importance. In addressing this challenge, the employment of strained cyclic systems has emerged as a powerful strategy, offering potential for the development of novel synthetic approaches.[17,18,19] The term "ring strain" of a cyclic molecule refers to the increased potential energy resulting from structural distortions from the optimal geometry of a molecule. In numerical terms, strain energy ($\Delta\Delta H_f^\circ$) is defined as the difference between the experimental heat of combustion of a molecule and the theoretical heat of formation. The latter can for example be estimated by the group increment method, which is based on summing the contributions of the structural groups contained in a molecule.[20] For cyclic hydrocarbons with small or medium size, a significant difference is found between theoretical and experimental heat of formation, except for cyclohexane (Figure 2, left). The ring strain of cycloalkanes increases in the series from cyclohexane to cyclopropane with decreasing ring size.[21–23]

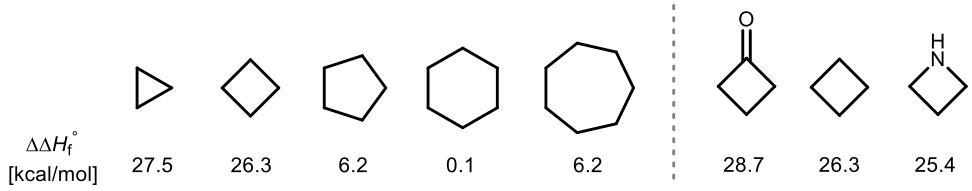

Figure 2. Strain energies of selected cycloalkanes and derivatives.[21–23]

In 1885, *Baeyer* attributed this observation to the increasing de*via*tion in the bond angle from the ideal tetrahedral angle of 109.5°, which is found in acyclic analogues.[24] The impact of this phenomenon is also evident when comparing

derivatives of carbocycles. As exemplified for four-membered systems, the introduction of a ketone functionality increases the strain energy due to the enhanced deviation of the actual bond angle from the ideal sp^2-hybridised carbonyl bond angle of 120° (Figure 2, right).[22,25] In addition to *Baeyer* strain, the total ring strain of a molecule consists of two further components, all of which contribute to the strain energy in different amounts depending on the structural properties. Torsional strain arises from an unfavourable eclipsed conformation of a molecule (*Pitzer* strain). Therefore, cyclic molecules often adopt non-planar conformations to reduce the number of repulsive interactions. In this context, the incorporation of a nitrogen into the ring system introduces flexibility due to its ability to adopt a pyramidal geometry, which allows for some strain relief (Figure 2, right).[21] As a third component, transannular strain, also called *Prelog* strain, predominantly occurs in medium-sized rings (7-12 members) through repulsive interactions of groups on non-adjacent carbons.[26]

The utilisation of strained molecules allows for reaction development of novel transformations, making small cyclic compounds to valuable intermediates in organic synthesis. Thus, various methodologies exploit ring strain to drive skeletal diversification by means of ring-opening, -expansion or -contraction reactions (Figure 3).

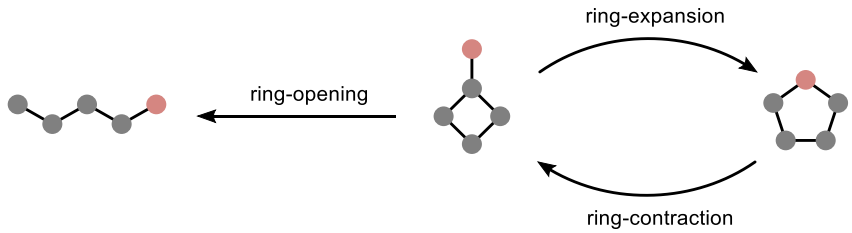

Figure 3. Transformations of small cyclic molecules.

In the following, selected reactions will be discussed that exemplify these three general strategies for using strained molecules to synthesise and modify nitrogen-containing compounds.

Driven by the release of the inherent strain energy present in small-ring systems, ring-opening reactions achieve bond cleavage, which leads to the formation of open-chain or larger ring structures. In this context, the ring-opening of aziridines has been established as an important strategy in organic chemistry.[27] While release of ring strain of the three-membered nitrogen-containing heterocycle promotes ring-opening reactions, analogous four-membered structures, namely azetidines, exhibit significantly lower propensity for *C–N* bond cleavage.[28] In 2015, the *Sun* group reported a catalytic asymmetric desymmetrisation of azetidines **1.1**, thereby addressing the challenge of their low reactivity and difficult stereocontrol in ring-opening reactions (Scheme 1).[29] Using thiol **1.2** as a nucleophile, Brønsted acid-catalysed ring-opening enables the formation of chiral amide **1.3** with high efficiency and enantioselectivity of 98:2 enantiomeric ratio (*er*) in presence of chiral phosphoric acid (*R*)-**1.4**. The reaction is accelerated

by acylation of the azetidine ring with a 3,4,5-trimethoxybenzoyl group. The nitrogen-activated transition state formed by interaction between the catalyst, substrate and nucleophile is kinetically favoured over the carbonyl oxygen activation. Hence, cleavage of the *C*–*N* bond is facilitated by selective attack of the nucleophile **1.2**.

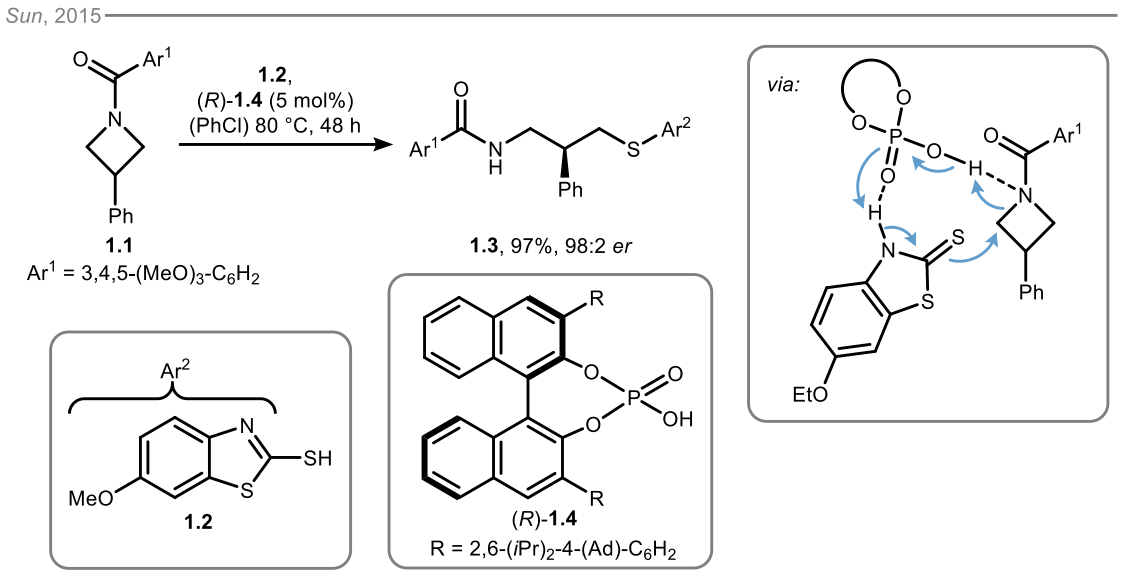

Scheme 1. Ring-opening strategy for the enantioselective synthesis of acyclic amide 1.3 by *Sun* and coworkers.[29] PhCl = chlorobenzene, Ad = adamantyl.

Ring-contraction allows for the transformation of larger cyclic systems into smaller intermediates and represents a powerful tool for one-step skeletal modification. Recently, *Oestreich* and coworkers developed an approach to modify amine scaffolds by ring-contraction of hydroxylamines towards tertiary amines using hydrosilanes and catalytic tris(pentafluorophenyl)borane (Scheme 2).[30] Depending on the substrate used, experimental and computational studies suggest, that the reaction proceeds *via* two different pathways. The reaction is initiated by dehydrogenative silylation forming *O*-disilyloxonium intermediates **1.5** or **1.6**. For aliphatic substrate **1.7** it is proposed, that the reaction follows a selective 1,2-alkyl shift leading to the formation of pyrrolidine **1.8**. In contrast, the high regioselectivity for the reaction of hydroxylamine **1.9** is maintained by electrophilic substitution leading to a phenonium ion intermediate **1.10**, which undergoes hydride transfer to form the final ring-contracted product **1.11**.

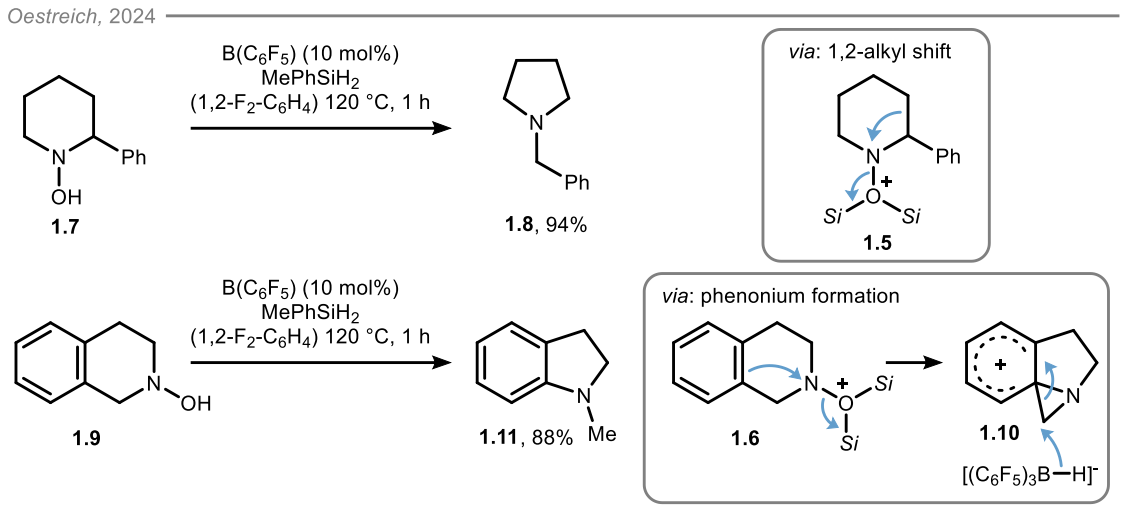

Scheme 2. Ring-contraction strategy for the synthesis of pyrrolidines 1.8 and 1.11 by *Oestreich* and coworkers.[30]

While the two strategies presented above are examples of approaches for the transformation of nitrogen-containing molecules, strained molecules are likewise applied to the synthesis of nitrogen-containing heterocycles. *Sandvoß* and *Wahl* recently reported a transition-metal-free method for the nitrogen insertion reaction between cyclic alcohol **1.12** and *O*-mesitylsulfonylhydroxylamine **1.13** as an aminating reagent (Scheme 3).[31] Key of this transformation is the ring-expansion towards five-membered heterocycle **1.14** by skeletal rearrangement *via* 1,2-carbon shift from intermediate **1.15**. Optimisation studies highlighted the crucial role of the fluorinated alcoholic solvent, which enhances substrate activation and thus allows for efficient interaction with the ambiphilic aminating agent. Combination of the nitrogen insertion strategy with a photochemical *Norrish-Yang*-type cyclisation offers a novel route to 2-methylindole **1.16** by generation of alcohol **1.17** from *ortho*-substituted acetophenone **1.18**. The combined approach demonstrates a stepwise build-and-release strategy, that provides a new pathway for indole synthesis, a key structural motif in pharmaceuticals.

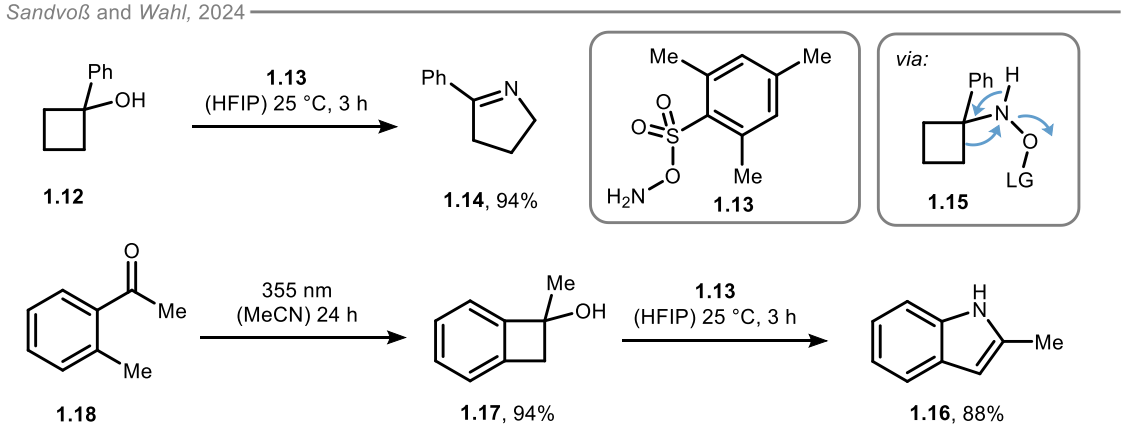

Scheme 3. Ring-expansion strategy for the synthesis of pyrrolidine 1.14 and build and release strategy for the synthesis of 2-methylindole 1.16 by *Sandvoß* and *Wahl*.[31] HFIP= 1,1,1,3,3,3-hexafluoroisopropanol, LG = leaving group. MeCN= acetonitrile.

2 Development of a selective nitrogen insertion strategy

2.1 Introduction

A prevalent structural motif of nitrogen-containing drugs are γ-lactams. The five-membered heterocycles exhibit a wide range of therapeutic potential, including antibiotic[32] and antiviral[33], anti-inflammatory[34], cytotoxic[35] and anti-tumor[36] properties.[37] Thus, racemic and enantioselective γ-lactam structures can be found in various drug candidates, such as lenalidomide[38], brivaracetam[39] and nimatrelvir[40] (Scheme 4). The pharmaceutical importance of the motif is accompanied by considerable interest in the synthetic accessibility.

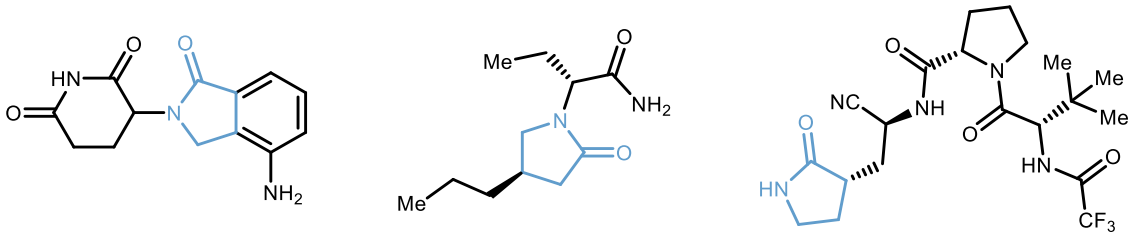

lenalomide
treatment of multiple myeloma

brivaracetam
antieleptic drug

nirmatrelvir
SARS-CoV-2 inhibitor

Scheme 4. Selected examples of drugs including a γ-lactam core with various therapeutic applications.

Common methodologies employed in the synthesis of γ-lactams rely on the cyclisation of linear compounds, which bear a carboxylic acid and an amine functionality, as found in amino acid derivatives.[41] In addition to amide formation facilitated by activating reagents, cyclisation is also possible by intramolecular *N*-alkylation of an amide[42], nitrene *C*–*H* insertion[43] or transition metal catalysed *C*–*C* bond formation.[44]

2.1.1 Nitrogen insertion *via* Beckmann and Schmidt reaction

A complementary strategy of lactam synthesis is the nitrogen insertion into a cyclic ketone by *Beckmann*[45] or *Schmidt*[46,47] rearrangement. The former transformation describes the acid-catalysed rearrangement of oximes and is one of the oldest and most common methodologies used for the formation of amides. In industry, the *Beckmann* reaction is an established process synthesising ε-caprolactam, a precursor of Nylon-6.[48] Similarly, the synthesis of γ-lactams can be achieved through the *Beckmann* rearrangement of 4-membered cyclic oximes, as illustrated by *Jeffs et al.* for the formation of bicyclic lactam **2.1** from oxime **2.2** albeit in modest yield (Scheme 5, top left).[49]

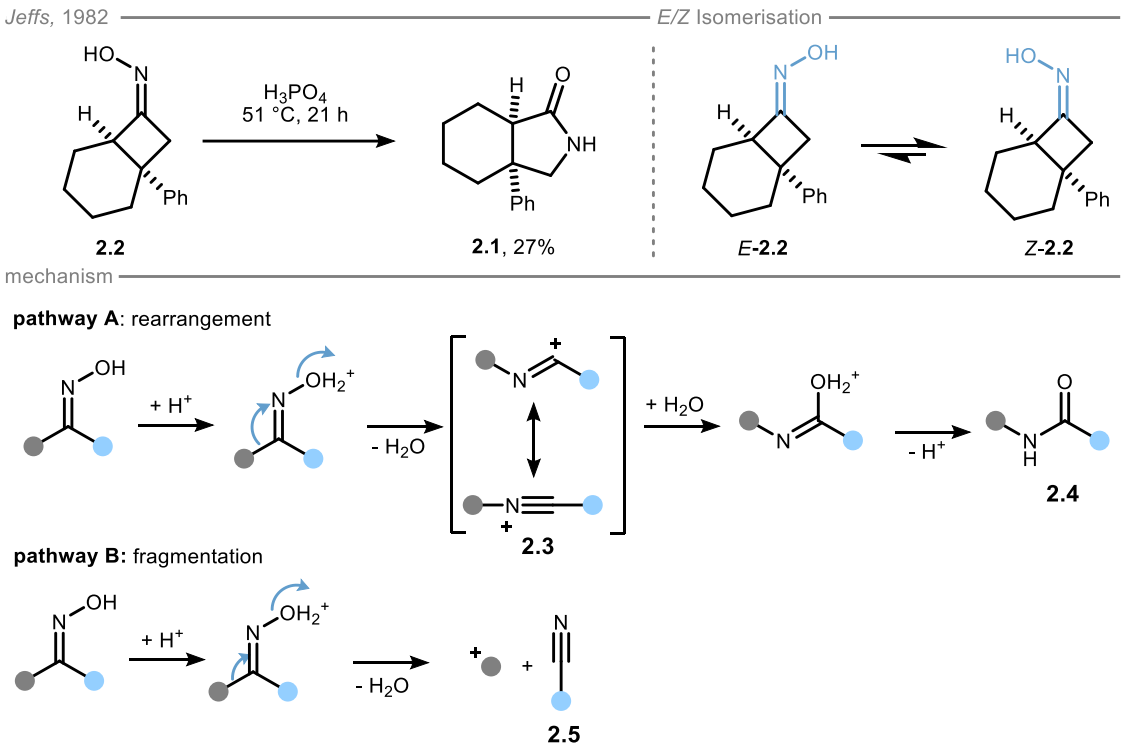

Scheme 5. Top left: Acid-catalysed *Beckmann* rearrangement of cyclobutanone oxime 2.2 by *Jeffs et al.*[49] Top right: Thermodynamic equilibrium for the *E*/*Z* isomerisation of the cyclobutanone oxime determining the regioselectivity.[49] Bottom: General mechanism of the *Beckmann* reaction with the rearrangement towards the formation of an amide 2.4 and the fragmentation towards the formation of a nitrile 2.5.

Product regioselectivity of *Beckmann* rearrangements depend on the *E*/*Z* isomerisation of the starting material (Scheme 5, top right), as the acidic activation of the oxime group facilitates a migration of the substituent placed antiperiplanar to the *N*–*O* bond (Scheme 5, bottom pathway A).[50,51] The concerted migration and departure of the leaving group affords a cationic nitrilium intermediate **2.3**, which can be attacked from a nucleophile, such as water.[52] Finally, the amide **2.4** is formed through tautomerisation. Thus, the observed regioselectivity in the seminal study by *Jeffs et al.* is explained by the prevalence of the thermodynamically favoured *Z*-isomer of oxime **2.2**. Furthermore, selectivity can be affected by a competing *C*–*C* fragmentation, resulting in the formation of a nitrile **2.5** rather than amide **2.4** (Scheme 5, bottom pathway B).[53] During this process, a carbocation is formed in *α*-position to the oxime. Accordingly, structural properties stabilising carbocations, such as functional groups or quaternary centres, assist the *Beckmann* fragmentation.[50,54] In addition to this lack of controllability, the required oximes have to be synthesised from ketones through a condensation reaction with hydroxylamine, thus representing a resource-intensive method. Whilst classical *Beckmann* reaction conditions require strong acidic conditions to promote the rearrangement, it has been demonstrated that oxime activation can also be achieved through esterification, thereby enhancing the leaving group ability.[55]

Similarly, the *Schmidt* reaction describes the formation of an amide **2.4** from the reaction between a ketone **2.6** and an azide compound (Scheme 6, top left).[46,47] These transformations generally require the presence of strong protic acids, thus enhancing the reactivity of the carbonyl group. In the last decades, the development of the reaction conditions has enabled the synthesis of *N*-alkylated amides, utilising alkyl azides in the presence of *Lewis* acids.[56] Among these studies, *Aubé et al.* reported the formation of *N*-alkylated lactams from various cyclic ketones by *Lewis* acid-catalysed nitrogen insertion reaction of *n*-hexyl azide (*n*-$HexN_3$)(Scheme 6, top right). With this methodology, *γ*-lactam **2.7** was accessible in moderate yields, starting from 3-phenylcyclobutanone **2.8**.[57]

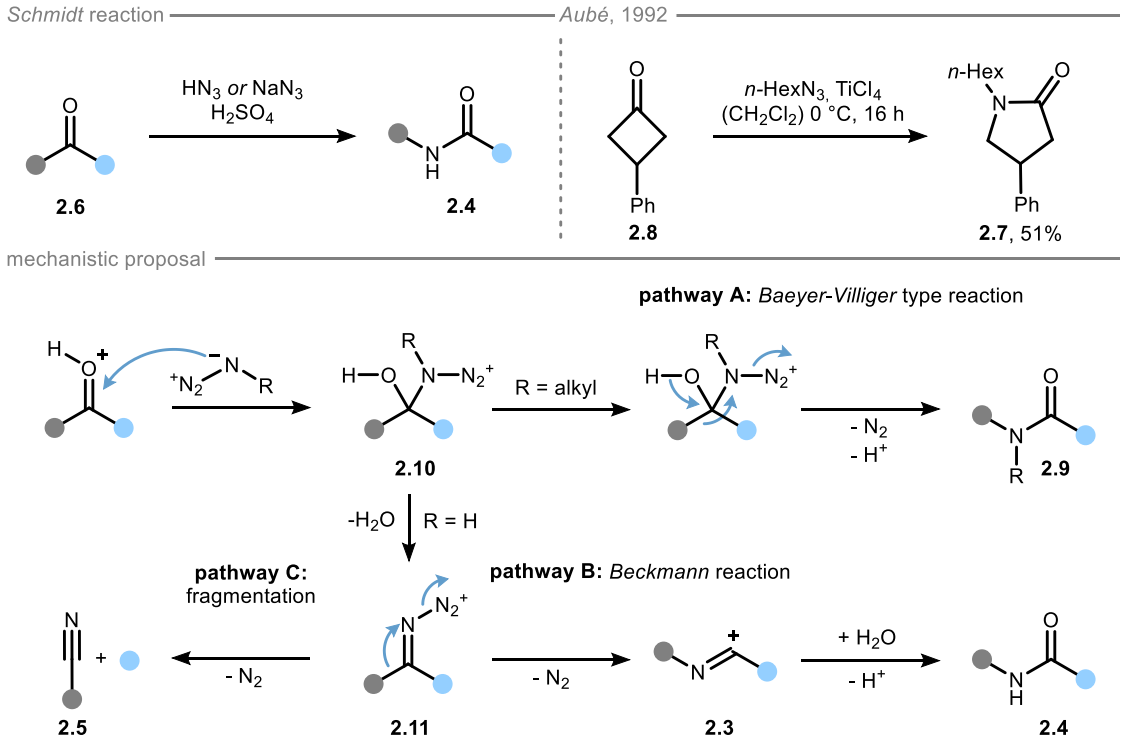

Scheme 6. Top left: General *Schmidt* reaction of ketone 2.6 with hydrazoic acid or sodium azide and sulfuric acid affording amide 2.4. Top right: *Schmidt* reaction of cyclobutanone 2.8 with *n*-hexyl azide catalysed by titanium tetrachloride by *Aubé et al.*[57] Bottom: Proposed mechanism of the *Schmidt* reaction with three different pathways after nucleophilic attack of the azide compound to the ketone.

The authors postulate that the rearrangement affording *N*-alkylated lactams **2.9** occurs *via* a *Baeyer-Villiger* type reaction from tetrahedral intermediate **2.10**, since condensation towards imine type intermediate **2.11** is hindered by alkyl substitution (Scheme 6, bottom pathway A). Nevertheless, a second mechanistic pathway is commonly discussed for the nitrogen insertion reaction towards unsubstituted amines **2.4**.[58] This pathway involves the condensation of the tetrahedral intermediate **2.10**, resulting in the formation of intermediate **2.11**. The following process bears similarity to the *Beckmann* reaction, wherein intermediate **2.11** can undergo either a rearrangement that affords the desired amide **2.4** (Scheme 6, bottom pathway B), or an undesired fragmentation that produces a nitrile **2.5** (Scheme 6, bottom pathway C). As indicated by earlier studies,

tetrazoles have been reported as byproduct resulting from the reaction between nitrilium ion **2.3** and a second equivalent of hydrazoic acids, thus providing evidence for pathway B.[47,59] Furthermore, recent mechanistic investigations have revealed a late path bifurcation between *Beckmann* rearrangement and fragmentation depending on the ketone used.[60] Consequently, *Schmidt* reactions face similar drawbacks as *Beckmann* reactions, resulting in a hampered predictability of the selectivity. Moreover, both transformations require harsh conditions including strong acids, high temperatures and hazardous or explosive reagents.
Therefore, improved variants of the aforementioned methodologies where developed in the early 1970s, including the rearrangement of nitrones[61] and the reaction of ketones with *O*-sulfonylated hydroxylamines.[62] The potential of *O*-mesitylene sulfonylhydroxylamine **1.13**, a representative of the latter reagents, was highlighted by *DeMesmaeker* and coworkers in their investigation of the nitrogen insertion rection with cyclobutanone **2.12** (Scheme 7).[63] While the conventional *Beckmann* reaction gave solely fragmentation product **2.13**, the desired lactam **2.14** was successfully formed using hydroxylamine **1.13** under aqueous acidic conditions. Herein, the rearrangement is postulated to occur *via* tetrahedral intermediate **2.15**, which is thermodynamically favoured by the release of the ring strain present in the four-membered substrate.

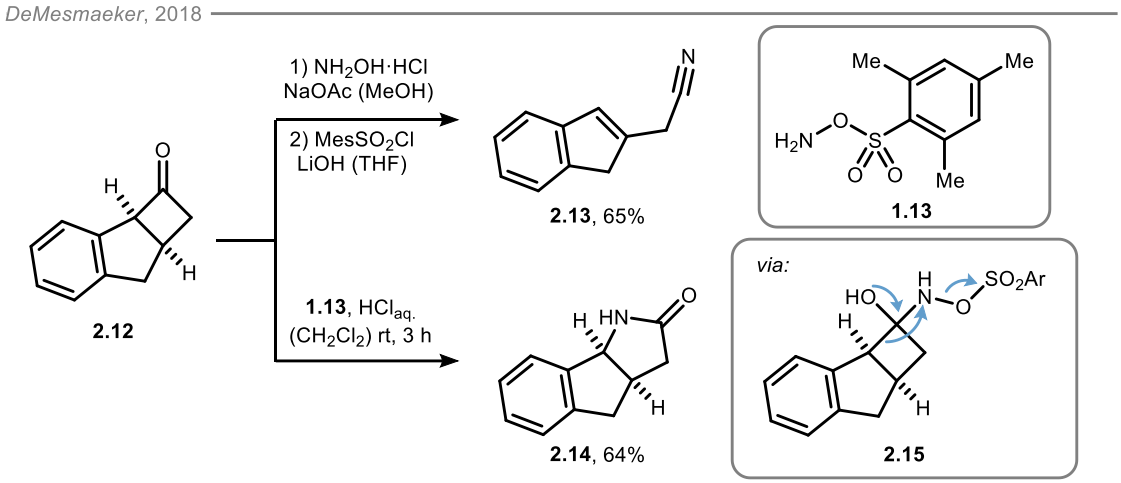

Scheme 7. *Beckmann* fragmentation of ketone 2.12 using classical *Beckmann* reaction conditions (top) and *Beckmann* rearrangement of ketone 2.12 *via* a tetrahedral intermediate 2.15 using aminating reagent 1.13 (bottom) by *DeMesmaeker* and coworkers.[63] Mes= mesitylene.

2.1.2 Oxygen insertion *via* Baeyer-Villiger oxidation

As previously discussed, several mechanistic explanations are often considered reasonable for nitrogen insertion processes and therefore extensively debated in literature (*vide supra*, Scheme 6). Whereas the common methodologies are often considered to include *Beckmann* reaction pathways, recent works proposed *Baeyer-Villiger* type rearrangements. In order to be able to discuss the nuances of the mechanistic differences in the following work, the *Baeyer-Villiger* reaction will be briefly summarised for the corresponding oxygen insertion reaction of

cyclobutanones **2.16** to γ-lactones **2.17** (Scheme 8, top). Starting from the initial reports on an insertion of oxygen into the *C–C* bond of a ketone through treatment with peroxymonosulfonic acid, the frequently used *Baeyer-Villiger* reaction has undergone significant enhancements.[64–66] Thus, the replacement of the oxidant with peroxy acids, such as *meta*-chlorobenzoic acid **2.18** (*m*CPBA), has enabled the development of mild and selective methods.[67]

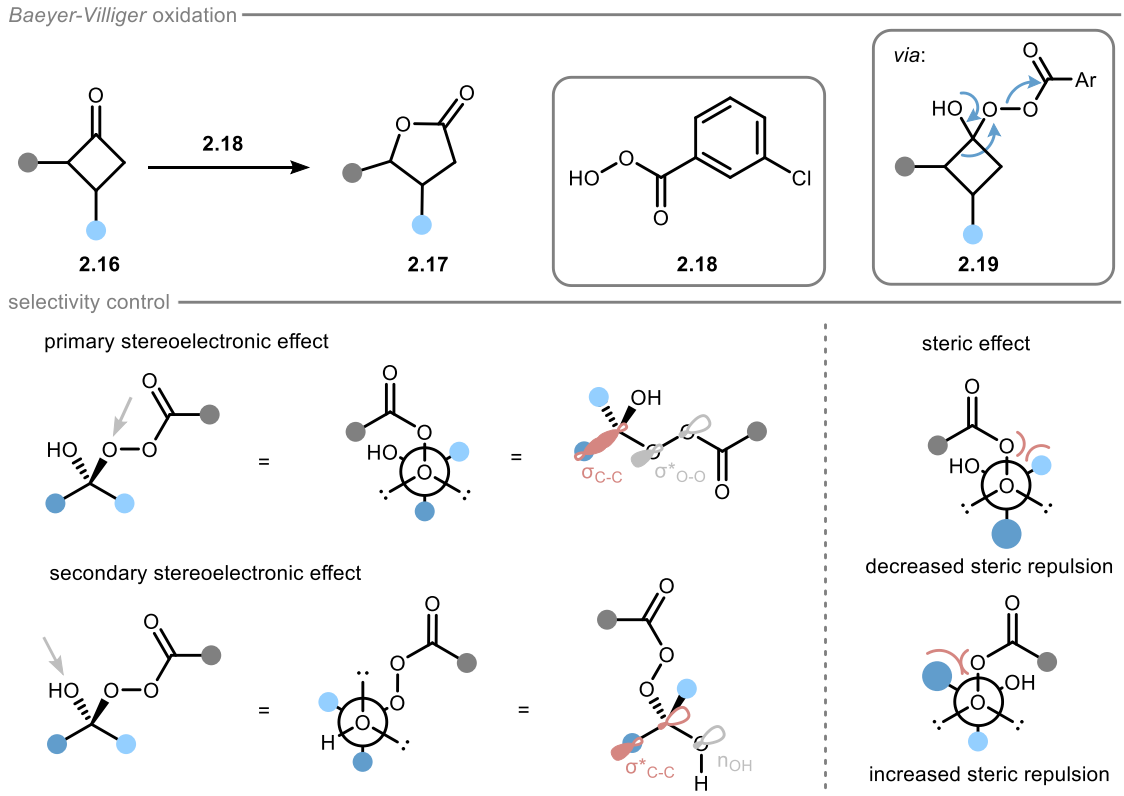

Scheme 8. Top: General example for the formation of γ-lactones 2.17 *via Baeyer-Villiger* oxidation of cyclobutanones 2.16 with *m*CPBA (2.18). Bottom left: Representation of the stereoelectronic effects with the involved orbital interactions in the "*Criegee* intermediate" 2.19. Bottom right: Representation of the steric repulsion for transformation of ketones with different substituents.

In 1953, *Doering* and *Dorfmann* confirmed the mechanistic course of the reaction *via* the formation of a tetrahedral adduct **2.19** known as the "*Criegee* intermediate", which is formed by nucleophilic addition of the peroxyacid to the ketone.[68,69] Migration of one substituent, and subsequent release of the leaving group leads to product formation. In the second step of the reaction, the migration is controlled through stereoelectronic effects, including the antiperiplanar alignment of the migrating residue and the leaving group (Scheme 8, bottom).[70] This orientation allows for the best orbital overlap between the σ-orbital of the *C–C* bond and the σ*-orbital of the *O–O* bond. In addition, a secondary effect arises due to the overlap of the n-orbital of the hydroxy group and the σ*-orbital of the *C–C* bond.[71] Consequently, rearrangement occurs by migration of the *C–C* bond placed antiperiplanar to the *O–O* bond of the leaving group within retention of the stereochemistry of the migrating substituent. Besides stereospecific transformations, application of chiral catalysts allow for stereoselective

desymmetrisation of cyclobutanones as a straightforward and effective approach in asymmetric synthesis.[19] Furthermore, regioselectivity can be predicted considering electronic and steric properties of the substituents.[66,72] In order to minimise steric interactions in the transition state, the biggest substituent is preferably oriented in antiperiplanar alignment to the *O–O* bond. This configuration is beneficial for the rearrangement, resulting in an increased migratory aptitude that is correlated with the degree of substitution (tertiary alkyl> secondary alkyl> primary alkyl). Additionally, it was found that the migration ability is increased for substituents with better stabilisation of the partial positive charge formed in the transition state.[69,73] Therefore, the presence of electron-donating groups increases the migration rate, whereas electron-withdrawing groups decrease the migrating ability.

2.1.3 Motivation and aim

The *Baeyer-Villiger* oxidation represents a powerful tool for the mild and selective synthesis of esters *via* oxygen insertion reactions using ketones and peroxy acids. Thus, γ-lactones are easily accessed from cyclobutanones by ring-expansion reaction. In contrast, analogous nitrogen insertion reaction *via Beckmann* and *Schmidt* rearrangements requires highly acidic reaction media, challenging its synthetic utility. Recent developments include the utilisation of amine reagents like *O*-mesitylene sulfonylhydroxylamine **1.13**.[63,74] However, while benefiting the rearrangement, the weak *N*–*O* bond of the aminating reagent **1.13** is minimising the working safety and storage ability of the reagent due to the increased tendency for spontaneous decomposition. Additionally, the concomitant formation of fragmentation products as a concurrent reaction impedes the performance and synthetic applicability of common protocols (*vide supra*, Scheme 7). Therefore, a mild nitrogen insertion process using a stable and selective amine reagent was investigated in collaboration with [redacted]. According to the proposed mechanism of an aza-*Baeyer-Villiger* rearrangement, [redacted] identified an *O*-substituted hydroxylamine as suitable aminating reagent, which was inspired by established reagents as nitrogen sources and the structural similarity to peroxy acids commonly used for oxygen insertion. Nucleophilic addition of a hydroxylamine to the carbonyl group of 3-substituted cyclobutanones is proposed to form a tetrahedral intermediate **2.20** (Scheme 9). The process of the nitrogen insertion relies on the subsequent rearrangement, which is facilitated by the effective leaving group (LG) ability of the substituent at the nitrogen and the release of ring strain.

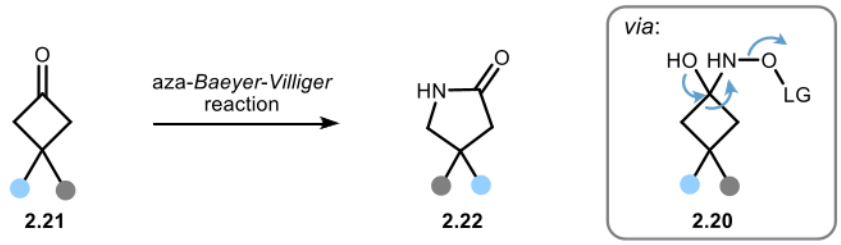

Scheme 9. Synthesis of γ-lactams *via* aza-*Baeyer-Villiger* oxidation.

In this collaborative endeavour, mechanistic investigations for the transformation of cyclobutanones **2.21** towards γ-lactams **2.22** were conducted. As part of this work, the use of α-substituted cyclobutanones for a stereochemical analysis determining analogies to the *Bayer-Villiger* oxidation was envisaged. In this regard, the exploration will investigate the regioselectivity and stereospecificity of the transformation. The knowledge gained from this study was used to evaluate the synthetic utility, with the aim to explore the substrate scope of the developed methodology.

2.2 Synthesis of starting materials

A library of cyclobutanones was synthesised in order to study their reactivity in a nitrogen insertion reaction. For the purpose of conducting a stereochemical analysis of an aza-*Baeyer-Villiger* rearrangement, a series of *α*-substituted cyclobutanones **2.23** to **2.25** were prepared, in accordance with established literature procedures (Scheme 10).[75,76] 2-Methylenecyclobutanones **2.26** to **2.28** were obtained in moderate yields by aldol condensation of cyclobutanone **2.29** with the corresponding aldehyde. Homocondensation of cyclobutanone occurred as a side reaction, thus limiting the overall performance of the transformations. The synthesis of the desired cyclobutanones **2.23** to **2.25** was achieved by reduction of the olefin formed during the initial synthesis step. While **2.23** and **2.24** were accessed in satisfactory yields, the synthesis of the thiophenyl derivative **2.25** was less successful. For overcoming limitations due to catalyst inhibition, a second portion of palladium on charcoal was added after 6 h reaction time to yield cyclobutanone **2.25** in 29%.

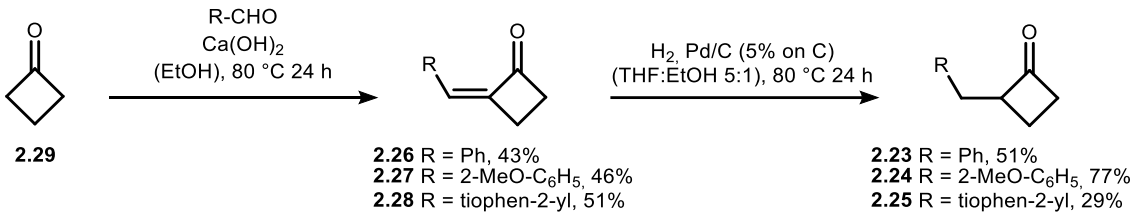

Scheme 10. Synthesis of α-substituted cyclobutanones 2.23 to 2.25 *via* aldol condensation of cyclobutanone 2.29 and the corresponding aldehyde followed by subsequent hydrogenation of the formed alkene. EtOH = ethanol, THF = tetrahydrofuran.

The analysis of the aza-*Baeyer-Villiger* reaction prompted to investigate the stereospecificity of the nitrogen insertion process. Therefore, enantioselective cyclobutanone (*S*)-**2.23** was prepared from 2-methylene cyclobutanone **2.26** *via* asymmetric hydrogenation in presence of chiral complex **2.30**. Stereocontrol in the reduction derives from the coordination of a chiral *P*,*N*-ligand **2.31** to iridium. Starting from 2,2'-dihydroxyl biphenyl **2.32**, ligand **2.31** was prepared according to modified literature known procedures by the *Zhang* group.[77–79] The synthesis was initiated through the triflation of biphenyl **2.32** with trifluoromethanesulfonic anhydride (Tf_2O) in the presence of diisopropylethylamine. Palladium catalysed insertion with diphenyl phosphine oxide afforded phosphine oxide **2.33** in good yield. Compound **2.34** was prepared from precursor **2.33** through a one-pot reaction method that involved palladium catalysed carbonylation using carbon monoxide and subsequent coupling of (1*S*,2*R*)-1-amino-2-indanole. To mitigate the inherent safety risks associated with the use of toxic gases, small portions of CO were generated *in situ* by treating formic acid with sulfuric acid. The final oxazoline ligand **2.31** was obtained after intramolecular condensation under acidic conditions, followed by reduction with trichlorosilane. Completion of the synthesis of complex **2.30** was achieved through the complexation

of ligand **2.31** with cyclooctadiene iridium chloride dimer and counterion exchange with sodium tetrakis [3,5-bis(trifluoromethyl)phenyl]borate (BAr_F).

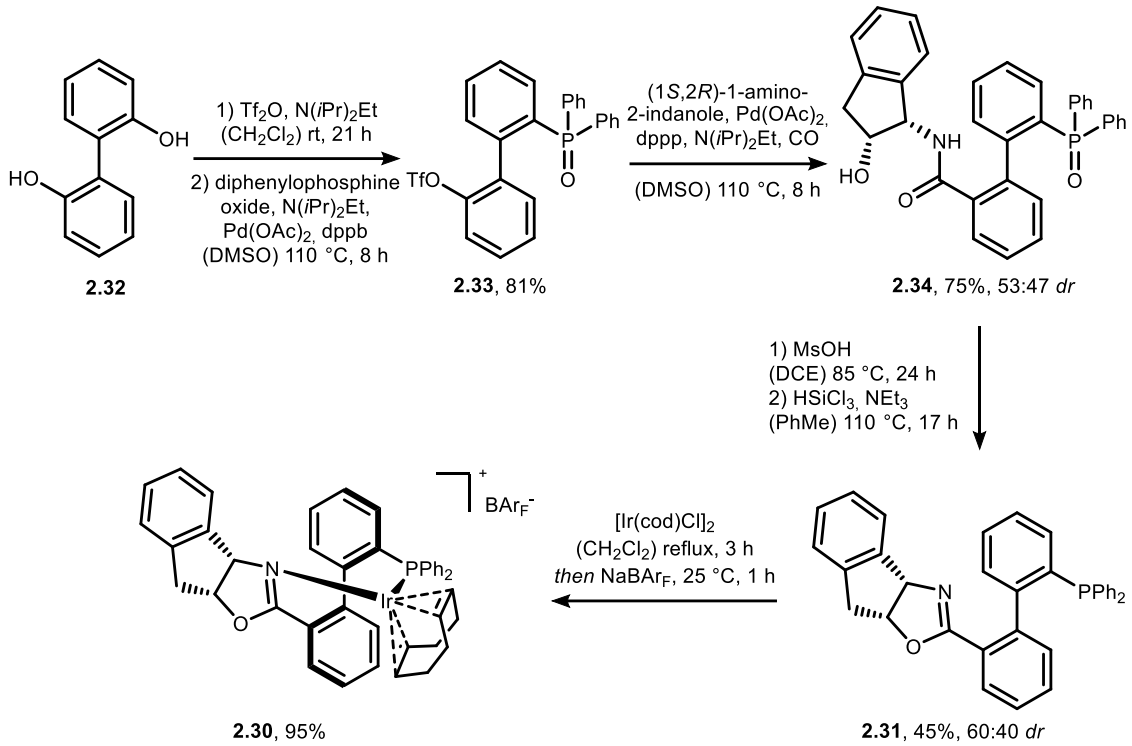

Scheme 11. Synthesis route for the formation of complex 2.30. cod = cyclooctadiene, dppb = 1,4-bis(diphenylphosphino)butane, dppp = 1,3-bis(diphenylphosphino)propane, DMSO = dimethyl sulfoxide, MsOH = methanesulfonic acid, *dr* = diastereomeric ratio.

The successfully synthesised complex **2.30** was employed to enable the stereoselective synthesis of cyclobutanone (*S*)-**2.23**. Following a modified literature procedure from *Xia et al.*[80], the asymmetric hydrogenation of alkene **2.26** afforded cyclobutanone (*S*)-**2.23** with an enantioselectivity of 95:5 *er*.

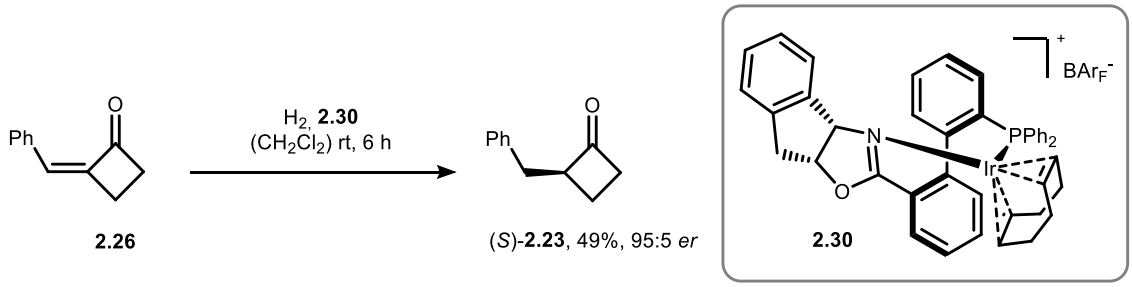

Scheme 12. Synthesis of chiral α-substituted cyclobutanone (*S*)-2.23 *via* enantioselective reduction in presence of chiral complex 2.30.

For the exploration of the substrate scope of the nitrogen insertion reaction, versatile cyclobutanones were obtained *via* thermal [2+2]-cycloaddition between an alkene and an *in situ* generated ketene-type intermediate. In contrast to alkene alkene [2+2]-cycloadditions, the employment of allene or ketene derivatives allows for thermal [2+2]-cycloaddition.[81] Frequently, dichloroketene[82,83] or ketene iminium ions[84,85] are used in these approaches.

The latter was applied in the preparation of cyclobutanone **2.35**. The ketene iminium species **2.36** was generated *in situ* by triflation of *N*,*N*-

dimethylisobutyramide **2.37** and base-induced elimination.[86] The isolation of the target product **2.35** was achieved through the hydrolysis of the cyclobutanone iminium salt that was formed during [2+2]-cycloaddition of ketene iminium intermediate **2.36** with styrene **2.38**.[84]

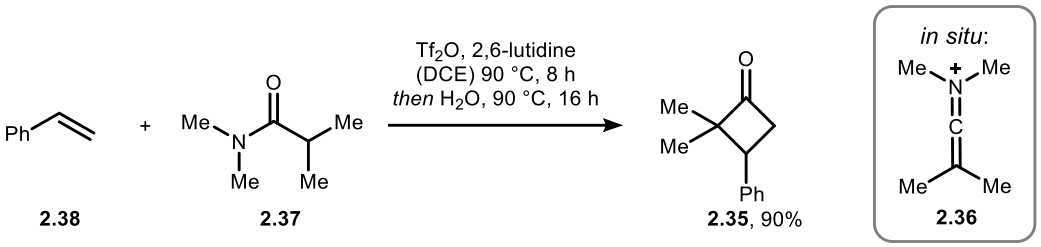

Scheme 13. Synthesis of α-disubstituted cyclobutanone *via* [2+2] cycloaddition between styrene an *in situ* formed ketene iminium ion. DCE = 1,2-dichloroethane.

Cyclobutanone **2.12**, a substrate that is known to undergo fragmentation reaction using harsh conditions (*cf.* chapter 2.1.2), was prepared to demonstrate the mild reaction conditions of the developed aza-*Baeyer-Villiger* reaction. The tricyclic compound was obtained *via* an intramolecular [2+2]-cycloaddition from precursor **2.39** that was synthesised according to a procedure by *Lachia et al.*[87] First, synthesis of amide **2.40** was achieved starting from 2-iodobenzoic acid **2.41** after acid chloride formation and nucleophilic attack of diisopropylamine. *Stille* coupling with allylstannane and tetrakistriphenylphosphine palladium introduced alkene functionality affording precursor **2.39** in good yields. The subsequent generation of ketene iminium salt **2.42** and intramolecular cycloaddition delivered tricyclic cyclobutanone **2.12** after hydrolysis of the resulting cyclobutanone iminium salt. It should be noted that the hydrolysis was only accomplished under basic conditions, as the reaction with water was found to be unsuccessful.

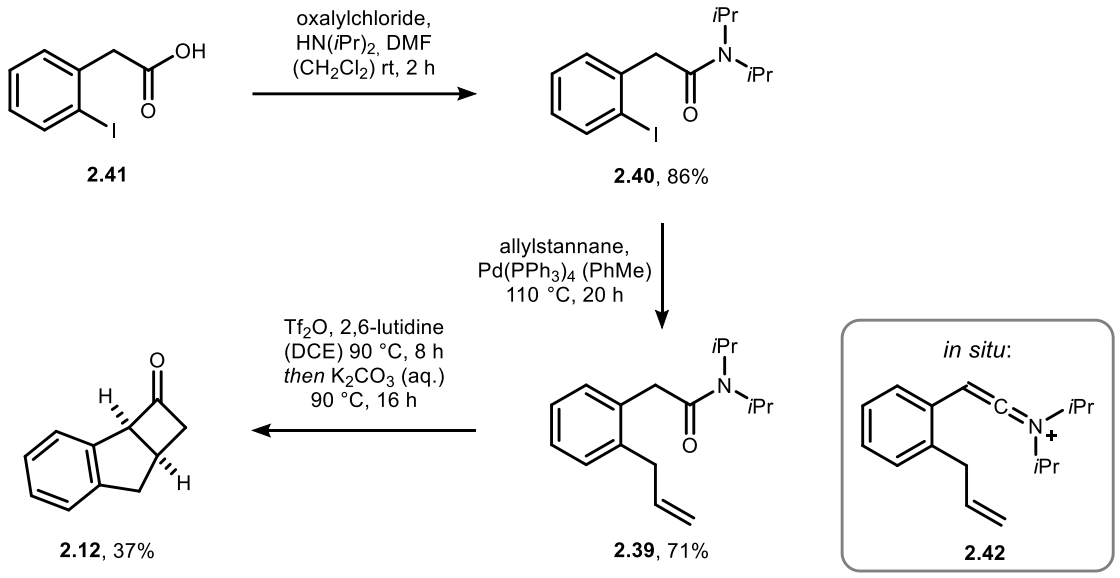

Scheme 14. Synthesis route of precursor 2.39 for intramolecular [2+2] cycloaddition and synthesis of cyclobutanone 2.12. DMF = dimethylformamide.

[2+2]-Cycloaddition and dehalogenation using dichloroketene **2.43** and commercially available indene **2.44** resulted in the formation of tricyclic cyclobutanone **2.45**, a regiosiomer of **2.12**. The formation of dichlorketene **2.43** was conducted under ultrasonication, facilitating the zinc-mediated dehalogenation of trichloroacetyl chloride.[88,89] [2+2]-Cycloaddition with dichloroketene **2.43** afforded a *α,α*-dichlorinated cyclobutanone, which was subsequently dehalogenated using zinc and acetic acid (AcOH).[83,90]

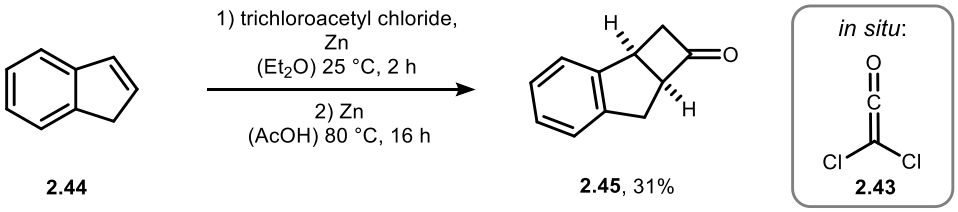

Scheme 15. Synthesis of tricyclic cyclobutanone 2.45 *via* [2+2]-cycloaddition between indene 2.44 and dichloroketene 2.43 and subsequent reductive dehalogenation. Et_2O = diethyl ether.

Besides structurally diverse cyclobutanones, the use of a substrate with a different ring size was sought to be explored in the aza-*Baeyer-Villiger* reaction. Therefore, cyclopentanone **2.46** was prepared following a literature known procedure by *Müller et al.*[91] First, cyclopentanone derivative **2.47** was formed *via* aldol condensation between benzil **2.48** and acetone and subsequent nucleophilic substitution with acetyl chloride. Dehalogenation and reduction of the alkene moiety gave the desired product **2.46** in good yields.

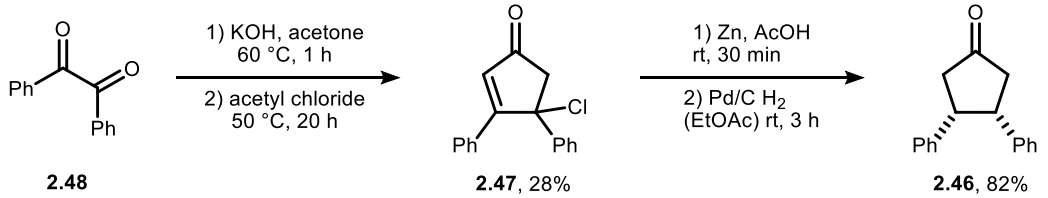

Scheme 16. Synthesis of cyclopentanone 2.46. EtOAc = ethyl acetate.

2.3 Investigation of the nitrogen insertion reaction

The nitrogen insertion of cyclobutanones with hydroxylamines was investigated in collaboration with [redacted]. The development of a mild method following a *Baeyer-Villiger* type rearrangement is advantageous in terms of synthetic utility in comparison to the established nitrogen insertion protocols (*cf.* chapter 2.1.1). The scope and synthetic applicability of such an aza-*Baeyer-Villiger* reaction was sought to be expanded as part of this work. The initial optimisation, mechanistic investigations and parts of the exploration of the substrate scope were performed by [redacted] and [redacted]. The ensuing discussion will provide a concise overview of these findings. Initially, the potential of aminating reagents bearing good leaving groups at the nitrogen atom were investigated by [redacted] using 3-phenylcyclobutanone **2.8** as a model substrate (Scheme 17). The corresponding lactam **2.49** was expected to be formed *via* ring-expansion rearrangement of intermediate **2.50**. Although the aminating reagent **1.13** has been used previously in synthesis of γ-lactams,[63] it was not considered for this study due to its limited accessibility and low stability. Rather, the choice of *O*-(diphenylphosphinyl)hydroxylamine **2.51** (DPPH) and amino benzoate **2.52** was inspired by the structural properties of *O*-substituted hydroxylamine **1.13**. The reaction with aminating reagent **2.51**, resulted in the predominant formation of the expected γ-lactam **2.49** (entry 1). In contrast, application of amino benzoate **2.52** favoured the condensation pathway affording oxime ester **2.53** (entry 2). Thus, [redacted] determined that the stability of the leaving group was deemed to be crucial for the desired nitrogen insertion. In this regard, hydroxylamine **2.51** has been shown to outcompete other aminating agents due to the properties of the leaving group and its overall high stability. Another beneficial aspect is the commercial availability of the reagent. A solvent screening performed by [redacted] revealed that DMF further improves the ratio between γ-lactam **2.49** and cyclobutanone oxime derivative **2.53**. Mechanistic investigations by [redacted] discovered the condensation process to be a side reaction rather than part of the mechanism towards γ-lactam formation, assisting the postulated aza-*Baeyer-Villiger* rearrangement.[92]

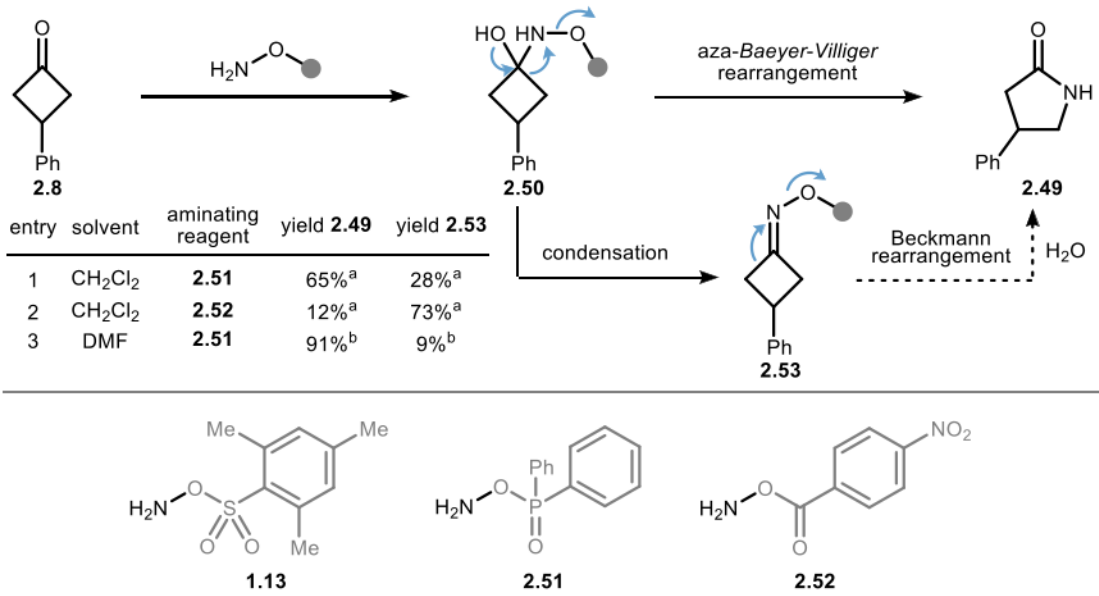

entry	solvent	aminating reagent	yield **2.49**	yield **2.53**
1	CH_2Cl_2	**2.51**	65%[a]	28%[a]
2	CH_2Cl_2	**2.52**	12%[a]	73%[a]
3	DMF	**2.51**	91%[b]	9%[b]

Scheme 17. Top: Mechanistic proposal and initial results of the aza-*Baeyer-Villiger* reaction between cylobutanone 2.8 and different aminating reagents. Bottom: Aminating reagents sorted by their leaving group ability decreasing from left to right. [a] Results obtained by [redacted]. [b] Results obtained by [redacted].

The focus of this work is to emphasise the benefits in using the aminating reagent **2.51**. Therefore, the reaction with cyclobutanone **2.12** was investigated under optimised reaction conditions. Tricyclic lactam **2.14** was obtained as the major isomer with 82% yield. The nitrogen insertion process afforded the corresponding lactam as a separable mixture of both regioisomers in a regioisomeric ratio (*rr*) of 97:3. In contrast to the absence of *Beckmann* fragmentation observed in this study, *DeMesmaeker* and coworkers reported the formation of a significant amount of fragmentation product **2.13** formed during the reaction between cyclobutanone **2.12** and hydroxylamine **1.13**. The desired lactam **2.14** was obtained with a reduced yield of 35%.[63] The regioselectivity of the nitrogen insertion is consistent with the expected regioselectivity for a classical *Baeyer-Villiger* process, with migration of the most electron rich carbon (*cf.* chapter 2.1.2).[64,66]

Table 1. Reaction of cyclobutanone 2.12 with different hydroxylamine reagents.

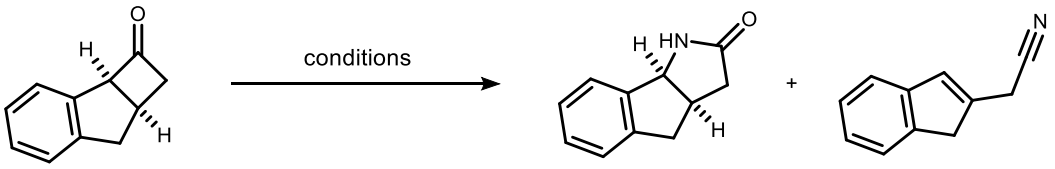

entry	conditions	yield 2.14	yield 2.13
1	**2.51** (DMF) 25 °C, 24 h	82%, 97:3 *rr*	0%
2	**1.13** (CH_2Cl_2) 25 °C[a]	35%[a]	27%[a]

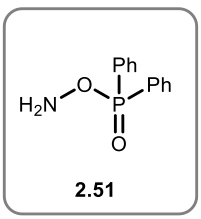

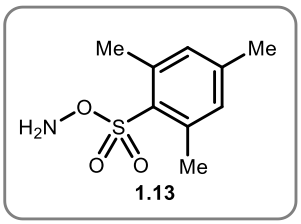

[a] Results obtained by DeMesmaeker and coworkers.[63]

The reliability of the migration aptitude was substantiated by a comparison of the nitrogen insertion process with the corresponding *Bayer-Villiger* oxidation, using the *α*-substituted cyclobutanones **2.23** and **2.24**, amine reagent **2.51** and *m*CPBA **2.18**. Adjusting the reaction conditions, these transformations where performed in ethyl acetate at 35 °C. Lactone **2.54** was obtained in 89% yield with a regioisomeric ratio of 96:4 *rr* by reaction of cyclobutanone **2.23** with *m*CPBA. The corresponding nitrogen insertion reaction resulted in the formation of lactam **2.55**, exhibiting a slightly reduced regioselectivity of 90:10 *rr*. Similar results were obtained for the reactions with cyclobutanone **2.24**. Nevertheless, the major regioisomers formed *via* nitrogen insertion matched the one of the *Baeyer-Villiger* reaction, thus indicating a strong resemblance between the two processes.

Table 2. Comparison of the regioselectivity of the oxygen and nitrogen insertion.

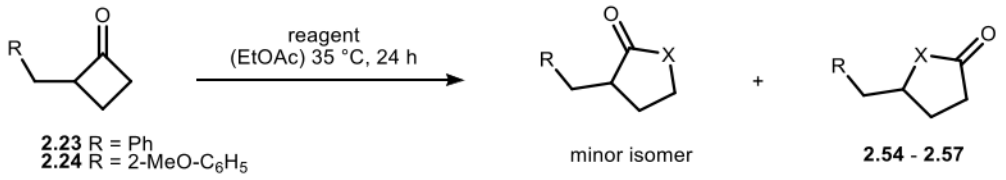

2.23 R = Ph
2.24 R = 2-MeO-C_6H_5

minor isomer

2.54 - **2.57**

entry	reagent	cyclobutanone	R	X	yield
1	**2.18**	**2.23**	Ph	O	**2.54** 89%, 96:4 *rr*
2	**2.51**	**2.23**	Ph	NH	**2.55** 94%, 90:10 *rr*
3	**2.18**	**2.24**	2-MeO-C_6H_5	O	**2.56** 88%, 96:4 *rr*
4	**2.51**	**2.24**	2-MeO-C_6H_5	NH	**2.57** 90%, 88:12 *rr*

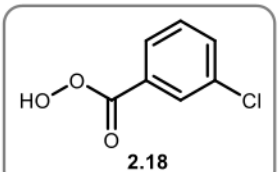

2.18

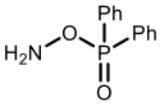

2.51

In order to explore further analogies between the oxygen and nitrogen insertion reaction, the stereospecificity of the nitrogen insertion process was examined. In accordance with the findings of previous studies concerning a stereospecific *Baeyer-Villiger* reaction,[80] the reaction of enantiomerically enriched cyclobutanone (*S*)-**2.23** afforded γ-lactam (*S*)-**2.55** with 86% yield, 83:17 *rr* and 95:5 *er*. Comparing the enantiopuritiy of the starting material with the obtained product the transformation occurred with higher than 99% enantiospecifity (*es*). Furthermore, the stereospecific insertion of methylated nitrogen was accomplished, giving *N*-alkylated lactam (*S*)-**2.58** within comparable results. The synthesis of methylated lactam (*S*)-**2.58** was achieved by reaction of cyclobutanone (*S*)-**2.23** with alkylated aminating reagent **2.59**, which was prepared by [redacted]. The observed trends of the 1,2-shifts indicate a strong correspondence between the oxygen and nitrogen insertion reaction, thus supporting the proposed mechanism of an aza-*Baeyer-Villiger* rearrangement.

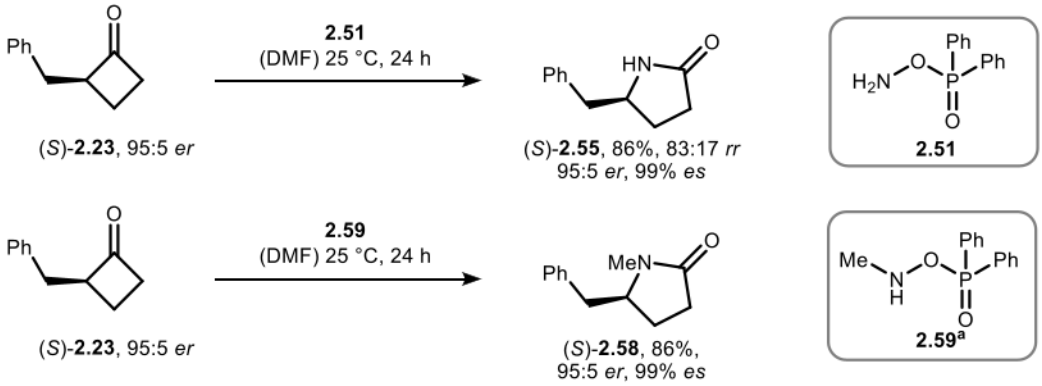

Scheme 18. Stereospecific nitrogen insertion *via* aza-*Baeyer-Villiger* reaction. [a]Reagent prepared by [redacted].

In the following course of the project, the investigation was focused on the expansion of the substrate scope of the aza-*Baeyer-Villiger* reaction. Besides the substrates presented above, versatile *α*-substituted cyclobutanones, including both steric and electronic alterations, in addition to heterocyclic substitution and annulated structures, were examined. Notably, the performance and regioselectivity of the nitrogen insertion reaction were found to remain unperturbed by steric alterations (Scheme 19). The tolerance of thiophene substituted lactam **2.60** serves to highlight the mild nature of the methodology. *α*,*α*-Disubstituted lactam **2.61** and tricyclic lactam **2.62** were obtained in good yields and regioselectivities. Furthermore, the scalability of the reaction was demonstrated by the synthesis of 3-substituted *γ*-lactam **2.49** on a gram-scale with >97% purity. Noteworthy, on the big reaction scale, small residues of the unreacted aminating reagent **2.51** remained as impurities after separation *via* flash column chromatography.
The investigations of [redacted] further explored the applicability of 3-substituted cyclobutanones with diverse functional groups and the use of *N*-alkylated hydroxylamines.[92] These results are part of his own work and will therefore not be discussed herein.

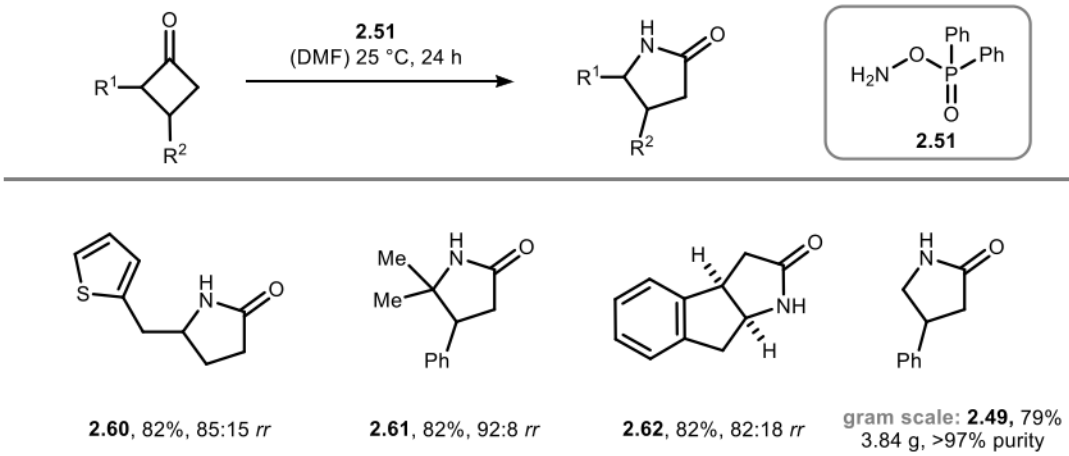

Scheme 19. Further substrate scope of the aza-*Baeyer-Villiger* reaction.

It was further investigated whether cyclopentanones are also suitable for nitrogen insertion reactions. Therefore, the reaction between cyclopentanone **2.46** and amine reagent **2.51** was tested in a small selection of different solvents. The reactions in toluene and dichloromethane afforded small amounts of oxime ester **2.63** besides mainly unreacted starting material **2.46**. For the activation of the ketone functionality, HFIP and acetic acid were applied as more acidic solvents, resulting in an increased reactivity towards the formation of oxime ester **2.63**. However, ring-expansion giving the lactam **2.64** remained unsuccessful.

Table 3. Reaction between cyclopentanone 2.46 and amine reagent 2.51 in different solvents.

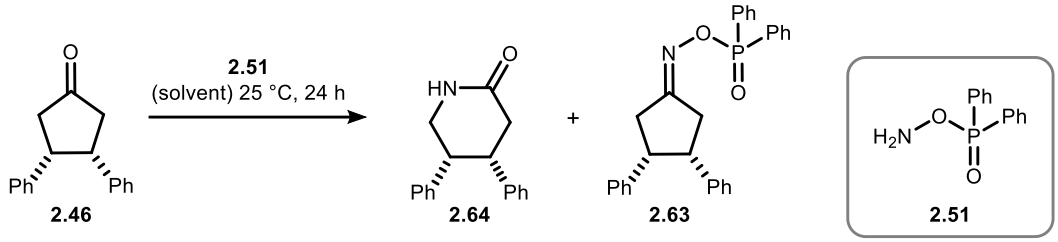

entry	solvent	yield 2.64	yield 2.63	conversion
1	PhMe	0%	7%	10%
2	CH_2Cl_2	0%	15%	22%
3	HFIP	0%	25%	26%
4	acetic acid	0%	86%	88%

2.4 Summary and outlook

The nitrogen insertion reaction of cyclobutanones with hydroxylamines was investigated in collaboration with [redacted], who found reagent **2.51** to be a promising nitrogen source for the synthesis of γ-lactams (Scheme 20). The mild nature of the developed reaction conditions was witnessed by the suppressed *Beckmann* fragmentation process, which was previously limiting established nitrogen insertion protocols. A detailed analysis of the regioselectivity and stereospecificity of the transformation was conducted, revealing significant parallels with the analogous formation of γ-lactones *via Baeyer-Villiger* oxidation. These results lend support to the mechanistic investigations conducted by [redacted] on an aza-*Baeyer-Villiger* rearrangement, thereby facilitating the prediction of reaction selectivity. In this work, the scope of the reaction was expanded to α-substituted cyclobutanones, incorporating steric and electronic alterations, as well as heterocyclic moieties, with high yields up to 94% and good regioisomeric ratios from 82:18 to 92:8 *rr*. In particular, the enantiospecific transfer of alkylated nitrogen, in combination with the gram scale synthesis of cyclobutanone **2.49**, underlines that the developed method may become a powerful tool in organic synthesis.

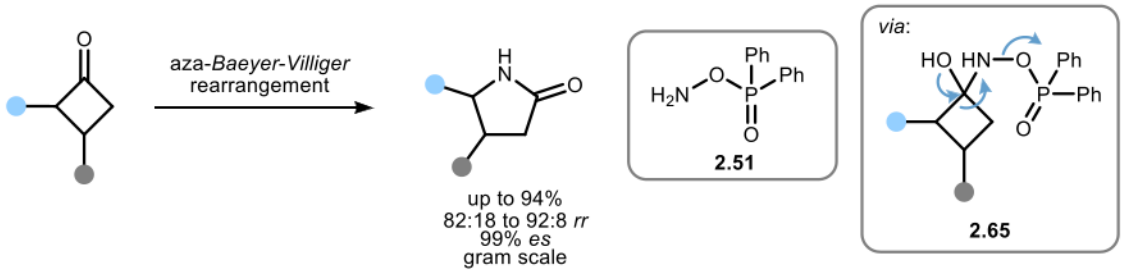

Scheme 20. Synthesis of γ-lactams from cyclobutanones *via* aza-*Baeyer-Villiger* reaction.

In order to further develop the presented nitrogen insertion strategy, it is necessary to overcome the substrate limitations, thus extending the methodology to ketones with varying ring size. Consequently, the exploration of differing reaction conditions or the employment of more reactive amine reagents could be a fruitful endeavour for investigation. Further, the development of an enantioselective protocol remains to be accomplished. In this regard, the potential of chiral amine reagents to introduce stereoselectivity through selective formation of the tetrahedral intermediate **2.65** is a promising prospective for exploration. In the context of atom economy and process sustainability, the ideal approach would involve the identification of a catalytic process. The introduction of enantioselectivity by asymmetric catalytic rearrangement of the tetrahedral intermediate **2.65** has the feasibility of achieving enantioselective γ-lactam formation. Therefore, the identification of a suitable catalytic system is pivotal, with the inspiration deriving from established protocols for an enantioselective *Baeyer-Villiger* oxidation.

3 Development of a catalytic asymmetric nitrogen incorporation strategy

3.1 Introduction

In the preceding chapter, commercially available *O*-substituted hydroxylamine **2.51** was used as a mild reagent for the synthesis of γ-lactams *via* aza-*Baeyer-Villiger* rearrangement of cyclobutanones. Despite the identification of strong analogies to the classical *Baeyer-Villiger* oxidation, enantioselective conditions remain to be developed. As previously outlined, the development of new synthetic strategies for the formation of γ-lactams is of great importance due to their application in drug discovery (*cf.* chapter 2.1). Most of the drug candidates under consideration are chiral molecules, with a single enantiomer frequently displaying divergent biological activities with regard to pharmacokinetics or toxicity.[93] In light of the fact, that enzymes, receptors and proteins in the human body are chiral, it follows that one enantiomer possesses the potential to deliver the desired therapeutic effect, while the other is inactive, toxic or may cause side effects. As a consequence, the synthesis of the desired enantiomer with high selectivity is pivotal in current drug development. Furthermore, selective access to both enantiomers is essential to evaluate the efficacy of a drug candidate.[94] A plethora of strategies have been developed for the asymmetric synthesis of target structures, including the utilisation of chiral reagents, chiral auxiliaries, and asymmetric catalysis.[95] Among these, asymmetric catalysis has emerged as a particular potent tool, facilitating the selective formation of a single enantiomer through interaction of the substrate with a chiral catalyst. The utilisation of this approach entails the minimisation of synthesis steps and the requirement of stoichiometric reagents, thus enhancing the sustainability of the overall process.[96] Furthermore, the use of chiral catalysts in the conversion of prochiral compounds, especially 3-substituted cyclobutanones, enables desymmetrisation, thereby facilitating the direct introduction of a stereogenic centre in a distal position of the molecule.[19,97] In this regard, considerable attention has been focused on the asymmetric *Baeyer-Villiger* oxidation of prochiral cyclobutanones using catalytic systems including organocatalysts, as well as transition metals or *Lewis* acids with coordinating chiral ligands.[98,99]

3.1.1 Asymmetric nitrogen insertion

In contrast to the asymmetric *Baeyer-Villiger* oxidation, the corresponding catalytic formation of chiral γ-lactams is an underexplored field. Limitations in the stereocontrol of nitrogen insertion reactions arise from the harsh acidic conditions typically required for common methodologies like *Schmidt* and *Beckmann* reaction (*cf.* chapter 2.1.1). Therefore, recent studies have explored alternative methodologies for the desymmetrisation of cyclobutanones. These approaches include the formation of enantiopure γ-lactams by nitrogen-based ring-expansion using chiral reagents. In this field, pioneering work was made by the group of *Aubé*, who developed an asymmetric *Schmidt* reaction of cyclic ketones with chiral amine reagents. The approach hence enabled desymmetrisation of cyclobutanone **2.8** through a hydroxyl azide-mediated ring-expansion reaction to generate *N*-alkylated γ-lactam **3.1** with a modest selectivity of 65:35 *dr* (Scheme 21).[100,101] The process is initiated by *Lewis* acid activation of the ketone, facilitating a nucleophilic attack of the hydroxy group of the hydroxyl azide **3.2**. Thus, electrophilic intermediate **3.3** is formed, which is reacting to the spirocyclic intermediate **3.4** *via* intramolecular trapping with the azide tethered on the alkyl chain. Here, the regioselectivity of the following rearrangement is determined by the preferred conformation of the newly formed six-membered ring, with the phenyl group positioned equatorially. Migration occurs from the *C*–*C* bond, which is located antiperiplanar to the leaving group. However, the kinetic effects controlling the selective attack of the azide on the activated carbonyl, hence the prediction of the diastereoselectivity are not fully understood.[100] While the presented strategy represents an early example for an asymmetric nitrogen insertion process for cyclic ketones, the reaction of cyclobutanones remains lacking in selectivity.[101]

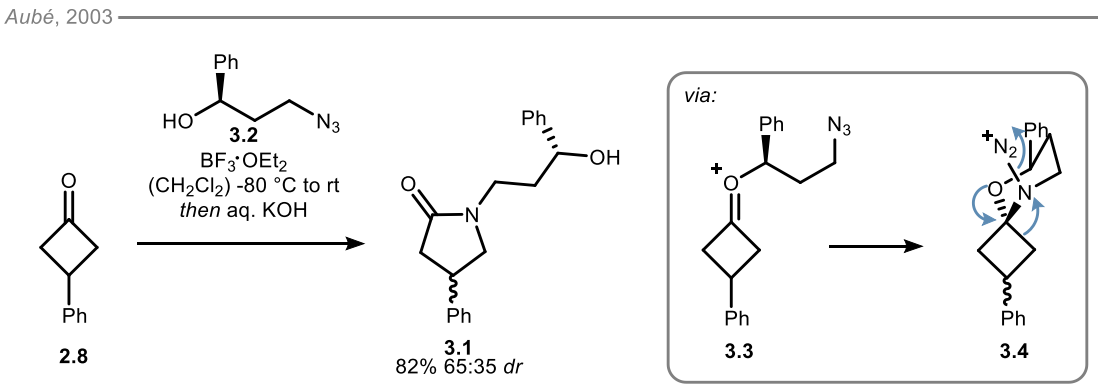

Scheme 21. Synthesis of *N*-alkylated γ-lactam 3.1 *via* asymmetric *Schmidt*-type reaction by *Aubé* and coworkers.[100,101]

An improved strategy that uses an auxiliary as a chiral nitrogen source was published by *Wahl* and coworkers in 2021 (Scheme 22).[102] The reaction provides a highly selective route to *N*-substituted γ-lactams tolerating steric and electronic alterations, versatile functional groups and quaternary all-carbon centres. The mechanism of this process is described through the reaction between (1*S*,2*R*)-1-amino-2-indanol **3.5** and prochiral cyclobutanone **2.8** to form an *N*,*O*-ketal intermediate *via* nucleophilic addition and dehydration. Subsequent halogenation with tichloroisocyanuric acid **3.6** introduces a leaving group at the nitrogen, thus facilitating the rearrangement of intermediate **3.7**. Following the ring-expansion process, a nucleophilic attack by water affords the desired substituted γ-lactam **3.8**. Intermediate **3.7** undergoes an interconversion *via* an iminium species **3.9**, which results in the occurrence of the isomers **3.7** and *epi*-**3.7** in an equilibrium of 49:51 *dr*. Mechanistic studies provide evidence that this transformation operates under a *Curtin–Hammett* scenario. Thus, isomer **3.13** is preferentially formed *via* the favourable transition state with a selectivity of 80:20 *dr*. The separation of the formed diastereoisomers and mild oxidative cleavage with cerium ammonium nitrate (CAN) affords the formation of enantiopure lactam (*S*)-**2.49** by removal of the indanol auxiliary. Nevertheless, the utilisation of auxiliaries demands additional synthetic steps, causes increased waste production, and consequently diminishes overall efficiency. These drawbacks are mitigated by the development of catalytic approaches, which remain a major challenge in the field of asymmetric nitrogen insertion reactions.

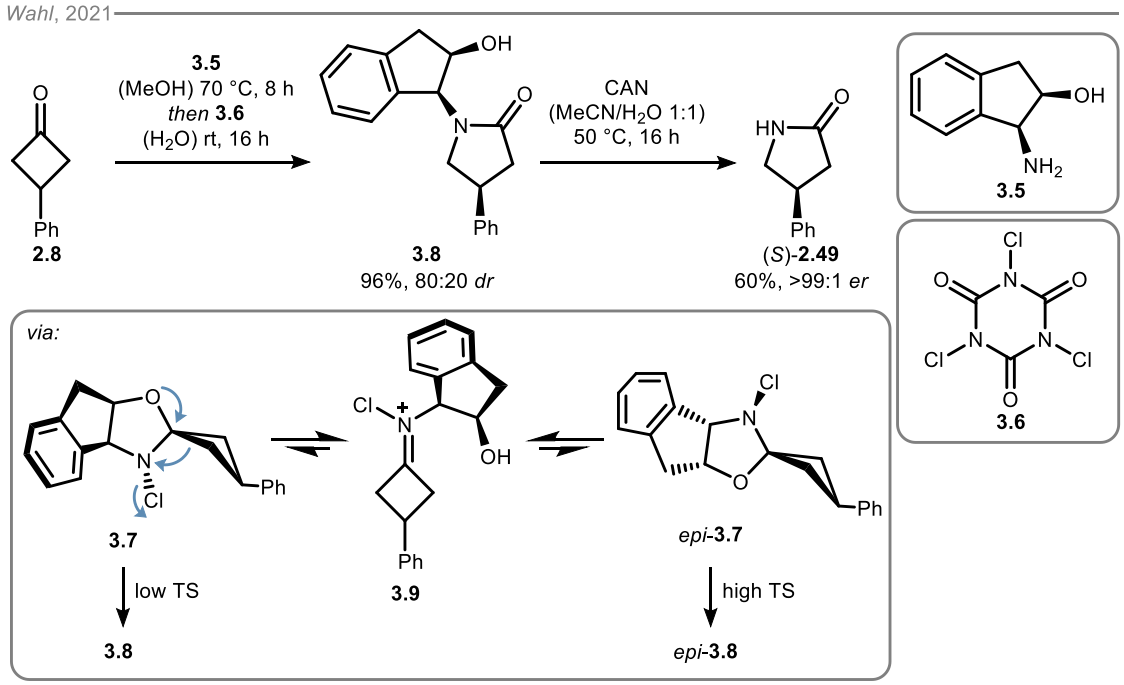

Scheme 22. Synthesis of enantioselective γ-lactams by *Wahl* and coworkers *via* selective nitrogen insertion and cleavage of the auxiliary.[102]

3.1.2 Catalytic nitrogen incorporation

A groundbreaking example of a catalytic asymmetric incorporation of nitrogen into prochiral substrates was described by *Antilla* and coworkers with the formation of axially chiral oxime ether (*R*)-**3.10** (Scheme 23, top).[103] The desymmetrisation of 4-substituted cyclohexanone **3.11** was achieved by asymmetric condensation with *O*-substituted hydroxylamine **3.12** in the presence of the strontium salt of chiral phosphoric acid (*R*)-**3.13**. The products are bearing a stereogenic axis, due to the restricted rotation of the *C–N* double bond formed during the reaction. The fixation of the substituent prevents interconversion of the two possible conformers, leading to the existence of two distinct enantiomers. The axial chirality of the oxime ethers is set by selective interaction of one enantiomer of the tetrahedral intermediate **3.14** with the chiral phosphoric acid (*S*)-**3.13**. A computational study of the desymmetrisation reaction was in excellent agreement with the obtained experimental enantioselectivity. Herein, the dehydration of the intermediate alcohol in presence of the *Brønsted* acid was identified as the stereocontrolling step. Consequently, the mode of stereoinduction was attributed to a complementary shape between the substrate and the chiral binding pocket of the catalyst enabling stabilizing *π–CH* interactions.
While the application of 4-substituted oxime ethers was limited due to missing enantiospecific transformations of the introduced chirality, *He et al.* developed a strategy for the conversion of axially chiral oxime (*R*)-**3.15** in an acid-catalysed *Beckmann* rearrangement towards enantioenriched point chiral nitrogen-containing heterocycles (*S*)-**3.16** (Scheme 23, bottom).[104] The desired oxime (*R*)-**3.15** is derived from anthrone **3.17** *via* asymmetric condensation with *O*-substituted hydroxylamine **3.18** in the presence of chiral phosphoric acid (*R*)-**3.19** and subsequent palladium catalysed deallylation. Thus, the sequence of an enantioselective condensation followed by conversion of axial-to-point chirality through a *Beckmann* rearrangement offers a new approach for the synthesis of chiral lactam-structures. Nevertheless, the strategy requires a multistep protocol and is confined to anthrone structures, thereby restricting its applicability.

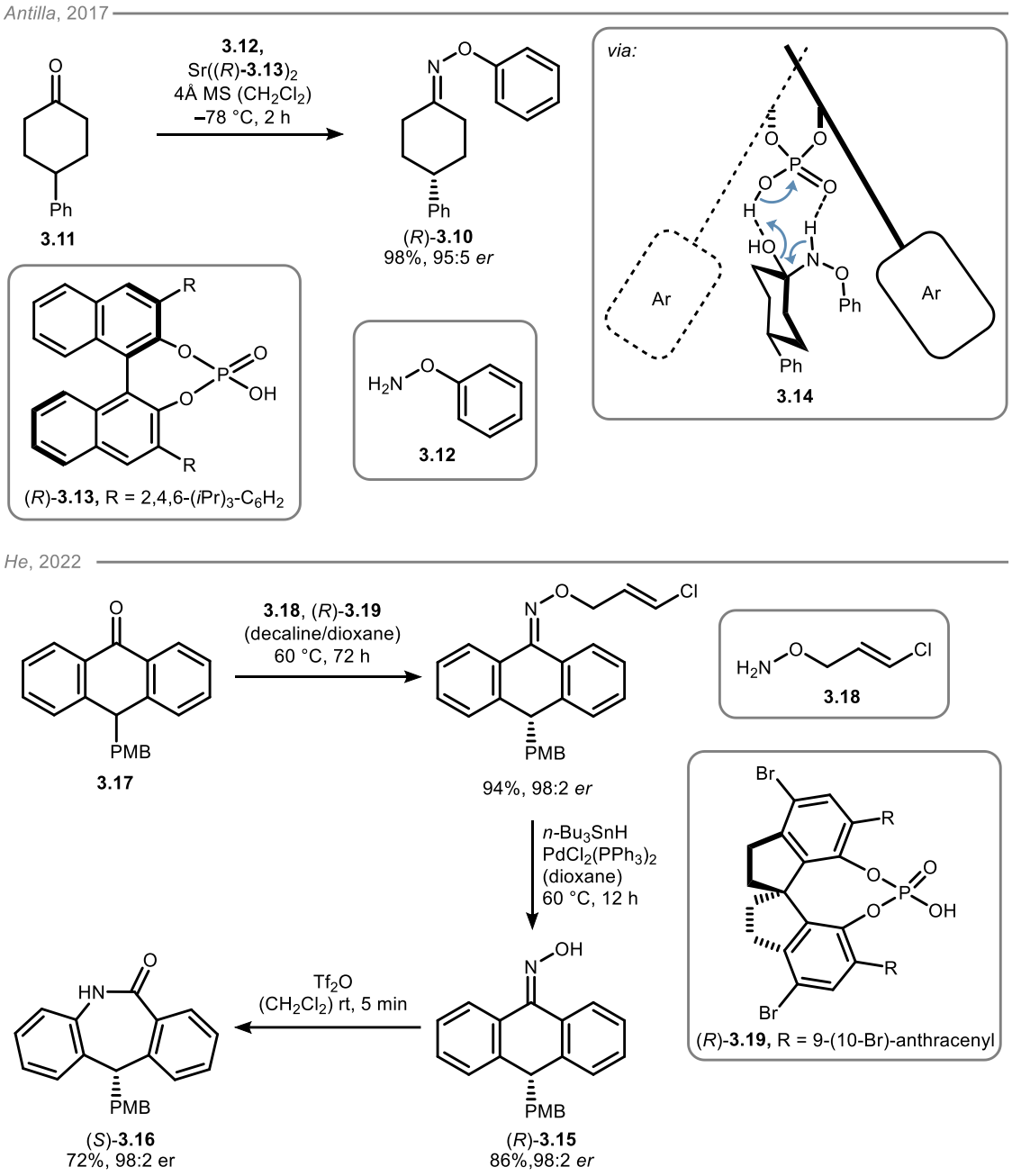

Scheme 23. Top: Asymmetric condensation of cyclohexanones with *O*-substituted hydroxylamines catalysed by chiral phosphoric acid by *Antilla* and coworkers.[103] Bottom: Enantioselective synthesis of lactams *via* enantioselective condensation, oxime ether cleavage and Beckmann rearrangement by *He et al.*[104] PMB = *p*-methoxybenzyl.

3.1.3 Motivation and aim

The development of efficient and enantioselective methodologies of nitrogen insertion reactions *via* desymmetrisation of cyclobutanones continues to be a major challenge. While various catalytic protocols are available for the *Baeyer-Villiger* oxidation of prochiral cyclobutanones, nitrogen insertion strategies are limited to the use of chiral reagents or auxiliaries. Therefore, the present study sets out to investigate the development of an efficient catalytic nitrogen insertion reaction, building on the analogies between the previously presented aza-*Baeyer-Villiger* rearrangement and the corresponding oxygen insertion reaction. Inspired by the implemented catalytic systems for enantioselective *Baeyer-Villiger* oxidation, a suitable catalyst was sought to be identified for the reaction of 3-substituted cyclobutanones **2.22** with hydroxylamine **2.51**.[99] Hence, a selective rearrangement towards enantioenriched γ-lactams **2.22** is envisaged through the interaction of a catalyst with the tetrahedral intermediate **3.20** (Scheme 24). For the optimisation of a reaction protocol, various organocatalysts were investigated, focussing on chiral phosphoric acids, due to their facile structural adaptability.[105]

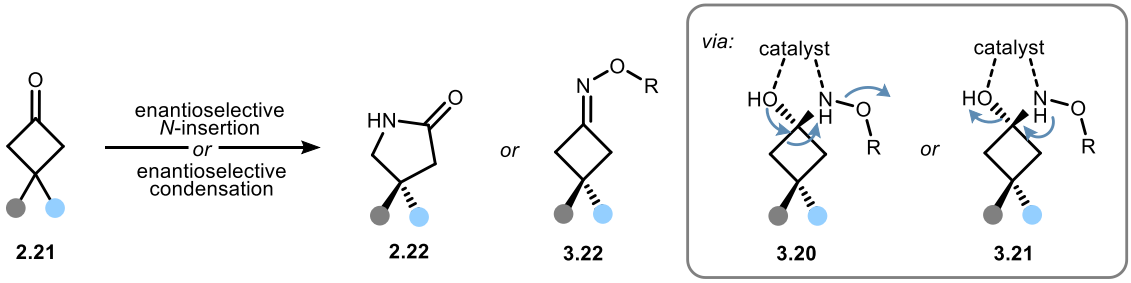

Scheme 24. Catalytic asymmetric *N*-incorporation by selective rearrangement or condensantion *via* transition states 3.20 or 3.21.

As outlined above, chiral phosphoric acids are known to accelerate enantioselective condensation of hydroxylamines with cyclohexanone derivatives to generate axially chiral oxime ethers.[103,104] Formation of structurally comparable cyclobutanone oxime esters was observed as side products of the aza-*Baeyer-Villiger* reaction (*cf.* chapter 2.3). Enantioselective condensation *via* transition state **3.21** is achieving asymmetric condensation towards enantioenriched cyclobutanone oxime esters **3.22**. The enantioselective synthesis of the axially chiral four-membered compounds remains unexplored, although their reactivity allows for the development of versatile transformations (*vide infra*, *cf.* chapter 4). Therefore, the formation of both chiral γ-lactams **2.22** and cyclobutanone oxime esters **3.22** will be considered during the initial optimisation. The influence of different organocatalysts and amine reagents on the reactions outcome will be investigated. Furthermore, mechanistic studies will be presented to shine light on the synergy between enantioselective nitrogen insertion and condensation process. Based on these results, the scope for the developed methodology is envisaged to be investigated including substrates with versatile substitution pattern and ring sizes.

3.2 Synthesis of starting materials

As described above, the influence of various amine reagents was sought to be investigated over the course of this study. Therefore, versatile *O*-substituted hydroxylamines with similar structural properties to amine reagent **2.51** were synthesised. During this investigation, a degradation of deprotected hydroxylamines became evident, even when stored –20 °C. Therefore, the amine reagents were prepared immediately before use from the bench stable hydroxylamines substituted with a *tert*-butyloxycarbonyl (Boc) group. The Boc-protected hydroxylamines were synthesised from the corresponding phosphinic acids. Synthesis of the phosphinic acids **3.23** to **3.25** was conducted *via* nucleophilic substitution of the corresponding Grignard reagent to diethoxyphosphite and subsequent oxidation with sodium hydroxide and hydrogen peroxide (Scheme 25). The corresponding products **3.23** to were obtained in moderate to good yields adapting literature known procedures.[106]

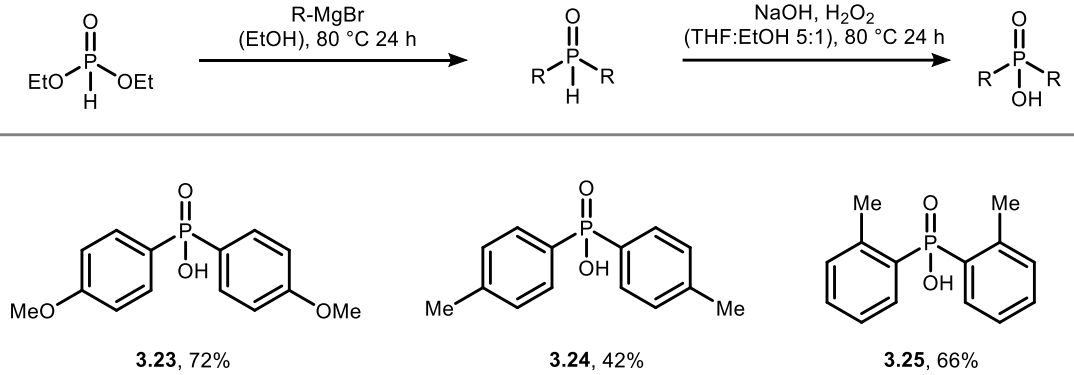

Scheme 25. Preparation of phosphinic acids 3.23 to 3.25.

O-Phosphinyl substituted hydroxylamines **3.26** and **3.27** were prepared from the corresponding phosphinic acids **3.23** and **3.24** following the typical synthetic route *via* formation of the Boc-protected hydroxylamines and deprotection (Scheme 26, top).[107,108] The Boc-protected hydroxylamines were obtained *via* phosphoroxy chloride formation and subsequent nucleophilic substitution with *N*-Boc-hydroxylamine. According to a literature known protocol,[108] Boc-deprotection with trifluoroacetic acid (TFA) in dichloromethane (CH_2Cl_2) enabled the formation of the free hydroxylamines **3.26** to **3.27** in good yields.
Since the formation of Boc-protected hydroxylamine **3.28** from phosphinic acid **3.25** was not possible following the route presented above, the synthesis of amine reagent **3.29** was achieved *via* active ester coupling with *N*,*N*'-dicyclohexalcarbodiimide (DCC) and *N*-Boc-hydroxylamine and subsequent deprotection with TFA (Scheme 26, bottom).

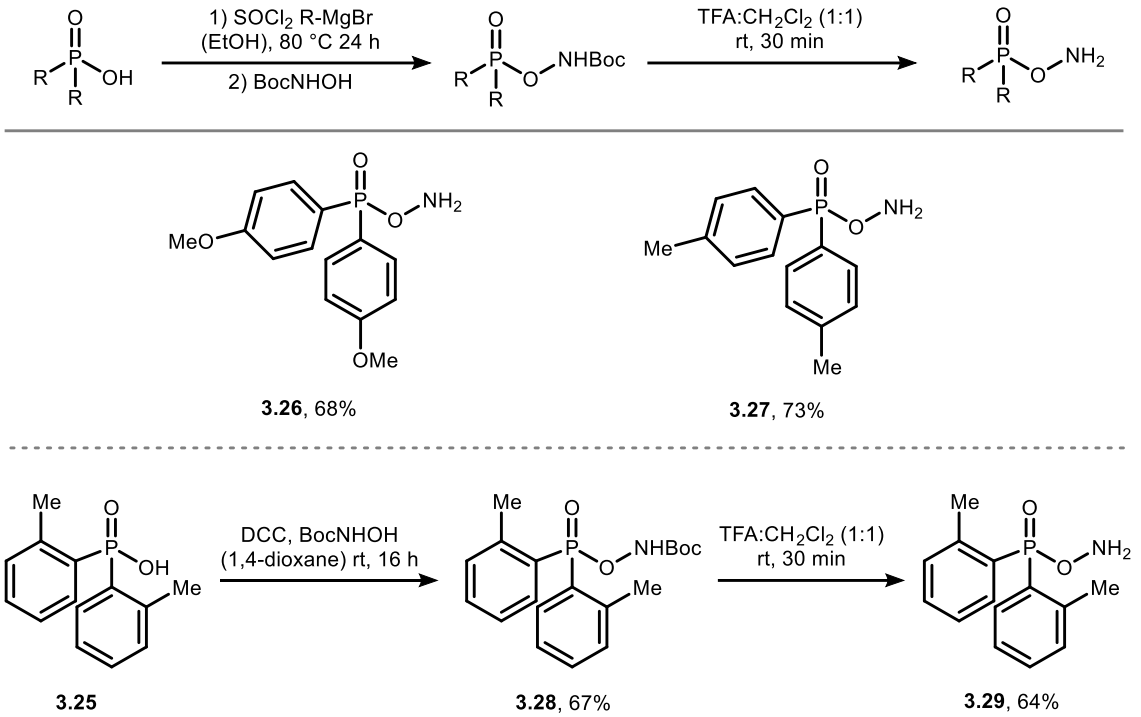

Scheme 26. Top: Preparation of phosphinyl hydroxylamines 3.26 and 3.27. Bottom: Preparation of phosphinyl hydroxylamine 3.29.

3.3 Development of reaction conditions

3.3.1 Initial results

The preliminary results regarding an asymmetric nitrogen insertion protocol were gathered in collaboration with [redacted], who was engaged in the development of a protocol employing *Lewis* acids with chiral ligands. These outcomes constitute part of his own work and are therefore not included in the results of this optimisation.[92] Reactions performed by [redacted] that are pivotal to this work are indicated as such. In view of the results from the aforementioned study about the aza-*Baeyer-Villiger* reaction (*cf.* chapter 2.2), prochiral cyclobutanone **2.8** and amine reagent **2.51** were selected as model substrates for the ensuing study. Starting the development of a catalytic asymmetric nitrogen incorporation strategy, the application of various chiral organocatalysts was investigated (Table 4). Over the course of the uncatalyzed rearrangement between cyclobutanone **2.8** and amine reagent **2.51**, equimolar amounts of phosphinic acid **3.30** are formed as the leaving group (Scheme 27). Recent DFT calculations have suggested the participate in the formation γ-lactam **2.49**.[109]

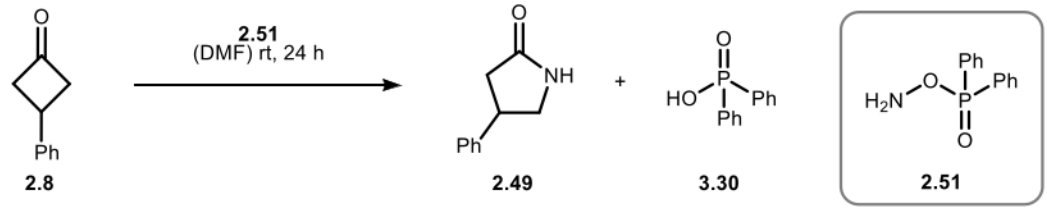

Scheme 27. Aza-*Baeyer-Villiger* reaction of 3-phenylcyclobutanone 2.8 with formation of γ-lactam 2.49 and phosphinic acid 3.30.

Hence, the use of related C2-symmetric and therefore chiral phosphinic acid **3.31** with similar acidity was probed for catalytic activity in an asymmetric nitrogen insertion approach. However, *Brønsted* acid **3.31** demonstrated no significant stereoinduction, with the formation of γ-lactam **2.49** in 84% yield and an enantiomeric ratio of 48:52 *er* (entry 1). Highly selective asymmetric *Baeyer-Villiger* oxidation can be performed with chiral phosphoric acids.[99] For this reason, *Brønsted* acid (*S*)-**3.13** was estimated to be a potential catalyst for the nitrogen insertion reaction in analogy. The reaction between cyclobutanone **2.8** with amine reagent **2.51** in presence of catalytic amounts of (*S*)-**3.13** was conducted by [redacted]. Interestingly, the oxime ester **3.32** was formed in 91% yield with an enantiomeric ratio of 73:27 *er*, whereas the desired γ-lactam **2.49** was obtained with 7% yield and a selectivity of 58:42 *er* (entry 2). The shift in product selectivity indicates, that while the phosphoric acid effectively catalyses the asymmetric condensation process, the majority of the lactam is formed by a racemic background reaction. As *Brønsted* acids **3.31** and **3.13** showed limited catalytic activity towards the anticipated γ-lactam formation, the investigation turned to chiral amine **3.33**. The desired lactam **2.49** was successfully formed, but it was

obtained virtually in a racemic fashion with an enantiomeric ratio of 51:49 *er* (entry 3). These preliminary results indicate that the development of a catalytic nitrogen incorporation reaction by rearrangement is challenging due to the stoichiometric formation of phosphinic acid **3.30** and the properties of prevalent catalysts. Nevertheless, the unexpected shift of the reaction outcome towards an asymmetric condensation in the presence of phosphoric acid (*S*)-**3.13** prompted for further investigation of this transformation.

Table 4. Initial results of an asymmetric *N*-incorporation reaction, reactions were carried out on a 0.05 mmol scale, yield based on ^{1}H NMR experiments using CH_2Br_2 as an internal standard, *er* determined by chiral HPLC analysis.

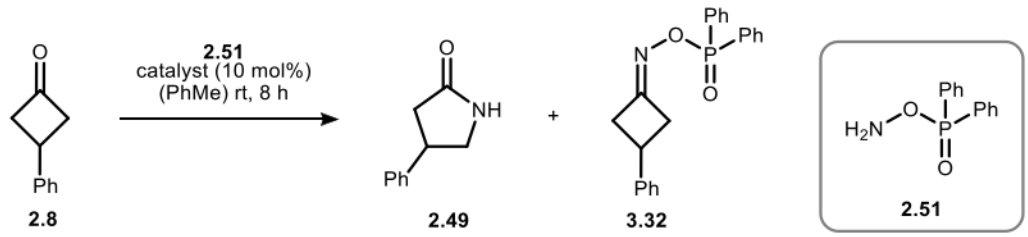

entry	catalyst	yield **2.49**	er **2.49**	yield **3.32**	er **3.32**
1	**3.31**	84%	48:52	16%	-
2[a]	(*S*)-**3.13**	7%	58:42	91%	73:27
3	**3.33**[b]	59%	51:49	-	-

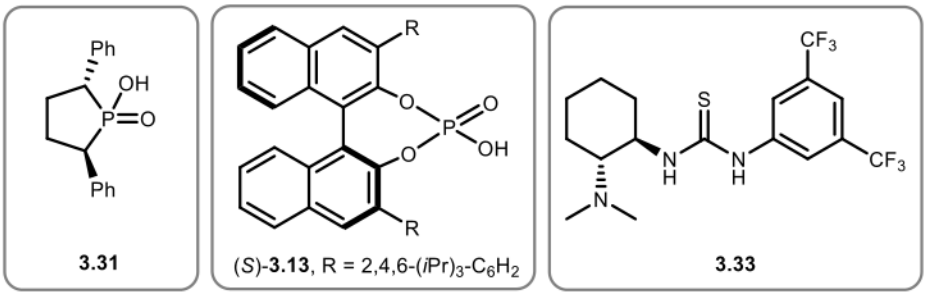

[a] reaction was performed by [redacted] [b] compound was prepared by [redacted].

3.3.2 Optimisation of the reaction conditions

Similar to cyclohexanone oxime ethers,[103] the chirality of the cyclobutanone oxime esters arises from the restricted rotation of the *C–N* double bond formed during the condensation process, thus classifying them as axially chiral compounds. Although the condensation of the tetrahedral intermediate **2.50** is an undesired side reaction in the racemic aza-*Baeyer-Villiger* reaction (*cf.* chapter 2.3), enantioselective formation of the axially chiral compounds offers novel synthetic potential by application in chirality transfer reactions (*vide infra*, chapter 4). Methodologies for the asymmetric condensation between cyclobutanones and hydroxylamine derivatives are still unexplored. Therefore, the results from the preliminary experiments were used as the basis for an optimisation towards the improvement of the stereoselective condensation process. The yields of the reactions were analysed by quantitative ^{1}H NMR techniques using CH_2Br_2 as internal standard and the enantiomeric ratios were determined after separation by chiral HPLC

analysis. Firstly, the role of different additives was investigated (Table 5). Noteworthy, the reaction between cyclobutanone **2.8** and hydroxylamine **2.51** in toluene without any additive gave the oxime ester **3.32** in 13% yield, with the corresponding γ-lactam **2.49** being the major product (entry 1). Addition of 4 Å molecular sieves (MS) had a negligible effect on the formation of oxime ester **3.32** (entry 2). Indicated by the preliminary results, significant change in the reactions outcome was achieved by employing racemic and chiral phosphoric acids **3.34** and **3.13** (entry 3 & 4). A negative impact of the formation of side products, namely water and phosphinic acid, was excluded by the addition of 4 Å MS and phosphinic acid **3.30** in presence of catalyst **3.13** (entry 5 & 6).

Table 5. Initial optimisation with screening for additives. Reactions were carried out on a 0.05 mmol scale in 1.0 mL solvent, yield based on ^{1}H NMR experiments using CH_2Br_2 as an internal standard, *er* determined by chiral HPLC analysis.

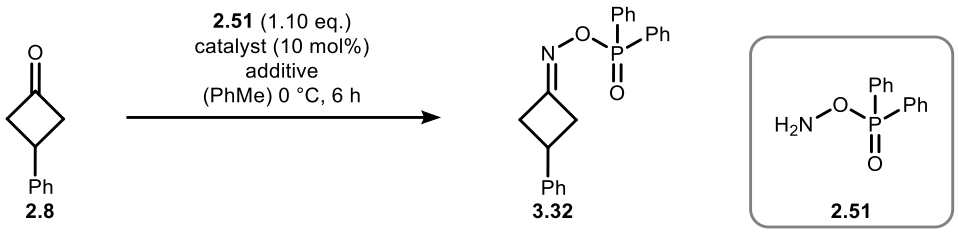

entry	catalyst	additives	yield **3.32**	*er*
1	-	-	13%	-
2	-	4 Å MS	25%	-
3	**3.34**	-	75%	-
4	(*S*)-**3.13**	-	78%	15:85
5	(*S*)-**3.13**	4 Å MS	74%	15:85
6	(*S*)-**3.13**	**3.30**	69%	16:84

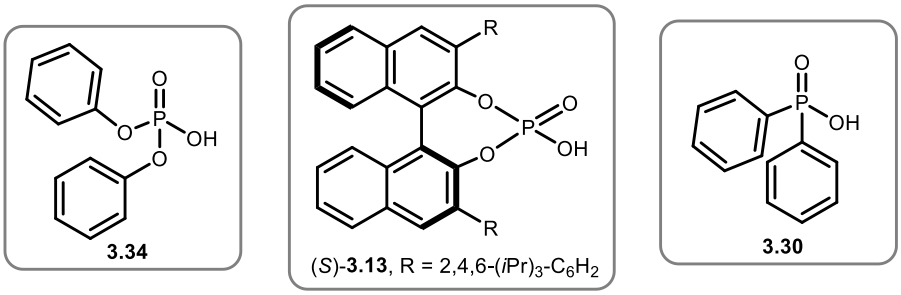

Subsequently, various amine reagents were employed to identify the best hydroxylamine for the desired condensation in presence of chiral phosphoric acid (*S*)-**3.13** (Table 6). The initial part of that investigation was conducted in CH_2Cl_2. Compared to the results obtained with amine reagent **2.51**, utilisation of commercially available hydroxylamine **3.35** and **2.52** afforded the corresponding oxime derivatives in high yields but reduced enantioselectivities (entries 1 – 3). During the previous study about the development of an aza-*Baeyer-Villiger* reaction the strength of leaving group was deemed to be crucial to enable nitrogen insertion reaction (*cf.* chapter 2.3). When hydroxylamines with low leaving group stability were used in the reaction with cyclobutanone **2.8**, oxime derivatives **2.53** were obtained as side products. Therefore, it was assumed that a stronger leaving group is key for successful enantioinduction in a catalytic condensation process, due to an otherwise uncatalyzed background formation of the oxime derivatives. In contrast, *O*-sulfonyl substituted hydroxylamine **1.13** is characterised by an increased reactivity in nitrogen insertion reactions. Reaction of amine **1.13** resulted in the absence of oxime ester formation (entry 4). Consequently, *O*-phosphinyl-substituted hydroxylamines involving electronic and steric alterations were subject of subsequent investigations. During the study, significant improvements of the stereocontrol were achieved by solvent change (entry 5), the following investigation was thus performed in toluene. Changes in the electronic properties of the hydroxylamine **3.26** and **3.27** had minor influences on the reactivity, while resulting in slightly reduced enantioselectivities of the oxime esters formed (entries 6 and 7). Conversely, the reaction was found to be inhibited with the more sterically demanding amine reagent **3.29** (entry 7). In addition to the experiments presented herein, [redacted] contributed to the identification of a suitable amine reagent for oxime ester formation as part of a research internship. A detailed investigation on the synthesis and employment of aminobenzoates and their corresponding salts is found in her own work.[110] As these results do not influence the further course of the project, they will not be discussed at this point.

Table 6. Hydroxylamine reagent optimisation, reactions were carried out on a 0.05 mmol scale, yield based on ^{1}H NMR experiments using CH_2Br_2 as an internal standard, *er* determined by chiral HPLC analysis.

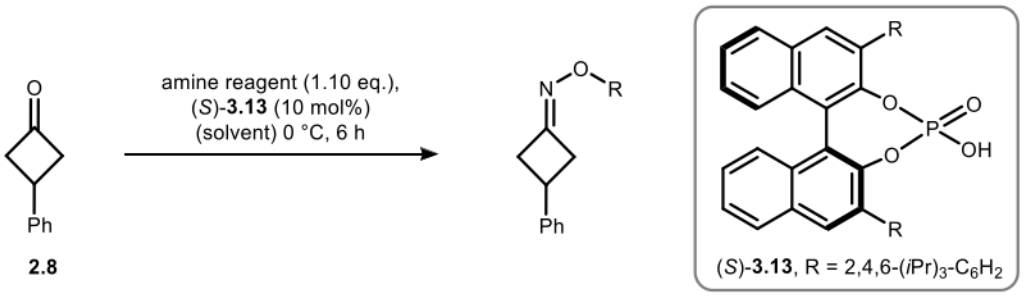

entry	amine reagent	solvent	yield oxime	er
1	**2.51**	CH_2Cl_2	82%	20:80
2	**3.35**	CH_2Cl_2	90%	32:68
3	**2.52**	CH_2Cl_2	94%	59:41
4	**1.13**[a]	CH_2Cl_2	0%	-
5	**2.51**	PhMe	78%	15:85
6	**3.26**	PhMe	77%	19:81
7	**3.27**	PhMe	96%	17:83
8	**3.29**	PhMe	0	-

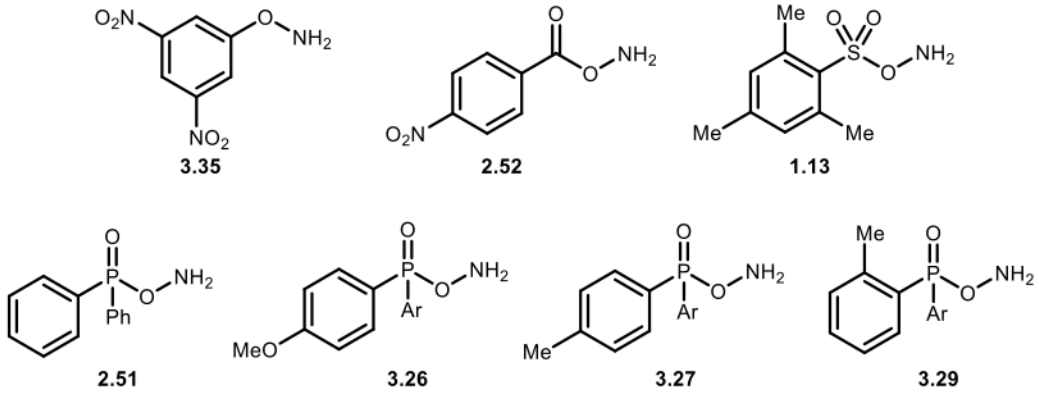

[a] compound was prepared by [redacted]

In the following, the reaction was performed in a set of different solvents, to illustrate the influence of solvent polarity. Therefore, the polarity was altered systematically to cover the whole range from polar protic to apolar aprotic solvents (Table 7). Examining the reaction in protic or polar solvents exerted a considerably deleterious effect on the reaction process (entries 1 and 2). On the other hand, an enhancement in stereoselectivity was observed when less polar solvents were employed (entries 3 – 6). Here, a reduced reaction rate was observed for the use of *n*-hexane due to the low solubility of the reagents (entry 7). Therefore, best results were obtained performing the asymmetric condensation in toluene (entry 6). In consideration with earlier studies about the asymmetric formation of cyclohexanone oxime ethers by *Nimmagadda et al.*[103] (*cf.* chapter 3.1.1), these observations gave first insights about the reaction mechanism. The stereoselectivity of the process is assumed to be derived from *H*-bonding interaction between the tetrahedral intermediate **2.50** and the catalyst in the transition state (*vide infra*,

cf. chapter 3.4). The effect that occurs is clearly illustrated by the employment of polar protic solvents. Utilisation of methanol is going along with a poor enantioinduction, resulting from competing *H*-bonding interactions with the solvent, which weakens the interaction with the catalyst.

Table 7. Solvent and concentration optimisation, reactions were carried out on a 0.05 mmol scale, yield based on ^{1}H NMR experiments using CH_2Br_2 as an internal standard, *er* determined by chiral HPLC analysis.

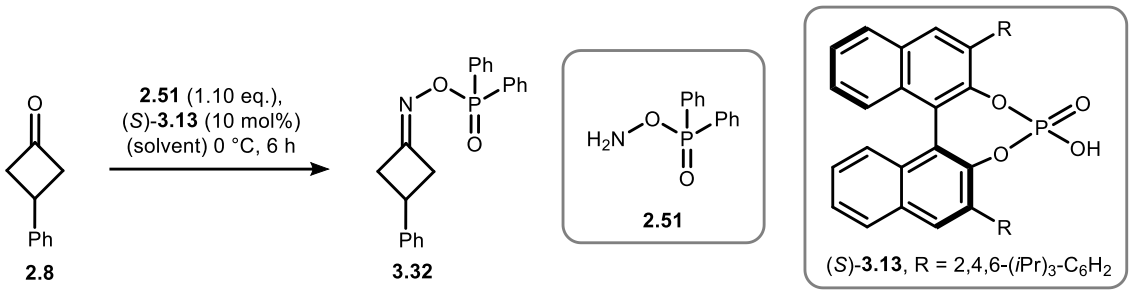

entry	solvent	yield **3.32**	er
1	MeOH	61%	45:55
2	MeCN	90%	39:61
3	THF	85%	30:70
4	CH_2Cl_2	82%	20:80
5	$PhCF_3$	35%	13:87
6	PhMe	78%	15:85
7	*n*-hexane	44%	13:87

Following the identification of the optimal solvent, utilisation of various chiral phosphoric acids were systematically investigated as potential catalysts (Table 8). Depending on availability, catalysts were used either in (*S*)- or (*R*)-configuration, accordingly the formation of the major enantiomer is inverted. Based on the studies regarding the enantioselective condensation of cyclohexanones with hydroxylamines by *Nimmagadda et al.*,[103] the impact of magnesium *tert*-butanolate and the magnesium salt of (*S*)-**3.13** was studied. While effective in the literature-known protocol, utilisation of the salts was not beneficial for the condensation of cyclobutanone **2.8** with hydroxylamine **2.51** (entries 1 – 3). Alteration of the chiral phosphoric acid's backbone by using catalyst (*R*)-**3.36** gave the product **3.32** with a consistent selectivity of 84:16 *er*, but reduced yield of 67% compared to the application of (*S*)-**3.13**. The substituents in 3,3'-positions of the BINOL backbone define the environment of the catalytic centre. Thus, catalysts with differing substitutions (**3.37** to **3.40**) were investigated (entries 4 – 8). As a result, it was found that both, steric and electronic alterations possess a substantial impact on the reactivity and selectivity of the reaction, giving oxime ester **3.32** in a range of 37% to 96% yield with selectivity of 30:70 to 91:9 *er*. (2,4,6-Tricyclohexylphenyl)-substituted catalyst (*R*)-**3.40** was identified to give the most favourable outcome in terms of reactivity and enantioselectivity (entry 8).

Table 8. Catalyst and additive optimisation, reactions were carried out on a 0.05 mmol scale, yield based on ^{1}H NMR experiments using CH_2Br_2 as an internal standard, *er* determined by chiral HPLC analysis.

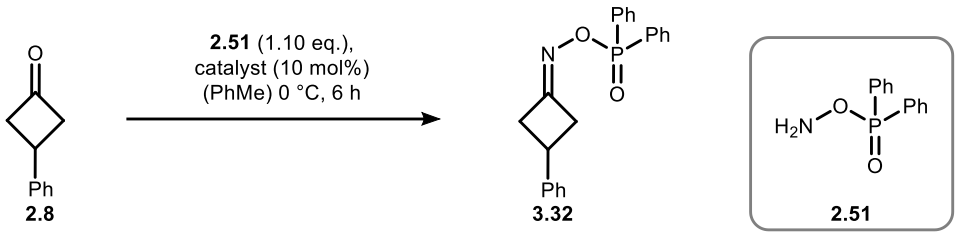

entry	*Brønsted* acid	yield 3.32	*er*
1	(*S*)-**3.13**	78%	15:85
2	$Mg(OtBu)_2$	8%	-
3	$Mg((S)\text{-}\mathbf{3.13})_2$	48%	18:82
4	(*R*)-**3.36**	67%	84:16
5	(S)-**3.37**	25%	27:73
6	(S)-**3.38**	96%	30:70
7	(S)-**3.39**	37%	35:65
8	(*R*)-**3.40**	72%	91:9

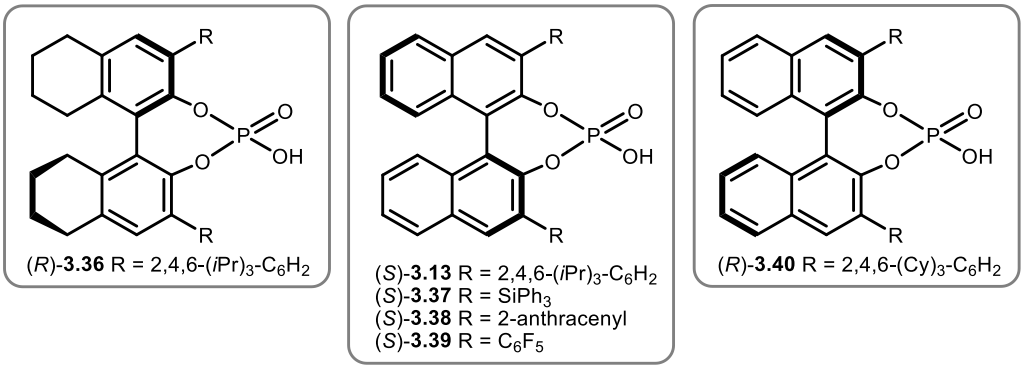

Concluding the optimisation, the reaction with the best performing catalyst (*R*)-**3.40** was exposed to different temperatures. While effectively increasing the enantioselectivity, a significantly reduced reaction rate was observed at temperatures below –20 °C. Consequently, the subsequent exploration of the substrate scope was conducted at –20 °C with a reaction time of 24 hours.

Table 9. Temperature optimisation, reactions were carried out on a 0.05 mmol scale, yield based on ^{1}H NMR experiments using CH_2Br_2 as an internal standard, *er* determined by chiral HPLC analysis.

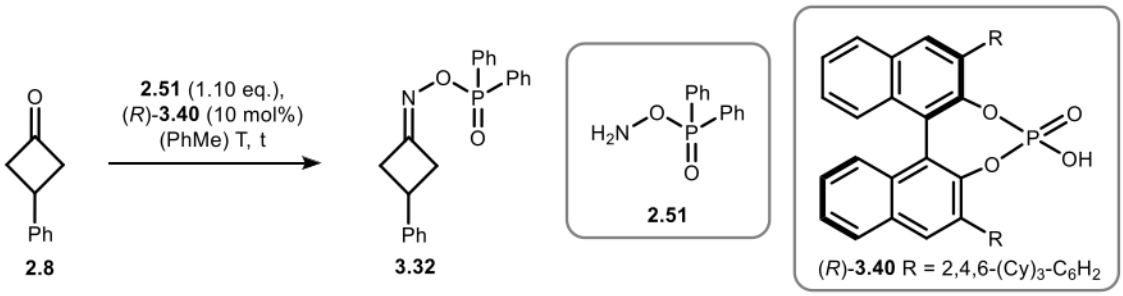

entry	temperature	time	yield 3.32	*er*
1	0 °C	6 h	72 %	91:9
2	–20 °C	24 h	70%	95:5
3	–33 °C	24 h	35%	97:3

3.4 Mechanistic studies and absolute configuration

In order to investigate the reaction mechanism and to determine the absolute configuration of the axially chiral oxime esters, density functional theory (DFT) calculations were performed by [redacted]. Catalyst (*S*)-**3.40** was used for the calculations and four different isomers were considered for all steps of the reaction process forming two distinct enantiomers. In the following, a concise summary of these results is provided, thus offering valuable insights into the reaction process, which are pivotal for the progress of this work. For better understanding, only the most favourable pathways leading to each enantiomer are depicted, while all four transition states are shown for the stereo determining step (Scheme 28). The stepwise mechanism consists of the complexation of the chiral phosphoric acid (*S*)-**3.40** to cyclobutanone **2.8** and amine reagent **2.51**, with the formation of the tetrahedral intermediate **INT1**. Condensation of the intermediate results in the generation of the *C–N* double bond and cyclobutanone oxime ester **2.8** is released after decomplexation. The study revealed that the phosphoric acid is catalysing both the water extrusion and the addition of the hydroxylamine to the ketone. Nevertheless, the first step is reversible and therefore the formation of the tetrahedral intermediate **INT1** is not specific. The stereoselectivity is determined by water extrusion proceeding preferentially *via* transition state **TS2a**, due to the lower energy of at least 2.4 kcal/mol compared to the other three stereochemically distinct transition states **TS2b** to **TS2d** (Scheme 28, bottom). As a result, oxime ester (*S*)-**3.32** is formed as major enantiomer.

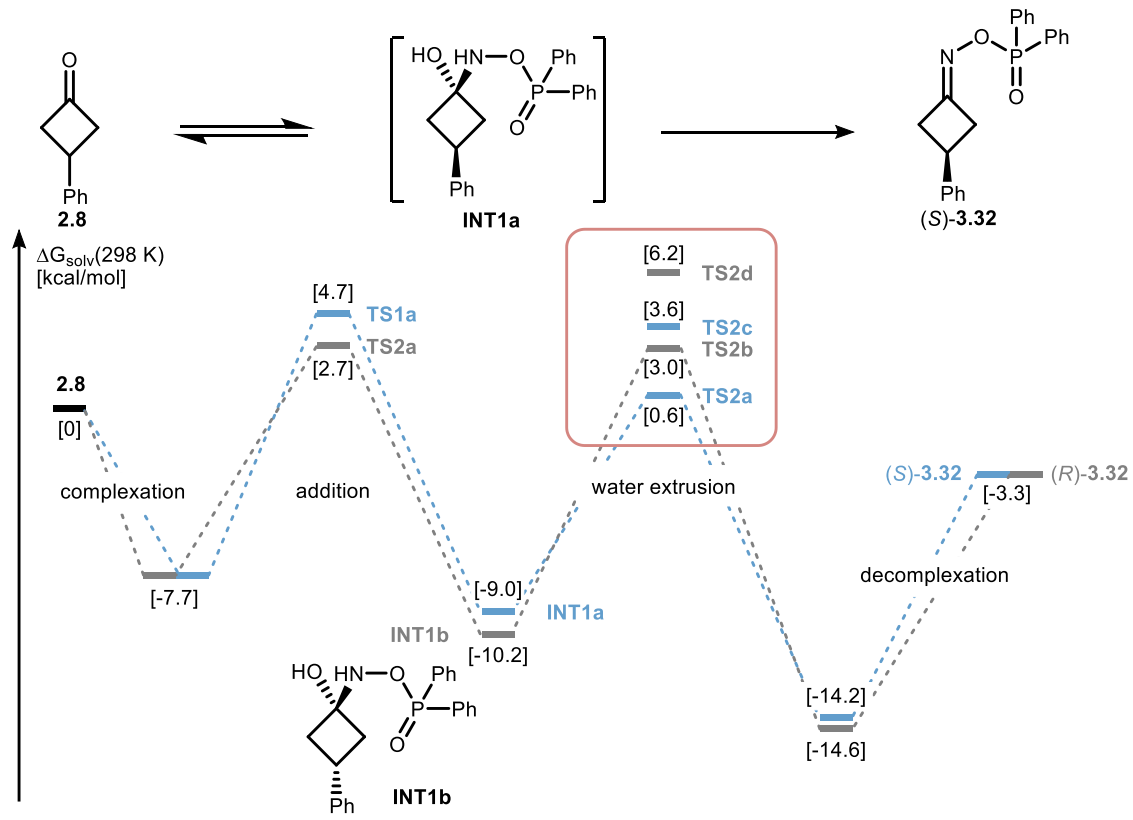

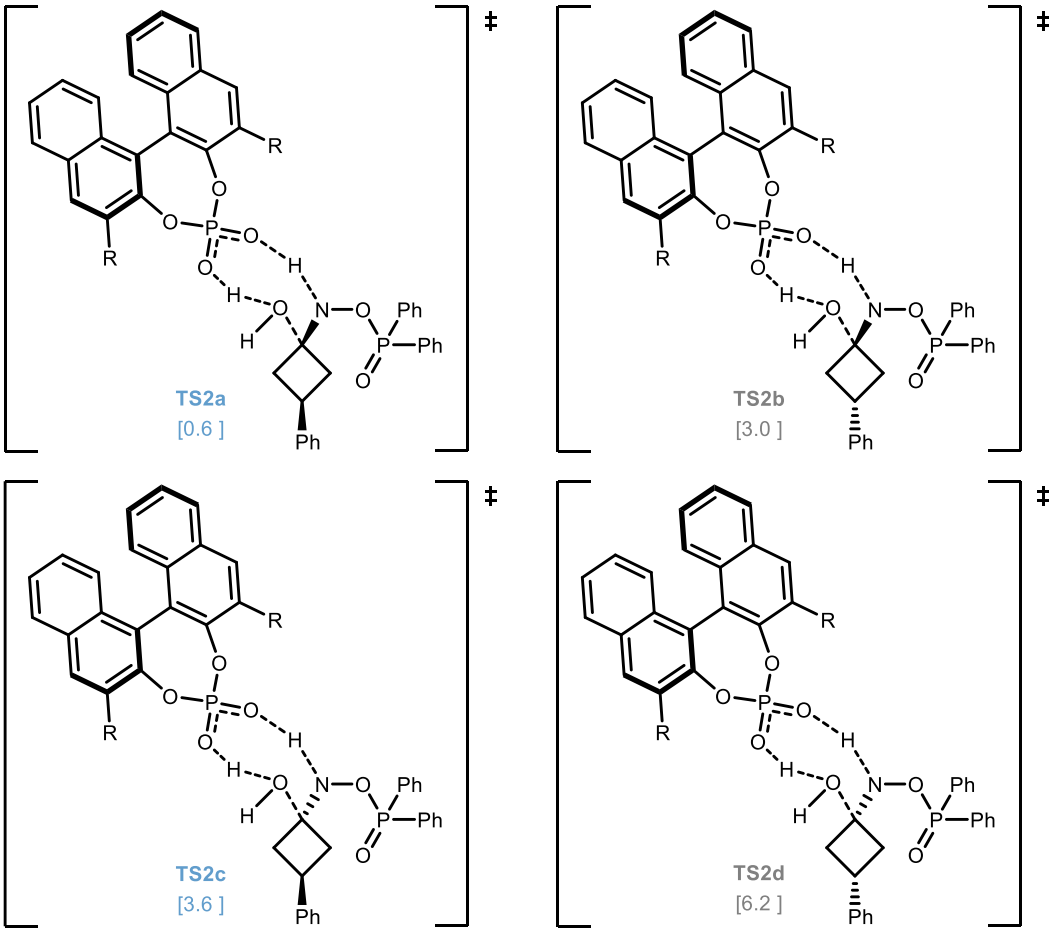

Scheme 28. R = 2,4,6-(Cy)$_3$-C$_6$H$_2$. Top: Energy profile for the most favourable pathway towards (*S*)-3.32 (blue) and (*R*)-3.32 (grey). Bottom: All four transition states for the stereodetermining condensation step.

The absolute configuration was confirmed by the synthesis of cyclobutanone oxime esters **3.41** and **3.42** using the corresponding enantiomer of the chiral phosphoric acid. X-ray diffraction proofed the formation of (*R*)-configured oxime esters as major products by employment of *Brønsted* acid (*R*)-**3.40**.

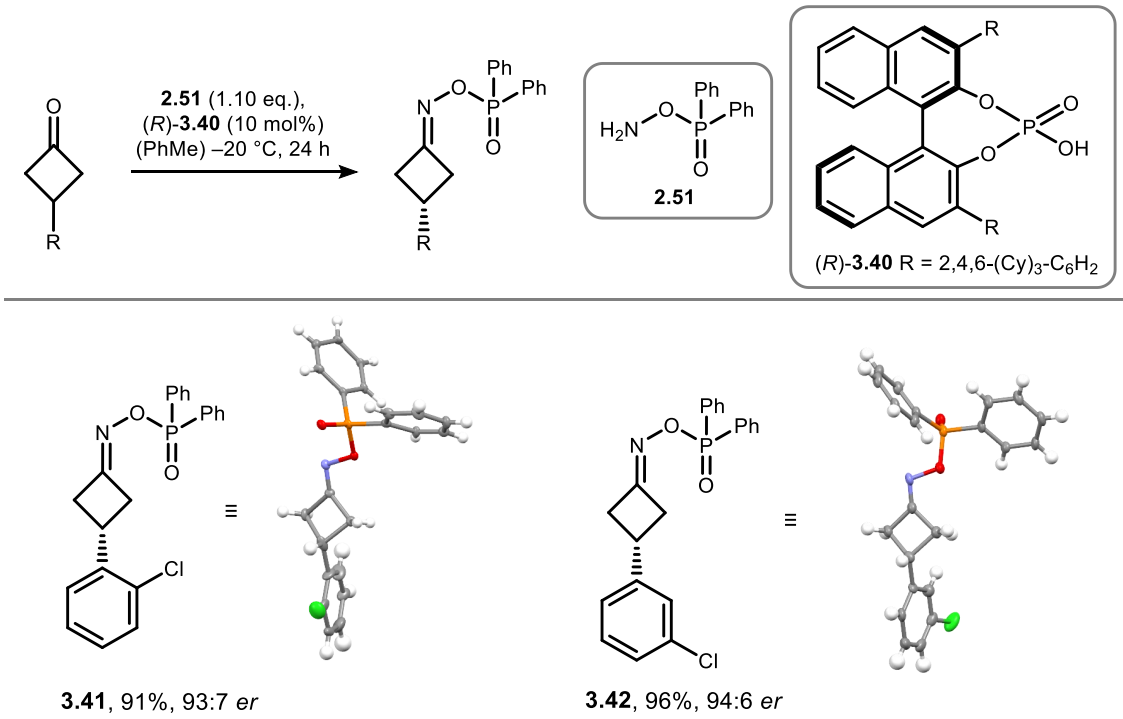

Scheme 29. Determination of the absolute configuration of oxime esters 3.41 and 3.42 *via* X-ray diffraction, thermal ellipsoids are depicted at 20% probability.

3.5 Scope

With the optimised reaction conditions and the insights from the mechanistic investigation at hand, the scope of the asymmetric condensation was explored. If not stated otherwise, the transformations were conducted on a 0.2 mmol scale using *Brønsted* acid (*R*)-**3.40** as catalyst in toluene. The synthetic applicability of the developed method was demonstrated by upscaling of the reaction with substrate **2.8** used during the optimisation process (Scheme 30). Performing the asymmetric condensation on a 1.0 mmol scale allowed for the synthesis of oxime ester (*R*)-**3.32** without the loss of reactivity and selectivity. With the increased reaction scale, a purification and recovery of the catalyst was possible. After acidic extraction and recrystallisation, reuse of the recovered catalyst without reduction in catalytic activity was feasible for the transformation of cyclobutanone **2.8** on standard reaction scale.

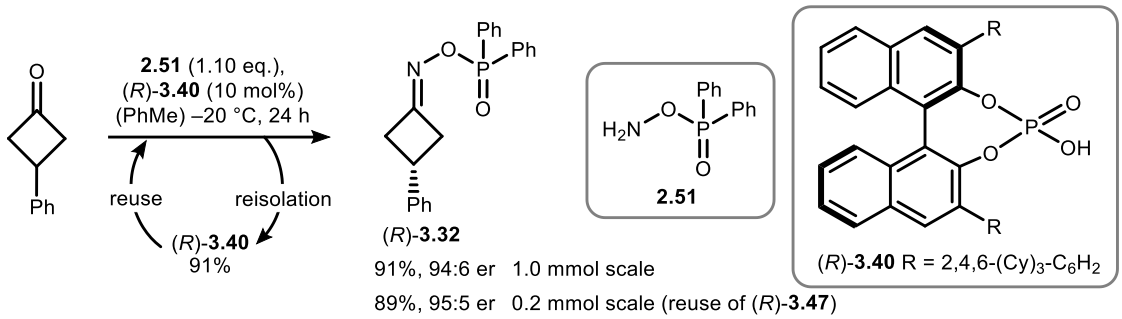

Scheme 30. Upscaling of the asymmetric condensation on a 1.0 mmol scale with reisolation of the catalyst. Reuse of the catalyst was performed on a 0.2 mmol scale.

To explore the scope and limitations of the asymmetric condensation, a series of electronically and sterically differing 3-substituted cyclobutanones were treated with amine reagent **2.51** in the presence of chiral phosphoric acid (*R*)-**3.40** in toluene (Scheme 31). For identification of conditions for chiral HPLC analysis racemic oxime esters were prepared by reaction of the corresponding cyclobutanone and hydroxylamine **2.51** in presence of diphenyl phosphate. First aromatic substituents on the cyclobutanone were investigated. Whilst altering the *para*-position of the aromatic ring, slightly reduced selectivity for oxime esters with electron withdrawing groups like halogen atoms ((*R*)-**3.43** to (*R*)-**3.45**) and trifluoromethyl ((*R*)-**3.46**) was observed. Increase of the electron density of the cyclobutanone resulted in the formation of the corresponding oxime esters (*R*)-**3.47** and (*R*)-**3.48** with good yields and a stereoselectivity of 91:9 *er*. Furthermore, the stereoinduction of the reaction was mostly unaffected by steric perturbations on the aromatic ring, giving oxime esters (*R*)-**3.49** to (*R*)-**3.51** in excellent enantioselectivities with good yields. Interestingly, alkyl substituents at the cyclobutanone were tolerated without a significant loss of selectivity and moderate reactivity (entries (*R*)-**3.52** to (*R*)-**3.54**). However, the introduction of sterically bulkier alkyl substituents resulted in a decline in enantioselectivity. Sterically challenging 3,3-disubstituted oxime esters (*R*)-**3.55** and (*R*)-**3.56** were obtained with diminished results of 65:35 *er* and 57% and 51% yield, respectively. While synthesis of protected alcohol (*R*)-**3.57** could be afforded with moderate enantioselectivity, other functional groups, such as protected hydroxyl or carboxyl, directly attached to cyclobutanones were significantly less well tolerated (entries (*R*)-**3.58** and (*R*)-**3.59**). The observed compatibility of aromatic and alkyl substituents, in combination with the decline in electronic susceptibility leads to the assumption, that *π–π* and *π–CH* interactions are requisite for high selectivity.

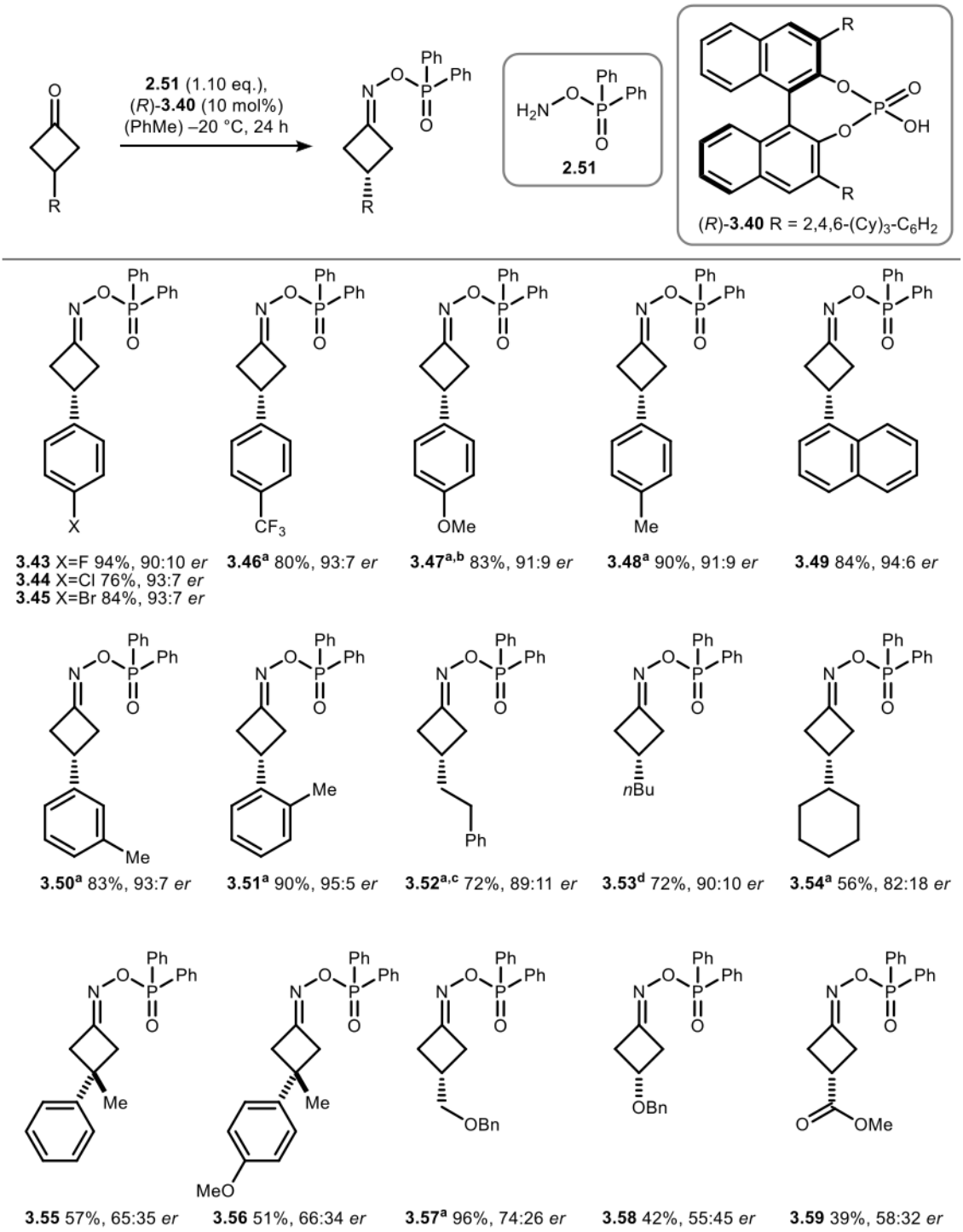

Scheme 31. Substrate scope for the enantioselective condensation of cyclobutanones. Reactions were run in toluene (0.05 M) on a 0.2 mmol scale. Yields of isolated compounds, *er* determined by chiral HPLC analysis.[a] Racemic sample was prepared by [redacted]. [b] Reaction was performed by [redacted] [c] Reaction was performed by [redacted]. [d] Racemic sample was prepared by [redacted].

In addition to the use of cyclobutanones as substrates, the substrate scope was extended to the utilisation of prochiral cyclic ketones with differing ring size (Scheme 33, top). The transformation of cyclopentanone **2.46** gave the corresponding oxime ester (3*R*,4*S*)-**2.63** with 87% yield and an excellent enantioselectivity of 99:1 *er*. In contrast, cyclohexanone oxime ester **3.60** was formed with good yield but diminished enantioselectivity of 66:34 *er*. In order to elucidate whether the observed reduction in stereospecificity was the result of competing

uncatalysed background reaction, a further transformation of cyclohexanone **3.11** was undertaken at a reduced temperature of –78 °C. As evident from the slightly improved stereoselectivity of 70:30 *er*, the use of very low temperature had only little influence on the enantioselectivity of the transformation.

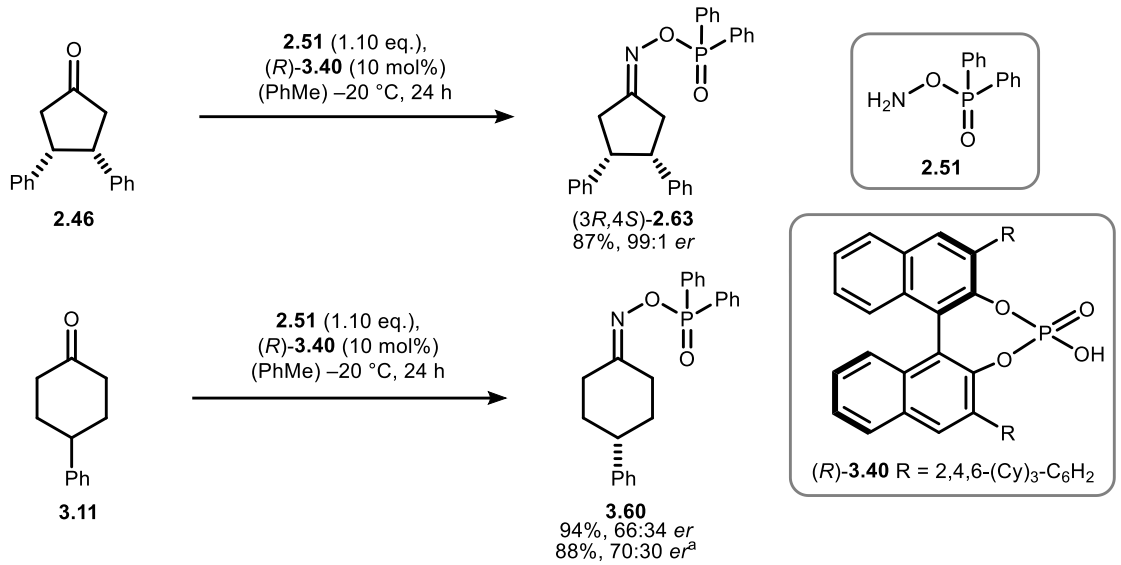

Scheme 32. Enantioselective condensation of cyclopentanone 2.46 and 4-phenylcyclohexanone 3.11. Reactions were run in toluene (0.05 M) on a 0.2 mmol scale. Yields of isolated compounds, *er* determined by chiral HPLC analysis. [a]Reaction was performed at –78 °C.

It was further investigated whether the developed protocol can be applied to *α*-substituted cyclobutanones reacting in a kinetic resolution. Therefore, the reaction of cyclobutanones **3.61** and **2.23** with amine reagent **2.51** in presence of catalyst (*S*)-**3.13** (Scheme 33, bottom) was tested. Instead of the expected oxime esters **3.62** and **3.63**, the corresponding *γ*-lactams **3.64** and **2.55** were formed with enantiomeric ratios of 50:50 and 60:40 *er*, respectively. Thus, the nitrogen insertion process occurred without or with only low stereocontrol.

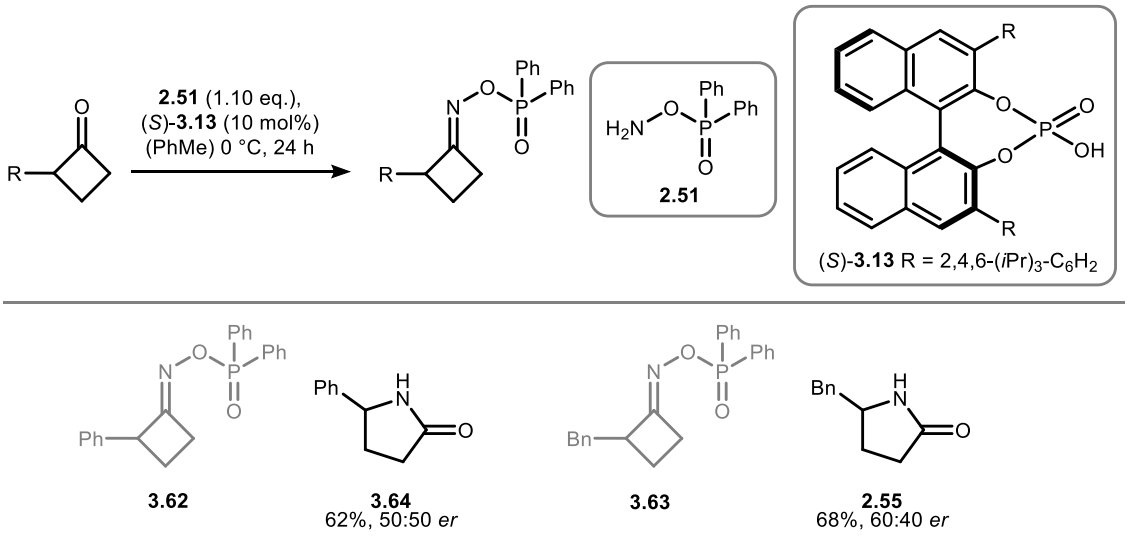

Scheme 33. Investigation of the kinetic resolution of *α*-substituted cyclobutanones. Reactions were run in toluene (0.05 M) on a 0.05 mmol scale. Yields of isolated compounds, *er* determined by chiral HPLC analysis.

3.6 Summary and outlook

The asymmetric nitrogen incorporation reaction of cyclic ketones with hydroxylamines was investigated using versatile catalysts. Instead of enantioselective nitrogen insertion by ring-expansion rearrangement, asymmetric condensation was found to be catalysed by chiral phosphoric acids (Scheme 34). Extensive optimisation of the reaction conditions led to an improved protocol using phosphoric acid (*R*)-**3.40** in toluene at –20 °C. The developed protocol represents a novel method and facilitates the synthesis of axially chiral cyclobutanone oxime esters for the first time. DFT calculations performed by [redacted] revealed a bifunctional role of the chiral phosphoric acid accelerating the formation of the tetrahedral intermediate **INT1**, as well as enabling water extrusion as the stereodetermining step. Thus, catalytic oxime formation was demonstrated to result in the formation of (*R*)-oxime esters as major enantiomers using (*R*)-configured catalyst. The scope of the methodology includes the synthesis of various 3-subsituted cyclobutanone oxime esters with aryl- and alkyl-substitution in high enantioselectivities with up to 95:5 *er* and excellent yields up to 94%. Furthermore, the transformation of a prochiral cyclopentanone was conducted giving the corresponding oxime ester in excellent stereoselectivity of 99:1 *er*.

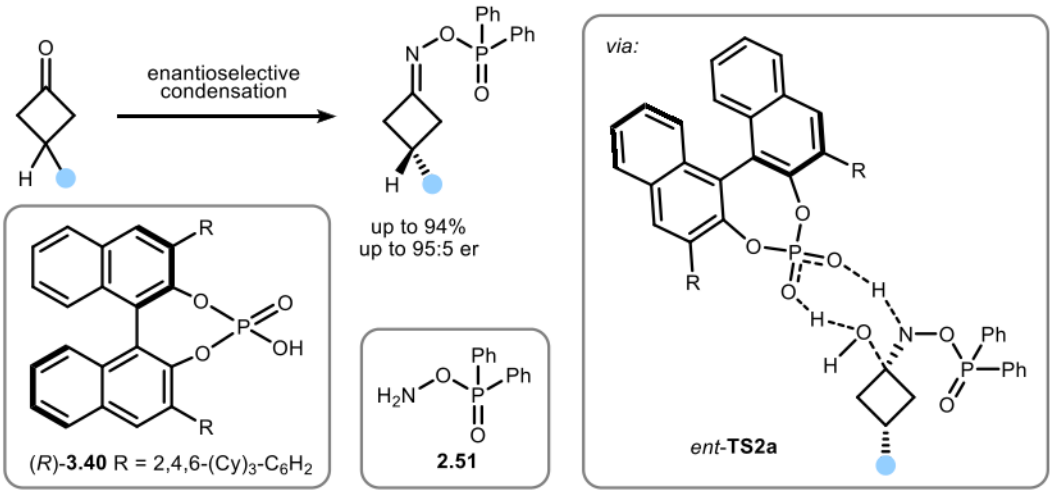

Scheme 34. Asymmetric condensation of 3-substituted cyclobutanones with hydroxylamine and chiral phosphoric acid.

Limitations were encountered for substrates bearing functional groups, 3,3-disubstituted cyclobutanones, and cyclohexanone derivatives. The diminished stereoinduction is hypothesised to result either from competing background reaction or poor interaction between the substrate and the catalyst. Therefore, further research is required to evaluate a better performing catalyst for these specific substrates. Furthermore, the development of a kinetic resolution protocol presents itself as an opportunity for the transformation of α-substituted cyclobutanone substrates.

To further leverage the introduced axial chirality in following transformations, a development of protocols for the conversion of the enantioenriched oxime esters

under preservation of the stereoselectivity is necessary. In this regard, the manifold of methodologies for the utilisation of cyclobutanone oxime esters as valuable intermediates in organic synthesis should be given due consideration (*vide infra*, *cf*. chapter 4).

4 Strategies towards the conversion of axial-to-point chirality

4.1 Introduction

In the previous chapter, the first enantioselective synthesis of cyclobutanone oxime esters was presented. The selective formation of the axially chiral compounds was accomplished by asymmetric condensation in excellent yields and enantioselectivities. Apart from oxime esters, synthetic approaches for the enantioselective construction of axially chiral oxime ethers with varying core structures are well-established.[103,104,111] In contrast, synthetic strategies for their stereocontrolled transformation to point chiral compounds remain scarce. One of the major challenges lies in the low reactivity of oxime ethers, due to their steric and electronic characteristics. Additionally, *E*/*Z* isomerisation of the oxime functionality is resulting in racemisation, thus limiting synthetic approaches for chirality transfer. An outstanding example was demonstrated by *Tan* and coworkers with the development of an approach for the transformation of enantiopure anthrone-derived oxime ethers to point chiral lactam-structures *via Beckmann* rearrangement (*cf.* chapter 3.1.1).[104] Selective migration of the antiperiplanar carbon bond to the *N*–*O* bond of the oxime ensures stereointegrity of the rearrangement process (*cf.* chapter 2.1.1).

4.1.1 Application of cyclobutanone oxime esters

While enantioselective protocols are limited, several strategies for the transformation of racemic cyclobutanone oxime esters have emerged, mainly focussing on ring-opening reactions affording acyclic nitriles.[112] Nitriles possess a distinctively short and polarised triple bond, rendering them as remarkable functionalities in molecular recognition due to their ability to form hydrogen bond interactions in sterically dense environments.[113] Furthermore, the strong dipole present in nitrile groups facilitates polar interaction, rendering the functional group suitable for bioisosteric replacement of hydroxyl or carboxyl moieties. Nitriles are hence suitable for targeting a wide range of therapeutic fields.[114,115] The relative metabolic stability of nitriles contributes to prolonged drug activity and bioavailability.[114,116] Nevertheless, nitrile groups are capable of undergoing a variety of reactions, such as amide formation by hydrolysis or reduction to primary amines, highlighting their relevance as key intermediates for drug discovery.[117] Given the widespread significance of nitriles in medicinal chemistry, efficient methods for their synthesis are of great interest. Among the numerous synthetic approaches towards nitriles, *C*–*C* bond cleavage strategies of cyclic oxime esters have emerged as a powerful tool for generating nitrile building blocks under mild

conditions. Selective cleavage of the relatively weak *N–O* bond, with an average of 57 kcal/mol, facilitates the generation of reactive intermediates that undergo fragmentation.[118] Commonly, the key intermediates are formed by single electron transfer (SET) or oxidative addition (OA) of metals,[119] leading either to the formation of iminyl radical **4.1** or imino-metal complexes **4.2**. *β*-Carbon cleavage of the cyclic intermediates results in the formation of acyclic nitriles intermediates **4.3** and **4.4** *via* the release of molecular strain of the cyclobutane skeleton (Scheme 35).[18,112] In the two-electron process, *β*-H-elimination of intermediate **4.4** and subsequent isomerisation of the external double results in the formation of cyclopropane alkenes **4.5**. In contrast, radical intermediates **4.3** can be trapped with radical acceptors. Trapping of the *C*-centred radical **4.3** enables further diversification by incorporation of additional functional groups leading to functionalised alkyl nitriles **4.6**.

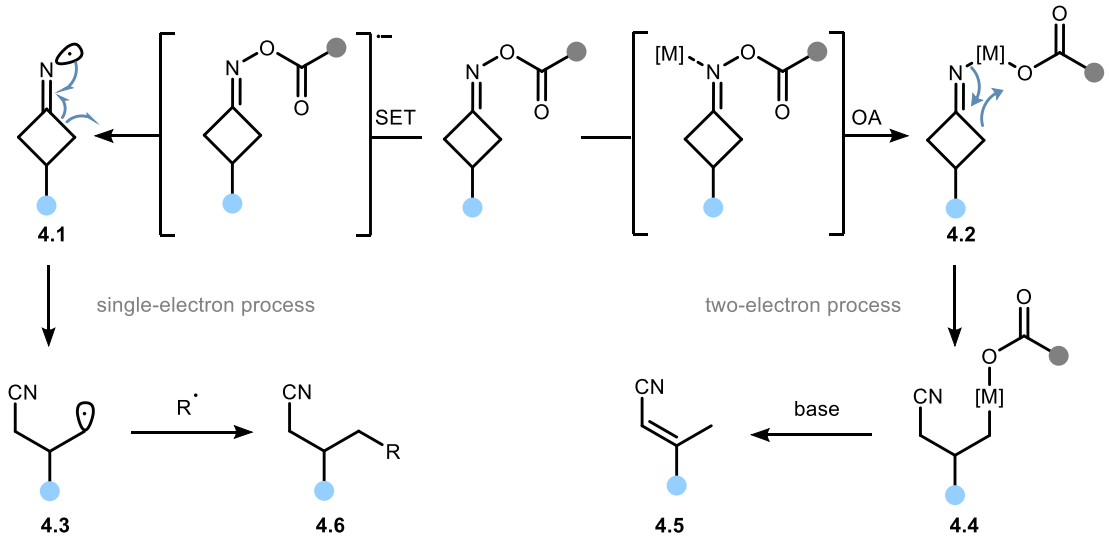

Scheme 35. General strategies of ring-opening reactions of cyclobutanone oxime esters *via* SET or OA and subsequent *β*-carbon cleavage of the iminyl radical 4.1 or imino-metal complex 4.2.

The plethora of scientific publications about the transformation of oxime esters does not only include the utilisation of versatile radical acceptors, but also a series of radical formation methodologies.[120] First examples employing cyclic oxime derivatives mentioned in the early 90s by *Zard* and coworkers were based on the generation of radicals under comparably harsh conditions using stoichiometric amounts of toxic radical initiators or UV irradiation.[121] In contrast, current strategies rely on milder methods, like photoredox processes or transition-metal-mediated *N–O* bond fragmentation.[122]

Shi and *Zhao*, for example, reported a copper catalysed iminyl radical formation from oxime ester **4.7** by single electron reduction (Scheme 36, top).[123] Homolytic *C–C* bond cleavage of radical **4.8** enables generation of an acyclic radical like **4.1**, which reacts with olefin **4.9** to form acyclic intermediate **4.10**. Radical oxidation by the reduced copper species and elimination of cationic intermediate **4.11** results in the formation of product **4.12**. In a similar fashion, different

transition metals like nickel,[124] iron[125] or iridium[126] can be used for radical initiation. Iridium-based photocatalysts find application in photoredox processes, enabling mild radical generation *via* visible-light mediated excitation of the photocatalyst and subsequent SET reduction of the oxime (Scheme 36, bottom).[127,128] After *C*–*C* bond cleavage of the generated iminyl radical **4.8** and attack of the radical acceptor **4.9**, the catalyst is recovered by a second SET with the formation of carbocation **4.11**. As described above, the product **4.12** is generated by elimination. Employing these general tools of radical initiation, the synthesis of diverse alkyl-nitriles has been demonstrated, depending on the radical acceptor used. Besides the formation of *C*–heteroatom bonds, including oxygen,[129] nitrogen,[130] sulfur,[131] boron[132] or halogen atoms,[133] cyclisation reactions are possible, enabling the generation of heterocycles and other complex molecular structures.

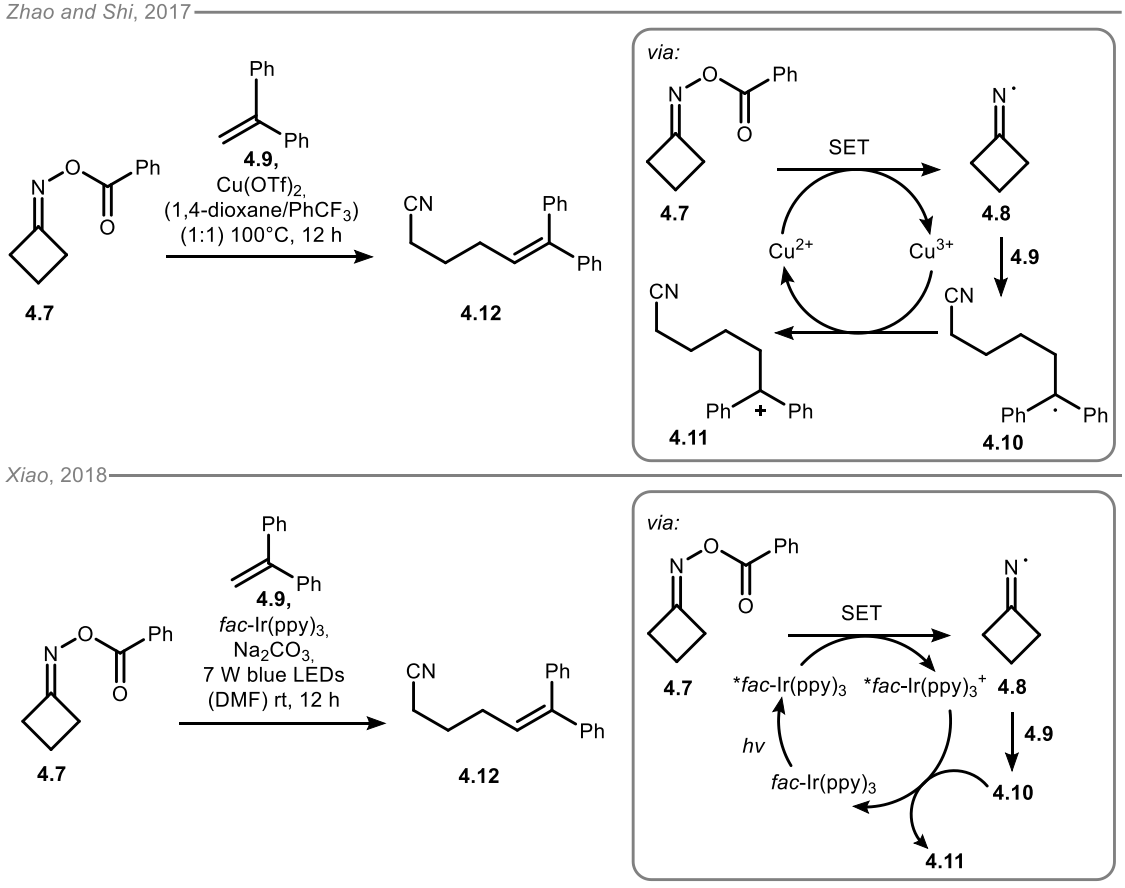

Scheme 36. Top: Ring-opening strategy of cyclobutanone oxime ester 4.7 *via* transition metal catalysed formation of iminyl radical 4.8 by *Zhao* and *Shi*. [123] Bottom: Ring-opening strategy of cyclobutanone oxime ester 4.7 *via* photoredox catalysed formation of iminyl radical 4.8 by *Xiao* and coworkers.[127] ppy = 2-phenylpyridine.

Pioneering studies for the oxidative addition (OA) of Pd(0) to the *N*–*O* bond of cyclobutanone oxime esters with subsequent *β*-carbon elimination were published by *Nishimura* and *Uemura* by the beginning of this century.[134,135] OA of palladium to oxime ester **4.13** results in the formation of intermediate **4.14**. Ring-opening reaction by *β*-carbon elimination leads to the formation of alkylpalladium intermediate **4.15**, which is eliminated with potassium carbonate

affording terminal alkene **4.16**. Double bond isomerisation results in the formation of *α,β*-unsaturated nitriles **4.17** (Scheme 37, top). The authors found, that the reaction is strongly influenced by ligand and substrate choice, with the *E*/*Z* configuration of the oxime ester **4.18** is controlling the direction of the *C–C* bond cleavage. Therefore, product **4.19** or **4.20** were obtained depending on the isomer of the oxime ester used in the transformation (Scheme 37, middle). While *β*-H elimination is difficult to avoid in the two-electron catalytic cycles, utilization of quaternary substrate **4.21** changes the reactions outcome towards the formation of cyclopropane nitrile **4.22**. By prevention of the elimination process, *C–H* activation results in the formation of a four-membered palladacycle **4.23**, which is undergoing a ring-contraction reaction due to reductive elimination (Scheme 37, bottom).

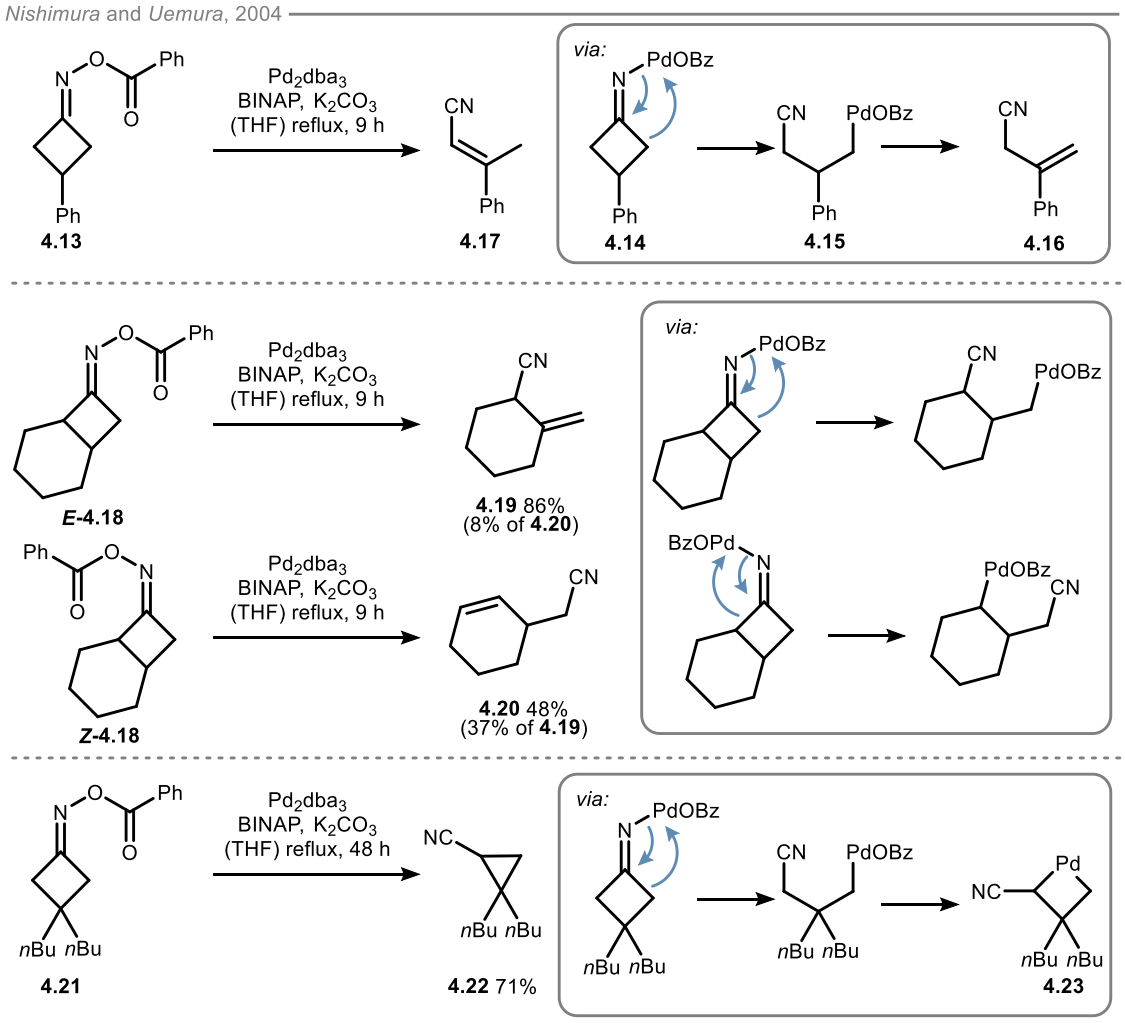

Scheme 37. Top: Ring-opening strategy of cyclobutanone oxime ester 4.13 *via* oxidative addition of Pd(0) to the *N–O* bond with subsequent *β*-hydride elimination and rearrangement of the double bond affording *α,β*-unsaturated nitrile 4.16. Middle: Selectivity control of the palladium catalysed ring-opening reactions of cyclobutanone oxime esters *E*-4.18 and *Z*-4.18. Bottom: Ring-contraction strategy of all quaternary substituted cyclobutanone oxime ester 4.21 forming cyclopropane nitrile 4.22 by *Nishimura* and *Uemura*.[134,135] dba = dibenzylideneacetone, Bz = benzoyl, BINAP = 2,2'-(diphenylphosphino)-1,1'-binaphthyl.

In 2019, *Shuai et al.* demonstrated the formation of cyclopropane nitrile **4.24** from oxime ester **4.25** *via* ring-contraction reaction with lithium hexamethylsilylamide (LiHMDS) in presence of a nickel catalyst.[136] Similar to the ring-contraction using palladium catalysts, the authors propose a ring-opening reaction initiated by oxidative addition of nickel to the *N–O* bond, with subsequent formation of a four-membered metalate-intermediate **4.26**. In case of *α*-substituted cyclobutanone oxime esters **4.27**, the rearrangement occurred without the addition of the transition metal. Therefore, the authors postulated an alternative pathway based on the formation of anion **4.28**, which is stabilised by *α*-substitution. Finally, ring-contraction rearrangement delivers to the corresponding product **4.29**.

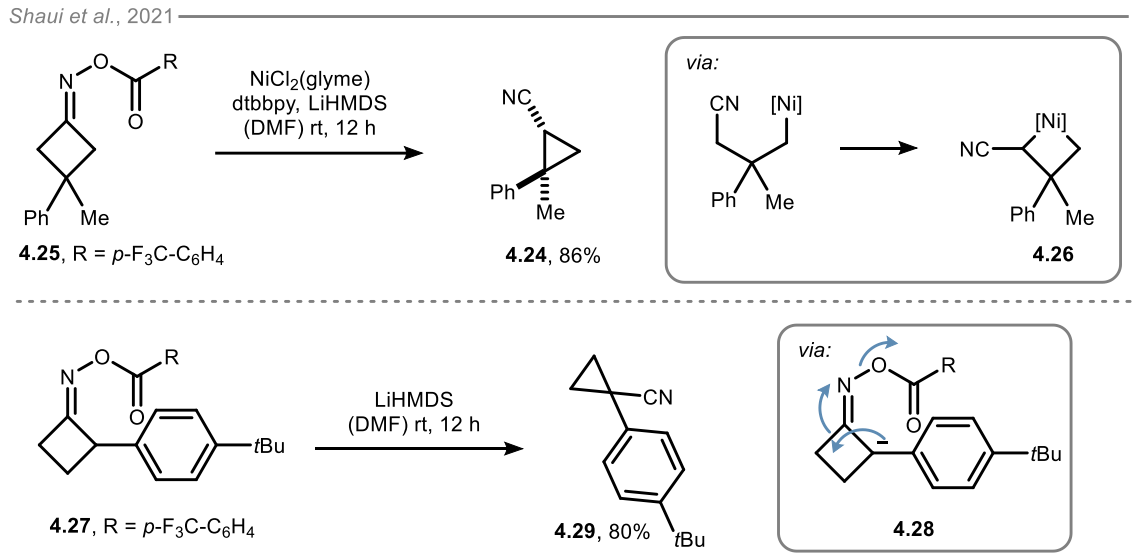

Scheme 38. Top: Ring-contraction strategy of 3-substituted cyclobutanone 4.25 *via* OA of nickel and formation of four-membered intermediate 4.26. Bottom: Ring-contraction strategy of α-substituted cyclobutanone 4.27 with LiHMDS *via* concerted ring-contraction rearrangement of anionic intermediate 4.28 by *Shuai et al.*[136] dtbby = 2,6-di-*tert*-butylpyridine, glyme = dimethoxyethane.

4.1.2 Motivation and aim

The presented examples show the versatility of oxime esters as important intermediates in organic synthesis for the build-up of complex molecular structures. However, approaches for the stereocontrolled conversion from axial-to-point chirality are comparably underexplored and are part of recent research interests (*cf.* chapter 3.1.2). In three distinct projects, transfer of axial-to-point chirality is investigated by harnessing the specific properties of cyclobutanone oxime esters in ring-expansion, -opening and -contraction reactions (Scheme 39). Thereby, the transformation of axially chiral oxime esters **4.30** into point chiral lactams **4.31**, acyclic alkyl nitriles **4.32** and cyclopropane nitriles **4.33** was to be studied.
First, a mild and enantiospecific ring-expansion strategy from cyclobutanone oximes towards chiral lactams was investigated, exploiting the molecular strain of the four-membered ring. Following the studies presented in chapter 3, *Beckmann*-type rearrangement should be triggered by increasing the leaving group propensity of the ester moiety using different acidic conditions, including *Brønsted* and *Lewis* acids. Selective migration of the antiperiplanar bond of the *N–O* bond was envisaged to ensure an enantiospecific process (*cf.* chapter 2.1.1). As part of this work, development of a proof of concept for a catalytic enantioselective nitrogen insertion reaction based on the asymmetric condensation between 3-substituted cyclobutanones and amine reagent **2.51** with subsequent selective ring-expansion rearrangement will be conducted.
Second, ring-opening reactions *via* β-carbon scission will be explored. In this regard, different approaches for initiating the reaction are sought to be examined, using generation of both iminyl-radical and imino-metal intermediates. Initiation strategies will include implementation of transition metals like palladium and copper, as well as photoredox methodologies. The selective and rapid bond cleavage of successfully formed cyclic intermediates **4.34** and **4.35** is proposed to provide access to acyclic alkyl nitriles with a chiral centre in 3-position, before racemisation of the cyclic intermediate is occurring. Further functionalisation is envisaged through the trapping of the acyclic intermediates with a range of radical acceptors or coupling reagents, depending on the initiation method employed.
Third, the focus will be directed towards the investigation of reactions of axially chiral cyclobutanone oxime esters **4.30** under basic conditions. The study was envisaged to cover functionalisation reactions of the ester moiety with *Brønsted* bases and detailed investigation of the formation of chiral cyclopropane nitriles **4.33**. For the latter, the reaction conditions for a site selective deprotonation were aimed to be optimised, to assure a stereospecific ring-contraction reaction. In this regard, control experiments will shine light on the mechanism of an unusual rearrangement, which facilitates selective access to *cis*- and *trans*-cyclopropanes by adjustment of the reaction conditions. Finally, synthetic application of

the developed methodology was demonstrated by the exploration of a substrate scope and formal synthesis of an FDA-approved drug candidate.

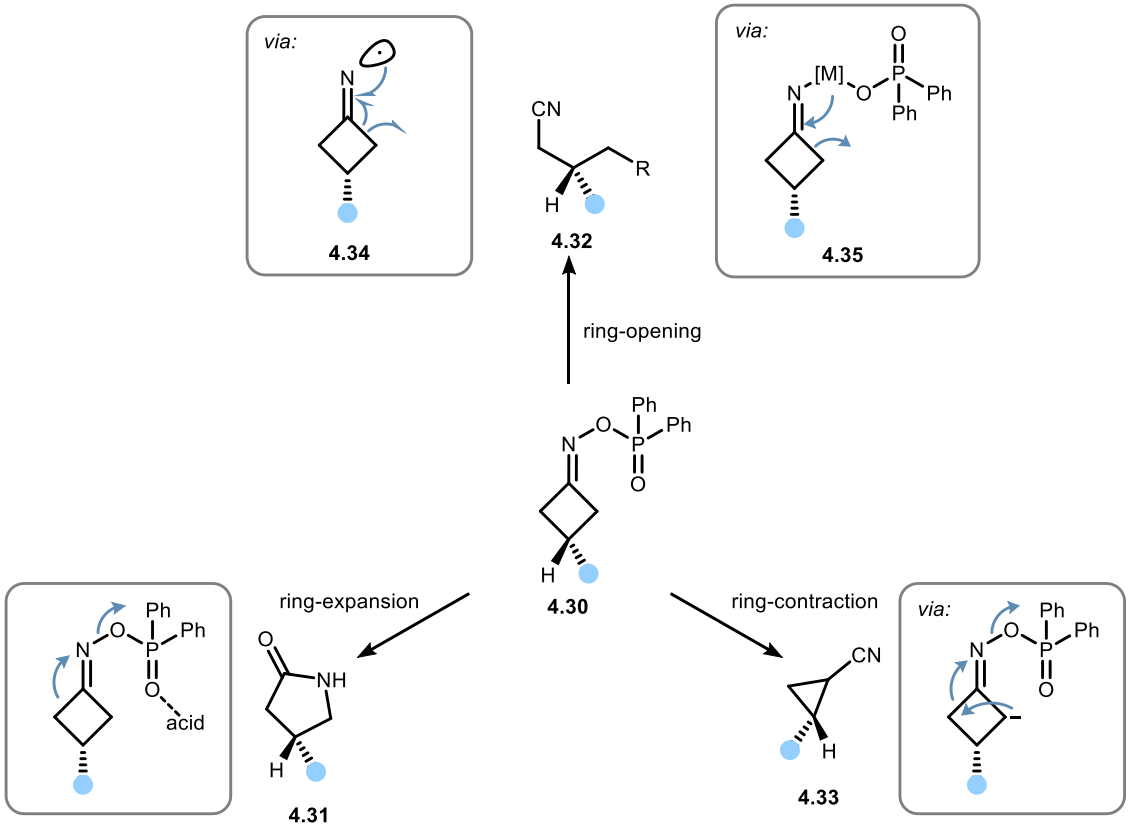

Scheme 39. Approaches for the conversion of axial-to-point chirality by transformation of cyclobutanone oxime esters 4.30 into lactams 4.31, acyclic nitriles 4.32 and cyclopropane nitriles 4.33 using ring-opening, -expansion and-contraction reactions *via* versatile intermediates.

4.2 Ring-expansion of cyclobutanone oxime esters

The previously described attempts to develop an enantioselective nitrogen insertion reaction resulted in the asymmetric formation of axially chiral cyclobutanones instead of chiral γ-lactams (*cf.* chapter 3). For realising this general endeavour, various strategies for the rearrangement of such cyclobutanone oxime esters were investigated. As discussed above, ring-expansion reactions of cyclobutanone derivatives either follow an aza-*Baeyer-Villiger* or *Beckmann* rearrangement, accelerated by relief of the inherent molecular strain (*cf.* chapter 2). In order to achieve a stereoselective conversion of axially chiral cyclobutanone oxime ester (*R*)-**3.32** to point chiral lactam (*R*)-**2.49** *via* an aza-*Baeyer-Villiger* mechanism, specific formation of only one diastereomer of the tetrahedral intermediate **4.36** must be ensured (Scheme 40, pathway A). In contrast, stereoselectivity of the *Beckmann* rearrangement is determined by the *E*/*Z* configuration of the oxime functionality, which is preset due to the asymmetric condensation affording cyclobutanone (*R*)-**3.32** in a selectivity of 95:5 *er* (*vide supra*, chapter 3.5). In this study, migration of the antiperiplanar carbon bond is envisaged to be facilitated by increase of the leaving group propensity employing acidic conditions (Scheme 40, pathway B).

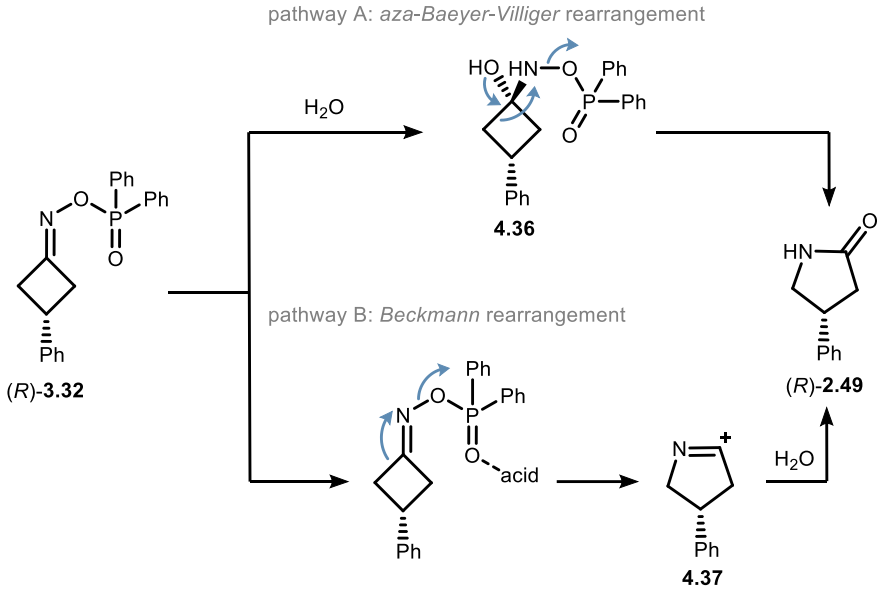

Scheme 40. Strategies for a selective ring-expansion rearrangement of enantioenriched cyclobutanone oxime ester following two possible pathways. Pathway A: Selective formation of the tetrahedral intermediate 4.36 by nucleophilic addition of water with subsequent aza-*Baeyer-Villiger* rearrangement. Pathway B: *Beckmann* rearrangement affording nitrilium intermediate 4.37 with formation of lactam (*R*)-2.49 after water addition.

4.2.1 Optimisation of reaction conditions

As before, cyclobutanone oxime ester **3.32** was chosen as model substrate for the investigation of the chirality transfer *via* ring-expansion reaction. After ensuring the successful transformation of oxime ester **3.32** to lactam **2.49** under racemic conditions, the enantiospecificity of the different reaction conditions was determined by employment of chiral oxime ester (*R*)-**3.32** with an enantiopurity of 95:5 *er*. Since the focus of this work is the development of an enantiospecific methodology, in the following only the results of the reactions using enantioenriched starting material are discussed (Table 10). The yields of the transformations were determined by quantitative ^{1}H NMR analysis using CH_2Br_2 as internal standard and the enantiopurity of the products was determined *via* chiral HPLC analysis after purification. First, ring-expansion *via* an aza-*Baeyer-Villiger* reaction was investigated. Enforcing the formation of the tetrahedral intermediate **4.36**, the oxime ester (*R*)-**3.32** was heated in a solvent mixture of water and THF for 16 hours. The desired lactam (*R*)-**2.49** was obtained with 88% yield and an enantiopurity of 60:40 *er* (entry 1). The low enantiospecificity of 22% *es* is presumed to result from the unselective addition of water to the oxime carbon. Therefore, the reaction conditions were changed to ensure a *Beckmann* rearrangement by activation of the leaving group. Employing *para*-toluene sulfonic acid (*p*-TsOH) as a strong *Brønsted* acid, the corresponding γ-lactam (*R*)-**2.49** was obtained with 95% yield in a racemic fashion. The loss of stereoinformation over the course of the reaction is assumed to be caused by protonation of the oxime nitrogen, thus facilitating isomerisation of the *C–N* double bond *via* formation of intermediate **4.38** (Scheme 41).[137] In contrast, treatment of enantioenriched oxime ester (*R*)-**3.32** with boron trifluoride diethyl etherate ($BF_3{\cdot}OEt_2$) at room temperature initiated the ring-expansion reaction to yield γ-lactam (*R*)-**2.49** quantitatively with an enantioselectivity of 92:8 *er* (entry 3). Thus, the transformation occurred with excellent specificity of 98% *es*.

Table 10. Initial results of a stereospecific ring-expansion reaction of chiral cyclobutanone oxime ester (*R*)-3.32 with an enantiopurity of 95:5 *er*, reactions were carried out on a 0.05 mmol scale, yield based on ^{1}H NMR experiments using CH_2Br_2 as internal standard, *er* determined by HPLC analysis after separation.

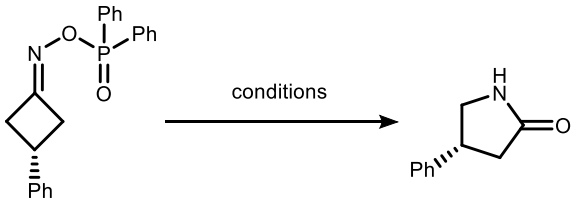

(*R*)-**3.32**, 95:5 *er* (*R*)-**2.49**

entry	conditions	yield	*er*	*es*
1	H_2O : THF (1:1), 90 °C, 16 h	88%	60:40	22%
2	pTsOH (1.0 eq.), (PhMe) rt, 16 h	82%	50:50	0%
3	$BF_3{\cdot}OEt_2$ (1.0 eq.), (PhMe) 0 °C, 16 h	98%	92:8	96%

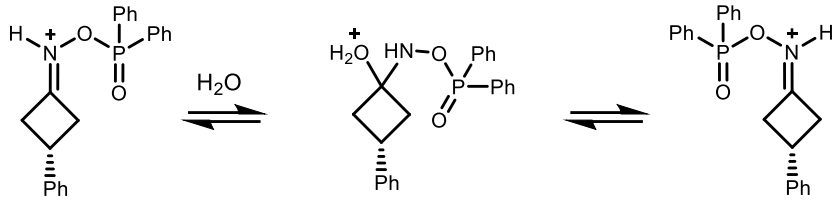

(*R*)-**4.32** **4.38** (*S*)-**4.32**

Scheme 41. Isomerisation of the *C–N* double bond of oxime ester *via* formation of the tetrahedral intermediate 4.38 by employment of *Brønsted* acids.

Following the initial results of a stereoselective rearrangement using a *Lewis* acid, the reaction conditions were optimised (Table 11). Performing the reaction at –20 °C resulted in a reduced conversion of cyclobutanone oxime ester (*R*)-**3.32** but similar stereoselectivity compared to the initial experiments conducted at 0 °C (entry 1 and 2). For easier handling on small reaction scales, the use of solid *Lewis* acid $B(C_6F_5)_3$ was investigated, affording the formation of the desired product (*R*)-**2.49** with reduced yield but similar specificity of 97% *es* (entry 3). For developing a catalytic method, reducing the amount of *Lewis* acid was probed in the following. Employment of 20 mol% of $BF_3{\cdot}OEt_2$ resulted in a lower reaction rate, giving γ-lactam (*R*)-**2.49** in 58% yield (entry 4). However, the specificity of the reaction was in a comparable range to the results of the stoichiometric addition of *Lewis* acid, indicating that a catalytic process is possible. Interestingly, catalytic use of $B(C_6F_5)_3$ resulted in a significant drop in both reactivity and selectivity (entry 5).

Table 11. Optimisation of the reaction of cyclobutanone oxime ester (*R*)-3.32 towards γ-lactam (*R*)-2.49 with *Lewis* acids, reactions were carried out on a 0.05 mmol scale, yield based on ^{1}H NMR experiments using CH_2Br_2 as an internal standard, *er* determined by HPLC analysis after separation.

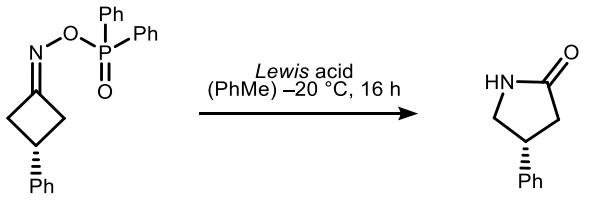

(*R*)-**3.32** (*R*)-**2.49**

entry	*Lewis* acid	*er* (*R*)-**3.32**	yield (*R*)-**2.49**	*er* (*R*)-**2.49**	*es*
1	$BF_3{\cdot}OEt_2$[a] (1.00 eq.)	94:6	98%	92:8	96%
2	$BF_3{\cdot}OEt_2$ (1.00 eq.)	94:6	87%	93:7	98%
3	$B(C_6F_5)_3$ (1.00 eq.)	89:11	72%	88:12	97%
4	$BF_3{\cdot}OEt_2$ (0.20 eq.)	92:8	58%	90:10	95%
5	$B(C_6F_5)_3$ (0.20 eq.)	91:9	19%	85:15	85%

[a]reaction was performed at 0 °C.

Based on the results for the selective formation of γ-lactam (*R*)-**2.49**, the one-pot reaction of the asymmetric condensation and *Lewis* acid-induced rearrangement was investigated in the following course of the project. With the aim of developing a catalytic asymmetric nitrogen insertion reaction, the transformation of cyclobutanone **2.8** in a one-step dual *Brønsted* and *Lewis* acid catalysis approach was

investigated. Therefore, catalytic amounts of chiral phosphoric acid (*R*)-**3.40** and $BF_3{\cdot}OEt_2$ or $B(C_6F_5)_3$ were applied from the beginning of the reaction between cyclobutanone **2.8** and hydroxylamine **2.51** (Table 12). ^{1}H-NMR analysis of the crude reaction mixture revealed full conversion of the starting material to a mixture of the desired lactam (*R*)-**2.49** and oxime ester (*R*)-**3.32**. As before, lactam (*R*)-**2.49** was obtained in a higher yield in the reaction with $BF_3{\cdot}OEt_2$ than in the reaction with $B(C_6F_5)_3$. The enantiomeric ratio of the lactam formation was significantly decreased in both transformations than in the direct catalytic conversion starting from enantioenriched oxime ester (*R*)-**3.32** (*vide supra*, Table 11 entries 4 & 5). The oxime ester (*R*)-**3.32** was isolated with enantiopurities of 77:23 and 85:15 *er*, which is significantly lower than the enantioselectivities obtained before (cf. chapter 3). These results indicate that both steps, the asymmetric condensation and the stereospecific rearrangement, are negatively affected by the simultaneous presence of *Brønsted* and *Lewis* acid.

Table 12. Test reaction of a one pot asymmetric nitrogen insertion from cyclobutanone 2.8 towards γ-lactam (*R*)-2.49 under dual *Brønsted* and *Lewis* acid catalysis. Reactions were carried out on a 0.05 mmol scale, yield based on ^{1}H NMR experiments using CH_2Br_2 as an internal standard, *er* determined by HPLC analysis after separation.

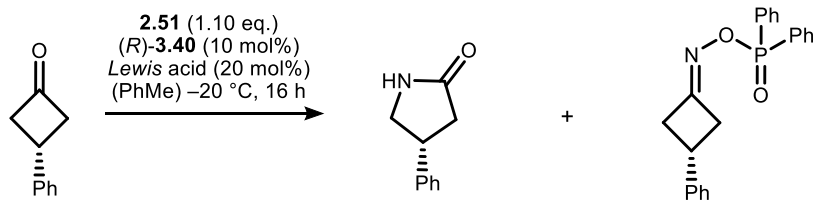

2.8 (*R*)-**2.49** (*R*)-**3.32**

Entry	*Lewis* acid	yield (*S*)-**2.49**	*er* (*S*)-**2.49**	*er* (*S*)-**3.32**	*es*
1	$BF_3{\cdot}OEt_2$	48%	70:30	77:23	74%
2	$B(C_6F_5)_3$	27%	72:28	85:15	63%

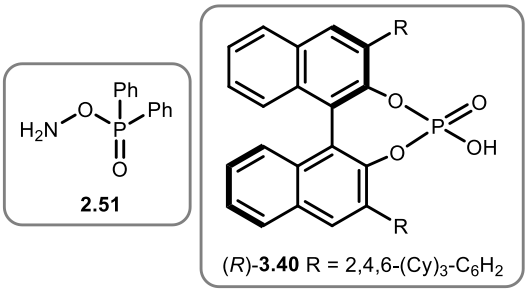

In order to avoid the interference of the *Lewis* acid on the asymmetric condensation, a sequential one-pot protocol of enantioselective oxime formation with subsequent addition of stoichiometric amounts of $BF_3{\cdot}OEt_2$ was explored (Table 13). Due to the unsatisfactory results obtained with $B(C_6F_5)_3$, this *Lewis* acid was not considered for further investigations. For all reactions, the chiral oxime ester (*S*)-**3.32** was not isolated, thus the intermediate is assumed to be formed with an enantioselectivity of 95:5 *er* according to the results obtained before (*cf.* chapter 3.5). The desired lactam (*R*)-**2.49** was obtained in a good yield and with a low

enantioselectivity of 70:30 *er*, which corresponds to 46% *es* (entry 1). Therefore, the reaction conditions for the rearrangement were systematically adjusted to elucidate the influencing parameters. Employment of an excess of *Lewis* acid improved the selectivity of the rearrangement (entry 2), thus suggesting that the rapid rearrangement is essential for maintaining stereointegrity. Similar results were obtained by using a reduced amount of hydroxylamine **2.51**, ensuring the absence of interaction between excess hydroxylamine and *Lewis* acid (entry 3). Addition of 4Å MS revealed that presence of water is significantly affecting the specificity of the rearrangement process (entry 4). Racemisation might occur through the addition of water to the oxime **3.32** forming the tetrahedral intermediate **4.38**. Presumably, either trace amounts of hydrogen fluoride, generated *in situ* through hydrolysis of $BF_3{\cdot}OEt_2$, or $BF_3{\cdot}OEt_2$ itself catalyse this unwanted isomerisation.

Table 13. Optimisation of a sequential one-pot asymmetric nitrogen insertion from cyclobutanone 2.8 towards *γ*-lactam (*R*)-2.49 with oxime ester formation and subsequent rearrangement, reactions were carried out on a 0.05 mmol scale, yield based on ^{1}H NMR experiments using CH_2Br_2 as an internal standard, *er* determined by HPLC after separation, *es* was calculated based on the average *er* (95:5) of (*R*)-3.32 isolated in previous experiments.

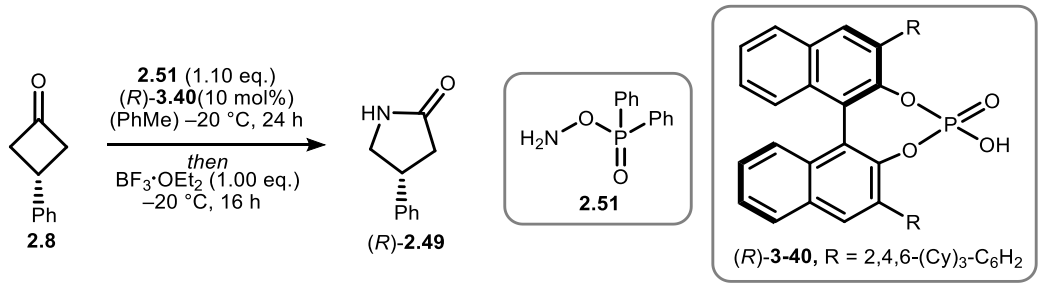

entry	deviation to standard conditions	yield	*er*	*es*
1	-	78%	70:30	46%
2	3.0 eq. *Lewis* acid	71%	87:13	85%
3	0.5 eq. DPPH	17%	87:13	85%
4	4Å MS	82%	90:10	92%

Finally, the detrimental effect of the phosphoric acid on the rearrangement process was confirmed by the reaction of oxime ester (*R*)-**3.32** in the presence of chiral phosphoric acid (*R*)-**3.13**, giving the chiral lactam (*R*)-**2.49** in an enantiomeric ratio of 89:11 *er* (90% *es*).

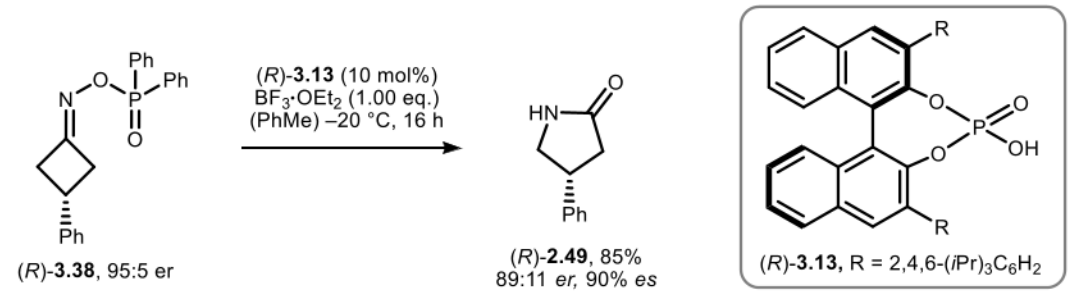

Scheme 42. Ring-expansion reaction of enantioenriched cyclobutanone (*R*)-3.32 with BF_3·OEt_2 in presence of chiral phosphoric acid (*R*)-3.13.

4.2.2 Mechanistic picture

Based on the results obtained during the optimisation an initial mechanistic picture for the transformation of oxime ester (*R*)-**3.32** to lactam (*R*)-**2.49** can be drawn (Scheme 43). Over the course of this study, the absolute configuration of the lactam was determined by comparison of the HPLC-trace and optical rotation to literature known data.[19] The formation of (*R*)-configured γ-lactam **2.49** is consistent with the expected stereoconfiguration obtained *via* a *Beckmann*-type rearrangement by migration of the bond placed antiperiplanar to the leaving group. Nevertheless, in presence of water, formation of the tetrahedral intermediate **4.36** is occurring as an undesired side reaction. The unspecific addition of water leads to racemisation of the oxime ester (*R*)-**3.32** and subsequent aza-*Baeyer-Villiger* rearrangement contribute to reducing the enantiospecificity of the entire transformation. The complete elucidation of the mechanistic picture remains to be accomplished, but the results presented herein provide a solid foundation for further investigation. Further studies on catalytic one-step methodologies for asymmetric nitrogen insertion processes will be continued by [redacted] as part of her own work.

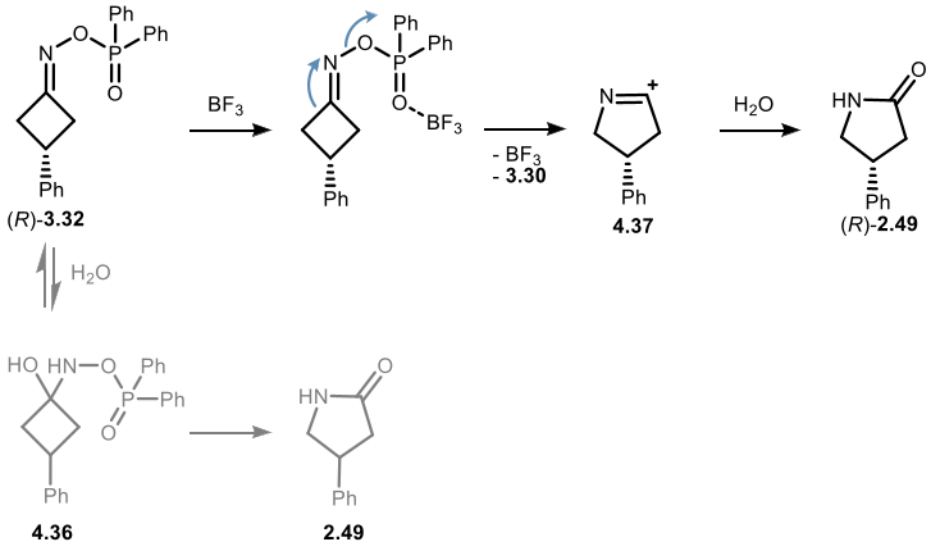

Scheme 43. Mechanistic picture of the stereospecific ring-expansion rearrangement of chiral cyclobutanone oxime ester (*R*)-3.32.

4.3 Ring-opening of cyclobutanone oxime esters

In addition to the use of cyclobutanone oxime esters as intermediates in the synthesis of lactams, the selective formation of the axially chiral compounds has opened new possibilities to access enantioenriched acyclic nitriles. As outlined above, cyclobutanone oxime esters are important intermediates in organic synthesis due to their versatile applicability in ring-opening reactions (*cf.* chapter 4.1.1). In such transformations, iminyl radicals **4.1** or imino-metalate complexes **4.2** are involved as intermediates (*vide supra*). To achieve chirality transfer from axial-to-point chirality, *β*-carbon cleavage has to occur faster than racemisation of the cyclic intermediates **4.1** and **4.2** (Scheme 44).

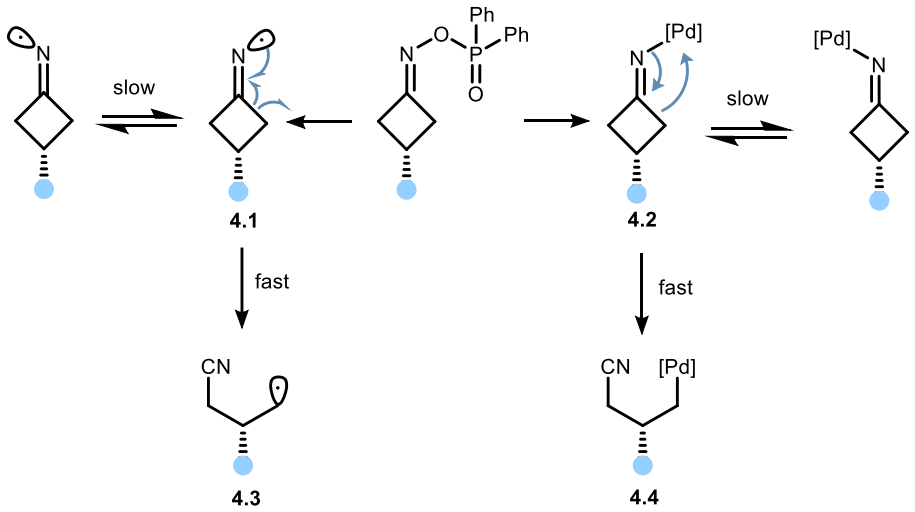

Scheme 44. Strategy for a selective ring-opening reaction of enantioenriched cyclobutanone oxime esters *via* rapid *β*-carbon cleavage of intermediates 4.1 and 4.2

Therefore, different literature-known strategies were investigated using cyclobutanone oxime ester **3.32** as model substrate. First, all reactions were performed using racemic starting material. In order to determine stereospecificity, successful ring-opening approaches were transferred to the utilisation of enantioenriched oxime ester (*R*)-**3.32**. The results of *Nishimura* und *Uemura* shown potential for a stereospecific transformation by formation of imino-metalate complex **4.2** *via* OA of Pd(0)-catalyst to the weak *N–O* bond of the oxime moiety (*vide supra,* Scheme 37).[134,135] Following the literature-known procedure, ring-opening reaction of racemic cyclobutanone oxime ester **3.32** with palladium catalyst in presence of potassium carbonate afforded the expected alkene **4.17** in 86% yield (Table 14, entry 1). However, *β*-H elimination results in a loss of the previously introduced stereoinformation, thus limiting application for a chirality transfer reaction. Therefore, trapping of the acyclic Pd-intermediate **4.15** with a suitable coupling partner was envisaged in a *Suzuki* cross coupling reaction to produce nitrile **4.39**. Addition of phenylboronic acid resulted in the formation of alkene **4.17** in 68%, assuming that elimination is occurring preferred over transmetallation (entry 2). In order to avoid the undesired elimination reaction, BF_3K salt was used as coupling reagent, which is not dependent on the addition

of base. During the process a complete decomposition of both oxime ester and coupling reagent was observed (entry 3).

Table 14. Ring-opening reaction of oxime ester *rac*-3.32 with oxidative addition of Pd(0)-catalyst and *β*-H elimination or *Suzuki* cross coupling reaction, reactions were carried out on a 0.05 mmol scale, yield based on ^{1}H NMR experiments using CH_2Br_2 as an internal standard.

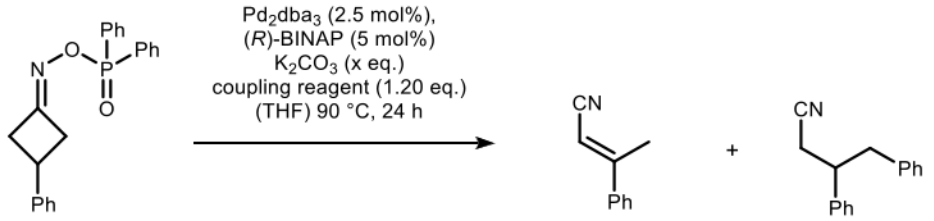

rac-**3.32** **4.17** **4.39**

entry	amount K_2CO_3	coupling reagent	yield **4.17**	yield **4.39**
1	1.00 eq.	-	86%	-
2	1.00 eq.	Ph-$B(OH)_2$	68%	0%
3	-	Ph-BF_3K[b]	traces	0%

[a]Reaction was performed without the addition of K_2CO_3. [b]Coupling reagent was prepared by [redacted].

While ring-opening reactions using two-electron processes are limited due to the elimination resulting in a loss of enantioselectivity, protocols following a ring-opening *via* radical pathway were tested (Scheme 45). Generation of the iminyl radical **4.40** with copper(II) triflate and radical trapping with alkene **4.9** gave the desired product **4.41** in good yields, but racemisation occurred during the transformation. Following the literature protocols the reaction was performed at 90 °C. During the project, stability of the enantioselective oxime was investigated, revealing racemisation takes place under thermal conditions. As the stereointegrity of the axially chiral oxime ester is depending on the *E*/*Z* configuration of the *C*–*N* double bond, thermal interconversion of the isomers was assumed to cause racemisation before chirality transfer is occurring. Therefore, a protocol by using copper(II) triflate and thiol **4.42** as nucleophile was applied.[131] Formation of nitrile **4.43** was achieved in good yields with an enantiomeric ratio of 50:50 *er*. The loss of stereoinformation during the reaction at room temperature indicates, that the formation of the iminyl radical **4.40** likewise limits the development of a stereospecific transformations by rapid interconversion of to the isomer *E*-**4.40**.

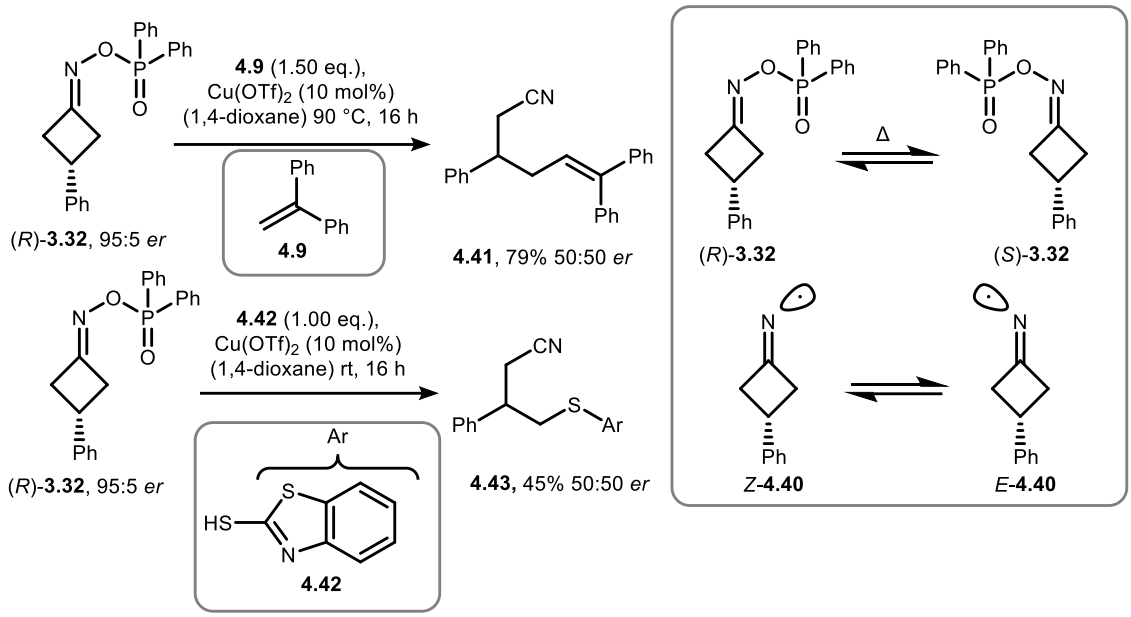

Scheme 45. Transformations of enantioselective cyclobutanone oxime ester (*R*)-3.32 in ring opening reactions.

Lastly, the formation of iminyl radical **4.40** *via* photoredox catalysis was investigated by visible light-irradiation of racemic oxime ester **3.32** in DMSO in the presence of a photoredox catalyst *fac*-Ir(ppy)$_3$. According to the approach developed by *Shi* and coworkers, formation of aldehyde **4.44** was expected by oxidation of the acyclic radical intermediate **4.3** with DMSO.[138] After 16 h, the cyclobutanone oxime *rac*-**3.32** was obtained in 90% and ^{1}H NMR analysis showed decomposition rather than selective formation of the desired product **4.44**.

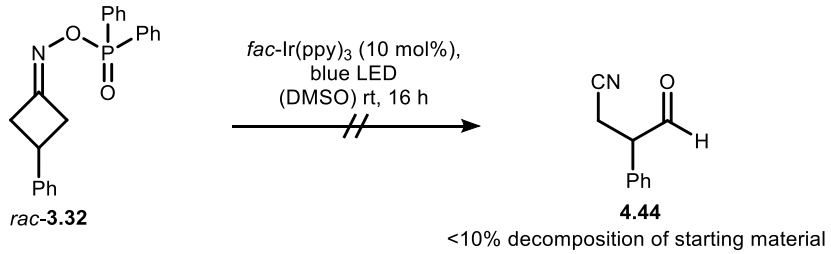

Scheme 46. Reaction of oxime ester rac-3.32 using a visible light mediated approach for radical initiation.

Apart from the lack of reactivity of the selected initiation by photoredox approaches or trapping methods for palladium intermediates, limitation of the ring-opening reactions was found to be attributed to the rapid racemisation of iminyl radical intermediate **4.40**. For this reason, no further investigations regarding ring-opening reactions of cyclobutanone oxime ester (*R*)-**3.32** were carried out. Instead, the focus of this work turned to the development of novel transformations of axially chiral cyclobutanone oxime esters under basic conditions.

4.4 Ring-contraction of cyclobutanone oxime esters

In the previous chapter, ring-opening reactions of cyclobutanone oxime ester **3.32** were explored. During this study, limitations were found in the lack of possibilities to suppress *β*-H elimination of palladium-intermediate **4.5** and rapid racemisation of iminyl-radical **4.40** formed as an intermediate. To circumvent these problems, further stereospecific functionalisation strategies of oxime ester (*R*)-**3.32** were sought to be achieved by the employment of basic conditions. While previous studies on the formation of axially chiral oxime derivatives were based on the synthesis of relatively unreactive oxime ethers, formation of phosphinyl oxime esters allows for saponification with hydroxide bases.[139] Thus, the reaction of enantioenriched cyclobutanone oxime ester (*R*)-**3.32** with sodium hydroxide was performed in methanol (Scheme 47). The desired product **4.45** was obtained in good yields as a racemic mixture. Similar to the results obtained before, formation of the anion **4.46** is assumed to cause the loss of stereoselectivity due to facile *E*/*Z* isomerisation *via* the anionic intermediate **4.47**.

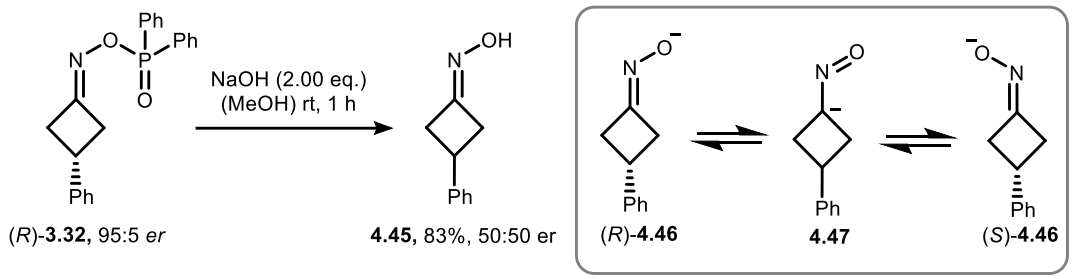

Scheme 47. Saponification of enantioenriched cyclobutanone oxime ester (*R*)-3.32 to cyclobutanone oxime 4.45. Racemisation *via* anionic intermediate 4.47.

Therefore, deprotonation of the cyclobutanone core was envisaged by application of non-nucleophilic bases. The study was inspired by the base-induced ring-contraction by *Shuai et al.*, which initiated a concerted rearrangement resulting in the formation of *trans*-cyclopropane nitriles (cf. chapter 4.1).[136] The stereointegrity of the ring-contraction rearrangement was assumed to result from site selective deprotonation facilitated either by steric or directing effects (Scheme 48).

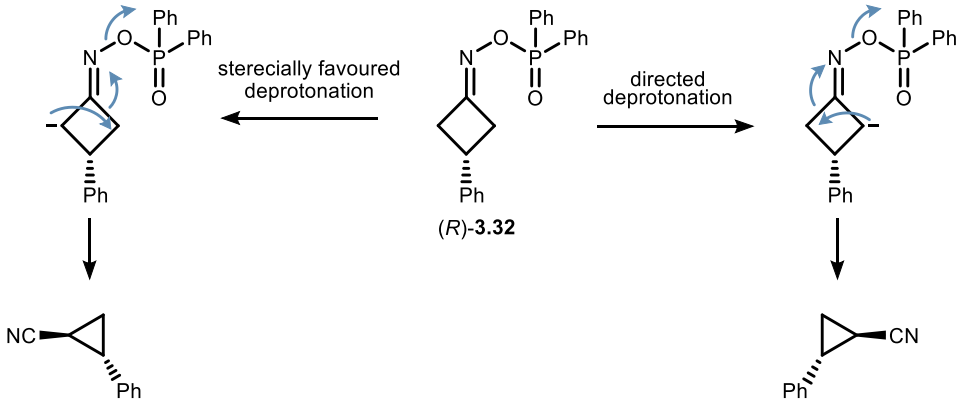

Scheme 48. Strategy for a selective ring-contraction reaction of enantioenriched cyclobutanone oxime esters by site selective deprotonation.

Initially, chiral oxime ester (*R*)-**3.32** was treated with LiHMDS in DMF at room temperature (Scheme 49). Cyclopropane nitriles **4.48** and **4.49** were obtained in a diastereomeric ratio of 62:38 *dr* (**4.48**:**4.49**) with an enantiopurity of 74:26 *er* respectively. The primary results with an enantiospecificity of 53% *es* and a combined yield of 45% encouraged for optimisation of the reaction conditions to improve both enantioselectivity and reactivity.

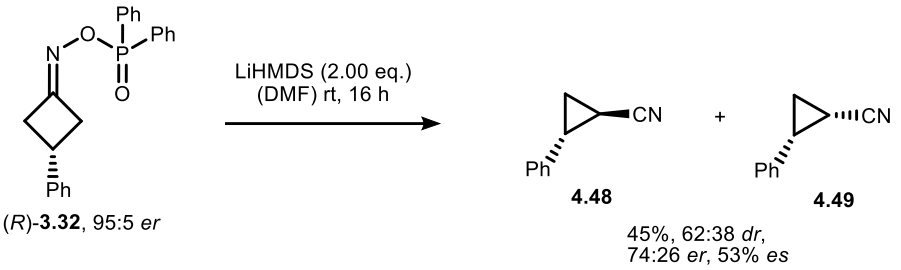

Scheme 49. Ring-contraction reaction of enantioenriched cyclobutanone oxime ester (*R*)-3.32 towards the formation of chiral cyclopropanes 4.48 and 4.4.49.

4.4.1 Optimisation of reaction conditions

First, the reaction of racemic oxime ester **3.32** in a series of solvents with varying polarity was investigated by quantitative ^{1}H NMR analysis with CH_2Br_2 as internal standard (Table 15). The yields given in the corresponding entries are based on the combined yields of the cyclopropanes **4.48** and **4.49**. Performing the reaction in cyclohexane gave almost no conversion to the desired products **4.48** and **4.49** (entry 1). Increased reactivity was obtained in toluene, whereas the transformation in benzene afforded 32% combined yield (entries 2 & 3). Both reactions gave the *trans*-isomer **4.48** as major product with a diastereomeric ratio of 71:29 *dr* and 75:25 *dr* respectively. The highest product formation was achieved by running the reaction in THF with a combined yield of 72% (entry 4). The employment of more polar solvents, like DMF led to diminished results in reactivity and diastereoselectivity (entry 5).

Table 15. Solvent optimisation, reactions were carried out on a 0.1 mmol scale, combined yield and dr based on ^{1}H NMR experiments using CH_2Br_2 as an internal standard.

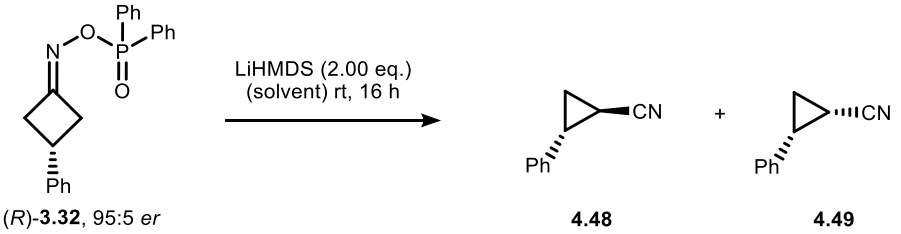

entry	solvent	combined yield	*dr* (**4.48**:**4.49**)
1	cyclohexane	<10%	n.d.
2	PhMe	62%	71:29
2	benzene	32%	75:25
4	THF	72%	67:34
5	DMF	51%	66:34

For the following optimisation employing different bases, 3-(*p*-fluorophenyl)-substituted oxime ester **3.43** was chosen as substrate, facilitating analysis of the reaction by quantitative ^{19}F NMR with $PhCF_3$ as internal standard. A series of bases with varying basicity were investigated running the reactions in toluene (Table 16). Utilisation of sodium and potassium salt of HMDS both resulted in diminished yields if cyclopropanes **4.50** and **4.51**, compared to LiHMDS (entries 1 – 3). 18-Crown-6 was employed coordinating the cation of the base, thus increasing the anionic character and by that the basicity. Interestingly, the diastereoselectivity was converted giving the *cis*-isomer **4.51** as the major product (entry 4). Employment of lithiumdiisopropylamide (LDA), a sterically less hindered base, gave similar results, with the cyclopropane **4.51** formed as a major product (entry 5). In contrast, lithiumtetramethylpiperidine (LiTMP) resulted in a decomposition of the starting material **3.43** without selective formation of the cyclopropane nitriles (entry 6). Application of potassium *tert*-butanolate led to a significant reduction of reactivity, with a conversion of 10% giving mainly the *cis*-product **4.51** (entry 7). Due to the low solubility of the inorganic salt, a solution of potassium *tert*-pentyloxide in toluene was employed, affording cyclopropanes **4.50** and **4.51** in a diastereomeric mixture of 59:41 *dr* with 44% of combined yield (entry 8).

Table 16. Base optimisation, reactions were carried out on a 0.1 mmol scale, yield based on ^{19}F NMR experiments using $PhCF_3$ as an internal standard.

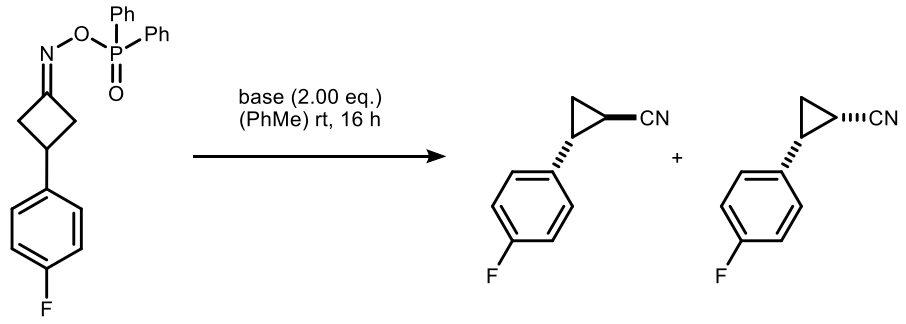

3.43 **4.50** **4.51**

entry	base	combined yield	*dr* (**4.50**:**4.51**)
1	LiHMDS	53%	75:25
2	NaHMDS	22%	72:28
3	KHMDS	36%	78:22
4	NaHMDS, 18-crown-6	37%	23:77
5	LDA	34%	34:66
6	LiTMP	0%	-
7	KOtBu	10%	8:92
8	KOtPent	44%	59:41

Combining the condensation and ring-contraction reaction in a sequential one-pot protocol was investigated using the best results obtained during the previous optimisation (Table 17). Racemic oxime esters were formed by reaction of cyclobutanone **4.52** with amine reagent **2.51** in presence of diphenyl phosphate

3.34. Subsequent addition of 2.00 equivalents of LiHMDS gave the desired cyclopropanes **4.50** and **4.51** with a diastereomeric ratio of 75:25 *dr*, in 38% yield over two steps (entry 1). As a change of the diastereomeric ratio was observed during the base optimisation, addition of different amounts of LiHMDS was investigated. While employment of 3.00 equivalents base did not significantly influence the reactions outcome, reversed diastereoselectivity was obtained with reduced amounts of LiHMDS (entries 2 & 3). Thus, employment of a stoichiometric amount of base afforded selective formation of *cis*-isomer **4.51** in a yield of 38% over two steps.

Table 17. Base equivalent optimisation, reactions were carried out on a 0.1 mmol scale, yield based on ^{19}F NMR experiments using $PhCF_3$ as an internal standard.

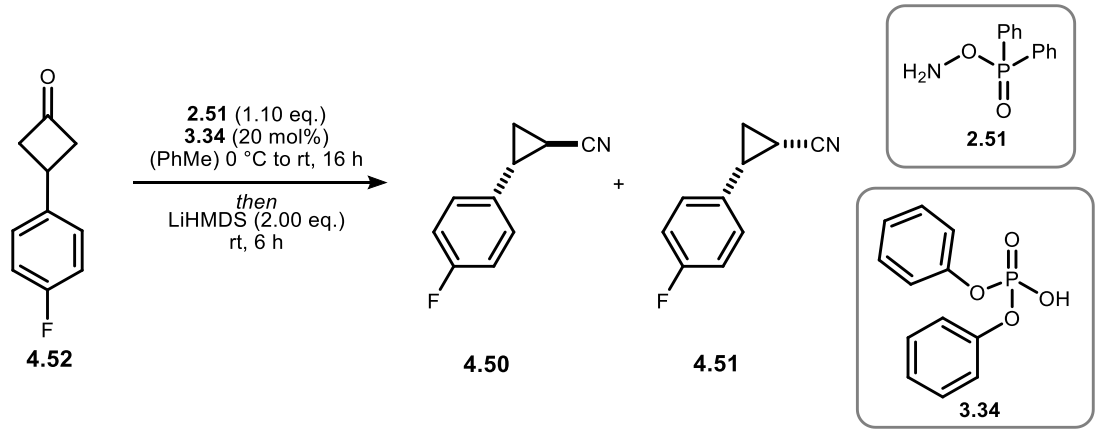

entry	amount of base	combined yield	*dr* (**4.50**:**4.51**)
1	2.00 eq.	38%	75:25
2	3.00 eq.	39%	78:22
3	1.50 eq.	37%	14:86
4	1.00 eq.	38%	>5:95

The absolute configuration of the *cis*-isomer **4.49** was determined by X-ray crystallography. The results obtained during the optimisation of the one-pot reaction led to the assumption, that the *cis*-isomer **4.49** is formed as the kinetic product whilst the thermodynamic *trans*-product **4.48** being generated by deprotonation of **4.49**. Investigating this hypothesis, enantioenriched cyclopropane (1*S*,2*R*)-**4.49** was treated under the standard reaction conditions (Scheme 50). Thereby, formation of the *trans*-isomer **4.48** with full prevention of the enantiopurity and 73% yield was achieved. The formation of the *trans*-product (1*R*,2*R*)-**4.48** was validated by comparison of the HPLC-traces of the foregoing optimisation and by comparing the optical rotation to literature data.[140] Thus, the possibility of selective formation of both diastereomers is emerging due to fine-tuning of the reaction parameters.

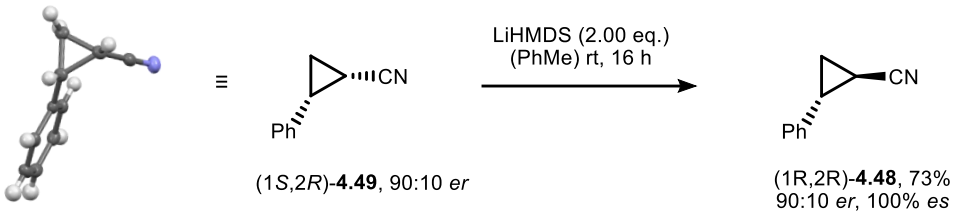

Scheme 50. Transformation of cyclopropane (1*S*,2*R*)-4.49 to trans-isomer (1*R*,2*R*)-4.48 by treatment under standard reaction conditions. Molecular structure and absolute configuration of *cis*-cyclopropane 4.49 determined *via* X-ray diffraction, thermal ellipsoids are depicted at 50% probability.

To conclude, the enantioselective one-pot reaction of cyclobutanone **2.8** with phosphoric acid (*R*)-**3.40** was investigated using LiHMDS in different solvent mixtures of toluene and THF (Table 18). The optimisation was conducted using 1.00 equivalents of base, thus only the yield and enantioselectivity for the formation of the *cis*-product (1*S*,2*R*)-**4.49** is determined. Further, the reaction conditions were adjusted to −78 °C due to the assumption, that *cis*-selective cyclopropane formation is ensured at lower temperatures. As the condensation towards the axially chiral cyclobutanone oxime ester (*R*)-**3.32** is performed in toluene, commercially available LiHMDS in toluene was initially employed for the second step. Surprisingly, cyclopropane (1*S*,2*R*)-**4.49** was formed with a poor enantioselectivity of 60:40 *er* (entry 1). Assuming that the oxime ester (*R*)-**3.32** was formed in a selectivity of 95:5 *er*, this result translates to 22% *es*. However, the initial results utilising chiral oxime ester in DMF and LiHMDS in THF gave the corresponding cyclopropanes with a selectivity of 74:26 *er* (*vide supra*, Scheme 49). Therefore, the ring-contraction reaction was conducted using LiHMDS in THF, giving cyclopropane (1*S*,2*R*)-**4.49** in similar yield of 56% with significantly improved selectivity of 90:10 *er* (entry 2). Performance of the ring-contraction in THF was investigated by removal of toluene after successful formation of oxime ester (*R*)-**3.32**. The crude reaction mixture was redissolved in THF and addition of LiHMDS in THF resulted in the formation of 12% yield with an enantioselectivity of 85:15 *er* (entry 3).

Table 18. Optimisation of the enantioselective one-pot protocol, reactions were carried out on a 0.1 mmol scale, combined yield and dr based on ^{1}H NMR experiments using CH_2Br_2 as an internal standard.

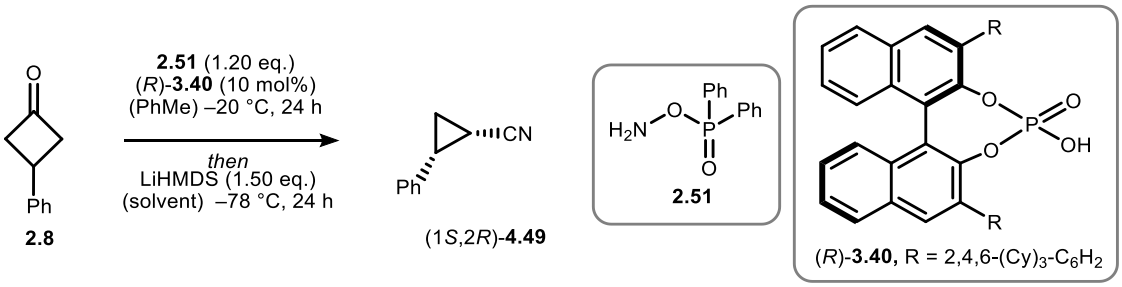

entry	base	solvent	yield	*er*
1	LiHMDS in PhMe	PhMe	56%	60:40
2	LiHMDS in THF	PhMe	56%	90:10
3	LiHMDS in THF	THF	12%	85:15

4.4.2 Mechanistic studies

Based on the results of the enantioselective optimisation, the solvent mixture of toluene and THF deemed to be crucial to ensure a high stereospecificity of the ring-contraction rearrangement. The importance of THF in the solvent mixture is assumed to result from the solvent dependent aggregation of LiHMDS. While oligomeric structures are predominant in noncoordinating solvents like toluene, mono or dimeric LiHMDS prevails in ethereal solution.[141] The structural proof of the formation of (1*S*,2*R*)-enantiomer determined by X-ray analysis, in combination with the results from the optimisation, indicates that directed deprotonation is present. Thus, it is assumed that the occurrence of low aggregated LiHMDS is essential to enable regioselective deprotonation directed by the phosphinyl group, to outcompete a sterically less hindered attack. From a mechanistic perspective, the generated anion **4.53** can undergo three distinguished pathways (Scheme 51). The first mechanistic proposal is based on a *Neber*-type rearrangement, including the formation of nitrene-type intermediate **4.54** which can also be described in a housane-type and zwitterionic structure **4.55** and **4.56**. The latter being the most likely intermediated enabling product formation *via* a 1,2-carbon shift. According to a study of *Shuai et al.*, the ring-contraction reaction can also be described in a concerted rearrangement of anion **4.57** towards the formation of cyclopropane nitrile.[136] Lastly, pathway C includes a [3,3]-sigmatropic rearrangement cleaving the weak *N–O* bond and simultaneously forming *α*-oxyphosphinylated intermediate **4.58**.[142] Thus, formation of the cyclopropane is facilitated by the good leaving group ability of the phosphinyl group.

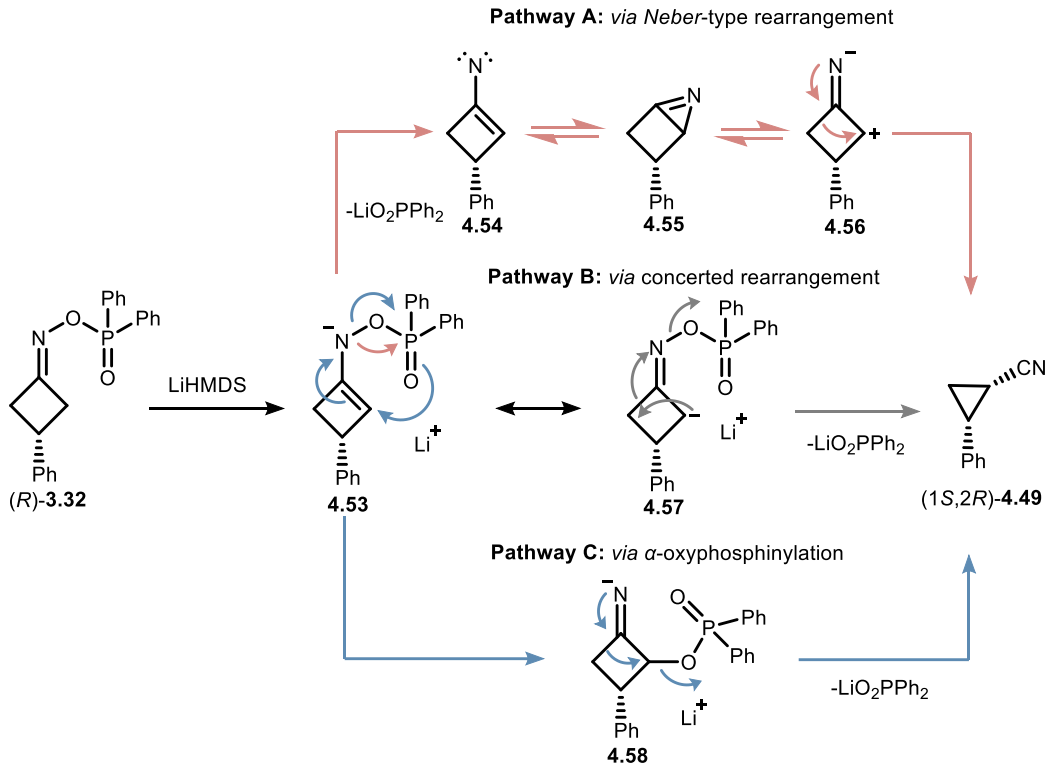

Scheme 51. Mechanistic proposals for the ring-contraction rearrangement initiated by directed deprotonation of oxime ester (*R*)-3.39 with LiHMDS. Pathway A (pink) follows a *Neber*-type rearrangement *via* nitrene formation and subsequent 1,2-carbon shift. Pathway B (grey) includes a concerted rearrangement of anion 4.57. Pathway C (blue) is based on the formation of *α*-phosphinylated intermediate 4.58 *via* [3,3]-sigmatropic rearrangement and ring-contraction by intramolecular substitution.

Different control experiments were conducted elucidating the mechanistic picture (Scheme 52). Treatment of cyclohexanone-derived oxime ester **3.60** under identical reaction conditions afforded pyrazine **4.59**. Formation of this product is explained by self-condensation of *α*-amino ketone **4.60** generated *via Neber* reaction followed by aromatization through oxidation. Attempts to trap the highly instable *α*-amino ketone **4.60** with di-*tert*-butyl dicarbonate failed, but generation of the corresponding HCl-salt was successful enabling the characterisation by mass spectrometry. Thus, proof is given that the reaction of cyclohexanone derivative **3.60** is following a *Neber*-type rearrangement, indicating the formation of cyclopropane nitrile (1*S*,2*R*)-**4.49** may follow pathway A. Nevertheless, it is worth mentioning that variation of the ring size can result in a change of the reaction mechanism. The reaction *via* a concerted rearrangement is considered implausible due to the lack of orbital interactions across the 4-membered core structure. In order to exclude the occurrence of *α*-substituted intermediate **4.58**, reaction of oxime ether **4.61** was investigated giving 32% of cyclopropanes **4.48** and **4.49** in 77:28 *dr*. The reduced yield indicated that the ring-contraction is dependent on the leaving group ability of the oxime functionality, which is correlating to the capability of nitrene formation.

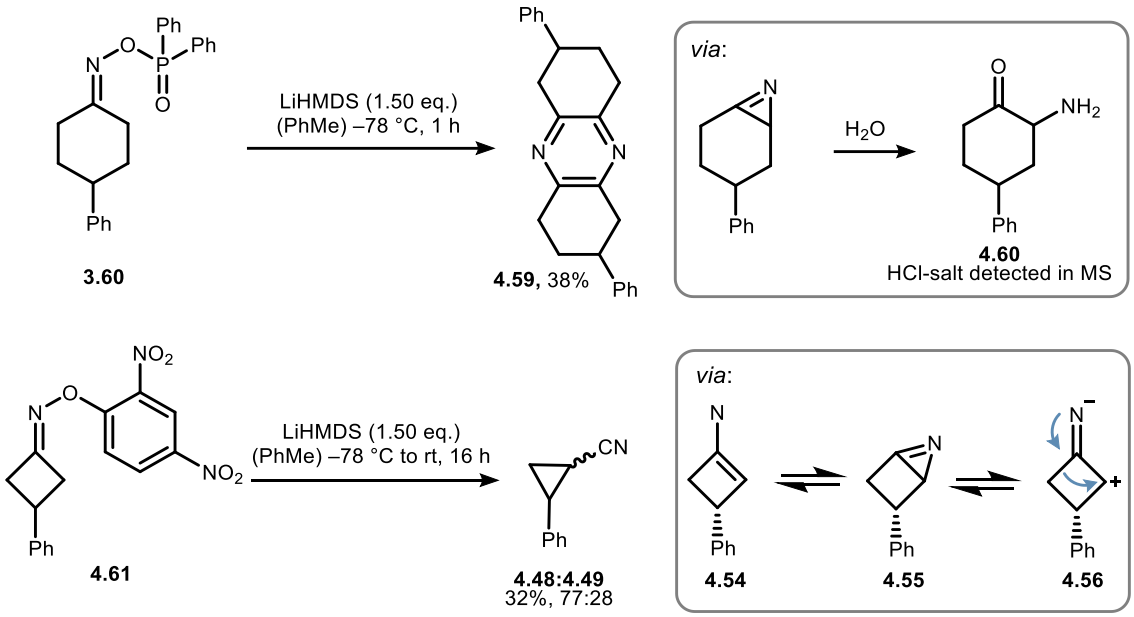

Scheme 52. Control experiments for the elucidation of the mechanism.

4.4.3 Scope

During the optimisation, fine-tuning of the reaction parameters enabled the diastereoselective formation of either the *cis*- or *trans*-isomer as major products. Thus, the kinetic product (1*S*,2*R*)-**4.49** is obtained performing the ring-contraction rearrangement with 1.00 equivalents of LiHMDS at −78 °C. In contrast, selective formation of diastereomer (1*R*,2*R*)-**4.48** is accomplished by employment of an excess of base at −20 °C. To highlight the stereodivergence of the developed methodology, the transformation of cyclobutanone **2.8** was conducted generating all four isomers existing for the corresponding cyclopropane. Synthesis of the different enantiomers was achieved by employment of the respective enantiomers of the phosphoric acid **3.40** used for the asymmetric condensation. In contrast, diastereoselectivity was guaranteed by adjustment of the reaction conditions. Thus, the conversion of axial-to-point-chirality was facilitated to give all products with moderate yields and good enantioselectivities. Enabling selective access to the specific isomers by simple adjustment of the reaction parameters demonstrates the synthetic value of the developed methodology.

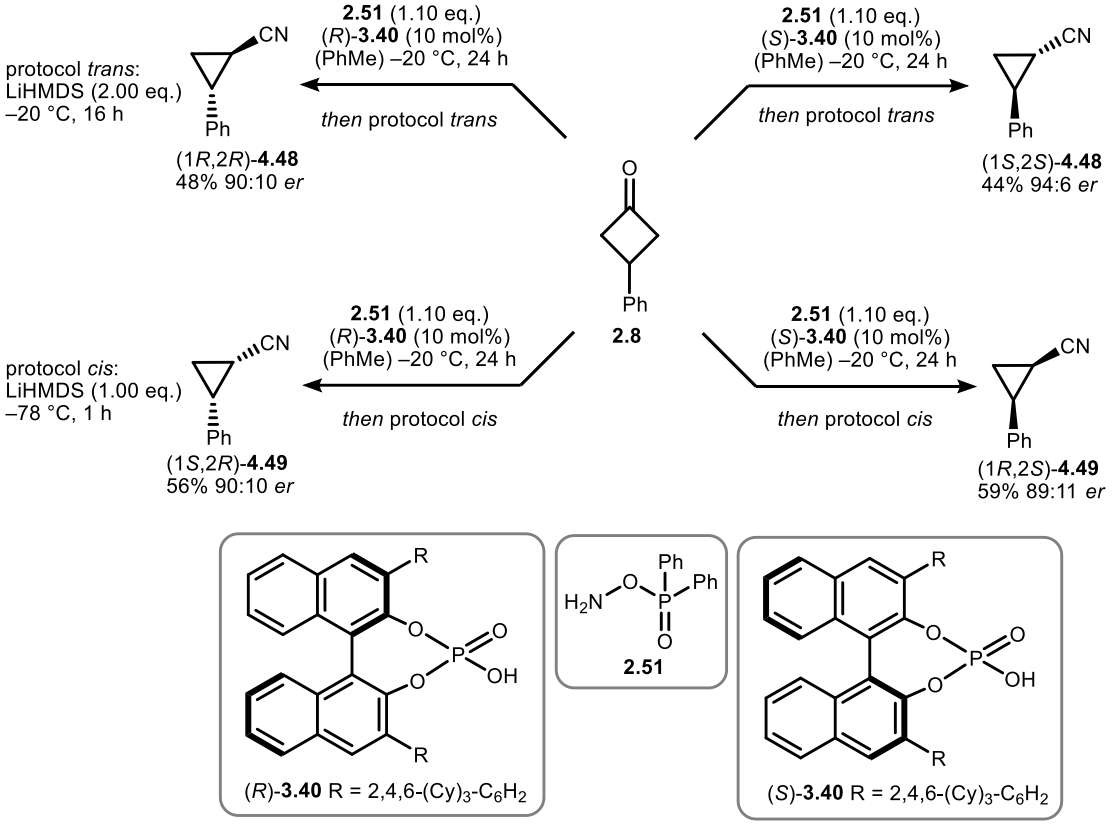

Scheme 53. Stereodivergent synthesis of all possible enantiomers of cyclopropane nitriles 4.48 and 4.49.

The substrate scope of the ring-contraction reaction was studied using a series of 3-substituted cyclobutanones and employing the conditions for the *cis*-selective cyclopropane formation. The combined yield and the diastereoselectivity of the reactions were determined by ^{1}H NMR analysis of the crude reaction mixture using CH_2Br_2 as internal standard. Separation of the diastereomers was achieved

via column chromatography and the enantiomeric ratio was determined by chiral HPLC analysis. Therefore, only the isolated yield and enantioselectivitiy of the major isomer will be discussed in the following. Similar to the previous study about the asymmetric formation of oxime esters (*cf.* chapter 3.5), racemic samples were prepared under standard reaction conditions using diphenyl phosphate as *Brønsted* acid. Electronic alteration at the aromatic substituent gave the electron poor *cis*-cyclopropanes **4.62** and **4.63** with a selectivity of 90:10 *dr* and 88:12 *er* and with moderate yields of 53% and 46% respectively. Synthesis of electron donating *p*-methoxybenzene substituted cyclopropane **4.64** was achieved with a selectivity of 92:8 *dr* and 88:12 *er* in 47% yield. Sterically perturbation enabled synthesis of the cyclopropanes **4.65** and **4.66** in similar enantioselectivities and with excellent diastereoselectivity of >99:1 *dr*. Application of alkylated substrates resulted in diminished stereoinduction, affording cyclopropane **4.67** in 47% yield with 79:21 *er*. The *trans*-selective synthesis of selected cyclopropanenitriles was conducted by [redacted] as part of her own work and will therefore not be discussed herein.

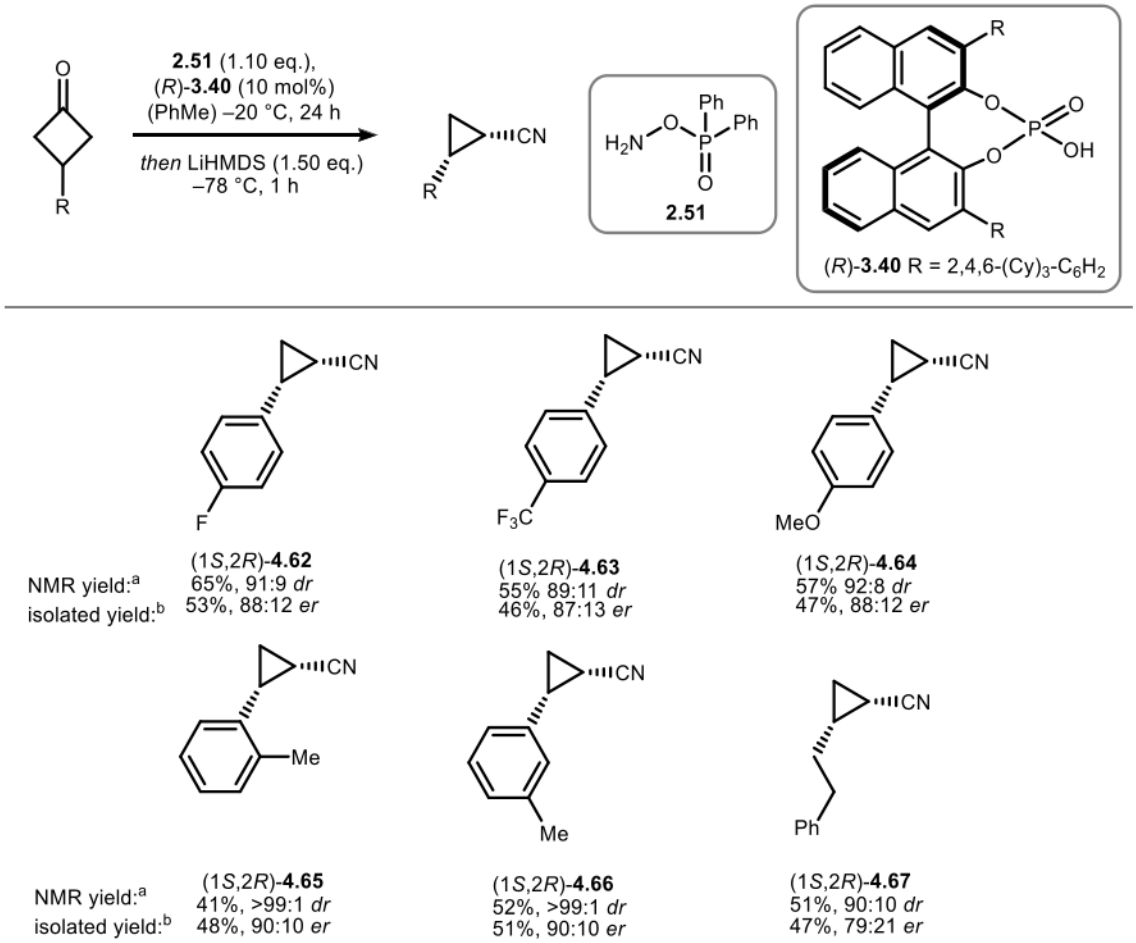

Scheme 54. Scope for the enantioselective condensation of cyclobutanones with subsequent ring-contraction towards *cis* cyclopropane nitriles. Reactions were run in toluene (0.05 M) with LiHMDS in THF (1.0 M) on a 0.2 mmol scale. [a] Determined by ^{1}H NMR using dibromomethane as internal standard. [b] Isolated yield and enantiomeric ratio correspond to the major isomer only.

4.4.4 Formal synthesis of Tasimelteon

Finally, synthetic utility of the ring-contraction rearrangement was demonstrated for the formal synthesis of the FDA-approved drug Tasimelteon (**4.68**), which is used for the treatment of non-24-hour sleep-wake-disorder.[143] Initially, styrene-derivative **4.69** was prepared from phenyl ethanol **4.70** by intramolecular cyclisation *via Goldberg-Ullmann* coupling and subsequent *Stille* coupling with tributylvinylstannane. [2+2]-Cycloaddition using dichloroketene and dehalogenation afforded the desired cyclobutanone **4.71**.

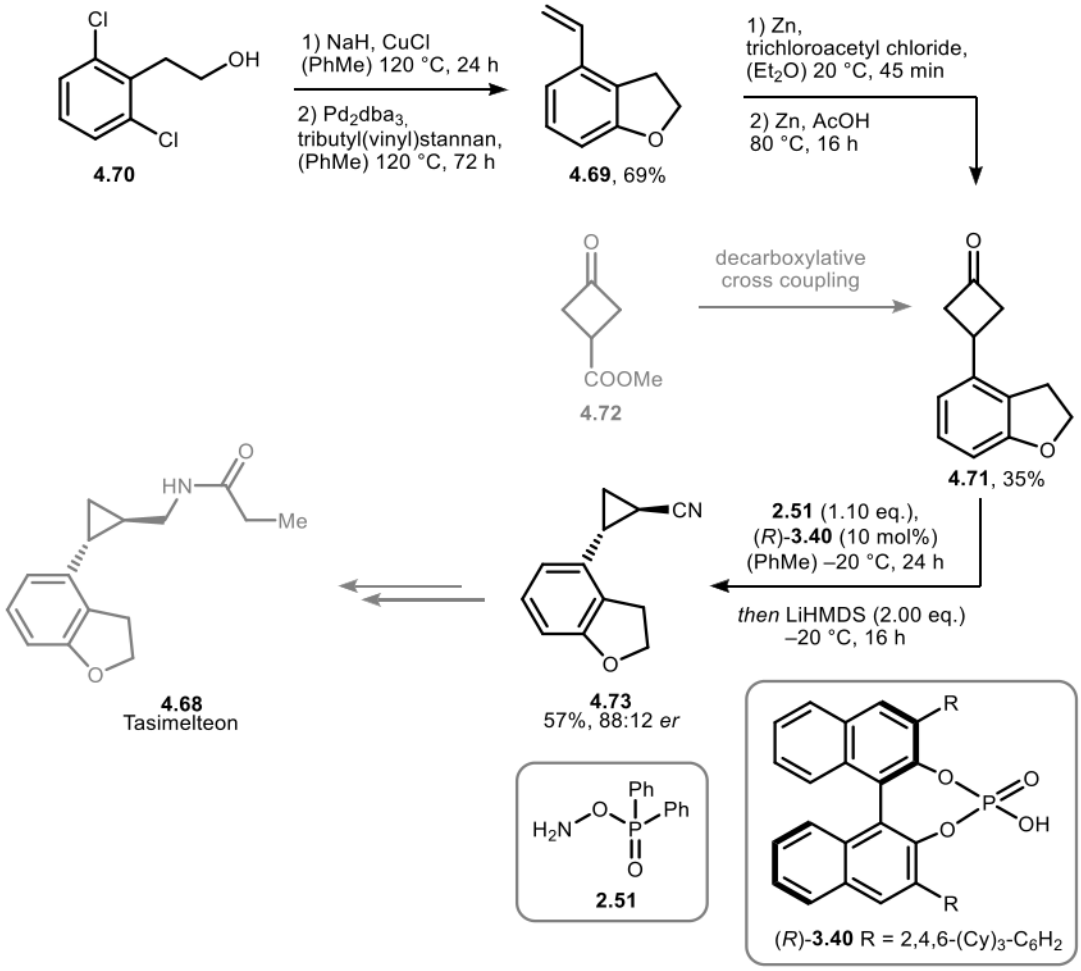

Scheme 55. Synthesis sequence for the formal formation of Tasimelteon 4.68.

As part of their research projects [redacted] and [redacted] independently investigated an alternative pathway for the synthesis of cyclobutanone **4.71** from methyl 3-oxocyclobutane-1-carboxylate **4.72** *via* a decarboxylative cross coupling strategy. The results are summarised in their own works and will not be discussed herein.[144] Application of the developed reaction conditions for the *trans*-selective protocol, enabled the synthesis of cyclopropane nitrile intermediate **4.73** *via* asymmetric condensation and chirality transfer by ring-contraction rearrangement. Thus, cyclopropane **4.73** was obtained in 45% yield and with an enantioselectivity of 88:12 *er*. Tasimelteon **4.70** can be obtained from this intermediate in two steps through reduction and subsequent amide coupling following the literature-known protocols by *Wang et al.*[145]

4.5 Summary and outlook

The major challenge encountered during the three projects were identified as the rapid isomerisation of the *C–N* double bond and the associated racemisation of the axially chiral oxime esters. The study revealed that heating, treatment with *Brønsted* acids and *Brønsted* bases result in a complete loss of stereointegrity. Furthermore, limitations were established in ring-opening procedures due to rapid isomerisation of iminyl radicals, which resulted in the formation of functionalised acyclic nitriles as racemic mixtures. Ring-opening approaches based on the oxidative addition of Pd(0)-catalysts were successfully providing the expected *α*,*β*-unsaturated nitrile **4.17**. However, the formation of imino-metal complexes proved to be obstacle to the development of a methodology incorporating a chirality transfer, due to the unavailability of methodologies to trap the acyclic palladium intermediate **4.15**. The employment of *Suzuki* coupling conditions resulted in the faster *β*-H elimination or decomposition of the starting materials in comparison to the formation of the targeted product.
Nevertheless, two different stereoretentive methodologies were developed, achieving conversion of axial-to-point chirality by ring-expansion or -contraction reaction. The combination of these novel approaches with the previously developed asymmetric condensation in sequential one-pot procedures enables the formation of chiral *γ*-lactam (*R*)-**2.49** or cyclopropane nitriles from simple prochiral cyclobutanones (Scheme 56).
The presented ring-expansion reaction accomplishes the initial goal of developing a mild and selective synthetic method of chiral *γ*-lactams *via* an asymmetric nitrogen insertion strategy (cf. chapter 3.1.3). Building on the results for an asymmetric formation of cyclobutanone oxime esters, a *Lewis* acid-initiated ring-expansion reaction was developed. Thus, the presented methodology demonstrates a proof of concept for a highly efficient synthesis of *γ*-lactams (*R*)-**2.49** *via* steroselective condensation and stereospecific ring-expansion reaction. Reaction under water-free conditions is deemed to be crucial to achieve a stereospecific rearrangement. Therefore, racemisation *via* formation of the tetrahedral intermediate **4.36** and aza-*Baeyer-Villiger* reaction are suggested to represent undesired side reactions. The application of the *Lewis* acid BF_3 is hypothesised to accelerate a *Beckmann* rearrangement by activating the leaving group. Consequently, enantioselective formation of the oxime ester (*R*)-**3.32** and subsequent migration of the antiperiplanar bond to the leaving group enables the generation of *γ*-lactam (*R*)-**2.49** with an enantiopurity of 90:10 *er*. Further investigation to explore the substrate scope of the reaction sequence, including the application of substrates with varying ring size remains to be accomplished. In addition, studies towards a one-step catalytic asymmetric nitrogen insertion strategy have to be conducted on the basis of the results presented herein.

Beyond accomplishing the development of an asymmetric nitrogen insertion protocol towards chiral γ-lactams, application of axially chiral cyclobutanone oxime esters paved the way for the synthesis of chiral cyclopropane nitriles. Detailed optimisation revealed a solvent dependency for the chirality transfer of the interesting ring-contraction rearrangement. Mechanistic experiments led to the suggestion, that the reaction is following a *Neber*-type rearrangement, involving formation of nitrene-type intermediate **4.54** and ring-contraction *via* a 1,2-carbon shift. Further validation of these mechanistic considerations remains to be accomplished by in-depth computational studies. By sequential combination with the asymmetric condensation of cyclobutanones, the ring-contraction rearrangement facilitates selective formation of chiral cyclopropane nitriles with an enantioselectivity of up to 90:10 *er*. The adjustment of the reaction parameters allows the target synthesis of the four possible product isomers, thus providing a stereodivergent approach for the formation of cyclopropane derivatives. The study was concluded with the representation of a substrate scope for the generation of *cis*-cyclopropane nitriles and the formal synthesis of the drug Tasimelteon. Therefore, the applicability of the methodology as a powerful tool in organic synthesis was demonstrated.

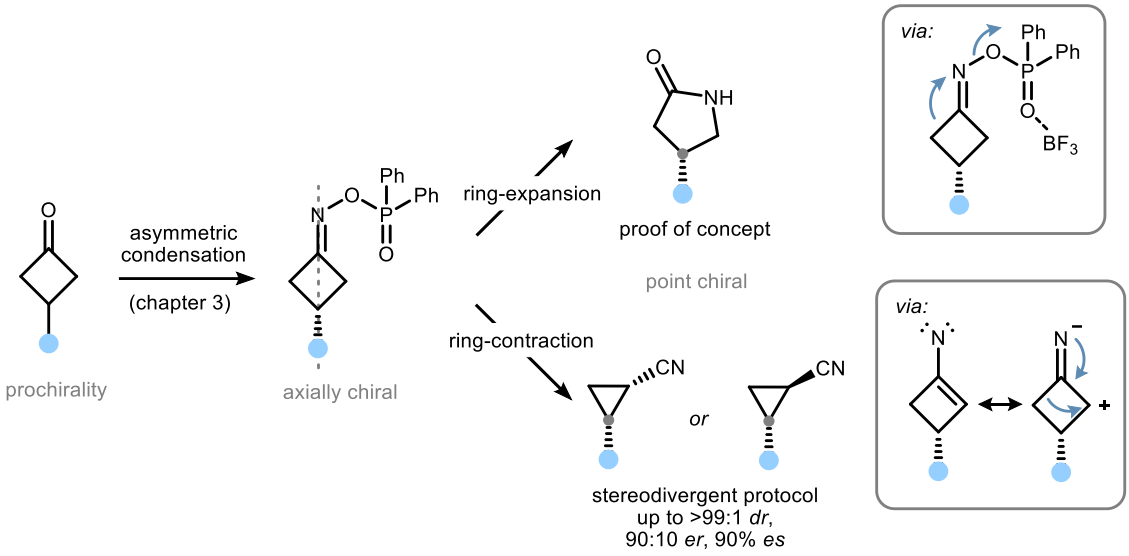

Scheme 56. Stereoselective synthesis of γ-lactams and cis- or trans-cyclopropanes by sequential one-pot approaches from cyclobutanones via asymmetric condensation and subsequent ring-expansion or ring-contraction rearrangement.

5 Experimental part

5.1 General information

Reaction Set-up: Chemicals were purchased from *Alfa Aesar*, *Acros Organics*, *Sigma Aldrich*, *BLDpharm*, *FluoroChem*, *Carbolution* or *ABCR* and (unless otherwise stated) used as received. All reactions involving air or moisture sensitive reagents were carried out in oven- (125 °C) and flame-dried glassware under nitrogen atmosphere using standard Schlenk techniques. Dry solvents were collected from an *MBraun MB SPS-800* (Et_2O: MB-KOL-A and MB-KOL MT2-250, THF: 2 × MB-KOL MT2-150°C, CH_2Cl_2: 2 × MB-KOL-A). A positive argon pressure was used to pass the solvents through the columns. Unless otherwise noted, all work-up and purification procedures were carried out with pre-distilled technical grade solvents.

Purification methods: Purification was performed either with standard column chromatography techniques using *Geduran*® Si 60 silica gel (0.063-0.200 mm, *Merck*), on an automated flash chromatography system *Biotage Isolera One* utilizing *Biotage Sfär Silica D-Duo* 60 µm columns (5 g, 25 g, 100 g), on an automated flash chromatography system *Teledyne Isco* with *Biotage Sfär Silica C18-Duo* 100 Å 30 µm columns (12 g) or with preparative thin layer chromatography (TLC) using glass plates coated with SiO_2-60 F254 and 0.5 mm thickness (*Merck*). Glass silica gel plates 60 F254 (*Merck*) were used for analytic thin layer chromatography applying either UV light (254/366 nm), $KMnO_4$ (1.5 g $KMnO_4$, 5 g $NaHCO_3$ and 5 mL NaOH 10% in 200 mL H_2O) or CAM (0.5 g $Ce(NH_4)_2(NO_3)_6$ and 24.0 g of $(NH_4)_6Mo_7O_{24}{\cdot}4H_2O$, 28 mL H_2SO_4 in 200 mL H_2O) for detection.

Analytical methods: Melting points (**M.P.**) were measured on a Büchi B-540 melting-point apparatus and are reported uncorrected.

Infrared (**IR**) spectra were obtained on a Tensor 27 spectrometer (Bruker) using a diamond ATR unit and are reported in wavenumbers (cm^{-1}). Bands are characterized as broad (br), strong (s), medium (m), and weak (w).

Nuclear magnetic resonance (**NMR**) spectra were recorded by the analytical department of the Department Chemie at Johannes Gutenberg-Universität Mainz. The following spectrometers were used: Avance III HD 300 (Bruker), Avance II 400 (Bruker), Avance III HD 400 (Bruker), and Avance III 600 equipped with a cryo-probe head (Bruker). Spectra were recorded at 26 °C (unless otherwise noted). Chemical shifts are reported in ppm with the solvent resonance as the internal standard (^{1}H NMR $CHCl_3$: δ = 7.26 ppm, C_6HD_5: δ = 7.16 ppm, $(CHD_2)(CD_3)SO$: δ = 2.50 ppm; ^{13}C NMR CDCl3: δ = 77.16 ppm, C_6D_6 δ = 128.06 ppm, $(CD_3)_2SO$: δ = 39.5 ppm). Chemical shifts of ^{19}F NMR are referenced to internal or external standards according to Togni and coworkers.[146]

The data is reported as follows: chemical shift, multiplicity (s = singlet, d = doublet, t = triplet, q = quartet, p = pentet, br = broad, m = multiplet or combinations of these), coupling constants (Hz) and integration. Apparent multiplicity, which occurs as a result of accidental equality of coupling constants to magnetically non-equivalent protons, is marked as *app*.

High Resolution Mass Spectrometry (**HRMS**) was performed by the analytical department of the Department Chemie at Johannes Gutenberg-Universität Mainz. Spectra were recorded on a Thermo-Fisher Scientific DFS (GC-MS, ionization *via* electron ionization (EI) or chemical ionization (CI)) or on an Agilent 6545 Q-ToF (LC-MS, ionization *via* electron spray ionization (ESI), atmospheric-pressure chemical ionization (APCI)). Signals are reported as mass to charge ratio m/z.

Optical rotations were measured on a *Perkin-Elmer* 241 polarimeter at 589 nm wavelength (Na D-line) using a standard 10 cm cell (1 mL). Specific rotations, [α]DT, are reported in ° mL/(g dm) at the specific temperature. Concentrations (c) are given in grams per 100 mL of the specific solvent.

Analytical high-performance liquid chromatography (**HPLC**) measurements were performed on the following systems: *Knauer* HPLC Pump Smartline 1000 with degassing unit, *Knauer* Autosampler Smartline 3950, *Knauer* UV-detector Smartline 2550, *Knauer* RI-detector Smartline 2300 or *Agilent Technologies* 1260 Infinity II HPLC-System with a binary pump, high performance degassing unit, automized liquid sampler, thermostatic column oven and diode array detector. Separation was performed using Lux® iCellulose-5 (4.6 × 250 nm × 5 µm, *Phenomenex* Ltd.), Lux® Cellulose-1 (4.6 × 250 nm × 5 µm, *Phenomenex* Ltd.), Lux® Amylose-1 (4.6 × 250 nm × 5 µm, *Phenomenex* Ltd.), Lux® i-Amylose-3 (4.6 × 250 nm × 5 µm, *Phenomenex* Ltd.), or Reprosil Chiral-AMS (4.6 × 250 nm × 5 µm, *Dr Maisch* GmbH).

X-ray diffraction: Data sets for compounds (*R*)-**3.41**, (*R*)-**3.42** and (1*S*,2*R*)-**4.59** were collected by [redacted] with a STOE Diffractometer system. Programs used: data collection X-Area WinXpose 2.022.0 (*X-RED* and *X-AREA*, Stoe & Cie, **2019**), cell-refinement: X-Area Recipe 1.36.0 (*X-RED* and *X-AREA*, Stoe & Cie, **2019**), structure solution SHELXT-2014 (G.M. Sheldrick *Acta Cryst*., **2015**, *A*71, 3-8); structure refinement SHELXT-2018/3 (A. L. Spek *Acta Cryst*., **2015**, *C*71, 3-8) and graphics Platon (A. L. Spek *Acta Cryst*., **2009**, *D*65, 148-155). R-values are given for observed reflections, and ωR^2 values are given for all reflections.

Documentation: The experimental work was partly documented using the electronic lab notebook (ELN) *Chemotion*. Otherwise, the documentation was carried out using conventional lab notebooks in paper form.

5.2 Nitrogen insertion *via* aza-*Baeyer-Villiger* reaction

5.2.1 Synthesis of starting materials

Synthesis of α-substituted cyclobutanones

General Procedure A (GP-A) for the synthesis of α-substituted methylenecyclobutanones

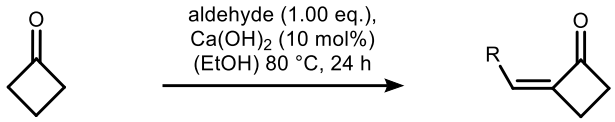

The olefin was prepared following a literature protocol by Song *et al.*[75] A Schlenk tube under N_2 atmosphere was charged with $Ca(OH)_2$ (2.10 g, 1.00 mmol, 0.100 eq.). A solution of cyclobutanone (2.10 g, 30.0 mmol, 3.00 eq.) and aldehyde (10.0 mmol, 1.00 eq.) in anhydrous EtOH (15 mL) was added. The resulting mixture was stirred at 80 °C for 24 h. The solvent was removed under reduced pressure. The olefin was obtained *via* flash column chromatography.

General Procedure B (GP-B) for the synthesis of α-substituted cyclobutanones

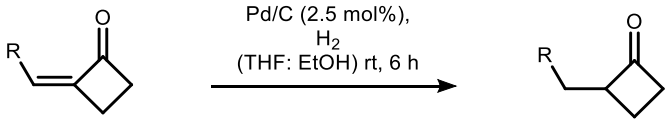

The *α*-substituted cyclobutanones were prepared following a literature protocol by Yang *et al.*[76] An oven dried round bottom flask under N_2 atmosphere was charged with Pd/C (5% on activated C, 2.35 mol%.). A solution of olefin in anhydrous THF:EtOH (4:1, 0.1 M) was added. The flask was purged with H_2 and the reaction mixture was stirred for 6 h at room temperature. The catalyst was removed by filtration through Celite® and elution with CH_2Cl_2. The filtrate was concentrated under reduced pressure and the product was obtained *via* flash column chromatography.

2-Benzylidenecyclobutan-1-one (2.26)

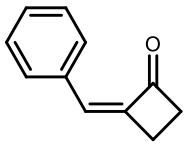

Following **GP-A** using benzaldehyde (1.0 mL, 1.06 g, 10.0 mmol, 1.00 eq.) the product **2.26** (687 mg, 4.34 mmol, 43%) was obtained *via* flash column chromatography (SiO_2, *n*-pentane:EtOAc, 95:5 to 90:10, stained with $KMnO_4$) as a light yellow solid.

^{1}H NMR (400 MHz, $CDCl_3$): δ = 7.55 – 7.49 (m, 2H), 7.45 – 7.37 (m, 3H), 7.04 (*app*. t, $J \approx 2.8$ Hz, 1H), 3.21 – 3.10 (m, 2H), 3.06 – 2.94 (m, 2H). **^{13}C NMR (101 MHz, $CDCl_3$)**: δ = 199.8, 146.3, 134.7, 130.3, 130.2, 129.1, 126.7, 45.9, 23.7. Spectroscopic data was in agreement to those previously reported.[77]

2-Benzylcyclobutan-1-one (2.23)

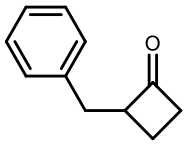

Following **GP-B** using olefin **2.25** (696 mg, 4.40 mmol, 1.00 eq.) the product **2.25** (358 mg, 2.23 mmol, 51%) was obtained *via* automated flash column chromatography (SiO_2, cyclohexane:EtOAc, 95:5, stained with $KMnO_4$) as colourless oil.

^{1}H NMR (400 MHz, $CDCl_3$): δ = 7.35 – 7.25 (m, 2H), 7.25 – 7.13 (m, 3H), 3.67 – 3.54 (m, 1H), 3.11 – 2.96 (m, 2H), 2.94 – 2.81 (m, 1H), 2.81 (dd, J = 14.1, 8.7 Hz, 1H), 2.23 – 2.09 (m, 1H), 1.75 (*app*. ddt, $J \approx 11.2$, 9.7, 7.7 Hz, 1H). **^{13}C NMR (101 MHz, $CDCl_3$)**: δ = 211.1, 139.0, 128.9, 128.7, 126.5, 61.4, 44.6, 35.3, 16.8. Spectroscopic data was in agreement to those previously reported.[147]

2-(2-Methoxybenzylidene)cyclobutan-1-one (2.27)

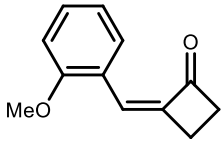

Following **GP-A** using 2-methoxybenzaldehyde (1.36 g, 10.0 mmol, 1.00 eq.) the olefin **2.27** (860 mg, 4.57 mmol, 46%) was obtained *via* automated flash column chromatography (SiO_2, *n*-hexane:EtOAc, 90:10, stained with $KMnO_4$) as yellow solid.

^{1}H NMR (400 MHz, $CDCl_3$): δ = 7.56 (dd, *J* = 7.8, 1.7 Hz, 1H), 7.53 (*app*. t, *J* ≈ 2.8 Hz, 1H), 7.36 (ddd, *J* = 8.3, 7.4, 1.7 Hz, 1H), 6.97 (*app*. t, *J* ≈ 7.6 Hz, 1H), 6.91 (d, *J* = 8.3 Hz, 1H), 3.86 (s, 3H), 3.15 – 3.08 (m, 2H), 2.99 – 2.92 (m, 2H). **^{13}C NMR (101 MHz, $CDCl_3$):** δ = 200.1, 159.4, 145.6, 131.7, 129.0, 123.6, 121.4, 120.7, 111.2, 55.7, 45.6, 23.6. Spectroscopic data was in agreement to those previously reported.[76]

2-(2-Methoxybenzyl)cyclobutanone (2.24)

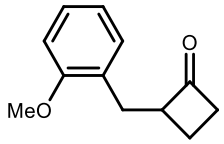

Following the **GP-B** using olefin **2.27** (860 mg, 4.57 mmol, 1.00 eq.) the product **2.24** (677 mg, 3.55 mmol, 77%) was obtained *via* automated flash column chromatography (SiO_2, cyclohexane:EtOAc, 95:5, stained with $KMnO_4$) as colourless oil.

^{1}H NMR (400 MHz, $CDCl_3$): δ = 7.21 (*app*. td, *J* ≈ 7.8, 1.8 Hz, 1H), 7.14 (dd, *J* = 7.4, 1.8 Hz, 1H), 6.89 (*app*. td, *J* ≈ 7.4, 1.1 Hz, 1H), 6.85 (dd, *J* = 8.2, 1.1 Hz, 1H), 3.81 (s, 3H), 3.70 – 3-60 (m, 1H), 3.08 (dd, *J* = 14.1, 5.6 Hz, 1H), 3.05 – 2.96 (m, 1H), 2.95 – 2.85 (m, 1H), 2.76 (dd, *J* = 14.1, 9.3 Hz, 1H), 2.16 – 2.04 (m, 1H), 1.78 – 1.68 (m, 1H). **^{13}C NMR (101 MHz, $CDCl_3$):** δ = 211.8, 157.6, 130.3, 127.7, 120.5, 110.3, 60.1, 55.3, 44.5, 30.0, 16.9. Spectroscopic data was in agreement to those previously reported.[148]

2-(Thiophen-2-ylmethylene)cyclobutan-1-one (2.28)

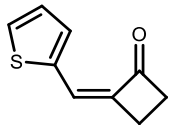

Following the **GP-A** using thiophen-2-carbaldheyde (1.12 g, 10.0 mmol, 1.00 eq.) the olefin **2.28** (963 mg, 5.10 mmol, 51%) was obtained *via* automated flash column chromatography (SiO_2, *n*-hexane:EtOAc, 90:10, stained with $KMnO_4$) as yellow solid.

^{1}H NMR (400 MHz, $CDCl_3$): δ = 7.51 (d, J = 5.1 Hz, 1H), 7.33 – 7.30 (m, 1H), 7.27 – 7.25 (m, 1H), 7.12 (dd, J = 5.1, 3.7 Hz, 1H), 3.15 – 3.07 (m, 2H), 2.89 – 2.83 (m, 2H). **^{13}C NMR (101 MHz, $CDCl_3$)**: δ = 198.9, 144.1, 139.1, 132.7, 130.3, 128.3, 119.6, 44.9, 23.1. Spectroscopic data was in agreement to those previously reported.[76]

2-(Thiophen-2-ylmethyl)cyclobutan-1-one (2.25)

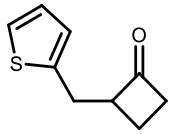

Following the **GP-B** using olefin **2.28** (820 mg, 5.00 mmol, 1.00 eq.) the product **2.25** (278 mg, 1.45 mmol, 29%) was obtained *via* automated flash column chromatography (SiO_2, cyclohexane:EtOAc, 80:20, stained with $KMnO_4$) as a yellow oil.

^{1}H NMR (400 MHz, $CDCl_3$): = 7.14 (dd, J = 5.1, 1.2 Hz, 1H), 6.93 (dd, J = 5.1, 3.4 Hz, 1H), 6.84 – 6.81 (m, 1H), 3.62 (m, 1H), 3.22 (dd, J = 15.4, 5.5 Hz, 1H), 3.14 – 2.96 (m, 2H), 2.95 – 2.84 (m 1H), 2.24 (*app*. dtd, $J \approx$ 11.3, 10.3, 5.1 Hz, 1H), 1.80 (*app*. ddt, $J \approx$ 11.3, 9.7, 7.7 Hz, 1H). **^{13}C NMR (101 MHz, $CDCl_3$):** δ = 210.2, 141.2, 127.1, 125.5, 123.9, 61.3, 44.8, 29.4, 16.7. Spectroscopic data was in agreement to those previously reported.[148]

Synthesis of iridium complex

[1,1'-Biphenyl]-2,2'-diyl bis(trifluoromethanesulfonate) (5.1)

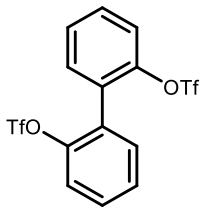

The title compound was prepared following a modified literature protocol by Tian *et al.*[79] In a Schlenk flask 2,2'-dihydroxybiphenyl (1.86 g, 10.0 mmol, 1.00 eq.) was dissolved in anhydrous CH_2Cl_2 (50 mL) under N_2 atmosphere. The stirring solution was cooled down with an ice/water bath, and *N*,*N*-diisopropylethylamine (5.23 mL, 3.88 g, 30.0 mmol, 3.00 eq.) was added. After 5 minutes triflic anhydride (Tf_2O) (4.20 mL, 7.05 g, 25.0 mmol, 2.50 eq.) was added dropwise. The reaction mixture was stirred at 0 °C for 3 h. The resulting mixture was washed with 1 M HCl (50 mL), saturated aqueous (sat. aq.) $NaHCO_3$ solution (50 mL) and brine (50 mL). The organic phase was dried over $MgSO_4$, filtered and the solvent was removed under reduced pressure. The product **5.1** (4.18 g, 9.30 mmol, 93%) was obtained *via* automated flash column chromatography (SiO_2, cyclohexane:EtOAc, 90:10, stained with $KMnO_4$) as colourless solid.

^{1}H NMR (400 MHz, $CDCl_3$): δ = 7.55 (ddd, J = 8.1, 7.2, 2.2 Hz, 2H), 7.51 (td, J = 7.4, 1.4 Hz, 2H), 7.48 – 7.45 (m, 2H), 7.43 (dd, J = 7.9, 1.4 Hz, 2H). **^{13}C NMR** (101 MHz, $CDCl_3$): δ = 146.9, 132.7, 130.9, 129.5, 128.7, 121.8, 118.8 (q, J = 320.3 Hz). Spectroscopic data was in agreement to those previously reported.[78]

2'-(Diphenylphosphoryl)-[1,1'-biphenyl]-2-yl trifluoromethanesulfonate (2.33)

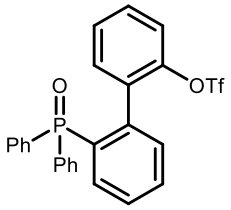

The title compound was prepared following a literature protocol by Tian *et al.*[79] In an oven dried Schlenk-flask 1,1'-biphenyl-2,2'-diyl bis(trifluoromethanesulfonate) (1.85 g, 4.10 mmol, 1.00 eq.), diphenylphosphine oxide (995 mg, 4.92 mmol, 1.20 eq.), $Pd(OAc)_2$ (46.0 mg, 205 µmol, 5 mol%) and dppb (87.4 mg, 205 µmol, 5 mol%) were dissolved in DMSO (20 mL) under N_2 atmosphere. *N*,*N*-Diisopropylethylamin (2.90 mL, 2.07 g, 16.0 mmol, 3.90 eq.) was added and the reaction mixture was stirred at 100 °C for 24 h. After cooling to room temperature, the mixture was diluted with CH_2Cl_2 (20 mL) and washed with 1 M HCl (20 mL), sat. aq. $NaHCO_3$ solution (20 mL) and brine (20 mL). The organic layer was dried over $MgSO_4$, filtered and the solvent was removed under reduced pressure. The product **2.33** was obtained *via* automated flash column chromatography (SiO_2, cyclohexane:EtOAc, 10:90, stained with $KMnO_4$) as a colourless powder (1.79 g, 3.57 mmol, 87%).

^{1}H NMR (400 MHz, $CDCl_3$): δ = 7.67 (ddd, J = 11.7, 8.3, 1.5 Hz, 2H), 7.62 – 7.56 (m, 1H), 7.55 – 7.35 (m, 10H), 7.33 – 7.27 (m, 2H), 7.26 – 7.19 (m, 2H), 6.95 – 6.86 (m, 1H).[a] Spectroscopic data was in agreement to those previously reported.[78]

[a] ^{13}C NMR was not assigned since ^{13}C NMR experiments with ^{31}P decoupling could not be performed on the NMR instruments.

2'-(Diphenylphosphoryl)-*N*-((1*S*,2*R*)-2-hydroxy-2,3-dihydro-1*H*-inden-1-yl)-[1,1'-biphenyl]-2-carboxamide (2.34)

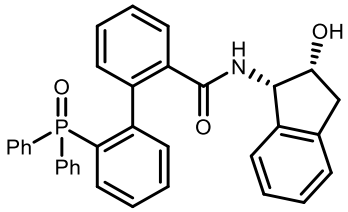

The title compound was prepared following a modified literature protocol by Xia *et al.*[77] A Schlenk flask was charged with $Pd(OAc)_2$ (105 mg, 472 µmol, 15 mol%) and dppp (193 mg, 472 µmol, 0.15 eq.). The flask was flushed with N_2 and *N*,*N*-diisopropylamine (1.52 mL, 1.13 g, 8.75 mmol, 2.80 eq.), a solution of the triflate **2.33** (1.57 g, 3.12 mmol, 1.00 eq.) and (1*S*,2*R*)-1-amino-2,3-dihydro-1H-inden-2-ol (699 mg, 4.69 mmol, 1.50 eq.) in DMSO (12 mL) were added. A double balloon was added and a second Schlenk tube was connected to the main reaction chamber by a short piece of rubber tubing. The second Schlenk tube was charged with sulfuric acid (0.42 mL, 766 mg, 7.81 mmol, 2.50 eq.) and heated to 70 °C. Formic acid (0.24 mL, 288 mg, 6.25 mmol, 2.00 eq.) was added dropwise to the second Schlenk tube. Carbon monoxide formation was observed by inflation of the balloon. After flushing the main reaction chamber with the generated carbon monoxide, the reaction mixture was heated to 110 °C for 18 h. The mixture was allowed to cool down to room temperature and water (15 mL) was added. After extraction with CH_2Cl_2 (3 × 15 mL) the combined organic phases were washed with brine (3 × 15 mL), dried over $MgSO_4$, filtered and the solvent was removed under reduced pressure. The product **2.34** (1.24 g, 2.34 mmol, 75%, 53:47 dr) the product *via* automated flash column chromatography (SiO_2, CH_2Cl_2:MeOH, 95:5, stained with $KMnO_4$) as colourless powder.

^{1}H NMR (400 MHz, $CDCl_3$): δ = 9.49 (d, *J* = 9.3 Hz, 1H), 8.77 (d, *J* = 7.2 Hz, 1H), 7.75 – 7.32 (m, 20H), 7.25 – 7.11 (m, 7H), 7.07 (ddd, *J* = 13.9, 7.5, 1.4 Hz, 1H), 6.99 – 6.85 (m, 3H), 6.81 – 6.69 (m, 3H), 6.19 (d, *J* = 7.7 Hz, 1H), 6.12 (d, *J* = 7.8 Hz, 1H), 5.72 (d, *J* = 7.5 Hz, 1H), 5.49 (dd, *J* = 9.3, 4.9 Hz, 1H), 5.34 (dd, *J* = 7.2, 4.6 Hz, 1H), 4.66 – 4.60 (m, 1H), 4.58 – 4.49 (m, 1H), 3.11 – 2.94 (m, 3H), 2.78 (dd, *J* = 16.3, 2.0 Hz, 1H).[a] Spectroscopic data was in agreement to those previously reported.[77]

[a] ^{13}C NMR was not assigned since ^{13}C NMR experiments with ^{31}P decoupling could not be performed on the NMR instruments.

(2'-((3a*S*,8a*R*)-3a,8a-Dihydro-8*H*-indeno[1,2-d]oxazol-2-yl)-[1,1'-biphenyl]-2-yl)diphenylphosphine oxide (5.2)

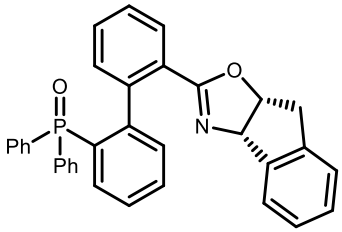

The title compound was prepared following a modified literature protocol by Xia *et al.*[77] In a round bottom flask methane sulfonic acid (370 µL, 544 mg, 5.60 mmol, 6.00 eq.) was slowly added to a stirring solution of **2.34** (500 mg, 900 µmol, 1.00 eq.) in 1,2-dichloroethane (5.0 mL) at 0 °C. After stirring for 30 minutes at 0 °C the reaction mixture was heated to 85 °C for 24 h. The reaction was quenched with water (10 mL) and extracted with CH_2Cl_2 (3 × 10 mL). The combined organic phases were washed with brine (3 × 10 mL), dried over $MgSO_4$, filtered and concentrated under reduced pressure. The product **5.2** (248 mg, 485 µmol, 51%, 64:36 dr) the product *via* flash column chromatography (SiO_2, CH_2Cl_2:MeOH, 97:3, stained with CAM) as white foam.

^{1}H NMR (300 MHz, $CDCl_3$): δ = 7.70 – 6.89 (m, 31H), 5.51 (dd, J = 7.7, 3.3 Hz, 1H), 5.18 (ddd, J = 8.1, 6.9, 1.5 Hz, 1H), 5.03 (ddd, J = 7.7, 6.5, 1.3 Hz, 1H), 3.39 – 3.06 (m, 3H), 2.69 (d, J = 17.9 Hz, 1H).[a] Spectroscopic data was in agreement to those previously reported.[77]

[a] ^{13}C NMR was not assigned since ^{13}C NMR experiments with ^{31}P decoupling could not be performed on the NMR instruments.

(3a*S*,8a*R*)-2-(2'-(diphenylphosphaneyl)-[1,1'-biphenyl]-2-yl)-3a,8a-dihydro-8*H*-indeno[1,2-d]oxazole (2.31)

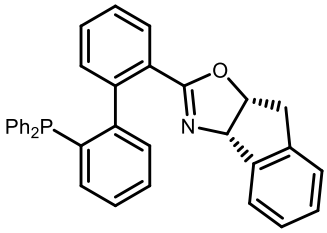

The title compound was prepared following a literature protocol by Xia *et al.*[77] In a Schlenk flask under N_2 atmosphere phosphine oxide **5.2** was dissolved in anhydrous and degassed toluene. NEt_3 and trichlorosilane were added, and the mixture was stirred at 110 °C for 16 h. After cooling to 0 °C, the reaction was quenched with an aqueous solution of $NaHCO_3$ (4 M). The phases were separated, and the aqueous layer was extracted with CH_2Cl_2 (3 × 5 mL). The combined organic phase was washed with water (3 × 5 mL) and brine (3 × 5 mL), dried over $MgSO_4$, filtered and concentrated under reduced pressure. The product **2.31** (87.0 mg, 176 µmol, 88%, 60:40 dr) the product *via* automated flash column chromatography (SiO_2, CH_2Cl_2:MeOH, 95:5, stained with $KMnO_4$) as colourless solid.

^{1}H NMR (400 MHz, $CDCl_3$): δ = 7.82 (ddd, J = 6.8, 5.2, 1.4 Hz, 1H), 7.47 – 7.40 (m, 2H), 7.35 – 7.01 (m, 30H), 6.99 – 6.90 (m, 3H), 6.89 – 6.81 (m, 2H), 6.76 (dd, J = 7.7, 1.3 Hz, 1H), 5.54 (dd, J = 8.0, 3.7 Hz, 2H), 5.15 (ddd, J = 8.0, 7.1, 1.7 Hz, 1H), 5.03 (ddd, J = 8.2, 7.1, 1.8 Hz, 1H), 3.25 – 3.08 (m, 2H), 2.75 (d, J = 18.0 Hz, 1H), 2.40 (d, J = 17.9 Hz, 1H).[a] Spectroscopic data was in agreement to those previously reported.[77]

[a] ^{13}C NMR was not assigned since ^{13}C NMR experiments with ^{31}P decoupling could not be performed on the NMR instruments.

[Ir(2.31)cod]BAr$_F$ (2.30)

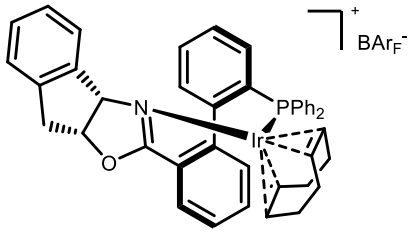

The title compound was prepared following a literature protocol by Xia *et al.*[77] In a Schlenk flask under N_2 atmosphere ligand **2.31** (50.0 mg, 100 µmol, 1.30 eq.) was dissolved in anhydrous CH_2Cl_2 (2.5 mL). $[Ir(cod)Cl]_2$ (50.0 mg, 1.00 µmol, 0.75 eq.) was added and the mixture was stirred at reflux for 3 h. After cooling to room temperature NaBArF (139 mg, 156 µmol, 2.10 eq.) was added followed by water (0.5 mL). The resulting mixture was stirred at room temperature for 1 h. CH_2Cl_2 (10 mL) was added and the organic phase was washed with brine (3 × 10 mL). The organic layer was dried over $MgSO_4$, filtered and concentrated under reduced pressure. The product **2.30** (118 mg, 71.0 µmol, 95%) the product *via* filtration through a short pad of silica eluting CH_2Cl_2 as orange solid.

^{1}H NMR (400 MHz, $CDCl_3$): δ = 8.08 (d, J = 7.4 Hz, 1H), 7.75 – 7.70 (m, 8H), 7.59 – 7.48 (m, 6H), 7.47 – 7.31 (m, 7H), 7.23 – 7.05 (m, 7H), 7.01 (td, J = 7.6, 1.5 Hz, 1H), 6.78 – 6.68 (m, 3H), 5.95 (d, J = 7.7 Hz, 1H), 5.71 (d, J = 8.4 Hz, 1H), 5.54 (td, J = 8.3, 3.9 Hz, 1H), 5.43 – 5.36 (m, 1H), 4.45 (p, J = 7.0 Hz, 1H), 3.14 (dd , J = 18.6, 8.3 Hz, 1H), 3.08 – 2.01 (m, 1H), 3.00 – 2.92 (m, 1H), 2.39 – 2.18 (m, 3H), 2.07 – 1.87 (m, 3H), 1.72 (d, J = 18.2, 3.9 Hz , 1H), 1.67 – 1.58 (m, 1H), 1.49 – 1.38 (m, 1H).[a] **^{31}P NMR** (162 MHz, $CDCl_3$): δ = 18.8. Spectroscopic data was in agreement to those previously reported.[77]

[a] ^{13}C NMR was not assigned since ^{13}C NMR experiments with ^{31}P decoupling could not be performed on the NMR instruments.

Synthesis of cyclobutanones

(*S*)-2-Benzylcyclobutan-1-one ((*S*)-2.23)

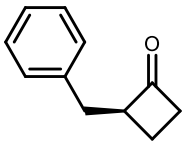

Following a modified literature protocol by Xia *et al.*[77] a round bottom flask under N_2 atmosphere was charged with complex **2.30** (12.0 mg, 75.0 µmol, 1 mol%). A solution of 2-benzylidenecyclo-butanone **2.26** (118 mg, 750 µmol, 1.00 eq.) in anhydrous CH_2Cl_2 (6.0 mL) was added. The reaction mixture was purged with H_2 and stirred at room temperature for 6 h. The catalyst was removed by filtration through Celite® and elution with CH_2Cl_2. The filtrate was concentrated under reduced pressure and the desired product (*S*)-**2.23** (59.2 mg, 326 µmol, 49%) the product *via* automated flash column chromatography (SiO_2, cyclohexane:EtOAc, 95:5, stained with $KMnO_4$) as colourless oil.

^{1}H NMR (400 MHz, $CDCl_3$): δ = 7.34 – 7.26 (m, 2H), 7.25 – 7.15 (m, 3H), 3.68 – 3.52 (m, 1H), 3.11 – 2.96 (m, 2H), 2.95 – 2.74 (m, 2H), 2.16 (*app*. dtd, $J \approx$ 11.2, 10.2, 5.2 Hz, 1H), 1.75 (*app*. ddt, $J \approx$ 11.2, 9.7, 7.7 Hz, 1H). **^{13}C NMR (101 MHz, $CDCl_3$):** δ = 211.1, 139.0, 128.9, 128.7, 126.5, 61.4, 44.6, 35.3, 16.8. **Optical Rotation**: $[\alpha]_D^{25}$ = −62.8 (*c* = 0.5, $CHCl_3$) for an enantiomerically enriched sample of 95:5 *er*. The enantiomeric purity was established by HPLC analysis using a chiral column (Lux® i-Amylose-3, 22 °C, 1 mL/min, 99:1 *n*-hexane : isopropanol, 210 nm, t = 9.454 min and 10.157 min). The absolute configuration was determined by comparison the optical rotation with reported data.[77] Spectroscopic data was in agreement to those previously reported.[77]

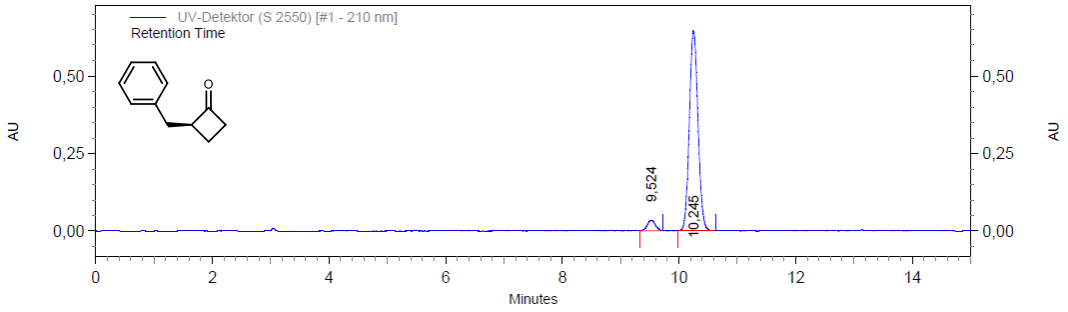

UV-Detektor (S 2550) [#1 - 210 nm] Results

Retention Time	Area	Area %
9,524	331817	4,73
10,245	6679214	95,27

Figure 4. HPLC chromatogram for (*S*)-2-benzylcyclobutan-1-one ((*S*)-2.23)

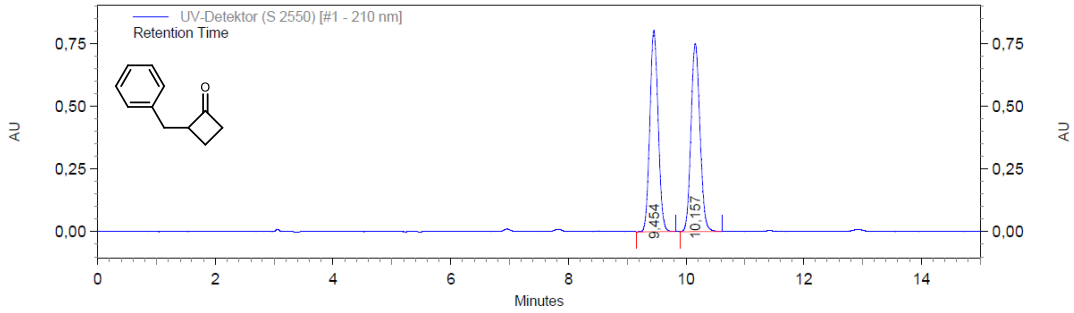

UV-Detektor (S 2550) [#1 - 210 nm] Results

Retention Time	Area	Area %
9,454	7897980	49,81
10,157	7958760	50,19

Figure 5. HPLC chromatogram for 2-benzylcyclobutan-1-one (2.23)

2,2-Dimethyl-3-phenylcyclobutan-1-one (2.35)

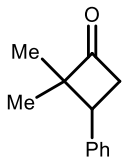

The cyclobutanone was prepared following a literature protocol by Flamagne *et al.*[84] In a Schlenk tube *N*,*N*-dimethylisobutyramide (1.38 g, 12.0 mmol, 1.20 eq.) was dissolved in 1,2-dichloroethane (24 mL). The solution was cooled with a water bath and Tf_2O (3.36 mL, 5.64 g, 20.0 mmol, 2.00 eq.) was added dropwise. After stirring the reaction mixture at room temperature for 10 minutes, a solution of styrene (2.62 mL, 1.04 g, 10.0 mmol, 1.00 eq.) and 2,6-lutidine (2.32 mL, 2.14 g, 20.0 mmol, 2.00 eq.) in 1,2-dichloroethane (5.0 mL) was added dropwise. The resulting mixture was stirred at 90 °C for 8 h. The mixture was allowed to cool to room temperature and water (30 mL) was added. The resulting mixture was stirred at 90 °C for 16 h. After cooling to room temperature, the layers were separated, and the aqueous layer was extracted with CH_2Cl_2 (4 × 50 mL). The combined organic layers were dried over $MgSO_4$, filtered and the solvent was removed under reduced pressure. The product **2.35** (1.57 g, 9.01 mmol, 90%) the product *via* bulb-to-bulb distillation (0.1 mbar, 95 °C) as colourless solid.

^{1}H NMR (400 MHz, $CDCl_3$): δ = 7.40 – 7.32 (m, 2H), 7.26 (tt, J = 7.0, 1.4 Hz, 1H), 7.22 – 7.18 (m, 2H), 3.52 – 3.38 (m, 2H), 3.29 (dd, J = 15.6, 7.7 Hz, 1H), 1.36 (s, 3H), 0.79 (s, 3H).**^{13}C NMR (101 MHz, $CDCl_3$):** δ = 213.8, 139.0, 128.6, 127.8, 126.8, 63.9, 46.1, 41.6, 23.6, 19.0. Spectroscopic data was in agreement to those previously reported.[149]

2-(2-Iodophenyl)-*N,N*-diisopropylacetamide (2.40)

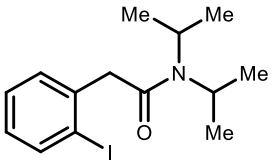

The product was prepared following a modified literature protocol by Lachia *et al.*[150] In a Schlenk flask under N_2 atmosphere 2-iodophenylacetic acid (1.31 g, 5.00 mmol, 1.00 eq.) was dissolved in anhydrous CH_2Cl_2 (10 mL). Oxalyl chloride (0.86 mL, 1.27 g, 10.0 mmol, 2.00 eq.) was slowly added to the solution, followed by two drops of DMF. The reaction mixture was stirred at room temperature for 2 h. The solvent was removed under reduced pressure. The residue was redissolved in anhydrous CH_2Cl_2 (12 mL) and the solution was cooled down to 0 °C with an ice/water bath. Diisopropylamine (2.11 mL, 3.94 g, 30.0 mmol, 3.00 eq.) was added dropwise. The reaction mixture was stirred for 16 h while warming to room temperature. Water was added and the layers were separated. The aqueous phase was extracted with CH_2Cl_2 (3 × 20 mL). The combined organic layer was washed with 1 M HCl (3 × 20 mL) and brine (3 × 20 mL), dried over $MgSO_4$, filtered, and concentrated under reduced pressure. The product **2.40** (1.50 g, 4.35 mmol, 86%) the product *via* automated flash column chromatography (SiO_2, cyclohexane:EtOAc, 90:10, stained with $KMnO_4$) as slightly yellow solid.

^{1}H NMR (400 MHz, $CDCl_3$): δ = 7.83 (d, J = 8.1 Hz, 1H), 7.34 – 7.27 (m, 2H), 6.93 (ddd, J = 7.9, 6.3, 2.8 Hz, 1H), 3.94 – 3.87 (m, 1H), 3.76 (s, 2H), 3.49 – 3.35 (m, 1H), 1.43 (d, J = 6.8 Hz, 6H), 1.14 (d, J = 6.7 Hz, 6H). **^{13}C NMR (101 MHz, $CDCl_3$):** δ = 169.0, 139.5, 139.5, 130.0, 128.5, 128.5, 101.5, 49.5, 48.0, 46.1, 20.9, 20.7. Spectroscopic data was in agreement to those previously reported.[150]

2-(2-Allylphenyl)-*N,N*-diisopropylacetamide (2.39)

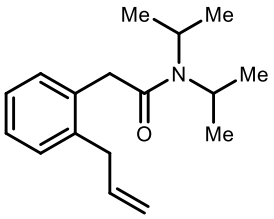

The product was prepared following a modified literature protocol by Lachia *et al.*[150] A Schlenk flask under N_2 atmosphere was charged with 2-(2-iodophenyl)-*N,N*-diisopropylacetamide **2.40** (1.04 g, 3.00 mmol, 1.00 eq.) and anhydrous toluene (30 mL). Allyltributylstannane (1.40 mL, 1.49 g, 4.50 mmol, 1.50 eq.) and tetrakis-(triphenylphosphine)-palladium (173 mg, 0.150 mmol, 5 mol%) was added to the solution. The reaction mixture was stirred at 110 °C for 20 h. The solvent was removed under reduced pressure. The residue was partitioned between *n*-hexane (20 mL) and acetonitrile (20 mL). The acetonitrile phase was

washed with *n*-hexane (3 × 20 mL) and concentrated under reduced pressure. The product **2.39** (555 mg, 2.13 mmol, 71%) the product *via* flash column chromatography (SiO_2, cyclohexane:EtOAc, 90:10, stained with $KMnO_4$) as yellow oil.

^{1}H NMR (400 MHz, $CDCl_3$): δ = 7.21 – 7.14 (m, 4H), 5.94 (ddt, *J* = 17.2, 10.1, 6.2 Hz, 1H), 5.07 (*app.* dq, *J* ≈ 10.1, 1.6 Hz, 1H), 4.98 (*app.* dq, *J* ≈ 17.0, 1.7 Hz, 1H), 3.84 (*app.* p, *J* ≈ 6.7 Hz, 1H), 3.65 (s, 2H), 3.47 – 3.37 (m, 1H), 3.35 (dt, *J* = 6.2, 1.7 Hz, 2H), 1.44 (d, *J* = 6.8 Hz, 6H), 1.07 (d, *J* = 6.7 Hz, 6H). **^{13}C NMR (101 MHz, $CDCl_3$):** δ = 170.1, 137.7, 136.8, 134.5, 130.0, 129.1, 127.1, 126.8, 115.9, 49.3, 46.0, 40.3, 37.7, 20.8, 20.7. Spectroscopic data was in agreement to those previously reported.[150]

1,2a,7,7a-Tetrahydro-2*H*-cyclobuta[a]inden-2-one (2.12)

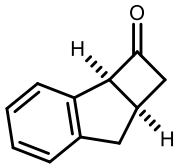

The product was prepared following a modified literature protocol by Lachia *et al.*[150] A Schlenk tube under N_2 atmosphere was charged with 2-(2-allylphenyl)-*N,N*-diisopropylacetamide **2.39** (260 mg, 1.00 mmol, 1.00 eq.) and 1,2-dichloroethane (10 mL). 2,6-Lutidine (140 µL, 129 mg, 1.20 eq., 1.20 mmol) and Tf_2O (180 µL, 310 mg, 1.10 eq., 1.10 mmoL) were added to the solution. The reaction mixture was stirred at 90 °C for 8 h. After cooling to room temperature an aqueous solution of K_2CO_3 (10%, 10 mL) was added, and the mixture was stirred at 90 °C for 16 h. The phases were separated, and the aqueous phase was extracted with CH_2Cl_2 (3 × 15 mL). The combined organic phase was dried over $MgSO_4$, filtered and concentrated under reduced pressure. The desired product **2.12** (58.0 mg, 370 µmol, 37%) the product *via* flash column chromatography (SiO_2, cyclohexane:EtOAc, 95:5, stained with $KMnO_4$) as colourless oil.

^{1}H NMR (400 MHz, $CDCl_3$): δ = 7.35 – 7.27 (m, 2H), 7.29 – 7.22 (m, 2H), 4.75 – 4.68 (m, 1H), 3.45 (dd, *J* = 16.9, 8.2 Hz, 1H), 3.35 (dd, *J* = 18.3, 4.9 Hz, 1H), 3.18 – 3.10 (m, 1H), 3.07 (d, *J* = 16.9, 1H), 2.87 (dd, *J* = 18.1, 3.2 Hz, 1H). **^{13}C NMR (101 MHz, $CDCl_3$):** δ = 206.5, 143.2, 137.7, 128.1, 127.5, 125.9, 125.3, 72.6, 53.1, 39.8, 26.9. Spectroscopic data was in agreement to those previously reported.[150]

2,2a,7,7a-Tetrahydro-1*H*-cyclobuta[a]inden-1-one (2.45)

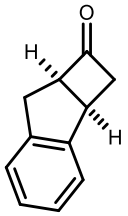

The title compound **2.45** was prepared *via* a two step procedure. First, the dichlorinated cyclobutanone was prepared following a literature protocol by Lu *et al.*[88]. To an oven dried Schlenk flask Zn powder (2.00 eq.) was suspended in anhydrous Et_2O (1.3 M) under inert atmosphere. Indene (1.00 eq.) was added and the flask was placed into a sonication bath. The mixture was irradiated with ultrasound, while a solution of trichloroacetyl chloride (1.50 eq.) in Et_2O (2.0 M) was added dropwise over a period of 40 min. The sonication bath was cooled by adding ice to maintain a temperature of <25 °C. Once the addition was completed, the mixture was kept under sonication. The progress of the reaction was monitored by TLC. The mixture was diluted with Et_2O (20 mL) and the solids were filtered off through a pad of Celite® and washed with Et_2O. The filtrate was washed with water (2 × 50 mL), an sat. aq. $NaHCO_3$ solution (4 × 50 mL) and brine. The organic phase was dried over $MgSO_4$, filtered and concentrated under reduced pressure. The crude reaction mixture was used without further purification.

In a round bottom flask, the crude reaction mixture of the first step was dissolved in glacial acetic acid (20 mL). The solution was cooled with a water bath and Zn dust (4.00 eq.) was slowly added. The reaction mixture was heated to 80 °C for 16 h. After cooling to room temperature, the mixture was filtered through a pad of Celite® and washed with CH_2Cl_2. The solvent was removed under reduced pressure. The residue was redissolved in Et_2O (20 mL), and the organic layer was washed with water (3 × 20 mL), sat. aq. $NaHCO_3$ solution (3 × 20 mL) and brine (3 × 20 mL). The organic phase was dried over $MgSO_4$, filtered and the solvent was removed under reduced pressure. The product **2.45** (487 mg, 3.08 mmol, 31%) was obtained as colourless oil by bulb-to-bulb distillation (0.1 mbar, 90 °C).

^{1}H NMR (400 MHz, $CDCl_3$): δ = 7.33 – 7.27 (m, 1H), 7.26 – 7.18 (m, 3H), 4.13 – 4.00 (m, 2H), 3.68 – 3.54 (m, 1H), 3.31 (*app.* dt, $J \approx 16.9$, 1.5 Hz, 1H), 3.18 – 3.04 (m, 1H), 2.96 – 2.83 (m, 1H). **^{13}C NMR (101 MHz, $CDCl_3$):** δ = 212.4, 144.7, 143.2, 127.6, 127.5, 125.5, 125.2, 62.9, 55.8, 36.7, 34.1. Spectroscopic data was in agreement to those previously reported.[151]

Synthesis of cyclopentanone

4-Hydroxy-3,4-diphenylcyclopent-2-en-1-one (5.3)

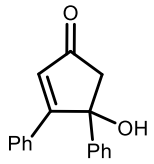

According to a procedure by *Müller et al.*,[91] an aqueous solution of KOH (32%, 0.3 mL) was added to a solution of benzil (15.0 g, 71.3 mmol, 1.00 eq.) in acetone (12.2 mL, 165 mmol, 2.32 eq.). The reaction mixture was stirred for 5 minutes at room temperature and another portion of aqueous KOH (32%, 6.0 mL) was added. After stirring for 1 h under reflux, the reaction mixture was allowed to cool to room temperature and poured into water (50 mL). The aqueous phase was extracted with CH2Cl2 (3 × 50 mL) and the combined organic layers were dried over $MgSO_4$, filtered and concentrated under reduced pressure. The product **5.3** (13.1 g, 52.3 mmol, 73%) was obtained *via* recrystallisation from toluene as yellow solid.

^{1}H NMR (400 MHz, $CDCl_3$): δ = 7.54 – 7.49 (m, 2H), 7.48 – 7.43 (m, 2H), 7.39 – 7.32 (m, 3H), 7.32 – 7.25 (m, 3H), 6.71 (s, 1H), 3.02 (d, J = 18.5 Hz, 1H), 2.90 (d, J = 18.5 Hz, 1H), 2.65 (s, 1H). **^{13}C NMR (101 MHz, $CDCl_3$):** δ = 204.8, 173.9, 144.2, 131.4, 131.1, 129.3, 129.2, 129.0, 129.0, 127.7, 124.3, 81.8, 56.7. Spectroscopic data was in agreement to those previously reported.[91]

4-Chloro-3,4-diphenylcyclopent-2-en-1-one (2.47)

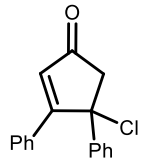

According to a procedure by *Müller et al.*,[91] a solution of 4-hydroxy-3,4-diphenylcyclopent-2-en-1-one **5.3** (6.23 g, 25.0 mmol, 1.00 eq.) in acetyl chloride (25 mL) was stirred for 16 h at 50 °C. The reaction mixture was allowed to cool to room temperature and the solvent was removed under reduced pressure. The crude product was redissolved in toluene and hexane was added until precipitation. The product **2.47** (2.54 g, 9.45 g, 38%) the product *via* filtration and wash with cold hexane as colourless solid.

^{1}H NMR (300 MHz, $CDCl_3$): δ = 7.57 – 7.46 (m, 4H), 7.42 – 7.27 (m, 6H), 6.86 (s, 1H), 3.49 (d, J = 19.0 Hz, 1H), 3.09 (d, J = 19.0 Hz, 1H). **^{13}C-NMR (101 MHz, $CDCl_3$)** δ = 202.6, 172.6, 142.5, 131.3, 131.2, 130.2, 129.8, 129.2,

128.8, 128.4, 125.9, 74.2, 59.7. Spectroscopic data was in agreement to those previously reported.[91]

3,4-Diphenylcyclopent-3-en-1-one (5.4)

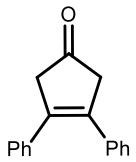

According to a procedure by *Müller et al.*,[91] a solution of 4-chloro-3,4-diphenylcyclopent-2-enone **2.47** (2.54 mg, 9.45 mmol, 1.00 eq.) in Et_2O (70 mL) was added to a suspension of zinc dust (20.7 g, 316 mmol, 33.5 eq.) in Et_2O (95 mL) and AcOH (5.0 mL). After stirring for 30 min at room temperature, the reaction mixture was filtered over a plug of Celite® and washed with Et_2O. The organic phase was washed with water (3 × 50 mL) and a sat. aq. $NaHCO_3$-solution, dried over $MgSO_4$, filtered and concentrated under reduced pressure. The product **5.4** (2.03 g, 8.64 mmol, 91%) was obtained without further purification as colourless solid.

^{1}H NMR (400 MHz, $CDCl_3$): δ = 7.26 – 7.14 (m, 10H), 3.49 (s, 4H). **^{13}C NMR (101 MHz, $CDCl_3$):** δ = 214.2, 136.5, 134.5, 128.6, 128.3, 127.7, 49.1. Spectroscopic data was in agreement to those previously reported.[91]

(*cis*)-3,4-Diphenylcyclopentan-1-one (2.46)

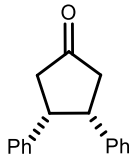

According to a procedure by *Müller et al.*,[91] a suspension of 3,4-diphenylcyclopent-3-enone **5.6** (996 mg, 4.25 mmol, 1.00 eq) and Pd/C (10%, 453 mg, 0.425 mmol) in EtOAc (22 mL) was stirred under an atmosphere of H_2 (balloon) for 4 h at room temperature. The reaction mixture was filtered over a plug of Celite®, washed with EtOAc and the solvent was removed under reduced pressure. The product **2.46** (904 mg, 3.83 mmol, 90%) was obtained *via* flash column chromatography (SiO_2, cyclohexane:EtOAc 90:10) as a colourless solid.

^{1}H NMR (400 MHz, $CDCl_3$): δ = 7.16 – 7.05 (m, 6H), 6.77 – 6.68 (m, 4H), 3.86 (ddt, J = 9.3, 6.0, 3.0 Hz, 2H), 2.86 – 2.61 (m, 4H). **^{13}C NMR (101 MHz, $CDCl_3$):** δ = 218.9, 139.5, 128.1, 128.1, 126.8, 47.5, 43.4. Spectroscopic data was in agreement to those previously reported.[91]

5.2.2 Investigation of the nitrogen insertion

General Procedure C (GP-C) for the ring-expansion of cyclobutanones to γ-lactams

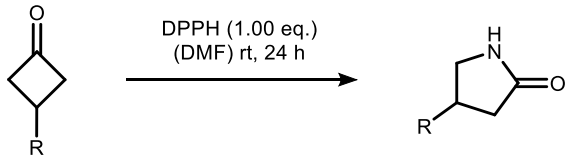

An oven dried tube was charged with *O*-(diphenylphosphinyl)hydroxylamine **2.51** (550 µmol, 1.10 eq.) and suspended in DMF (1.5 mL, 0.33 M). The corresponding cyclobutanone (500 µmol, 1.00 eq.) was dissolved in DMF (1.0 mL, 0.50 M) and added to the mixture. The mixture was stirred at room temperature for 24 h. The solvent was concentrated under reduced pressure and NMR yield of the crude reaction mixture was determined by ^{1}H NMR using dibromomethane (35.0 µL, 86.9 mg, 500 µmol) as the internal standard. The product was separated from the corresponding oxime byproduct by silica gel column chromatography.

General Procedure D (GP-D) for the ring-expansion of cyclobutanones to γ-lactones

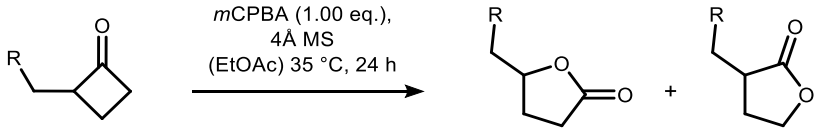

An oven dried tube was charged with 4 Å MS (150 mg), *m*CPBA (123 mg, 550 µmol, 1.10 eq.) in EtOAc (1.5 mL). A solution of cyclobutanone (500 µmol, 1.00 eq.) in EtOAc (1.0 mL) was added dropwise to the reaction and the mixture was stirred at 35 °C for 24 h. A sat. aq. K_2CO_3 solution (50 mL) was added, and the aqueous phase was extracted with CH_2Cl_2 (3 × 25 mL). The combined organic phases were dried over $MgSO_4$, filtered and the solvent was removed under reduced pressure.

3,3a,8,8a-Tetrahydroindeno[2,1-b]pyrrol-2(1*H*)-one, 3,3a,8,8a-tetrahydroindeno[1,2-c]pyrrol-1(2*H*)-one (2.14)

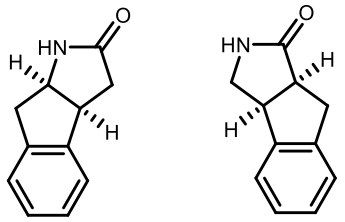

major minor

Following **GP-C** using 2,2a,7,7a-tetrahydro-1H-cyclobuta[a]inden-1-one **2.14** (79.1 mg, 500 µmol, 1.00 eq.) a mixture of regioisomers (82:18, 71.2 mg, 411 µmol, 83%) was obtained *via* flash column chromatography (SiO_2, EtOAc:MeOH, 95:5, stained with $KMnO_4$) as a white solid.

M.P.: 98 – 101 °C. **IR (neat)**: $\tilde{\nu}$ = 2358 (br), 1682 (s), 1458 (w), 1381 (w), 1310 (w), 1263 (m), 1060 (w), 750 (s).
Major regioisomer: ^{1}H NMR (400 MHz, $CDCl_3$): δ = 7.25 – 7.18 (m, 4H), 6.91 (s, 1H), 3.25 – 3.15 (m, 3H), 2.95 (d, *J* = 16.9 Hz, 1H), 2.85 (dd, *J* = 17.1, 9.3 Hz, 1H), 2.48 (dd, *J* = 17.1, 1.7 Hz, 1H). **^{13}C NMR (101 MHz, $CDCl_3$)**: δ = 177.4, 144.2, 140.5, 127.9, 127.5, 125.4, 124.8, 58.1, 45.0, 39.7, 37.3.
Minor regioisomer: ^{1}H NMR (400 MHz, $CDCl_3$): δ = 7.22 – 7.18 (m, 4H), 6.64 (s, 1H), 3.98 – 3.93 (m, 1H), 3.85 (dd, J = 9.7, 7.3 Hz, 1H), 3.49 (dt, *J* = 9.7, 1.3 Hz, 1H), 3.36 (d, *J* = 14.9 Hz, 1H), 3.25 (d *J* = 8.9 Hz, 1H), 3.21 – 3.19 (m, 1H). **^{13}C NMR (101 MHz, $CDCl_3$)**: δ = 180.4, 144.0, 142.2, 127.9, 127.2, 125.0, 124.0, 47.8, 44.7, 44.7, 34.9. Spectroscopic data of the major regioisomer was in agreement to those previously reported.[150]

5-Benzyldihydrofuran-2(3H)-one and 3-Benzyldihydrofuran-2(3H)-one (2.54)

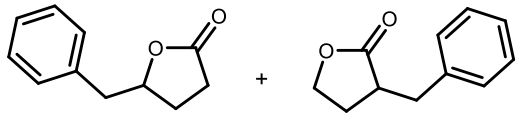

major minor

Following **GP-D** using 2-benzylcyclobutan-1-one **2.23** (80.1 mg, 500 µmol, 1.00 eq.) and *m*CPBA (123 mg, 550 µmol, 1.10 eq.) the major regioisomer **2.54** (76.7 mg, 435 µmol, 87%) and the minor regioisomer (2.2 mg, 12.5 µmol, 2%) were obtained *via* flash column chromatography (SiO_2, *n*-pentane:EtOAc, 80:20 to 70:30, stained with $KMnO_4$) both as colourless oil.

Major regioisomer: ^{1}H NMR (400 MHz, $CDCl_3$): δ = 7.36 – 7.29 (m, 2H), 7.29 – 7.20 (m, 3H), 4.74 (*app*. dq, $J \approx 7.5$, 6.3 Hz, 1H), 3.08 (dd, J = 14.0, 6.1 Hz, 1H), 2.93 (dd, J = 14.0, 6.3 Hz, 1H), 2.54 – 2.30 (m, 2H), 2.26 (dddd, J = 12.8, 9.5, 6.7, 4.7 Hz, 1H), 2.04 – 1.87 (m, 1H). **^{13}C NMR (101 MHz, $CDCl_3$):** δ = 177.2, 136.0, 129.6, 128.8, 127.1, 80.9, 41.4, 28.8, 27.3.
Minor regioisomer: ^{1}H NMR (400 MHz, $CDCl_3$): δ = 7.35 – 7.28 (m, 2H), 7.25 – 7.17 (m, 3H), 4.23 (*app*. td, $J \approx 8.8$, 3.1 Hz, 1H), 4.15 (*app*. td, $J \approx 9.3$, 6.7 Hz, 1H), 3.26 (dd, J = 13.6, 4.0 Hz, 1H), 2.90 – 2.80 (m, 1H), 2.76 (dd, J = 13.6, 9.4 Hz, 1H), 2.31 – 2.20 (m, 1H), 2.07 – 1.92 (m, 1H). **^{13}C NMR (101 MHz, $CDCl_3$):** δ = 178.9, 138.6, 129.0, 128.9, 126.9, 66.7, 41.3, 36.3, 28.2. Spectroscopic data was in agreement to those previously reported.[152]

5-Benzylpyrrolidin-2-one, 3-Benzylpyrrolidin-2-one (2.55)

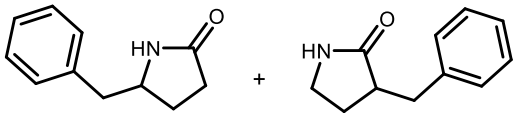

major minor

Following the **GP-C** using 2-benzylcyclobutan-1-one **2.23** (80.1 mg, 500 µmol, 1.00 eq.) and *O*-(diphenylphosphinyl)hydroxylamine **2.51** (128 mg, 550 µmol, 1.10 eq.) a mixture of regioisomers (78.6 mg, 449 µmol, 90%, 89:11 *rr*) was obtained *via* flash column chromatography (SiO_2, EtOAc:MeOH, 95:5, stained with $KmnO_4$) as colourless solid.

Major regioisomer: ^{1}H NMR (400 MHz, $CDCl_3$): δ = 7.39 – 7.12 (m, 5H), 5.95 (br s, 1H), 3.94 – 3.82 (m, 1H), 2.84 (dd, J = 13.4, 5.7 Hz, 1H), 2.72 (dd, J = 13.4, 8.0 Hz, 1H), 2.38 – 2.19 (m, 3H), 1.93 – 1.78 (m, 1H). **^{13}C NMR (101 MHz, $CDCl_3$)**: δ = 178.1, 137.6, 129.1, 128.8, 126.9, 55.8, 43.0, 30.2, 26.9.
Minor regioisomer: ^{1}H NMR (400 MHz, $CDCl_3$): δ = 7.39 – 7.12 (m, 5H), 6.23 (br s, 1H), 3.28 – 3.17 (m, 3H), 2.68 – 2.61 (m, 2H), 2.18 – 2.07 (m, 1H), 1.93 – 1.78 (m, 1H). **^{13}C NMR (101 MHz, $CDCl_3$)**: δ = 179.9, 139.6, 129.1, 128.6, 126.4, 42.8, 40.4, 36.7, 27.0. Spectroscopic data was in agreement to those previously reported.[153,154]

5-Benzyldihydrofuran-2(3H)-one and 3-Benzyldihydrofuran-2(3H)-one (2.56)

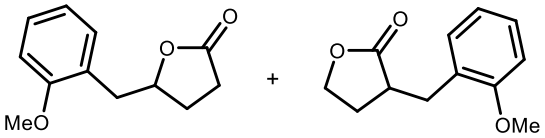

major minor

Following **GP-D** using 2-(2-methoxybenzyl)cyclobutanone **2.24** (95.1 mg, 500 µmol, 1.00 eq.) and *m*CPBA (123 mg, 550 µmol, 1.10 eq.) a mixture of regiosomers (90.3 mg, 441 µmol, 88%, 96:4 *rr*) was obtained *via* flash column chromatography (SiO_2, *n*-pentane:EtOAc, 80:20 to 70:30, stained with $KMnO_4$) both as colourless oil.

Major regioisomer: ^{1}H NMR (400 MHz, $CDCl_3$): δ =7.27 – 7.21 (m, 1H), 7.18 (dd, J = 7.4, 1.8 Hz, 1H), 6.95 – 6.82 (m, 2H), 4.80 (dq, J = 7.4, 6.7 Hz, 1H), 3.83 (s, 3H), 3.12 (dd, J = 13.6, 6.3 Hz, 1H), 2.91 (dd, J = 13.6, 6.8 Hz, 1H), 2.53 – 2.42 (m, 2H), 2.21 (dq, J = 12.8, 7.0 Hz, 1H), 2.03 – 1.87 (m, 1H). **^{13}C NMR (101 MHz, $CDCl_3$):** δ = 177.5, 157.6, 131.4, 130.7, 128.5, 128.2, 124.5, 120.8, 120.7, 110.5, 110.4, 80.3, 55.4, 35.9, 28.9, 27.4.

5-(2-Methoxybenzyl)pyrrolidin-2-one, 3-(2-methoxybenzyl)pyrrolidin-2-one (2.57)

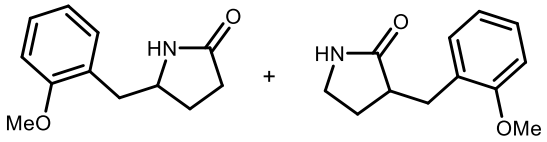

major minor

Following **GP-C** using 2-(2-methoxybenzyl)cyclobutanone **2.24** (95.1 mg, 500 µmol, 1.00 eq.) and *O*-(diphenylphosphinyl)hydroxylamine **2.51** (128 mg, 550 µmol, 1.10 eq.) a mixture of regioisomers (85.2 mg, 0.415 mmol, 83%, 88:12 *rr*) was obtained *via* flash column chromatography (SiO_2, EtOAc:MeOH, 97:3, stained with $KMnO_4$) as a white solid.

M.P.: 98 – 101 °C. **IR (neat)**: $\tilde{\nu}$ = 3235 (br), 2923 (br), 1692 (s), 1600 (w), 1494 (m), 1244 (s), 1119 (w), 1050 (m), 757 (m). **HRMS (ESI)**: Calculated for $C_{12}H_{16}NO_2$ $[M+H]^+$: 206.1181, Found: 206.1176.

Major regioisomer: ^{1}H NMR (400 MHz, $CDCl_3$): δ = 7.22 (td, J = 7.8, 1.8 Hz, 1H), 7.09 (dd, J = 7.3, 1.8 Hz, 1H), 6.91 – 6.84 (m, 2H), 5.95 (s, 1H), 3.97 – 3.87 (m, 1H), 3.81 (s, 3H), 2.87 (dd, J = 13.3, 5.4 Hz, 1H), 2.70 (dd, J = 13.2, 7.7 Hz, 1H), 2.35 – 2.26 (m, 2H), 2.25 – 2.16 (m, 1H), 1.90 – 1.76 (m, 1H). **^{13}C NMR (101 MHz, $CDCl_3$)**: δ = 178.0, 157.5, 131.0, 128.2, 126.0, 120.6, 110.5, 55.3, 54.4, 37.4, 30.2, 27.1.

Minor regioisomer: ^{1}H NMR (400 MHz, $CDCl_3$): δ = 7.22 – 7.18 (m, 1H), 7.18 – 7.13 (m, 1H), 7.09 (m, 1H), 6.87 (m, 1H), 6.41 (s, 1H), 3.80 (s, 3H), 3.35 – 3.24 (m, 1H), 3.26 – 3.03 (m, 2H), 2.73 (m, 1H), 2.56 (dd, J = 13.5, 10.4 Hz, 1H), 2.07 – 1.98 (m, 1H), 1.89 – 1.76 (m, 1H).**^{13}C NMR (101 MHz, $CDCl_3$)**: δ = 180.4, 157.7, 130.6, 128.1, 127.6, 120.4, 110.3, 55.2, 41.4, 40.4, 31.1, 27.1.

(*S*)-5-Benzylpyrrolidin-2-one and (*S*)-3-Benzylpyrrolidin-2-one ((*S*)-2.55)

major minor

Following **GP-C** using (*S*)-2-benzylcyclobutan-1-one (*S*)-**2.23** (48.1 mg, 300 µmol, 1.00 eq.) the product (*S*)-**2.55** was obtained as a mixture of regioisomers (45.1 mg, 257 µmol, 86%, 83:17 *rr*) *via* flash column chromatography (SiO_2, EtOAc:MeOH, 95:5, stained with $KMnO_4$) as a colourless oil.

Major regioisomer: ^{1}H NMR (400 MHz, $CDCl_3$): δ = 7.35 – 7.29 (m, 2H), 7.25 – 7.21 (m, 1H), 7.20 – 7.15 (m, 2H), 5.77 (s, 1H), 3.95 – 3.83 (m, 1H), 2.85 (dd, *J* = 13.4, 5.4 Hz, 1H), 2.72 (dd, *J* = 12.9, 4.5 Hz, 1H), 2.36 – 2.22 (m, 3H), 1.85 (m, 1H). **^{13}C NMR (101 MHz, $CDCl_3$)**: δ = 177.9, 137.7, 129.1, 129.0, 127.0, 55.8, 43.2, 30.2, 27.1.
Minor regioisomer: ^{1}H NMR (400 MHz, $CDCl_3$): δ = 7.28 – 7.26 (m, 2H), 7.24 – 7.20 (m, 3H), 5.96 (s, 1H), 3.31 – 3.17 (m, 3H), 2.69 – 2.64 (m, 2H), 2.14 (m, 1H), 1.94 – 1.88 (m, 1H). **^{13}C NMR (101 MHz, $CDCl_3$)**: δ = 179.7, 139.6, 129.1, 128.6, 126.5, 42.7, 40.3, 36.7, 27.0. **Optical Rotation**: $[\alpha]_D^{25}$ = +34.2 (*c* = 1.00, $CHCl_3$) for an enantiomerically enriched sample of 95:5 *er*. The enantiomeric purity was established by HPLC analysis using a chiral column (Lux® Cellulose-1, 22 °C, 1 mL/min, 85:15 *n*-hexane:isopropanol, 210 nm, major: t = 12.247 min and 15.339 min, minor: t = 9.149 min and 9.413 min). The absolute configuration was determined by comparison of HPLC with reported data.[155] Spectroscopic data was in agreement to those previously reported.[153,154]

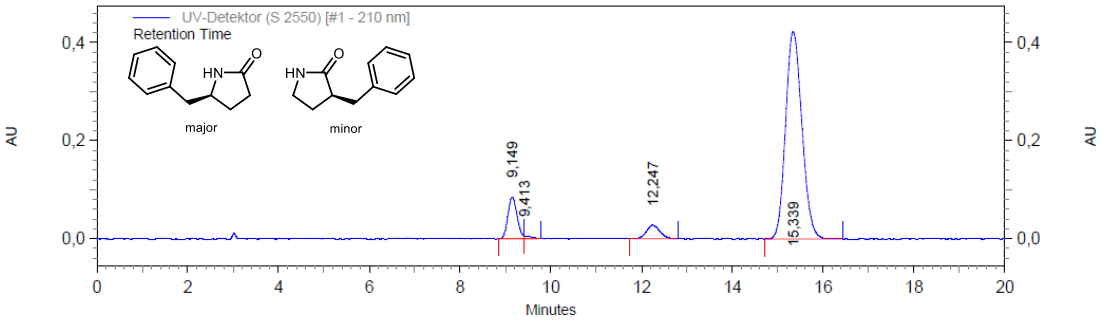

UV-Detektor (S 2550) [#1 - 210 nm] Results

Retention Time	Area	Area %
9,149	1192098	9,60
9,413	55333	0,45
12,247	572382	4,61
15,339	10597778	85,34

Figure 6. HPLC chromatogram for (S)-5-benzylpyrrolidin-2-one and (S)-3-benzylpyrrolidin-2-one (*S*)-2.55.

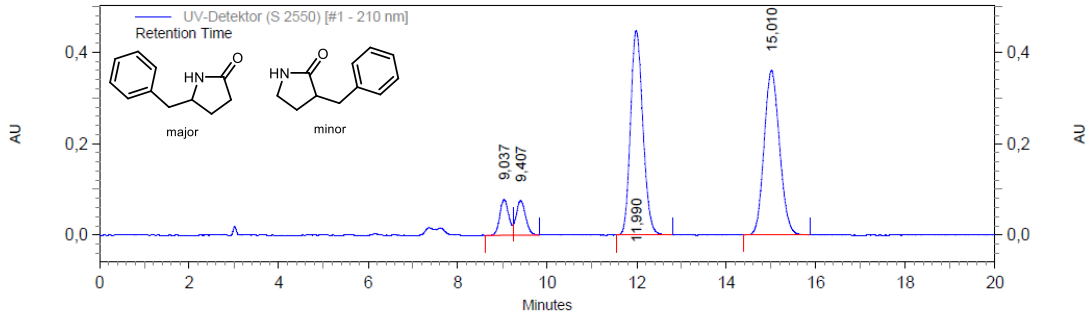

UV-Detektor (S 2550) [#1 - 210 nm] Results

Retention Time	Area	Area %
9,037	1095146	5,64
9,407	1100493	5,66
11,990	8603410	44,29
15,010	8628084	44,41

Figure 7. HPLC chromatogram for 5-benzylpyrrolidin-2-one and 3-benzylpyrrolidin-2-one 2.55.

(*S*)-5-Benzyl-1-methylpyrrolidin-2-one ((S)-2.58)

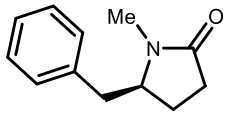

Following **GP-C** using (*S*)-2-benzylcyclobutan-1-one (*S*)-**2.23** (48.1 mg, 300 µmol, 1.00 eq.) and ((methylamino)oxy)diphenylphosphine oxide **2.59** (81.6 mg, 330 µmol, 1.10 eq.) The product (*S*)-**2.58** (48.8 mg, 258 µmol, 86%) was obtained *via* flash column chromatography (SiO_2, EtOAc, stained with $KMnO_4$) as a white solid.

^{1}H NMR (400 MHz, $CDCl_3$): δ = 7.35 – 7.29 (m, 2H), 7.27 – 7.22 (m, 1H), 7.19 – 7.14 (m, 2H), 3.75 (tt, *J* = 8.3, 4.3 Hz, 1H), 3.03 (dd, *J* = 13.5, 4.4 Hz, 1H), 2.88 (s, 3H), 2.64 (dd, *J* = 13.5, 8.2 Hz, 1H), 2.26 – 2.08 (m, 2H), 1.99 (dddd, *J* = 13.0, 9.9, 7.9, 7.3 Hz, 1H), 1.74 (dddd, *J* = 13.2, 9.1, 5.9, 4.2 Hz, 1H). **^{13}C NMR (101 MHz, $CDCl_3$)**: δ = 175.4, 137.1, 129.4, 128.8, 126.9, 61.3, 39.5, 29.8, 28.3, 23.7. **Optical Rotation**: $[\alpha]_D^{25}$ = –61.4 (*c* = 0.50, $CHCl_3$) for an enantiomerically enriched sample of 97:3 *er*. The enantiomeric purity was established by HPLC analysis using a chiral column (Lux® i-Amylose-3, 22 °C, 1 mL/min, 80:20 *n*-hexane:isopropanol, 210 nm, t = 9.076 min and 9.666 min). Spectroscopic data was in agreement to those previously reported.[156]

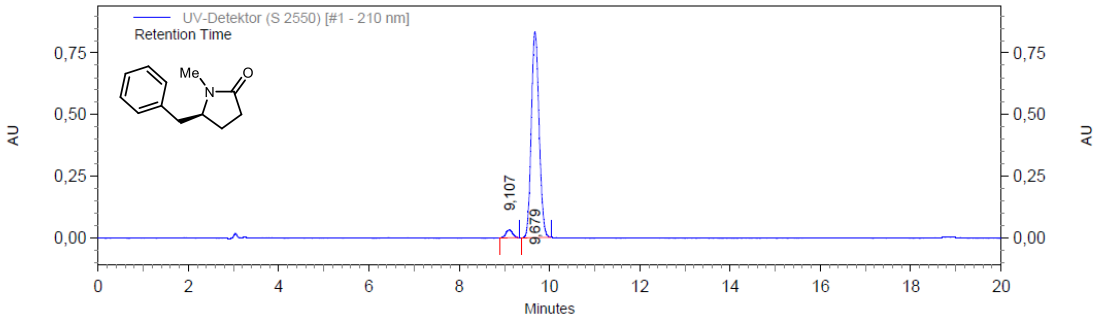

UV-Detektor (S 2550) [#1 - 210 nm] Results

Retention Time	Area	Area %
9,107	336936	3,26
9,679	10009402	96,74

Figure 8. HPLC chromatogram for (S)-5-benzyl-1-methylpyrrolidin-2-one (*S*)-2.58.

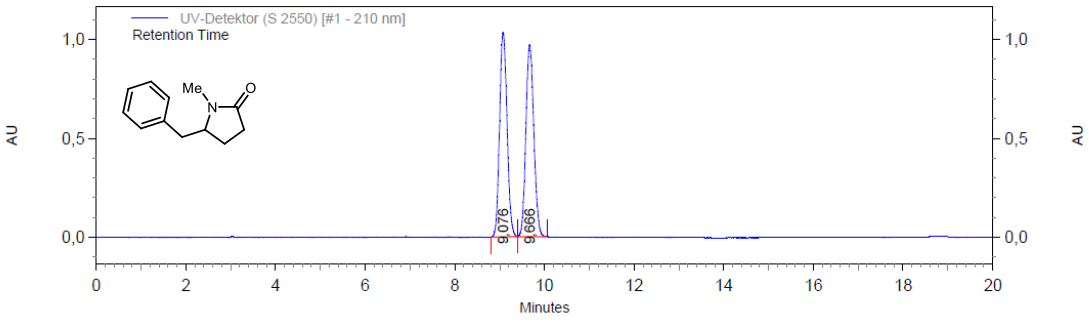

UV-Detektor (S 2550) [#1 - 210 nm] Results

Retention Time	Area	Area %
9,076	11987792	49,94
9,666	12018872	50,06

Figure 9. HPLC chromatogram for 5-benzyl-1-methylpyrrolidin-2-one 2.58.

5-(Thiophen-2-ylmethyl)pyrrolidine-2-one, 3-(thiophen-2-ylmethyl)pyrrolidine-2-one (2.60)

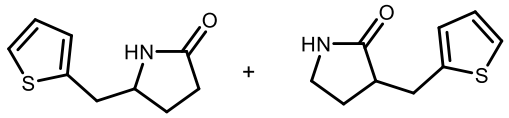

major minor

Following **GP-C** using 2-(thiophen-2-ylmethyl)cyclobutan-1-one **2.28** (83.1 mg, 500 µmol, 1.00 eq.) and *O*-(diphenylphosphinyl)hydroxylamine **2.51** (128 mg, 550 µmol, 1.10 eq.) a mixture of regioisomers (74.0 mg, 410 µmol, 82%, 85:15 *rr*) was obtained *via* flash column chromatography (SiO_2, EtOAc:MeOH, 95:5, stained with $KMnO_4$) as a yellow oil.

IR (neat): $\tilde{\nu}$ =3221 (br) 2920 (br), 2360 (w), 1691 (s), 1441 (w), 1275 (w), 1085 (w), 849 (w), 790 (m). **HRMS (ESI)**: Calculated for $C_9H_{12}NOS$ $[M+H]^+$: 182.0640, Found: 182.0627.

Major regioisomer: ^{1}H NMR (400 MHz, $CDCl_3$): δ = 7.18 (dd, J = 5.1, 1.2 Hz, 1H), 6.95 (dd, J = 5.2, 3.4 Hz, 1H), 6.86 – 6.82 (m, 1H), 6.33 – 6.20 (s, 1H), 3.95 – 3.86 (m,1H), 3.04 – 2.96 (m, 2H), 2.35 – 2.22 (m, 3H), 1.87 – 1.78 (m, 1H). **^{13}C NMR (101 MHz, $CDCl_3$)**: δ = 178.1, 139.5, 127.3, 126.2, 124.6, 55.7, 37.1, 30.1, 26.7.

Minor regioisomer: ^{1}H NMR (400 MHz, $CDCl_3$): δ = 7.14 (dd, J = 5.1, 1.2 Hz, 1H), 6.93 – 6.91 (m, 1H), 6.85 – 6.84 (m, 1H), 6.42 (s, 1H), 3.38 (dd, J = 14.9, 3.9 Hz, 1H), 3.33 – 3.20 (m, 2H), 2.97 – 2.88 (m, 1H), 2.68 (*app.* qd, ≈ 9.1, 3.9 Hz, 1H), 2.27 – 2.21 (m, 1H), 1.98 – 1.88 (m, 1H). **^{13}C NMR (101 MHz, $CDCl_3$)**: δ = 179.2, 141.7, 127.0, 125.7, 124.0, 42.9, 40.3, 30.9, 27.0.

5,5-dimethyl-4-phenylpyrrolidin-2-one, 3,3-dimethyl-4-phenylpyrrolidin-2-one (2.61)

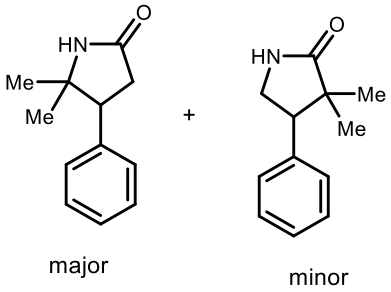

major minor

Following **GP-C**[a] using 2,2-dimethyl-3-phenylcyclobutan-1-one **2.35** (87.1 mg, 500 µmol, 1.00 eq.) and *O*-(diphenylphosphinyl)hydroxylamine **2.51** (128 mg, 550 µmol, 1.10 eq.) a mixture of regioisomers (77.6 mg, 410 µmol, 82%, 92:8 *rr*) was obtained *via* flash column chromatography (SiO_2, EtOAc:MeOH, 98:2, stained with $KMnO_4$) as a yellow oil.

IR (neat): $\tilde{\nu}$ = 3223 (br), 2963 (br), 1688 (s), 1499 (w), 1389 (m), 1196 (w), 774 (m), 702 (s). **Major regioisomer: ^{1}H NMR (400 MHz, $CDCl_3$)**: δ = 7.39 – 7.20 (m, 5H), 6.57 (s, 1H), 3.39 (dd, J = 10.2, 8.3 Hz, 1H), 2.83 (dd, J = 16.9, 10.2 Hz, 1H), 2.66 (dd, J = 16.9, 8.3 Hz, 1H), 1.39 (s, 3H), 0.88 (s, 3H). **^{13}C NMR (101 MHz, $CDCl_3$)**: δ = 176.2, 138.2, 128.6, 128.4, 127.5, 60.0, 51.7, 36.1, 28.9, 25.0. **Minor regioisomer: ^{1}H NMR (400 MHz, $CDCl_3$)**: δ = 7.39 – 7.20 (m, 5H), 3.65 (t, J = 9.4 Hz, 1H), 3.57 (dd, J = 9.8, 7.7 Hz, 1H), 3.32 (dd, J = 9.1, 7.6 Hz, 1H), 1.22 (s, 3H), 0.78 (s, 3H). **^{13}C NMR (101 MHz, $CDCl_3$)**: δ = 182.6, 137.9, 128.5, 128.5, 127.4, 52.5, 43.9, 43.7, 24.0, 19.9. **HRMS (ESI)**: Calculated for $C_{12}H_{16}NO$ $[M+H]^+$: 190.1232, Found: 190.1221. Spectroscopic data of the major regioisomer was in agreement to those previously reported.[157]

[a] Reaction was performed at 40 °C.

((3a,8b)-3,3a,4,8b-Tetrahydroindeno[1,2-b]pyrrol-2(1*H*)-one, (3a,8a)-1,3a,8,8a-tetrahydroindeno[1,2-c]pyrrol-3(2*H*)-one (2.62)

major minor

Following **GP-C** using 1,2a,7,7a-tetrahydro-2H-cyclobuta[a]inden-2-one **2.45** (47.5 mg, 300 µmol, 1.00 eq.) a mixture of regioisomers (>97:3, 42.5 mg, 245 µmol, 83%) was obtained *via* flash column chromatography (SiO_2, EtOAc:MeOH, 97:3, stained with $KMnO_4$) as a white solid.

M.P.: 188 – 191 °C. **Major regioisomer: ^{1}H NMR (400 MHz, $CDCl_3$)**: δ = 7.35 (s, 1H), 7.32 – 7.18 (m, 4H), 5.02 (d, J = 6.9 Hz, 1H), 3.35 – 3.22 (m, 2H), 2.91 – 2.79 (m, 1H), 2.76 – 2.63 (m, 1H), 2.26 – 2.14 (m, 1H).**^{13}C NMR (101 MHz, $CDCl_3$)**: δ = 178.0, 142.5, 141.8, 128.7, 127.4, 127.3, 125.4, 125.1, 125.0, 124.9, 63.6, 38.6, 37.8, 37.5. Spectroscopic data of the major regioisomer was in agreement to those previously reported.[157]

4-Phenylpyrrolidin-2-one (2.49)

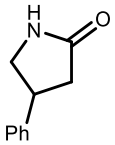

Following the general procedure **C** using 3-phenylcyclobutan-1-one **2.8** (4.39 g, 30.0 mmol, 1.00 eq.) and *O*-(diphenylphosphinyl)hydroxylamine **2.51** (8.10 g, 33.0 mmol, 1.10 eq.) the product **2.49** (3.84 g, 23.8 mmol, 79%, >97% purity) the product *via* flash column chromatography (SiO_2, EtOAc:MeOH, 95:5, stained with $KMnO_4$) as a colourless solid.

M.P.: 74–77 °C. **IR (neat)**: $\tilde{\nu}$ = 3236 (br), 2877 (br), 1693 (s), 1494 (m), 1454 (w), 1360 (w), 1290 (w), 1258 (m), 1050 (w), 759 (m), 700 (m), 472 (w). **^{1}H NMR (400 MHz, $CDCl_3$)**: δ = 7.36 – 7.32 (m, 2H), 7.29 – 7.23 (m, 3H), 7.12 – 7.01 (br s, 1H), 3.79 (dd, J = 9.6, 8.2 Hz, 1H), 3.69 (*app*. p, $J \approx$ 8.4 Hz, 1H), 3.43 (dd, J = 9.6, 7.4 Hz, 1H), 2.74 (dd, J = 16.9, 9.0 Hz, 1H), 2.51 (dd, J = 16.9, 8.9 Hz, 1H). **^{13}C NMR (101 MHz, $CDCl_3$)**: δ = 178.1, 142.2, 128.9, 127.2, 126.9, 49.7, 40.4, 38.2. **HRMS (ESI):** calculated for $C_{10}H_{12}NO$ $[M+H]^+$: 162.0913, found: 162.0911.

5.3 Nitrogen incorporation *via* asymmetric condensation

5.3.1 Synthesis of starting materials

General procedure E (GP-E) for the Grignard addition to diethylphosphite:

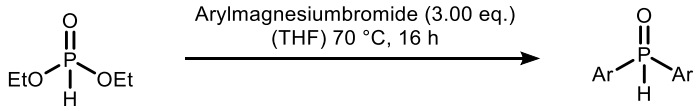

Arylmagnesiumbromide (1.0 M in THF, 3.00 eq.) was added to a Schlenk flask under N_2-atmosphere. The solution was cooled to 0 °C and a solution of diethylphosphite (1.00 eq.) in dry THF (1.0 M) was added dropwise. The reaction mixture was stirred for 3 h under reflux and 16 h at room temperature. The mixture was cooled to 0 °C and HCl (1.0 M, 30 mL) was slowly added. The solution was extracted with EtOAc (3 × 20 mL), dried over $MgSO_4$, filtered and concentrated under reduced pressure. The product the product *via* recrystallization with the conditions given in the corresponding entry.

General procedure F (GP-F) for the oxidation with sodium hydroxide and hydrogen peroxide:

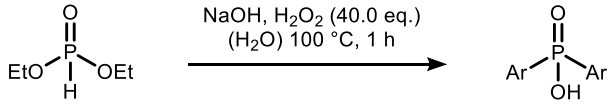

Hydrogen peroxide (35%, 40.0 eq.) was added dropwise to a suspension of phosphite (1.00 eq.) in aqueous NaOH-solution (5.0 N, 1.0 M). The reaction mixture was stirred at 100 °C for 1 h. After cooling to 0 °C, conc. HCl was added dropwise until precipitation was completed. The precipitate was collected by filtration and washed with water and Et_2O to obtain the corresponding phosphinic acid.

General procedure G (GP-G) for the synthesis of Boc-protected *O*-phosphorylated hydroxylamines:

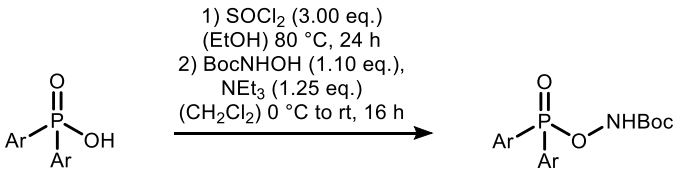

According to a procedure from *Smulik et al.*[158], to a suspension of phosphinic acid (1.00 eq.) in dry toluene (20 mL) was added thionyl chloride (3.00 eq.) under N_2-atmosphere. The reaction mixture was stirred at 80 °C for 3 h. After cooling to room temperature, the solvent was removed under reduced pressure (Schlenkline, cooling trap). The crude phosphinic acid chloride was redissolved in dry CH_2Cl_2 (3.0 M) and used without further purification.

In an oven dried Schlenk flask *N*-Boc hydroxylamine (1.10 eq.) was dissolved in dry CH_2Cl_2 (1.0 M) under N_2-atmosphere. The mixture was cooled with an ice bath and NEt_3 (1.25 eq.) was added dropwise over a period of 10 minutes. The solution of phosphinic acid chloride (1.00 eq.) in CH_2Cl_2 (3.0 M) was added dropwise to the reaction flask over a period of 10 minutes. The mixture was allowed to warm to room temperature over night. Water (10 mL) was added, and the mixture was extracted with CH_2Cl_2. The organic phase was dried over $MgSO_4$, filtered and concentrated under reduced pressure. The product was separated *via* flash column chromatography with the conditions given in the corresponding entry.

General procedure H (GP-H) for the Boc-deprotection with TFA:

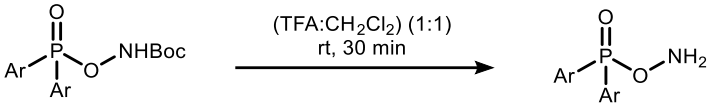

Boc-protected hydroxylamine (1.00 eq.) was dissolved in CH_2Cl_2 (1.0 M). The solution was cooled with an ice bath. TFA (1.0 M) was added and the solution was stirred at room temperature for 30 minutes. The solution was diluted with CH_2Cl_2 and water. $NaHCO_3$ was added until gas evolution stopped. The aqueous layer was extracted with CH_2Cl_2 and the combined organic phase was dried over $MgSO_4$, filtered and concentrated under reduced pressure. The residue was redissolved in CH_2Cl_2 (20 mL) and hexane was added. The product the product *via* filtration of the precipitate formed.

Bis(*p*-methoxyphenyl)phosphine oxide (5.5)

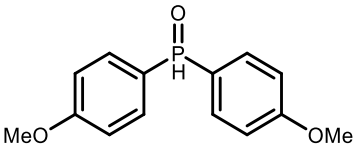

Following **GP-E** using 4-methoxyphenylmagnesiumbromide (1.0 M in THF, 30 mL, 30.0 mmol, 3.00 eq.) the product **5.5** (2.02 g, 7.70 mmol, 77%) was obtained *via* recrystallisation from EtOAc (30 mL) as a colourless powder.

^{1}H NMR (400 MHz, $CDCl_3$): δ = 8.02 (d, J = 477.8 Hz, 1H), 7.65 – 7.52 (m, 4H), 7.05 – 6.93 (m, 4H), 3.84 (s, 6H). **^{13}C NMR (101 MHz, $CDCl_3$)**: δ = 163.0 (d, J = 2.8 Hz), 132.8 (d, J = 12.9 Hz), 123.1 (d, J = 108.1 Hz), 114.5 (d, J = 13.9 Hz), 55.5. **^{31}P NMR (162 MHz, $CDCl_3$):** δ = 21.24. The spectroscopic data was in agreement to those previously reported.[159]

Bis-(*p*-methoxyphenyl)phosphinic acid (3.23)

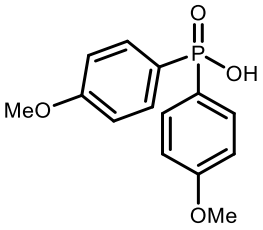

Following **GP-F** using bis(*p*-methoxyphenyl)phosphine oxide **5.5** (1.97 g, 7.5 mmol, 1.00 eq.) the product **3.23** (1.97 g, 7.06 mmol, 94%) was obtained as colourless powder.

^{1}H NMR (400 MHz, $CDCl_3$): δ = 9.49 (s, 1H), 7.71 – 7.44 (m, 4H), 6.83 (dq, J = 9.3, 2.6 Hz, 4H), 3.79 (s, 6H). **^{13}C NMR (101 MHz, $CDCl_3$)**: δ = 162.3 (d, J = 3.0 Hz), 133.2 (d, J = 12.0 Hz), 124.7 (d, J = 147.4 Hz), 113.9 (d, J = 14.4 Hz), 55.3. **^{31}P NMR (162 MHz, $CDCl_3$):** δ = 35.16. The spectroscopic data was in agreement to those previously reported.[108]

***tert*-Butyl ((bis-*p*-methoxyphenylphosphoryl)oxy)carbamate (5.6)**

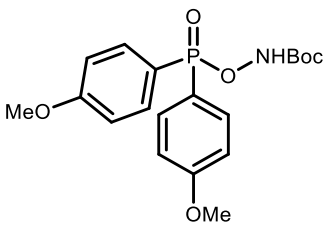

Following **GP-G** using bis-(*p*-methoxyphenyl)phosphinic acid **3.23** (1.48 g, 5.0 mmol, 1.00 eq.) the product **5.6** (1.65 g, 4.20 mmol, 84%) was obtained *via* automated flash column chromatography (SiO_2, cyclohexane:EtOAc (95:5 → 75:25)) as colourless powder.

M.P.: 166 – 171 °C. **IR (neat)**: $\tilde{\nu}$ = 3079 (w), 2927 (w), 1748 (m), 1598 (s), 1505 (m), 1297 (m), 1254 (s), 1217 (m), 1180 (m), 1161 (m), 1130 (s), 1082 (m), 1026 (m), 829 (m), 805 (m), 733 (m), 677 (m), 552 (s), 542 (s), 458 (m). **^{1}H NMR (600 MHz, $CDCl_3$)**: δ = 8.84 (s, 1H, N*H*), 7.92 – 7.78 (m, 4H, C$H_{arom.}$), 6.95 – 6.91 (m, 4H, C$H_{arom.}$), 3.82 (s, 6H, 2 × CH_3), 1.39 (s, 9H, 3 × CH_3).**^{13}C NMR (151 MHz, $CDCl_3$)**: δ = 163.1 (d, J = 2.9 Hz, C_q), 156.2 (d, J = 5.3 Hz, C_q), 134.4 (d, J = 11.4 Hz, *C*H), 121.0, 120.5 (d, J = 143.5 Hz, C_q), 114.0 (d, J = 14.6 Hz, *C*H), 82.6 (C_q), 55.5 (*C*H$_3$), 28.1 (*C*H$_3$). **^{31}P NMR (162 MHz, $CDCl_3$)** δ = 41.59. **HRMS (ESI):** Calculated for $C_{19}H_{25}NO_6P$ $[M+H]^+$: 395.1447, Found: 395.14487.

***O*-(bis-*p*-methoxyphenylphosphinyl)hydroxylamine (3.26)**

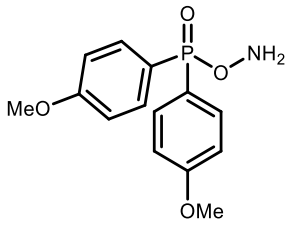

Following **GP-H** using *tert*-butyl ((bis-*p*-methoxyphenylphosphoryl)oxy)carbamate **5.6** (1.57 g, 4.0 mmol, 1.00 eq.) the product **3.26** (956 mg, 3.20 mmol, 81%) was obtained as a colourless powder.

^{1}H NMR (400 MHz, $CDCl_3$): δ = 7.80 – 7.71 (m, 4H), 6.97 (dq, J = 9.3, 2.6 Hz, 4H), 3.84 (s, 6H). **^{13}C NMR (101 MHz, $CDCl_3$):** δ = 162.9 (d, J = 3.0 Hz), 133.9 (d, J = 11.3 Hz), 122.8 (d, J = 148.3 Hz), 114.3 (d, J = 14.1 Hz), 55.5. **^{31}P NMR (162 MHz, $CDCl_3$)**: δ = 39.36. The spectroscopic data was in agreement to those previously reported.[108]

Di-*p*-tolylphosphine oxide (5.7)

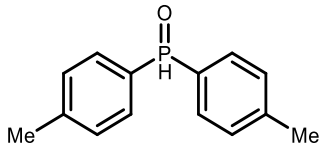

Following **GP-E** using 4-methylphenylmagnesiumbromide (1.0 M in THF, 60 mL, 60.0 mmol, 3.00 eq.) and diethylphosphite (2.76 g, 20.0 mmol, 1.00 eq.) the product **5.7** (1.97 g, 8.55 mmol, 43%) was obtained the product *via* recrystallisation from Et_2O (30 mL) as a colourless powder.

^{1}H NMR (400 MHz, $CDCl_3$): δ = 8.02 (d, J = 478.0 Hz, 1H), 7.61 – 7.53 (m, 4H), 7.29 (dd, J = 8.0, 2.6 Hz, 4H), 2.39 (s, 6H). **^{13}C NMR (101 MHz, $CDCl_3$)**: δ = 143.2 (d, J = 2.9 Hz), 130.9 (d, J = 11.8 Hz), 129.7 (d, J = 13.2 Hz), 128.5 (d, J = 103.9 Hz), 21.8. **^{31}P NMR (162 MHz, $CDCl_3$):** δ = 22.28. The spectroscopic data was in agreement to those previously reported.[159]

Di-*p*-tolylphosphinic acid (3.24)

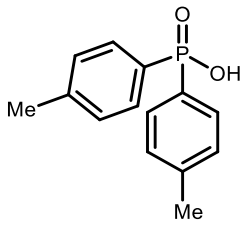

Following **GP-F** using di-*p*-tolylphosphine oxide **5.7** (1.97 g, 8.55 mmol, 1.00 eq.) the product **3.24** (2.07 g, 8.39 mmol, 98%) was obtained as a colourless powder.

^{1}H NMR (400 MHz, $CDCl_3$): δ = 8.86 (s, 1H), 7.71 – 7.45 (m, 4H), 7.12 (dd, J = 8.0, ,3.1 Hz, 4H, C$H_{arom.}$), 2.34 (s, 6H). **^{13}C NMR (101 MHz, $CDCl_3$)**: δ = 142.1 (d, J = 2.9 Hz), 131.34 (d, J = 10.9 Hz), 130.0 (d, J = 142.4 Hz), 129.06 (d, J = 13.7 Hz), 21.7. **^{31}P NMR (162 MHz, $CDCl_3$):** δ = 33.88. The spectroscopic data was in agreement to those previously reported.[108]

***tert*-Butyl ((di-*p*-tolylphosphoryl)oxy)carbamate (5.8)**

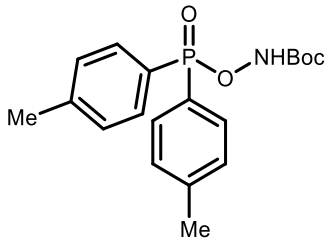

Following **GP-G** using di-*p*-tolylphosphinic acid **3.24** (2.65 g, 10.0 mmol, 1.00 eq.) the product **5.8** (3.00 g, 8.30 mmol, 83%) was obtained *via* automated flash column chromatography (SiO_2, cyclohexane:EtOAc (95:5 → 75:25)) as a colourless powder.

M.P.: 164 – 169 °C. **IR (neat)**: $\tilde{\nu}$ = 3090 (w), 2980 (w), 2895 (w), 1750 (m), 1719 (m), 1603 (w), 1368 (m), 1273 (w), 1253 (m), 1225 (s), 1209 (m), 1163 (m), 1129 (s), 1111 (m), 1082 (m), 836 (m), 810 (m), 770 (w), 744 (m), 710 (m), 671 (s), 622 (w), 544 (m), 527 (s), 483 (m), 465 (m), 452 (m), 430 (m), 414 (m). **^{1}H NMR (400 MHz, $CDCl_3$):** δ = 8.78 (d, J = 6.1 Hz, 1H, N*H*), 7.87 – 7.77 (m, 4H, C$H_{arom.}$), 7.24 (dddd, J = 7.6, 3.5, 1.6, 0.9 Hz, 4H, C$H_{arom.}$), 2.37 (s, J = 0.9 Hz, 6H, CH_3), 1.39 (s, 9H, CH_3). **^{13}C NMR (101 MHz, $CDCl_3$):** δ = 156.2 (d, J = 5.3 Hz, C_q), 143.4 (d, J = 2.9 Hz, C_q), 132.5 (d, J = 10.7 Hz, CH$_{arom.}$), 129.3 (d, J = 13.8 Hz, CH$_{arom.}$), 125.9 (d, J = 138.2 Hz, C_q), 82.7 (C_q), 28.2 (CH$_3$), 21.8 (CH$_3$). **^{31}P NMR (162 MHz, $CDCl_3$):** δ = 41.54. **HRMS (ESI):** Calculated for $C_{19}H_{24}NO_6PNa$ $[M+Na]^+$: 416.1233, Found: 416.1227.

***O*-(di-*p*-tolylphosphinyl))hydroxylamine (3.27)**

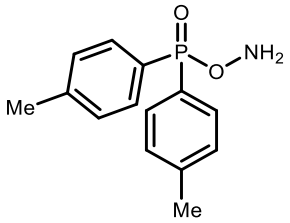

Following **GP-H** using *tert*-butyl ((di-*p*-tolylphosphoryl)oxy)carbamate **5.8** (361 mg, 1.00 mmol, 1.00 eq.) the product **3.27** (229 mg, 880 µmol, 88%) was obtained as a colourless powder.

^{1}H NMR (400 MHz, $CDCl_3$): δ = 7.77 – 7.66 (m, 4H), 7.31 – 7.24 (m, 4H), 2.39 (s, 6H). **^{13}C NMR (101 MHz, $CDCl_3$)**: δ = 143.7 (d, J = 2.9 Hz, C_q), 132.0 (d, J = 10.3 Hz, CH$_{arom.}$), 130.2 (d, J = 13.7 Hz, CH$_{arom.}$), 126.9 (d, J = 138.3 Hz, C_q), 21.8 (CH$_3$). **^{31}P NMR (162 MHz, $CDCl_3$):** δ = 36.99. The spectroscopic data was in agreement to those previously reported.[108]

5.3.2 Development of reaction conditions

The racemic products were prepared according to the following procedures:

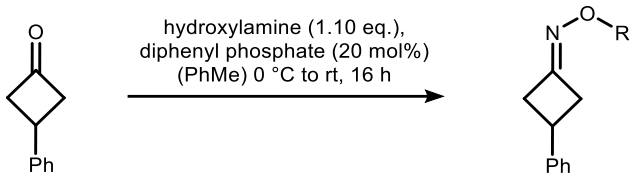

In a round bottom flask, diphenyl phosphate (20 mol%) and 3-phenylcyclobutanone **2.8** (0.05 mmol, 1.00 eq.) were dissolved in toluene (0.05 M). The mixture was cooled to 0 °C. The corresponding hydroxylamine (0.055 mmol, 1.10 eq.) was added, and the reaction mixture was allowed to warm to room temperature. NEt_3 (0.05 mmol, 1.00 eq.) was added. The solvent was removed under reduced pressure and the crude product was purified *via* flash column chromatography with the conditions given in the corresponding entry.

General procedure I (GP-I) for the optimisation reaction of enantioslective oximes:

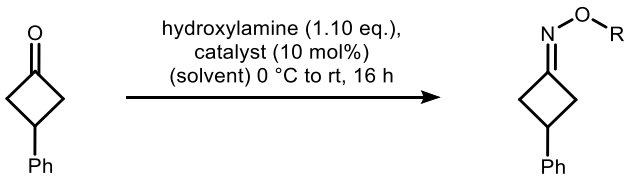

In a round bottom flask, catalyst (10 mol%) and 3-phenylcyclobutanone **2.8** (0.05 mmol, 1.00 eq.) were dissolved in the corresponding solvent (0.05 M). The mixture was cooled to 0 °C. The corresponding hydroxylamine (0.055 mmol, 1.10 eq.) was added, and the reaction mixture was stirred for 6 h. NEt_3 (0.05 mmol, 1.00 eq.) was added. The solvent was removed under reduced pressure and the crude product was purified *via* flash column chromatography with the conditions given in the corresponding entry.

(((3-Phenylcyclobutylidene)amino)oxy)diphenylphosphine oxide (3.32)

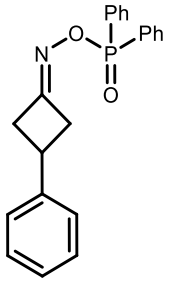

Following **GP-I** using 3-phenylyclobut-1-one **2.8** (7.31 mg, 50.0 µmol, 1.00 eq.), *O*-(diphenylphosphinyl)hydroxylamine **2.51** (12.8 mg, 55.0 µmol, 1.10 eq.) and toluene (1.0 mL) the product **3.32** (16.0 mg, 44.3 µmol, 89%) was obtained *via* automated flash column chromatography (SiO_2, Cyclohexane:EtOAc, 100:0 → 0:100, stained with $KMnO_4$) as a colourless solid.

The reaction was performed in similar fashion with other catalysts and solvents (*cf.* chapter 3.3).

^{1}H NMR (400 MHz, $CDCl_3$): δ = 7.93 – 7.81 (m, 4H), 7.61 – 7.42 (m, 6H), 7.38 – 7.30 (m, 2H), 7.29 – 7.20 (m, 3H), 3.72 – 3.53 (m, 2H), 3.49 – 3.34 (m, 1H), 3.27 – 3.03 (m, 2H).**^{13}C NMR (101 MHz, $CDCl_3$)**: δ = 166.5 (d, $^3J_{C\text{-}P}$ = 12.4 Hz), 143.2, 132.5 (d, $^4J_{C\text{-}P}$ = 2.7 Hz), 132.2 (*app.* t, $^2J_{C\text{-}P} \approx$ 10.5 Hz), 130.8 (d, $^1J_{C\text{-}P}$ = 136.1 Hz), 130.7 (d, $^1J_{C\text{-}P}$ = 135.7 Hz), 128.8 (d, $^3J_{C\text{-}P}$ = 13.3 Hz), 127.0, 126.5, 39.7, 39.5, 32.5. **^{31}P NMR (162 MHz, $CDCl_3$)**: δ = 35.2. The spectroscopic data was in agreement to those previously reported.[139] **HPLC:** The enantiomeric ratio of 14:86 *er* was established by HPLC analysis using a chiral column (Cellulose-1, 25 °C, 1 mL/min, 90:10 *n*hexane:isopropanol, 210 nm, t = 18.531 min and 21.142 min).

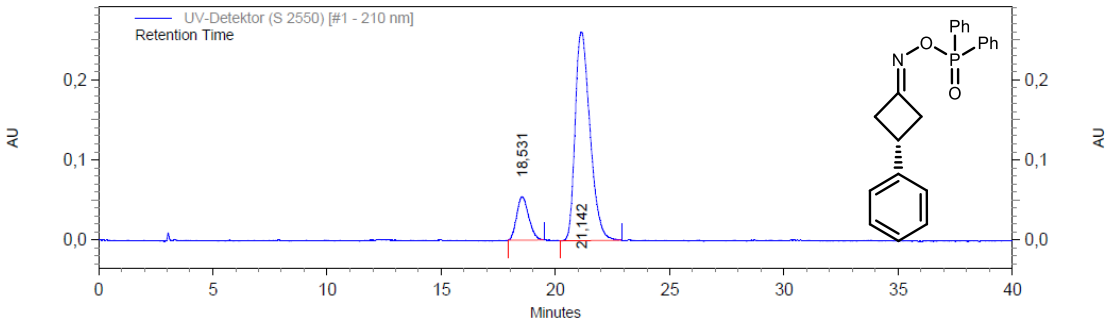

UV-Detektor (S 2550) [#1 - 210 nm] Results

Retention Time	Area	Area %
18,531	1984587	14,42
21,142	11781067	85,58

Figure 10. HPLC chromatogram for the enantioenriched sample of ((((3-phenylcyclobutylidene)amino)oxy)diphenylphosphine oxide (3.32).

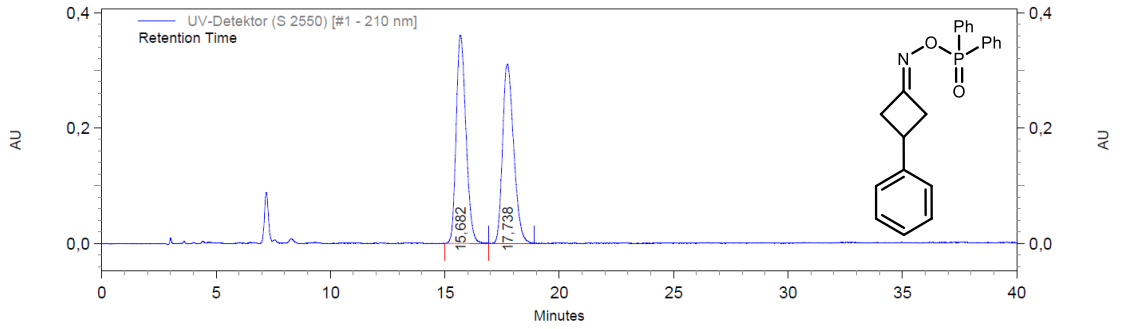

UV-Detektor (S 2550) [#1 - 210 nm] Results

Retention Time	Area	Area %
15,682	10736413	50,47
17,738	10537785	49,53

Figure 11. HPLC chromatogram for the racemic sample of (((3-phenylcyclobutylidene)amino)oxy)diphenylphosphine oxide (3.32).

3-Phenylcyclobutan-1-one *O*-(2,4-dinitrophenyl) oxime (5.9)

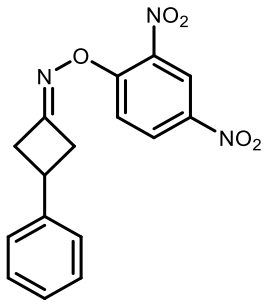

Following **GP-I** using 3-phenylyclobut-1-one **2.8** (7.31 mg, 50.0 µmol, 1.00 eq.), *O*-(2,4-dinitrophenyl)hydroxylamine **3.42** (11.0 mg, 55.0 µmol, 1.10 eq.) CH_2Cl_2 (1.0 mL) the product **5.9** (15.6 mg, 47.5 µmol, 95%) was obtained *via* automated flash column chromatography ((SiO_2, cyclohexane:EtOAc, 95:5 → 50:50, stained with $KMnO_4$) as a colourless powder.

M.P.: 93 – 101 °C. **IR (neat)**: $\tilde{\nu}$ = 1603 (s), 1524 (s), 1473 (m), 1341 (s), 1316 (m), 1285 (m), 1231 (w), 1142 (w), 1066 (w), 924 (m), 864 (m), 836 (w), 820 (m), 742 (m), 698 (m), 640 (w). **^{1}H NMR (400 MHz, $CDCl_3$)**: δ = 8.87 (d, J = 2.7 Hz, 1H, C$H_{arom.}$), 8.42 (dd, J = 9.4, 2.8 Hz, 1H, C$H_{arom.}$), 7.91 (d, J = 9.4 Hz, 1H, C$H_{arom.}$), 7.42 – 7.34 (m, 2H, C$H_{arom.}$), 7.33 – 7.27 (m, 3H, C$H_{arom.}$), 3.81 – 3.65 (m, 3H, CH, CH_2), 3.61 – 3.50 (m, 1H, CH_2), 3.38 – 3.19 (m, 2H, CH_2). **^{13}C NMR (101 MHz, $CDCl_3$)**: δ = 166.2 (C_q), 157.6 (C_q), 142.8 (C_q), 140.7 (C_q), 135.6 (C_q), 129.5 (*C*H), 129.0 (*C*H), 127.2 (*C*H), 126.5 (*C*H), 122.2 (*C*H), 117.2 (*C*H), 39.7 (*C*H_2), 39.2 (*C*H_2), 32.7 (*C*H). **HRMS (ESI):** Calculated for $C_{16}H_{13}N_3O_5Na$ $[M+Na]^+$: 350.0747, Found: 350.0746. **HPLC:** The enantiomeric ratio of 68:32 *er* was established by HPLC analysis using a chiral column (*i*Amylose-3, 25 °C, 1 mL/min, 90:10 *n*hexane:isopropanol, 210 nm, t = 18.458 min and 23.285 min).

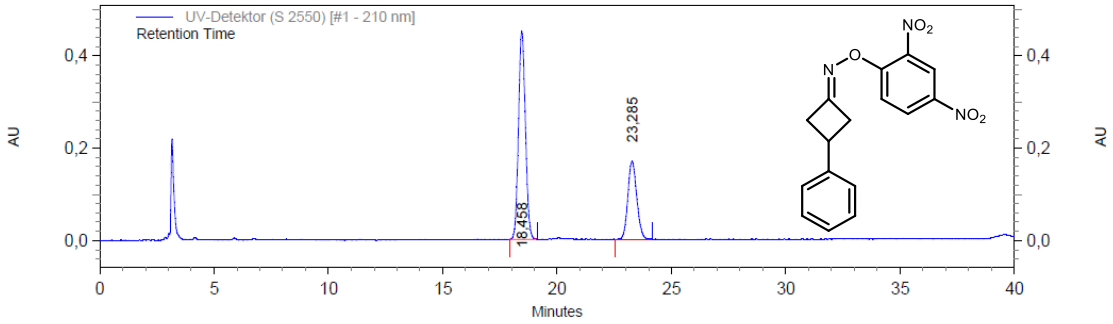

UV-Detektor (S 2550) [#1 - 210 nm] Results

Retention Time	Area	Area %
18,458	9491226	67,51
23,285	4568294	32,49

Figure 12. HPLC chromatogram for the enantioenriched sample of (((3-phenylcyclobutylidene)amino)oxy)diphenylphosphine oxide (5.9).

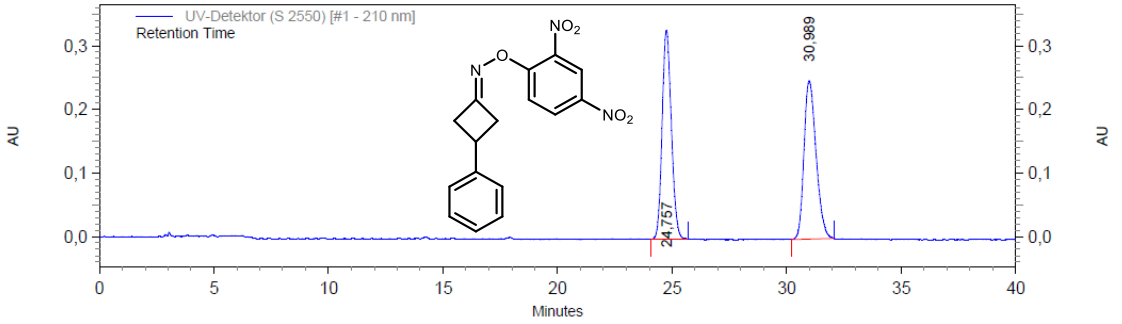

UV-Detektor (S 2550) [#1 - 210 nm] Results

Retention Time	Area	Area %
24,757	9216652	50,23
30,989	9133294	49,77

Figure 13. HPLC chromatogram for the racemic sample of (((3-phenylcyclobutylidene)amino)oxy)diphenylphosphine oxide (5.9).

3-Phenylcyclobutan-1-one *O*-(4-nitrobenzoyl) oxime (5.10)

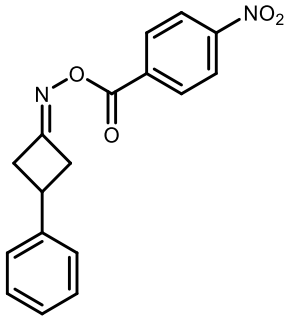

Following **GP-I** using 3-phenylyclobut-1-one **2.8** (7.31 mg, 50.0 µmol, 1.00 eq.), *O*-(4-nitrobenzoyl)hydroxylamine **2.52** (10.0 mg, 55.0 µmol, 1.00 eq.) and CH_2Cl_2 (1.0 mL) the product **5.10** (14.0 mg, 45.0 µmol, 90%) was obtained *via* automated flash column chromatography ((SiO_2, cyclohexane:EtOAc 95:5 → 50:50, stained with $KMnO_4$) as a colourless powder.

M.P.: 111 – 116 °C. **IR (neat)**: $\tilde{\nu}$ = 1743 (s), 1688 (w), 1606 (w), 1524 (s), 1496 (w), 1455 (w), 1398 (w), 1345 (m), 1320 (w), 1258 (s), 1235 (s), 1071 (s), 1013 (m), 872 (m), 853 (s), 777 (w), 743 (m), 715 (s), 698 (s), 670 (w), 505 (m). **^{1}H NMR (400 MHz, $CDCl_3$)**: δ = 8.35 – 8.29 (m, 2H, C$H_{arom.}$), 8.26 – 8.21 (m, 2H, C$H_{arom.}$), 7.42 – 7.34 (m, 2H, C$H_{arom.}$), 7.33 – 7.27 (m, 3H, C$H_{arom.}$), 3.81 – 3.70 (m, 1H, C*H*), 3.70 – 3.55 (m, 2H, CH_2), 3.35 – 3.21 (m, 2H, CH_2). **^{13}C NMR (101 MHz, $CDCl_3$)**: δ = 167.4 (C_q), 162.3 (C_q), 150.8 (C_q), 142.8 (C_q), 134.6 (C_q), 130.9 (*C*H), 129.0 (*C*H), 127.2 (*C*H), 126.4 (*C*H), 123.9 (*C*H), 39.7 (*C*H), 32.6 (*C*H). **HRMS (ESI):** Calculated for $C_{17}H_{14}N_2O_2Na$ $[M+Na]^+$: 333.0846, Found: 333.0847. **HPLC:** The enantiomeric ratio of 41:59 *er* was established by HPLC analysis using a chiral column (Amylose-1, 25 °C, 1 mL/min, 80:20 *n*hexane:isopropanol, 210 nm, t = 24.318 min and 28.746 min).

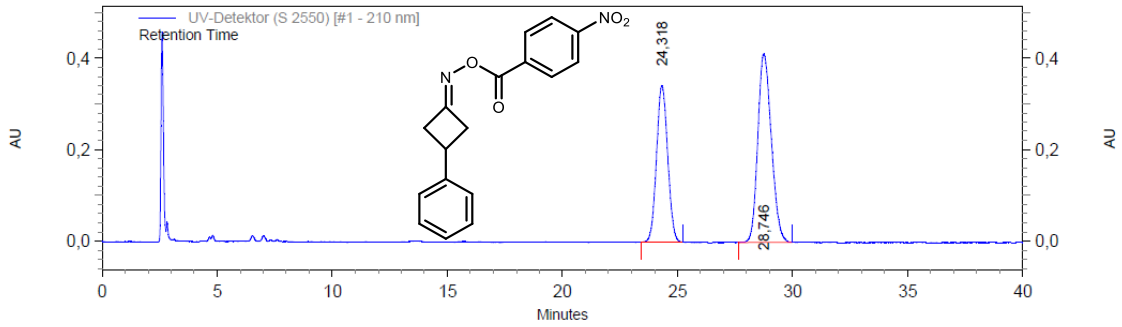

UV-Detektor (S 2550) [#1 - 210 nm] Results

Retention Time	Area	Area %
24,318	11592246	40,67
28,746	16910010	59,33

Figure 14. HPLC chromatogram for the enantioenriched sample of 3-Phenylcyclobutan-1-one *O*-(4-nitrobenzoyl) oxime (5.10).

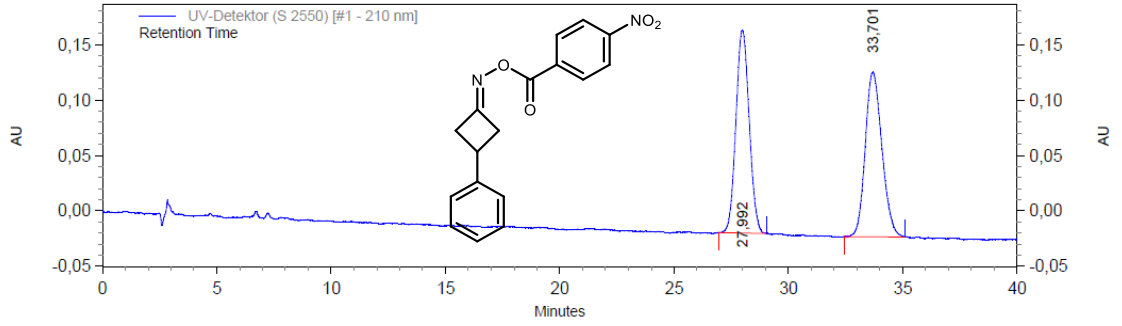

UV-Detektor (S 2550) [#1 - 210 nm] Results

Retention Time	Area	Area %
27,992	7395103	49,53
33,701	7536400	50,47

Figure 15. HPLC chromatogram for the racemic sample of 3-Phenylcyclobutan-1-one *O*-(4-nitrobenzoyl) oxime (5.10).

Bis(4-methoxyphenyl)(((3-phenylcyclobutylidene)amino)oxy)phosphine oxide (5.11)

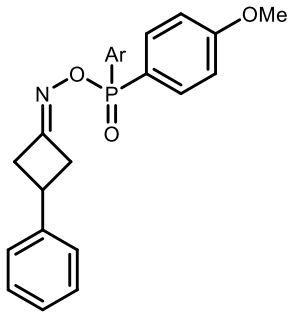

Following **GP-I** using 3-phenylyclobut-1-one **2.8** (7.31 mg, 50.0 µmol, 1.00 eq.), *O*-(bis-*p*-methoxyphenylphosphinyl)hydroxylamine **3.33** (16.0 mg, 55.0 µmol, 1.00 eq.) and toluene (1.0 mL) the product **5.11** (14.7 mg, 38.5 µmol, 77%) was obtained *via* automated flash column chromatography (SiO_2, cyclohexane:EtOAc (100:0 → 0:100)) as a colourless powder.

M.P.: 117 - 122 °C. **IR (neat)**: $\tilde{\nu}$ = 2925 (w), 1597 (s), 1571 (w), 1504 (m), 1457 (w), 1296 (m), 1253 (s), 1227 (s), 1179 (m), 1127 (s), 1025 (m), 871 (s), 831 (m), 805 (m), 749 (m), 699 (m), 672 (m), 543 (s), 457 (m). **^{1}H NMR (400 MHz, $CDCl_3$)**: δ = 7.78 (ddd, J = 11.9, 8.7, 3.4 Hz, 4H, C$H_{arom.}$), 7.38 – 7.31 (m, 2H, C$H_{arom.}$), 7.26 – 7.21 (m, 3H, C$H_{arom.}$), 6.99 – 6.93 (m, 4H, C$H_{arom.}$), 3.83 (s, 6H, CH_3), 3.65 – 3.54 (m, 2H, C*H*, CH_2), 3.41 (ddt, J = 16.9, 8.9, 3.2 Hz, 1H, CH_2), 3.20 – 3.12 (m, 1H, CH_2), 3.12 – 3.06 (m, 1H, CH_2). **^{13}C NMR (151 MHz, $CDCl_3$)**: δ = 166.0 (d, 12.4 Hz, $^3J_{C\text{-}P}$ = 12.4 Hz, C_q), 162.8 (d, $^4J_{C\text{-}P}$ = 3.0 Hz, C_q), 143.3 (C_q), 134.1 (d, $^2J_{C\text{-}P}$ 11.3 Hz, *C*H), 134.0 (d, $^2J_{C\text{-}P}$ 11.4 Hz, *C*H), 128.8 (*C*H), 126.9 (*C*H), 126.5 (*C*H), 122.2 (d, $^1J_{C\text{-}P}$ = 144.0 Hz, C_q), 122.1 (d, $^1J_{C\text{-}P}$ = 143.5 Hz, C_q), 114.2 (d, $^3J_{C\text{-}P}$ = 14.3 Hz, *C*H), 114.2 (d, $^3J_{C\text{-}P}$ = 14.3 Hz, *C*H), 55.5 (*C*H$_3$), 39.8 (*C*H$_2$), 39.5 (*C*H$_2$), 32.4 (*C*H). **^{31}P NMR (162 MHz, $CDCl_3$)**: δ = 36.26. **HPLC:** The enantiomeric ratio of 21:79 *er* was established by HPLC analysis using a chiral column (Cellulose-1, 25 °C, 1 mL/min, 70:30 *n*hexane:isopropanol, 210 nm, t = 24.318 min and 28.746 min).

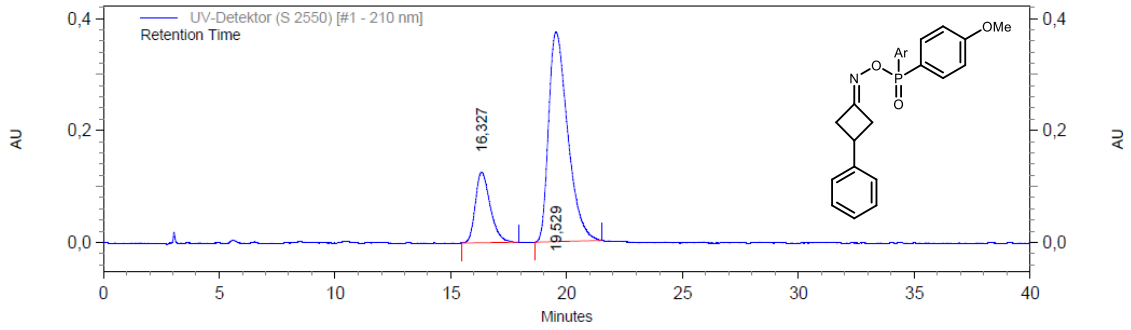

UV-Detektor (S 2550) [#1 - 210 nm] Results

Retention Time	Area	Area %
16,327	5608247	20,74
19,529	21436991	79,26

Figure 16. HPLC chromatogram for Bis(4-methoxyphenyl)(((3-phenylcyclobutylidene)amino)oxy)phosphine oxide.

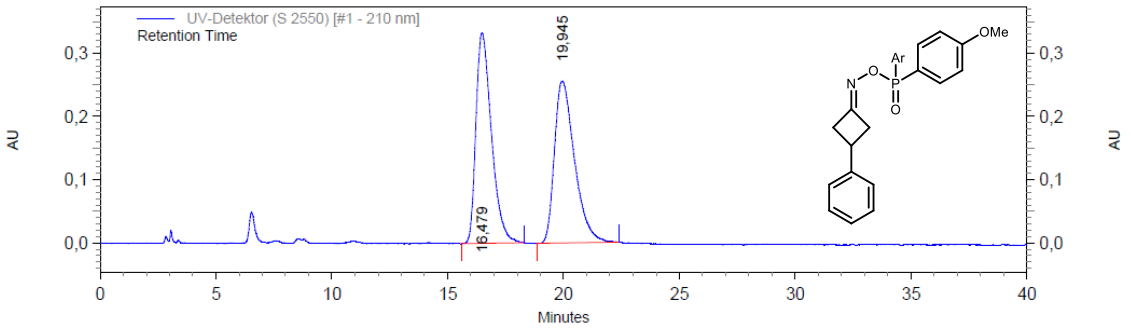

UV-Detektor (S 2550) [#1 - 210 nm] Results

Retention Time	Area	Area %
16,479	15494053	50,12
19,945	15417423	49,88

Figure 17. HPLC chromatogram for Bis(4-methoxyphenyl)(((3-phenylcyclobutylidene)amino)oxy)phosphine oxide.

(((3-Phenylcyclobutylidene)amino)oxy)di-p-tolylphosphine oxide (5.12)

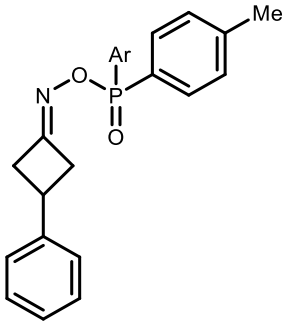

Following **GP-I** using 3-phenylyclobut-1-one **2.8** (7.31 mg, 50.0 µmol, 1.00 eq.), *O*-(di-*p*-tolylphosphinyl)hydroxylamine **3.34** (13.0 mg, 55.0 µmol, 1.00 eq.) and toluene (1.0 mL) the product **5.12** (18.7 mg, 48.0 µmol, 96%) was obtained *via* flash column chromatography ((SiO_2, *n*-pentane:EtOAc (100:0 → 0:100)) as a colourless powder.

M.P.: 115 - 119 °C. **IR (neat)**: $\tilde{\nu}$ = 3029 (w), 1699 (m), 1603 (m), 1233 (m), 1186 (m), 1128 (s), 1110 (m), 877 (s), 808 (m), 749 (m), 700 (m), 668 (s), 530 (s), 468 (m), 443 (m), 411 (m). **^{1}H NMR (400 MHz, $CDCl_3$)**: δ = 7.78 – 7.70 (m, 4H, C$H_{arom.}$), 7.38 – 7.31 (m, 2H, C$H_{arom.}$), 7.30 – 7.20 (m, 7H, C$H_{arom.}$), 3.67 – 3.51 (m, 2H, CH, CH_2), 3.47 – 3.35 (m, 1H, CH_2), 3.24 – 3.02 (m, 2H, CH_2), 2.39 (s, 6H, CH_3). **^{13}C NMR (101 MHz, $CDCl_3$)**: δ = 166.1 (d, $^3J_{C\text{-}P}$ = 12.4 Hz, C_q), 143.3 (C_q), 142.9 (d, $^4J_{C\text{-}P}$ = 2.7 Hz, C_q), 132.2 (*app.* t, $^2J_{C\text{-}P}$ ≈ 10.7 Hz, CH$_{arom.}$), 129.4 (d, $^3J_{C\text{-}P}$ = 13.3 Hz, CH$_{arom.}$), 128.8 (CH$_{arom.}$), 127.8 (d, $^1J_{C\text{-}P}$ = 138.6 Hz, C_q), 127.7 (d, $^1J_{C\text{-}P}$ = 138.3 Hz, C_q), 126.9 (CH$_{arom.}$), 126.5 (CH$_{arom.}$), 39.8 (CH$_2$), 39.5 (CH$_2$), 32.5 (CH), 21.8 (CH$_3$). **^{31}P NMR (162 MHz, $CDCl_3$)**: δ = 36.29. **HRMS (ESI):** Calculated for $C_{24}H_{25}NO_2P$ $[M+H]^+$: 390.1617, Found: 390.1613. **HPLC:** The enantiomeric ratio of 17:83 *er* was established by HPLC analysis using a chiral column (Amylose-1, 25 °C, 1 mL/min, 80:20 *n*hexane:iso-propanol, 210 nm, t = 24.318 min and 28.746 min).

5.3.3 Substrate scope cyclobutanone oxime esters

The racemic products were prepared according to the following procedure:

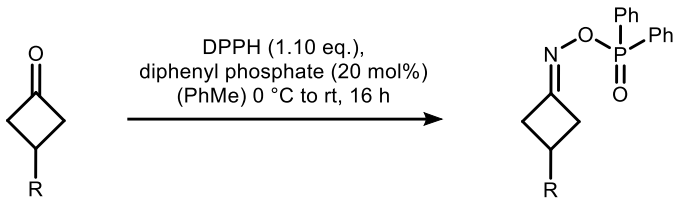

In a round bottom flask, diphenyl phosphate (20 mol%) and cyclobutanone (200 µmol, 1.00 eq.) were dissolved in toluene (0.05 M). The mixture was cooled to 0 °C. *O*-Diphenylphosphinylhydroxylamine (220 µmol, 1.10 eq.) was added and the reaction mixture was allowed to warm to room temperature over night. NEt_3 (200 µmol, 1.00 eq.) was added. The solvent was removed under reduced pressure and the crude product was purified *via* automated flash column chromatography with the conditions given in the corresponding entry.

General procedure J (GP-J) for the asymmetric condensation:

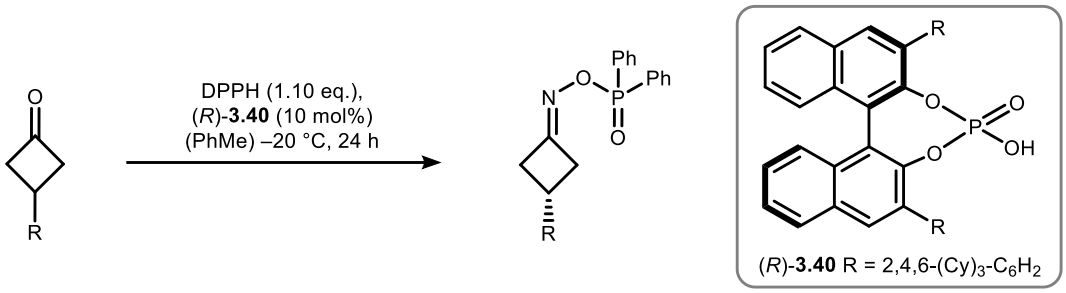

In a round bottom flask, (*R*)-**3.40** (10 mol%) and cyclobutanone (200 µmol, 1.00 eq.) were dissolved in toluene (0.05 M). The mixture was cooled to –20 °C. *O*-Diphenylphosphinylhydroxylamine (220 µmol, 1.10 eq.) was added and the reaction mixture was stirred at –20 °C for 24 h. NEt_3 (200 µmol, 1.00 eq.) was added. The solvent was removed under reduced pressure and the crude product was purified *via* automated flash column chromatography with the conditions given in the corresponding entry.

(*R*)-(((3-(2-chlorophenyl)cyclobutylidene)amino)oxy)diphenylphosphine oxide ((*R*)-3.41)

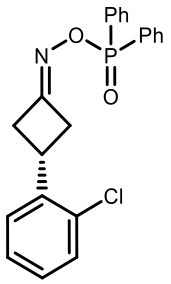

Following **GP-J** using 3-(2-chlorophenyl)cyclobut-1-one (90.3 mg, 500 µmol, 1.00 eq.), (*R*)-**3.40** (50.7 mg, 50.0 µmol, 10 mol%) and *O*-(diphenylphosphinyl)hydroxylamine **2.51** (128.3 mg, 550 µmol, 1.10 eq.) the product (*R*)-**3.41** (181 mg, 457 µmol, 91%) was obtained *via* automated flash column chromatography (SiO_2, Cyclohexane:EtOAc, 100:0 → 0:100, stained with $KMnO_4$) as colourless solid.

^{1}H NMR (400 MHz, $CDCl_3$): δ = 7.92 – 7.83 (m, 4H, C$H_{arom.}$), 7.58 – 7.51 (m, 2H, C$H_{arom.}$), 7.51 – 7.43 (m, 4H, C$H_{arom.}$), 7.39 – 7.35 (m, 1H, C$H_{arom.}$), 7.32 – 7.27 (m, 2H, C$H_{arom.}$), 7.22 – 7.18 (m, 1H, C$H_{arom.}$), 3.92 (tt, J = 8.8, 7.8 Hz, 1H, C*H*), 3.65 (*app*. ddt, $J \approx$ 17.5, 9.1, 3.4 Hz, 1H, CH_2), 3.45 (*app*. ddt, $J \approx$ 16.9, 9.0, 3.4 Hz, 1H, CH_2), 3.16 (dddd, J = 22.0, 16.9, 7.8, 3.0 Hz, 2H, CH_2). **^{13}C NMR (101 MHz, $CDCl_3$)**: δ = 166.1 (d, $^3J_{C\text{-}P}$ = 12.5 Hz, C_q), 139.7 (C_q), 134.1 (C_q), 132.5 (d, $^4J_{C\text{-}P}$ = 2.9 Hz, *C*H), 132.2 (d, $^2J_{C\text{-}P}$ = 10.1 Hz, *C*H), 132.2 (d, $^2J_{C\text{-}P}$ = 10.1 Hz, *C*H), 130.7 (d, $^1J_{C\text{-}P}$ = 136.1 Hz, C_q), 130.7 (d, $^1J_{C\text{-}P}$ = 135.9 Hz, C_q), 129.9 (*C*H), 128.7 (d, $^3J_{C\text{-}P}$ = 13.2 Hz, *C*H), 128.3 (*C*H), 127.2 (*C*H), 126.8 (*C*H), 38.2 (*C*H_2), 38.0 (*C*H_2), 30.7 (*C*H). **^{31}P NMR (162 MHz, $CDCl_3$)**: δ = 35.25. **Optical Rotation:** $[\alpha]_D^{25}$ = –67.8 (c = 0.5, $CHCl_3$) for an enantiomerically enriched sample of 93:7 *er*. The enantiomeric purity was established by HPLC analysis using a chiral column (Cellulose-1, 22 °C, 1 mL/min, 85:15 *n*-hexane:isopropanol, 214 nm, t = 14.493 min and 16.558 min).

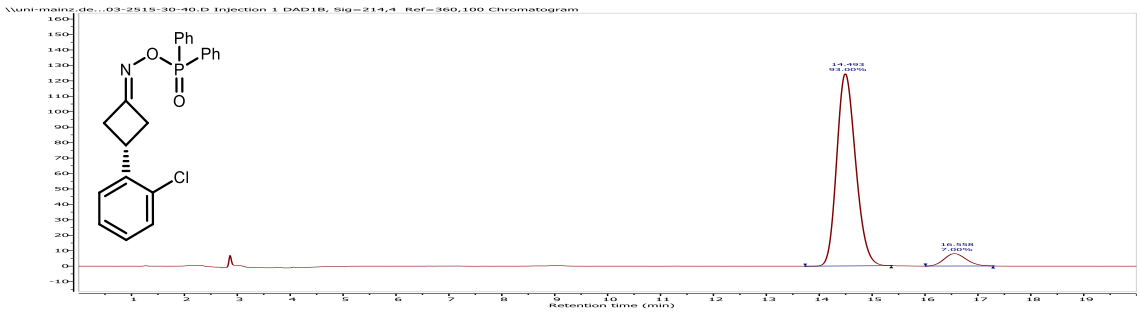

Retention Time	Area%
14.493	93.00
16.558	7.00

Figure 18. HPLC chromatogram for (*R*)-(((3-(2-chlorophenyl)cyclobutylidene)amino)oxy)diphenylphosphine oxide ((*R*)-3.41)

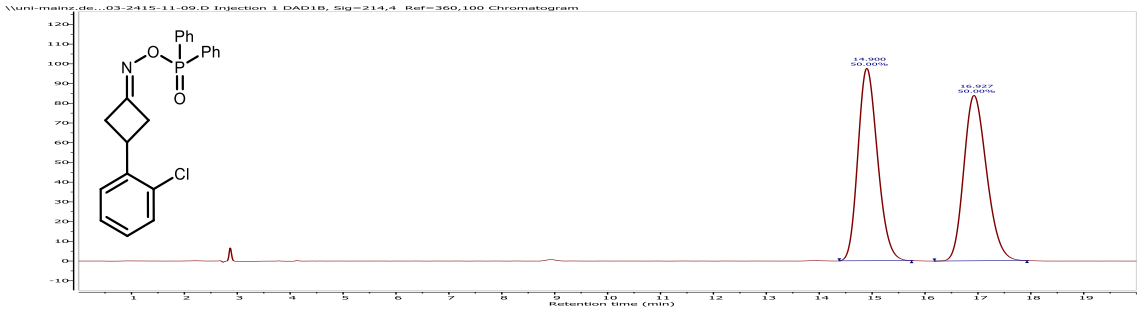

Retention Time	Area%
14.900	50.00
16.927	50.00

Figure 19. HPLC chromatogram for (((3-(2-chlorophenyl)cyclobutylidene)amino)oxy)diphenylphosphine oxide (3.41)

(*R*)-(((3-(3-chlorophenyl)cyclobutylidene)amino)oxy)diphenylphosphine oxide ((*R*)-3.42)

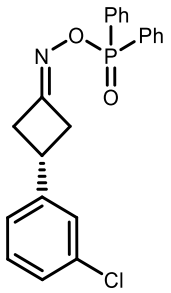

Following **GP-J** using 3-(3-chlorophenyl)cyclobut-1-one (90.3 mg, 500 µmol, 1.00 eq.), (*R*)-**3.40** (50.7 mg, 50.0 µmol, 10 mol%) and *O*-(diphenylphosphinyl)hydroxylamine **2.51** (128.3 mg, 550 µmol, 1.10 eq.) the product (*R*)-**3.42** (190 mg, 480 µmol, 96%) was obtained *via* automated flash column chromatography (SiO_2, Cyclohexane:EtOAc, 100:0 → 0:100, stained with $KMnO_4$) as colourless solid.

^{1}H NMR (400 MHz, $CDCl_3$): δ = 7.96 – 7.86 (m, 4H, C$H_{arom.}$), 7.62 – 7.54 (m, 2H, C$H_{arom.}$), 7.54 – 7.47 (m, 4H, C$H_{arom.}$), 7.34 – 7.27 (m, 1H), 7.27 – 7.23 (m, 2H), 7.17 – 7.12 (m, 1H), 3.72 – 3.56 (m, 2H, C*H*, CH_2), 3.51 – 3.38 (m, 1H, CH_2), 3.26 – 3.04 (m, 2H, CH_2). **^{13}C NMR (101 MHz, $CDCl_3$)**: δ = 165.6 (d, $^3J_{C\text{-}P}$ = 12.4 Hz, C_q), 145.1 (C_q), 134.6 (C_q), 132.4 (d, $^4J_{C\text{-}P}$ = 2.8 Hz, *C*H), 132.1 (d, $^2J_{C\text{-}P}$ = 10.4 Hz, *C*H), 132.0 (d, $^2J_{C\text{-}P}$ = 11.3 Hz, *C*H), 130.5 (d, $^1J_{C\text{-}P}$ = 136.1 Hz, C_q), 130.5 (d, $^1J_{C\text{-}P}$ = 135.4 Hz, C_q), 130.0 (*C*H), 128.6 (d, $^3J_{C\text{-}P}$ = 13.2 Hz, *C*H), 128.6 (d, $^3J_{C\text{-}P}$ = 13.2 Hz, *C*H), 127.1 (*C*H), 126.7 (*C*H), 124.6 (*C*H), 39.5 (CH_2), 39.3 (CH_2), 32.1 (*C*H). **^{31}P NMR (162 MHz, $CDCl_3$)**: δ = 34.86. **Optical Rotation:** $[\alpha]_D^{25}$ = –28.8 (c = 0.5, $CHCl_3$) for an enantiomerically enriched sample of 94:6 *er*. The enantiomeric purity was established by HPLC analysis using a chiral column (Cellulose-1, 22 °C, 1 mL/min, 85:15 *n*-hexane:isopropanol, 214 nm, t = 15.441 min and 17.354 min).

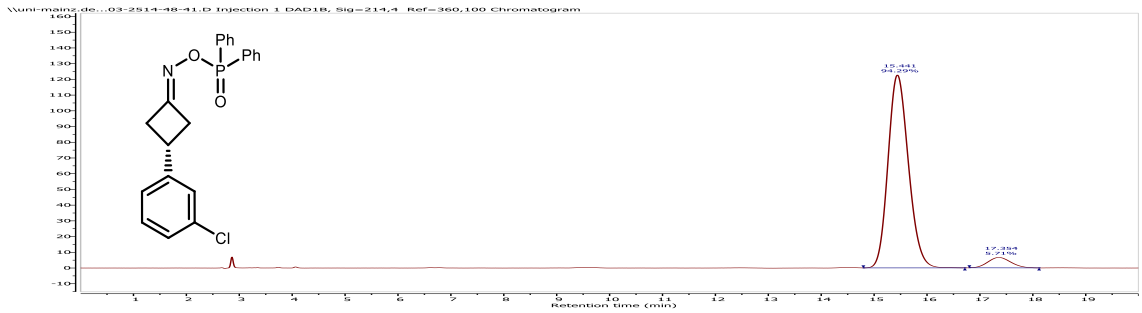

Retention Time	Area%
15.441	94.29
17.354	5.71

Figure 20. HPLC chromatogram for (*R*)-(((3-(3-chlorophenyl)cyclobutylidene)amino)oxy)diphenylphosphine oxide ((*R*)-3.42).

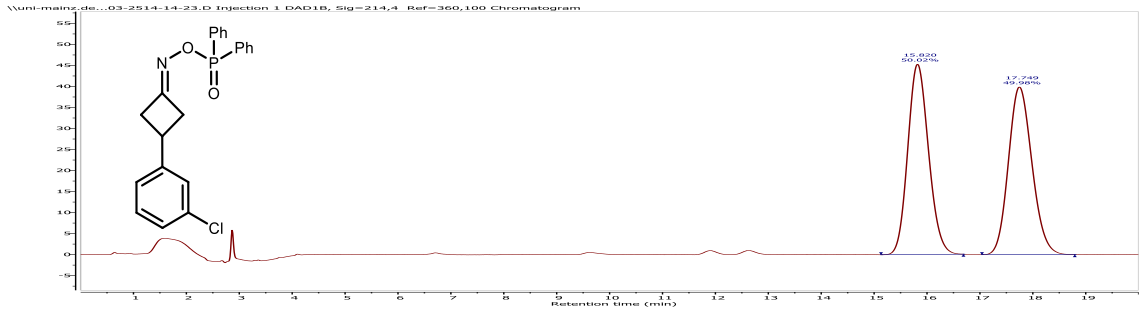

Retention Time	Area%
15.820	50.02
17.749	49.98

Figure 21. HPLC chromatogram for (((3-(3-chlorophenyl)cyclobutylidene)amino)oxy)diphenylphosphine oxide (3.42).

(*R*)-(((3-Phenylcyclobutylidene)amino)oxy)diphenylphosphine oxide ((*R*)-3.32)

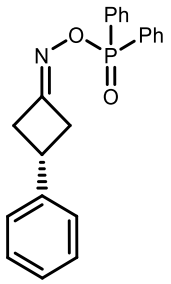

Following **GP-J** using 3-phenylyclobut-1-one **2.8** (29.2 mg, 200 µmol, 1.00 eq.), (*R*)-**3.40** (19.8 mg, 20.0 µmol, 10 mol%) and *O*-(diphenylphosphinyl)hydroxylamine **2.51** (51.3 mg, 220 µmol, 1.10 eq.) the product (*R*)-**3.32** (64.0 mg, 177 µmol, 89%) was obtained *via* automated flash column chromatography (SiO_2, Cyclohexane:EtOAc, 100:0 → 0:100, stained with $KMnO_4$) as colourless solid.

^{1}H NMR (400 MHz, $CDCl_3$): δ = 7.93 – 7.81 (m, 4H), 7.61 – 7.42 (m, 6H), 7.38 – 7.30 (m, 2H), 7.29 – 7.20 (m, 3H), 3.72 – 3.53 (m, 2H), 3.49 – 3.34 (m, 1H), 3.27 – 3.03 (m, 2H).**^{13}C NMR (101 MHz, $CDCl_3$)**: δ = 166.5 (d, $^3J_{C\text{-}P}$ = 12.4 Hz), 143.2, 132.5 (d, $^4J_{C\text{-}P}$ = 2.7 Hz), 132.2 (*app*. t, $^2J_{C\text{-}P}$ 10.5 Hz), 130.8 (d, $^1J_{C\text{-}P}$ = 136.1 Hz), 130.7 (d, $^1J_{C\text{-}P}$ = 135.7 Hz), 128.8 (d, $^3J_{C\text{-}P}$ = 13.3 Hz), 127.0, 126.5, 39.7, 39.5, 32.5. **^{31}P NMR (162 MHz, $CDCl_3$)**: δ = 35.23. The spectroscopic data was in agreement to those previously reported.[139] **Optical Rotation:** $[\alpha]_D^{25}$ = −65.1 (c = 0.5, $CHCl_3$) for an enantiomerically enriched sample of 95:5 *er*. The enantiomeric purity was established by HPLC analysis using a chiral column (Cellulose-1, 22 °C, 1 mL/min, 85:15 *n*-hexane:isopropanol, 210 nm, t = 15.855 min and 18.175 min).

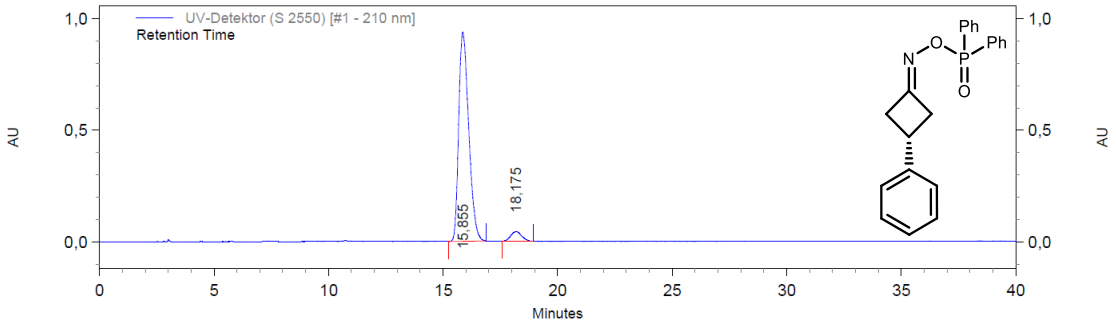

UV-Detektor (S 2550) [#1 - 210 nm] Results

Retention Time	Area	Area %
15,855	28423074	95,19
18,175	1435209	4,81

Figure 22. HPLC chromatogram for ((*R*)-(((3-Phenylcyclobutylidene)amino)oxy)diphenylphosphine oxide ((*R*)-3.32)

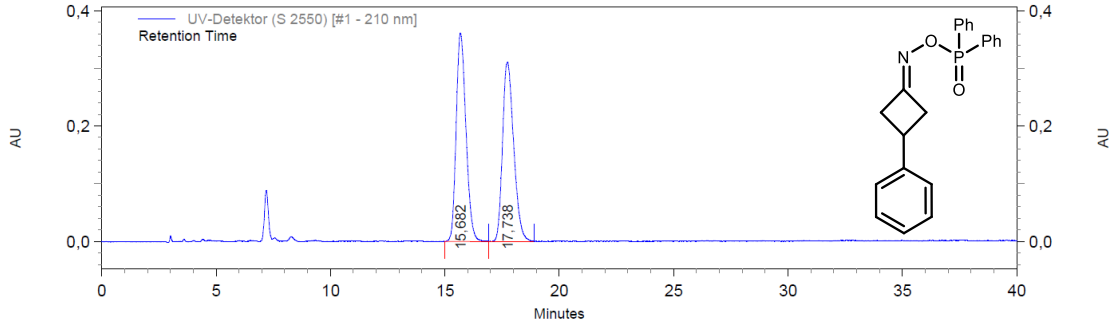

UV-Detektor (S 2550) [#1 - 210 nm] Results

Retention Time	Area	Area %
15,682	10736413	50,47
17,738	10537785	49,53

Figure 23. HPLC chromatogram for (((3-Phenylcyclobutylidene)amino)oxy)diphenylphosphine oxide (3.32)

1.0 mmol scale:

Following **GP-J** using 3-phenylyclobut-1-one **2.8** (146 mg, 1.00 mmol, 1.00 eq.), (*R*)-**3.40** (101 mg, 100 µmol, 10 mol%) and *O*-(diphenylphosphinyl)hydroxylamine [**2**] (257 mg, 1.10 mmol, 1.10 eq.) the product (*R*)-**3.32** (330 mg, 913 µmol, 91%) was obtained *via* automated flash column chromatography (SiO_2, Cyclohexane:EtOAc, 100:0 → 0:100, stained with $KMnO_4$) as colourless solid. **Optical Rotation:** $[\alpha]_D^{25}$ = –61.0 (c = 1.0, $CHCl_3$) for an enantiomerically enriched sample of 94:6 *er*. The enantiomeric purity was established by HPLC analysis using a chiral column (Cellulose-1, 40 °C, 1 mL/min, 85:15 *n*hexane:isopropanol, 214 nm, t = 14.009 min and 15.642 min).

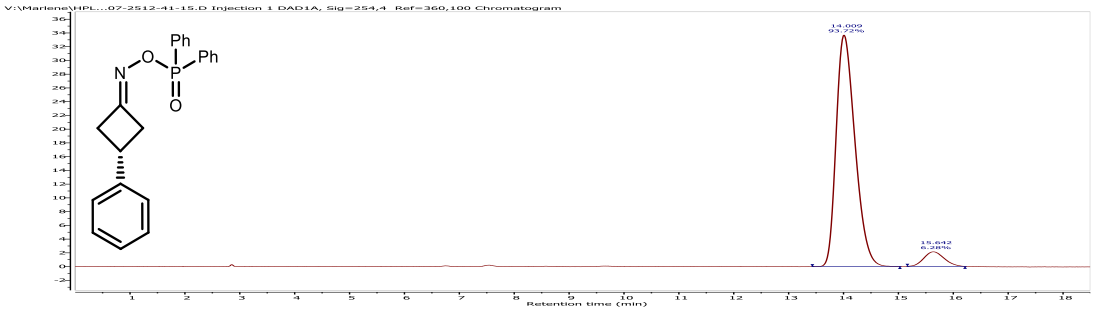

Retention Time	Area%
14.009	93.72
15.642	6.28

Figure 24. HPLC chromatogram for ((*R*)-(((3-Phenylcyclobutylidene)amino)oxy)diphenylphosphine oxide ((*R*)-3.32).

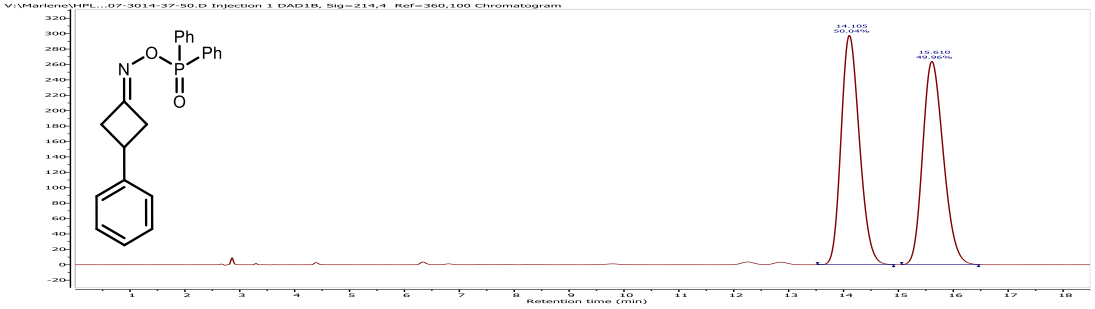

Retention Time	Area%
14.105	50.04
15.610	49.96

Figure 25. HPLC chromatogram for (((3-Phenylcyclobutylidene)amino)oxy)diphenylphosphine oxide (3.32).

Reisolation of the catalyst (*R*)-**3.40***:*
Following a procedure from Klussmann *et al.*[160], the catalyst isolated by flash column chromatography was dissolved in CH_2Cl_2 (20 mL). The organic phase was washed with 1.0 M HCl (3 x 10 mL), dried over Mg_2SO_4 and concentrated under reduced pressure. (R)-**3.40** (93 mg, 93.6 µmol, 91%) was obtained after recrystallization from acetonitrile as a colourless solid.

^{1}H NMR (400 MHz, $CDCl_3$): δ = 7.84 (d, *J* = 8.2 Hz, 2H), 7.70 (s, 2H), 7.44 (ddd, *J* = 8.1, 6.4, 1.5 Hz, 2H), 7.31 – 7.17 (m, 4H), 6.93 – 6.86 (m, 4H), 2.51 – 2.35 (m, 2H), 2.24 – 2.01 (m, 4H), 1.97 – 0.40 (m, 60H). **^{13}C NMR (101 MHz, $CDCl_3$)**: δ = 147.0, 146.6, 146.5, 146.4, 146.3, 132.3, 132.2, 131.9, 131.8, 131.0, 128.2, 126.8, 126.2, 125.6, 122.4, 121.8, 121.6, 44.9, 42.3, 41.9, 37.1, 35.2, 34.8, 34.3, 33.3, 32.7, 27.5, 27.3, 27.3, 27.10, 26.8, 26.5, 26.4, 25.9. **^{31}P NMR (162 MHz, $CDCl_3$)**: δ = 1.27. The spectroscopic data was in agreement to those previously reported.[161]

Reuse of the catalyst:
Following **GP-J** using 3-phenylyclobut-1-one **2.8** (29.2 mg, 200 µmol, 1.00 eq.), (*R*)-**3.40** (19.8 mg, 20.0 µmol, 10 mol%) and *O*-(diphenylphosphinyl)hydroxylamine **2.51** (51.3 mg, 220 µmol, 1.10 eq.) the product (*R*)-**3.32** (63.8 mg, 175 µmol, 88%) the product *via* flash column chromatography (SiO_2, Cyclohexane:EtOAc, 100:0 → 0:100, stained with $KMnO_4$) as colourless solid.

Optical Rotation: $[\alpha]_D^{25}$ = –59.7 (c = 1.0, $CHCl_3$) for an enantiomerically enriched sample of 94:06 *er*. The enantiomeric purity was established by HPLC analysis using a chiral column (Cellulose-1, 40 °C, 1 mL/min, 85:15 *n*hexane:isopropanol, 214 nm, t = 14.012 min and 15.615 min).

(*R*)-(((3-(4-Fluorophenyl)cyclobutylidene)amino)oxy)diphenylphosphine oxide ((*R*)-3.43)

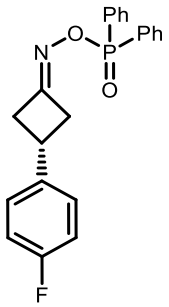

Following **GP-J** using 3-(4-fluorophenyl)cyclobutan-1-one (32.8 mg, 200 µmol, 1.00 eq.), (*R*)-**3.40** (19.8 mg, 20.0 µmol, 10 mol%) and *O*-(diphenylphosphinyl)hydroxylamine **2.51** (51.3 mg, 220 µmol, 1.10 eq.) the product (*R*)-**3.43** (71.0 mg, 187 µmol, 94%) was obtained *via* automated flash column chromatography (SiO_2, Cyclohexane:EtOAc, 100:0 → 0:100, stained with $KMnO_4$) as colourless solid.

M.P.: 84 – 89 °C. **IR (neat)**: $\tilde{\nu}$ = 2955 (w), 2924 (m), 2854 (w), 1604 (w), 1510 (s), 1439 (m), 1229 (s), 1180 (w), 1160 (w), 1129 (s), 1112 (m), 876 (s), 831 (m), 813 (m), 729 (s), 696 (s), 625 (w), 553 (s), 532 (s). **^{1}H NMR (600 MHz, $CDCl_3$)**: δ = 7.90 – 7.83 (m, 4H, C$H_{arom.}$), 7.57 – 7.52 (m, 2H, C$H_{arom.}$), 7.50 – 7.44 (m, 4H, C$H_{arom.}$), 7.23 – 7.17 (m, 2H, C$H_{arom.}$), 7.06 – 6.99 (m, 2H, C$H_{arom.}$), 3.65 – 3.56 (m, 2H, CH, CH_2), 3.46 – 3.38 (m, 1H, CH_2), 3.14 (qd, J = 10.3, 3.2 Hz, 1H, CH_2), 3.09 – 3.03 (m, 1H, CH_2). **^{13}C NMR (151 MHz, $CDCl_3$)**: δ = 166.1 (d, $^3J_{C\text{-}P}$ = 12.4 Hz, C_q), 161.8 (d, $^1J_{C\text{-}F}$ = 245.2 Hz, C_q), 138.9 (d, $^4J_{C\text{-}F}$ = 3.4 Hz, C_q), 132.5 (d, $^4J_{C\text{-}P}$ = 2.9 Hz, *C*H), 132.2 (d, $^2J_{C\text{-}P}$ = 9.8 Hz, *C*H), 132.1 (d, $^2J_{C\text{-}P}$ = 10.1 Hz, *C*H), 130.7 (d, $^1J_{C\text{-}P}$ = 136.0 Hz, C_q), 130.6 (d, $^1J_{C\text{-}P}$ = 135.6 Hz, C_q), 128.7 (d, $^3J_{C\text{-}P}$ = 13.2 Hz, *C*H), 128.0 (d, $^3J_{C\text{-}F}$ = 7.9 Hz, *C*H), 115.7 (d, $^2J_{C\text{-}F}$ = 21.4 Hz, *C*H), 39.90, 39.71, 31.85. **^{31}P NMR (162 MHz, $CDCl_3$)**: δ = 35.29. **^{19}F NMR** (376 MHz, $CDCl_3$) δ = −115.79 (tt, J = 8.8, 4.9 Hz). **HRMS (ESI):** Calculated for $C_{22}H_{19}FNO_2P$ $[M+H]^+$: 380.1210, Found: 380.1203. **Optical Rotation:** $[\alpha]_D^{25}$ = −63.3 (c = 0.5, $CHCl_3$) for an enantiomerically enriched sample of 90:10 *er*. The enantiomeric purity was established by HPLC analysis using a chiral column (Lux® Cellulose-1, 22 °C, 1 mL/min, 85:15 *n*-hexane:isopropanol, 210 nm, t = 16.751 min and 18.715 min).

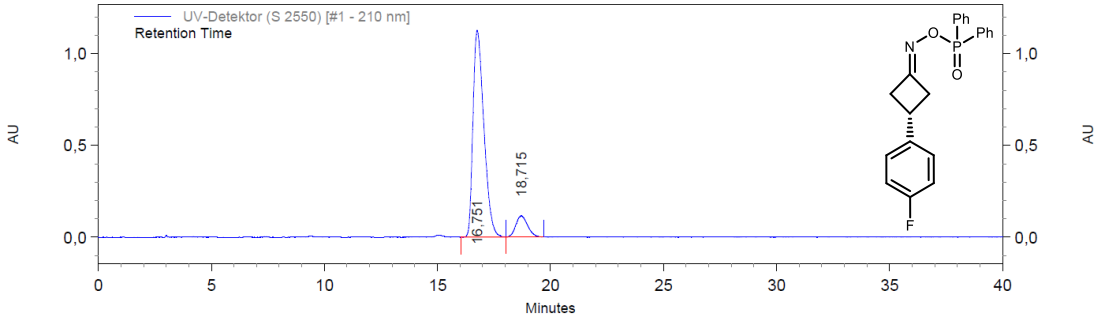

UV-Detektor (S 2550) [#1 - 210 nm] Results

Retention Time	Area	Area %
16,751	37770575	90,07
18,715	4164170	9,93

Figure 26. HPLC chromatogram for (*R*)-(((3-(4-fluorophenyl)cyclobutylidene)amino)oxy)diphenylphosphine oxide ((*R*)-3.43).

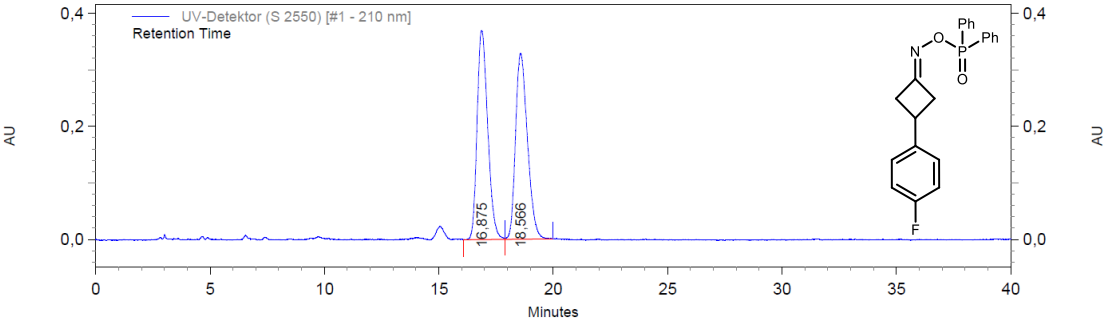

UV-Detektor (S 2550) [#1 - 210 nm] Results

Retention Time	Area	Area %
16,875	11975495	50,17
18,566	11892150	49,83

Figure 27. HPLC chromatogram for (((3-(4-fluorophenyl)cyclobutylidene)amino)oxy)diphenylphosphine oxide (3.43).

(*R*)-(((3-(4-Chlorophenyl)cyclobutylidene)amino)oxy)diphenylphosphine oxide ((*R*)-3.44)

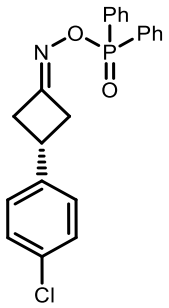

Following **GP-J** using 3-(4-chlorophenyl)cyclobutan-1-one (36.1 mg, 200 µmol, 1.00 eq.), (*R*)-**3.40** (19.8 mg, 20.0 µmol, 10 mol%) and *O*-(diphenylphosphinyl)hydroxylamine (*R*)-**3.44** (51.3 mg, 220 µmol, 1.10 eq.) the product (60.5 mg, 153 µmol, 76%) was obtained *via* automated flash column chromatography (SiO_2, Cyclohexane:EtOAc, 100:0 → 0:100, stained with $KMnO_4$) as colourless solid.

M.P.: 139 – 145 °C. **IR (neat)**: $\tilde{\nu}$ = 3057 (w), 2235 (w), 1693 (w), 1592 (w), 1493 (m), 1439 (m), 1399 (w), 1232 (s), 1180 (w), 1129 (s), 1112 (m), 1092 (m), 1014 (w), 876 (s), 817 (m), 763 (m), 729 (s), 695 (s), 584 (w), 553 (s), 537 (s). **^{1}H NMR (400 MHz, $CDCl_3$)**: δ = 7.87 (m, 4H, C$H_{arom.}$), 7.58 – 7.51 (m, 2H, C$H_{arom.}$), 7.51 – 7.43 (m, 4H, C$H_{arom.}$), 7.33 – 7.28 (m, 2H, C$H_{arom.}$), 7.20 – 7.13 (m, 2H, C$H_{arom.}$), 3.66 – 3.54 (m, 2H, C*H*, CH_2), 3.47 – 3.35 (m, 1H, CH_2), 3.21 – 3.01 (m, 2H, CH_2). **^{13}C NMR (101 MHz, $CDCl_3$)**: δ = 166.0 (d, $^3J_{C\text{-}P}$ = 12.4 Hz, *C*=N), 141.7 (C_q), 132.7 (C_q), 132.5 (d, $^4J_{C\text{-}P}$ = 2.9 Hz, *C*H), 132.2 (*app.* t, $^2J_{C\text{-}P}$ = 9.8 Hz, *C*H), 130.7 (d, $^1J_{C\text{-}P}$ = 136.2 Hz, C_q), 130.6 (d, $^1J_{C\text{-}P}$ = 135.7 Hz, C_q), 129.0 (*C*H), 128.7 (d, $^3J_{C\text{-}P}$ = 13.2 Hz, *C*H), 127.9 (*C*H), 39.7 (*C*H_2), 39.5 (*C*H_2), 32.0 (*C*H). **^{31}P NMR (162 MHz, $CDCl_3$)**: δ = 35.4. **HRMS (ESI):** Calculated for $C_{22}H_{19}ClNO_2P$ $[M+H]^+$: 309.0920, Found: 396.0916. **Optical Rotation:** $[\alpha]_D^{25}$ = –57.3 (c = 0.5, $CHCl_3$) for an enantiomerically enriched sample of 93:7 *er*. The enantiomeric purity was established by HPLC analysis using a chiral column (Lux® Cellulose-1, 22 °C, 1 mL/min, 93:07 *n*-hexane:isopropanol, 210 nm, t = 20.341 min and 23.495 min).

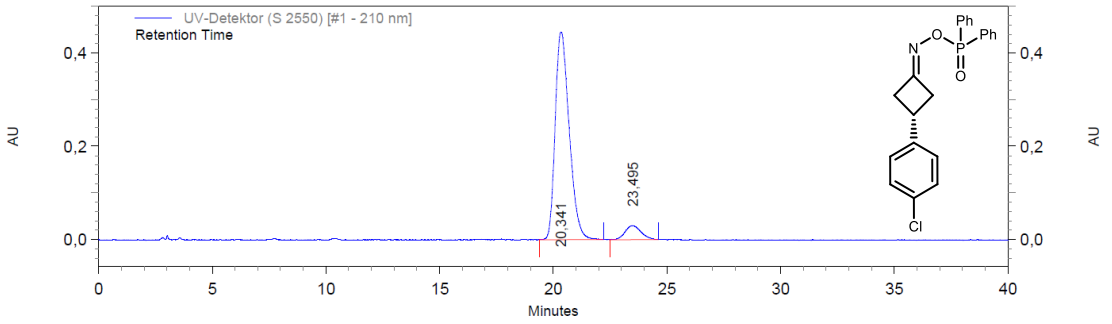

UV-Detektor (S 2550) [#1 - 210 nm] Results

Retention Time	Area	Area %
20,341	19041919	92,72
23,495	1494371	7,28

Figure 28. HPLC chromatogram for (*R*)-(((3-(4-chlorophenyl)cyclobutylidene)amino)oxy)diphenylphosphine oxide ((*R*)-3.44).

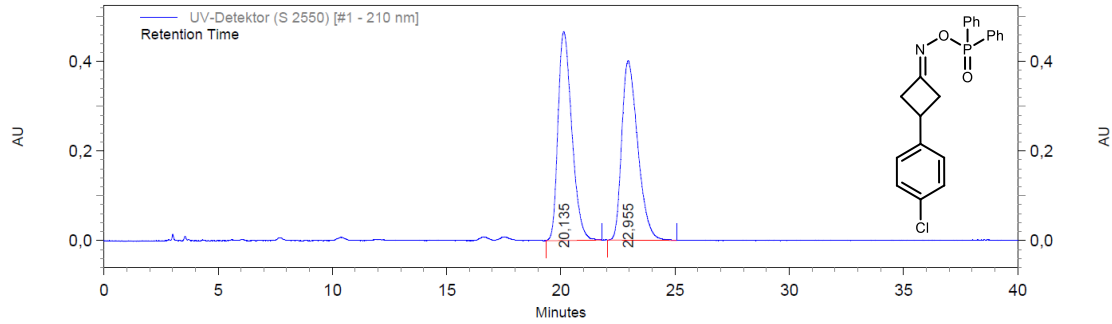

UV-Detektor (S 2550) [#1 - 210 nm] Results

Retention Time	Area	Area %
20,135	19575625	49,98
22,955	19591064	50,02

Figure 29. HPLC chromatogram for (((3-(4-chlorophenyl)cyclobutylidene)amino)oxy)diphenylphosphine oxide (3.44).

(*R*)-(((3-(4-Bromophenyl)cyclobutylidene)amino)oxy)diphenylphosphine oxide ((*R*)-3.45)

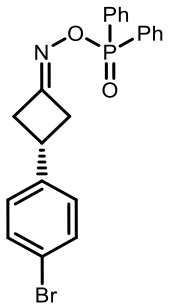

Following **GP-J** using 3-(4-bromophenyl)cyclobutan-1-one (45.0 mg, 200 µmol, 1.00 eq.), (*R*)-**3.40** (19.8 mg, 20.0 µmol, 10 mol%) and *O*-(diphenylphosphinyl)hydroxylamine **2.51** (51.3 mg, 220 µmol, 1.10 eq.) the product (*R*)-**3.45** (74.3 mg, 169 µmol, 84%) was obtained *via* automated flash column chromatography (SiO_2, Cyclohexane:EtOAc, 100:0 → 0:100, stained with $KMnO_4$) as colourless solid.

M.P.: 126 – 134 °C. **IR (neat)**: $\tilde{\nu}$ = 3059 (w), 2927 (w), 2230 (w), 2029 (w), 2003 (w), 1692 (w), 1592 (w), 1488 (m), 1439 (m), 1398 (w), 1230 (s), 1180 (w), 1129 (s), 1112 (m), 1072 (w), 1027 (w), 1010 (w), 965 (w), 890 (s), 874 (s), 814 (m), 753 (m), 728 (s), 695 (s), 645 (w), 553 (s), 536 (s), 524 (m), 452 (w), 419 (w). **^{1}H NMR (400 MHz, $CDCl_3$)**: δ = 7.90 – 7.82 (m, 4H, C$H_{arom.}$), 7.59 – 7.51 (m, 2H, C$H_{arom.}$), 7.50 – 7.43 (m, 6H, C$H_{arom.}$), 7.14 – 7.08 (m, 2H, C$H_{arom.}$), 3.66 – 3.53 (m, 2H, CH, CH_2), 3.48 – 3.36 (m, 1H, CH_2), 3.20 – 3.00 (m, 2H, CH_2). **^{13}C NMR (101 MHz, $CDCl_3$)**: δ = 165.9 (d, $^3J_{C\text{-}P}$ = 12.5 Hz, *C*=N), 142.2 (C_q), 132.5 (d, $^4J_{C\text{-}P}$ = 2.9 Hz, *C*H), 132.2 (*app*. t, $^2J_{C\text{-}P}$ = 9.8 Hz, *C*H), 131.9 (*C*H), 130.7 (d, $^1J_{C\text{-}P}$ = 136.1 Hz, C_q), 130.6 (d, $^1J_{C\text{-}P}$ = 135.7 Hz, C_q), 128.7 (d, $^3J_{C\text{-}P}$ = 13.2 Hz, *C*H), 128.3 (*C*H), 120.8 (C_q), 39.6 (*C*H$_2$), 39.5 (*C*H$_2$), 32.0 (*C*H). **^{31}P NMR (162 MHz, $CDCl_3$)**: δ = 35.42. **HRMS (ESI):** Calculated for $C_{22}H_{19}BrNO_2P$ $[M+H]^+$: 440.0415, Found: 440.0412. **Optical Rotation:** $[\alpha]_D^{25}$ = –60.8 (c = 0.5, $CHCl_3$) for an enantiomerically enriched sample of 93:7 *er*. The enantiomeric purity was established by HPLC analysis using a chiral column (Lux® Cellulose-1, 22 °C, 1 mL/min, 85:15 *n*hexane:isopropanol, 210 nm, t = 22.481 min and 26.136 min).

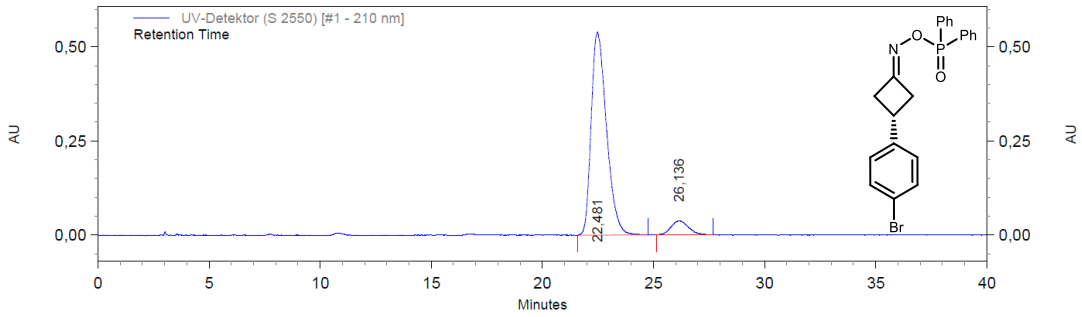

UV-Detektor (S 2550) [#1 - 210 nm] Results

Retention Time	Area	Area %
22,481	25816737	92,51
26,136	2089656	7,49

Figure 30. HPLC chromatogram for (*R*)-(((3-(4-bromophenyl)cyclobutylidene)amino)oxy)diphenylphosphine oxide ((*R*)-3.45).

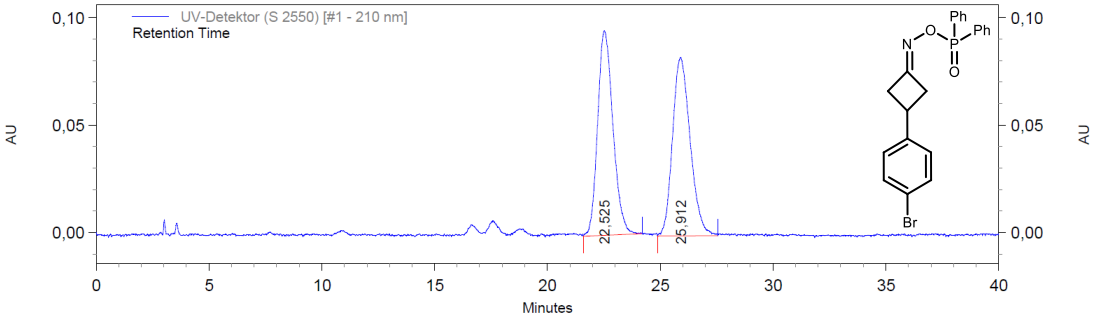

UV-Detektor (S 2550) [#1 - 210 nm] Results

Retention Time	Area	Area %
22,525	4492343	49,91
25,912	4508917	50,09

Figure 31. HPLC chromatogram for (((3-(4-bromophenyl)cyclobutylidene)amino)oxy)diphenylphosphine oxide (3.45).

(*R*)-(((3-(4-(Trifluoromethyl)phenyl)cyclobutylidene)amino)oxy)diphenyl phosphine oxide ((*R*)-3.46)

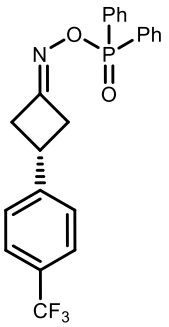

Following **GP-J** using 3-(4-(trifluoromethyl)phenyl)cyclobutan-1-one (42.8 mg, 200 µmol, 1.00 eq.), (*R*)-**3.40** (19.8 mg, 20.0 µmol, 10 mol%) and *O*-(diphenylphosphinyl)hydroxylamine **2.51** (51.3 mg, 220 µmol, 1.10 eq.) the product (*R*)-**3.46** (68.7 mg, 160 µmol, 80%) was obtained *via* automated flash column chromatography (SiO_2, Cyclohexane:EtOAc, 100:0 → 0:100, stained with $KMnO_4$) as colourless solid.

M.P.: 120 – 123 °C. **IR (neat)**: $\tilde{\nu}$ = 3061 (w), 2924 (w), 1619 (w), 1592 (w), 1439 (w), 1326 (s), 1232 (m), 1165 (m), 1128 (s), 1113 (s), 1069 (m), 1017 (w), 877 (m), 834 (w), 748 (w), 729 (m), 696 (m), 606 (w), 553 (m), 536 (m), 462 (w), 435 (w). **^{1}H NMR (400 MHz, $CDCl_3$)**: δ = 7.92 – 7.82 (m, 4H, C$H_{arom.}$), 7.60 (d, J = 8.0, 2H, C$H_{arom.}$), 7.58 – 7.52 (m, 2H, C$H_{arom.}$), 7.51 – 7.44 (m, 4H, C$H_{arom.}$), 7.36 (d, J = 8.1 Hz, 2H, C$H_{arom.}$), 3.75 – 3.59 (m, 2H, CH, CH_2), 3.51 – 3.42 (m, 1H, CH_2), 3.25 – 3.06 (m, 1H, 2xCH_2). **^{13}C NMR (101 MHz, $CDCl_3$)**: δ = 165.6 (d, $^3J_{C\text{-}P}$ = 12.4 Hz, *C*=N), 147.2 (*C*H), 132.5 (d, $^4J_{C\text{-}P}$ = 2.8 Hz, *C*H), 132.2 (t, $^2J_{C\text{-}P}$ = 10.2 Hz, *C*H)[a], 130.6 (d, $^1J_{C\text{-}P}$ = 136.1 Hz, C_q), 130.6 (d, $^1J_{C\text{-}P}$ = 135.8 Hz, C_q), 129.3 (q, $^2J_{C\text{-}F}$ = 32.5 Hz, C_q), 128.7 (d, $^3J_{C\text{-}P}$ = 13.2 Hz, *C*H), 126.9 (*C*H), 125.8 (q, $^3J_{C\text{-}F}$ = 3.8 Hz, *C*H), 124.2 3 (q, $^1J_{C\text{-}F}$ = 272.1 Hz, C_q), 39.6 (*C*H_2), 39.4 (*C*H_2), 32.3 (*C*H). **^{31}P NMR (162 MHz, $CDCl_3$)**: δ = 35.43. **^{19}F NMR (376 MHz, $CDCl_3$)** δ = –62.40. **HRMS (ESI):** Calculated for $C_{23}H_{19}F_3NO_2P$ $[M+H]^+$: 430.1184, Found: 430.1181. **Optical Rotation:** $[\alpha]_D^{25}$ = –22.0 (c = 0.5, $CHCl_3$) for an enantiomerically enriched sample of 93:7 *er*. The enantiomeric purity was established by HPLC analysis using a chiral column (Lux® Cellulose-1, 22 °C, 1 mL/min, 85:15 *n*hexane:isopropanol, 210 nm, t = 20.683 min and 26.437 min).

[a] Appears as triplett due to overlap of 2 carbon signals (dublett)

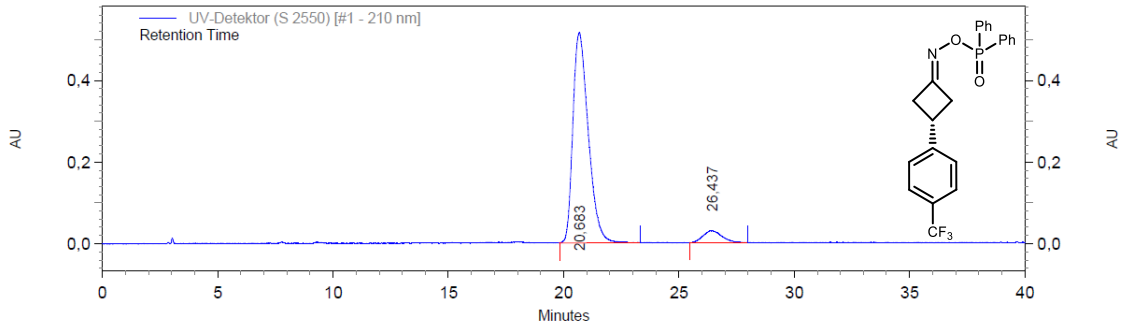

UV-Detektor (S 2550) [#1 - 210 nm] Results

Retention Time	Area	Area %
20,683	23852673	93,40
26,437	1686509	6,60

Figure 32. HPLC chromatogram for (*R*)-(((3-(4-(Trifluoromethyl)phenyl)cyclobutylidene)amino)oxy)diphenyl phosphine oxide ((*R*)-3.46).

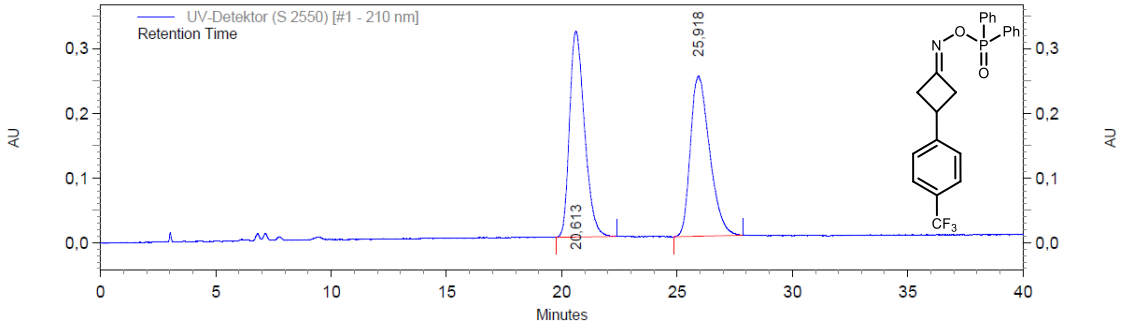

UV-Detektor (S 2550) [#1 - 210 nm] Results

Retention Time	Area	Area %
20,613	14331333	49,95
25,918	14362455	50,05

Figure 33. HPLC chromatogram for (((3-(4-(Trifluoromethyl)phenyl)cyclobutylidene)amino)oxy)diphenyl phosphine oxide (3.46).

(*R*)-(((3-(4-Methoxyphenyl)cyclobutylidene)amino)oxy)diphenylphosphin oxide ((*R*)-3.47)

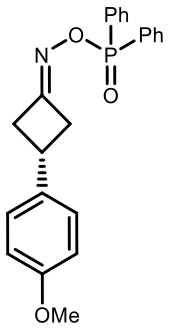

Following **GP-J** using 3-(4-methoxyphenyl)cyclobutan-1-one (35.2 mg, 200 µmol, 1.00 eq.), (*R*)-**3.40** (19.8 mg, 20.0 µmol, 10 mol%) and *O*-(diphenylphosphinyl)hydroxylamine **2.51** (51.3 mg, 220 µmol, 1.10 eq.) the product (*R*)-**3.47** (65.2 mg, 167 µmol, 83%) was obtained *via* automated flash column chromatography (SiO_2, Cyclohexane:EtOAc, 100:0 → 0:100, stained with $KMnO_4$) as colourless solid.

M.P.: 89 – 90 °C. **IR (neat)**: $\tilde{\nu}$ = 2956 (w), 2922 (w), 1688 (w), 1612 (w), 1592 (w), 1514 (m), 1488 (w), 1460 (w), 1439 (m), 1396 (w), 1247 (s), 1180 (m), 1127 (s), 1096 (m), 1070 (m), 1037 (m), 878 (s), 827 (m), 727 (s), 695 (s), 625 (w), 552 (s), 534 (s), 451 (w), 441 (w), 417 (w). **^{1}H NMR (400 MHz, $CDCl_3$)**: δ = 7.91 – 7.83 (m, 4H, C$H_{arom.}$), 7.57 – 7.51 (m, 2H, C$H_{arom.}$), 7.50 – 7.43 (m, 4H, C$H_{arom.}$), 7.19 – 7.12 (m, 2H, C$H_{arom.}$), 6.90 – 6.84 (m, 2H, C$H_{arom.}$), 3.80 (s, 3H, CH_3), 3.63 – 3.51 (m, 2H, CH_2), 3.44 – 3.34 (m, 1H, CH_2), 3.20 – 3.00 (m, 2H, 2xCH_2).**^{13}C NMR (101 MHz, $CDCl_3$)**: δ = 166.6 (d, $^3J_{C\text{-}P}$ = 12.4 Hz, *C*=N), 158.6 (C_q), 135.4 (C_q), 132.4 (d, $^4J_{C\text{-}P}$ = 2.8 Hz, *C*H), 132.2 (t, $^2J_{C\text{-}P}$ = 9.8 Hz, *C*H)[a], 130.8 (d, $^1J_{C\text{-}P}$ = 136.2 Hz, C_q), 130.7 (d, $^1J_{C\text{-}P}$ = 135.7 Hz, C_q), 128.6 (d, $^3J_{C\text{-}P}$ = 13.3 Hz, *C*H), 127.5 (*C*H), 114.2 (*C*H), 55.5 (*C*H$_3$), 40.0 (*C*H$_2$), 39.8 (*C*H$_2$), 31.8 (*C*H). **^{31}P NMR (162 MHz, $CDCl_3$)**: δ = 35.12. **HRMS (ESI):** Calculated for $C_{23}H_{22}NO_3P$ $[M+H]^+$: 392.1416, Found: 392.1411. **Optical Rotation:** $[\alpha]_D^{25}$ = –28.9 (c = 1.0, $CHCl_3$) for an enantiomerically enriched sample of 91:9 *er*. The enantiomeric purity was established by HPLC analysis using a chiral column (Lux® Cellulose-1, 22 °C, 1 mL/min, 85:15 *n*hexane:isopropanol, 210 nm, t = 47.464 min and 52.304 min).

[a] Appears as triplett due to overlap of 2 carbon signals (dublett)

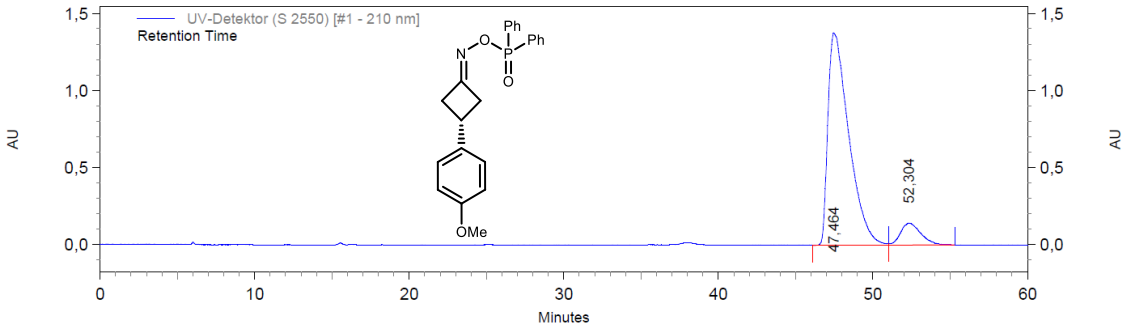

UV-Detektor (S 2550) [#1 - 210 nm] Results

Retention Time	Area	Area %
47,464	129075456	90,81
52,304	13059295	9,19

Figure 34. HPLC chromatogram for (*R*)-(((3-(4-Methoxyphenyl)cyclobutylidene)amino)oxy)diphenylphosphine oxide ((*R*)-3.47).

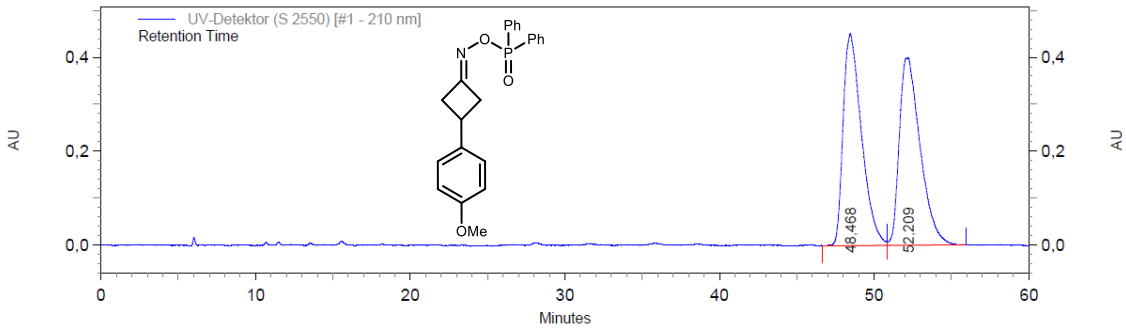

UV-Detektor (S 2550) [#1 - 210 nm] Results

Retention Time	Area	Area %
48,468	37413512	49,92
52,209	37531449	50,08

Figure 35. HPLC chromatogram for (((3-(4-Methoxyphenyl)cyclobutylidene)amino)oxy)diphenylphosphine oxide (3.47).

(*R*)-(((3-(*p*-Tolyl)cyclobutylidene)amino)oxy)diphenylphosphine oxide ((*R*)-3.48)

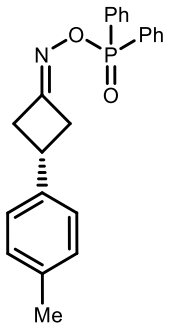

Following **GP-J** using 3-(4-methylphenyl)cyclobutanone (32.0 mg, 200 µmol, 1.00 eq.), (*R*)-**3.40** (19.8 mg, 20.0 µmol, 10 mol%) and *O*-(diphenylphosphinyl)hydroxylamine **2.51** (51.3 mg, 220 µmol, 1.10 eq.) the product (*R*)-**3.48** (67.8 mg, 181 µmol, 90%) was obtained *via* automated flash column chromatography (SiO_2, Cyclohexane:EtOAc, 100:0 → 0:100, stained with $KMnO_4$) as colourless solid.

M.P.: 97 – 100 °C. **IR (neat)**: $\tilde{\nu}$ = 3058 (w), 3021 (w), 2921 (w), 1690 (w), 1592 (w), 1516 (w), 1485 (w), 1439 (m), 1396 (w), 1233 (s), 1179 (w), 1129 (s), 1112 (m), 1072 (w), 1028 (w), 999 (w), 963 (w), 877 (s), 811 (m), 729 (s), 696 (s), 648 (w), 627 (w), 579 (w), 554 (s), 532 (s), 479 (w), 463 (w), 449 (w), 438 (w), 417 (w). **^{1}H NMR (400 MHz, $CDCl_3$)**: δ = 7.91 – 7.82 (m, 4H, C$H_{arom.}$), 7.58 – 7.51 (m, 2H, C$H_{arom.}$), 7.51 – 7.42 (m, 4H, C$H_{arom.}$), 7.18 – 7.10 (m, 4H, C$H_{arom.}$), 3.65 – 3.52 (m, 2H, C*H*, CH_2), 3.45 – 3.34 (m, 1H, CH_2), 3.21 – 3.01 (m, 2H, 2xCH_2), 2.34 (s, 3H, CH_3). **^{13}C NMR (101 MHz, $CDCl_3$)**: δ = 166.6 (d, $^3J_{C\text{-}P}$ = 12.5 Hz, *C*=N), 140.3 (C_q), 136.6 (C_q), 132.4 (d, $^4J_{C\text{-}P}$ = 2.9 Hz, *C*H), 132.2 (d, $^2J_{C\text{-}P}$ = 10.6 Hz, *C*H), 132.1 (d, $^2J_{C\text{-}P}$ = 10.6 Hz, *C*H), 130.8 (d, $^1J_{C\text{-}P}$ = 136.2 Hz, C_q), 130.7 (d, $^1J_{C\text{-}P}$ = 135.7 Hz, C_q), 129.5 (*C*H), 128.6 (d, $^3J_{C\text{-}P}$ = 13.2 Hz, *C*H), 126.4 (*C*H), 39.8 (*C*H_2), 39.6 (*C*H_2), 32.1 (*C*H), 21.1 (*C*H_3). **^{31}P NMR (162 MHz, $CDCl_3$)**: δ = 35.18. **HRMS (ESI):** Calculated for $C_{23}H_{22}NO_2P$ $[M+H]^+$: 376.1466, Found: 376.1461. **Optical Rotation:** $[\alpha]_D^{25}$ = –43.5 (c = 0.5, $CHCl_3$) for an enantiomerically enriched sample of 91:9 *er*. The enantiomeric purity was established by HPLC analysis using a chiral column (Lux® Cellulose-1, 22 °C, 1 mL/min, 85:15 *n*hexane:isopropanol, 210 nm, t = 13.930 min and 15.762 min).

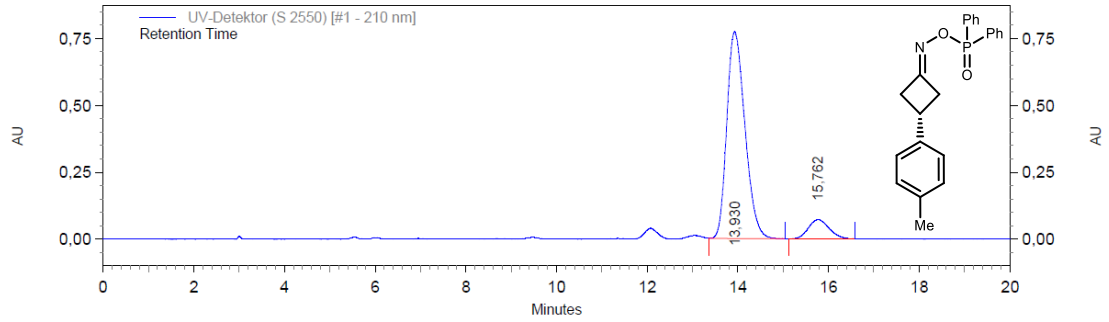

UV-Detektor (S 2550) [#1 - 210 nm] Results

Retention Time	Area	Area %
13,930	21528170	90,51
15,762	2258249	9,49

Figure 36. HPLC chromatogram for (*R*)-(((3-(*p*-tolyl)cyclobutylidene)amino)oxy)diphenylphosphine oxide ((*R*)-3.48).

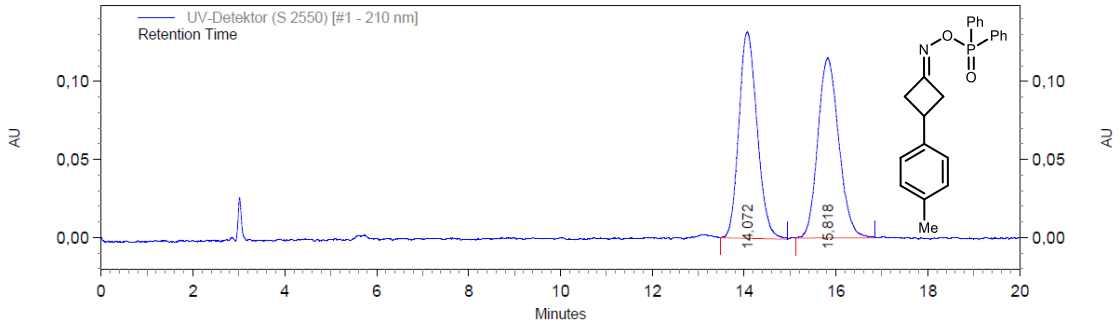

UV-Detektor (S 2550) [#1 - 210 nm] Results

Retention Time	Area	Area %
14,072	3654970	50,00
15,818	3655235	50,00

Figure 37. HPLC chromatogram for (((3-(*p*-tolyl)cyclobutylidene)amino)oxy)diphenylphosphine oxide (3.48).

(*R*)-(((3-(Naphthalen-1-yl)cyclobutylidene)amino)oxy)diphenylphosphine oxide ((*R*)-3.49)

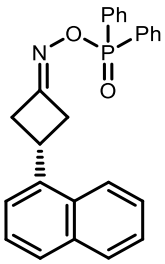

Following **GP-J** using 3-(naphthalen-2-yl)cyclobutan-1-one (39.3 mg, 200 µmol, 1.00 eq.), (*R*)-**3.40** (19.8 mg, 20.0 µmol, 10 mol%) and *O*-(diphenylphosphinyl)hydroxylamine **2.51** (51.3 mg, 220 µmol, 1.10 eq.) the product (*R*)-**3.49** (68.8 mg, 167 µmol, 84%) was obtained *via* automated flash column chromatography (SiO_2, Cyclohexane:EtOAc, 100:0 → 0:100, stained with $KMnO_4$) as colourless solid.

M.P.: 121 – 125 °C. **IR (neat)**: $\tilde{\nu}$ = 3053 (w), 2975 (w), 2926 (w), 2234 (w), 1693 (w), 1633 (w), 1592 (w), 1508 (w), 1485 (w), 1439 (m), 1397 (w), 1231 (s), 1180 (w), 1129 (m), 1112 (w), 1071 (w), 1028 (w), 877 (s), 816 (m), 729 (s), 696 (s), 651 (w), 602 (w), 553 (s), 531 (m), 479 (w), 448 (w), 427 (w), 417 (w). **^{1}H NMR (400 MHz, $CDCl_3$)**: δ = 7.96 – 7.86 (m, 4H, C$H_{arom.}$), 7.86 – 7.76 (m, 3H, C$H_{arom.}$), 7.67 (s, 1H, C$H_{arom.}$), 7.59 – 7.52 (m, 2H, C$H_{arom.}$), 7.52 – 7.43 (m, J = 10.9, 4.3 Hz, 6H, C$H_{arom.}$), 7.37 (dd, J = 8.5, 1.8 Hz, 1H, C$H_{arom.}$), 3.88 – 3.75 (m, 1H, C*H*), 3.68 (*app*. ddt, J ≈ 17.4, 9.1, 3.4 Hz, 1H, CH_2.), 3.49 (*app*. ddt, J ≈ 16.0, 8.9, 3.3 Hz, 1H, CH_2), 3.35 – 3.14 (m, 2H, CH_2).. **^{13}C NMR (101 MHz, $CDCl_3$)**: δ = 166.4 (d, $^3J_{C\text{-}P}$ = 12.4 Hz, *C*=N), 140.5 (C_q), 133.4 (C_q), 132.5 (d, $^4J_{C\text{-}P}$ = 2.6 Hz, *C*H)[a], 132.2 (t, $^2J_{C\text{-}P}$ = 10.4 Hz, *C*H)[b], 130.8 (d, $^1J_{C\text{-}P}$ = 136.1 Hz, C_q), 130.7 (d, $^1J_{C\text{-}P}$ = 135.7 Hz, C_q), 128.8 (*C*H), 128.7 (d, $^3J_{C\text{-}P}$ = 13.2 Hz, *C*H), 127.8 (*C*H), 127.8 (*C*H), 126.5 (*C*H), 126.0 (*C*H), 124.9 (*C*H), 124.8 (*C*H), 39.6 (*C*H), 39.4 (*C*H_2), 32.64 (*C*H_2). **^{31}P NMR (162 MHz, $CDCl_3$)**: δ = 35.30. **HRMS (ESI):** Calculated for $C_{26}H_{22}NO_2P$ $[M+H]^+$: 412.1466, Found: 412.1462. **Optical Rotation:** $[\alpha]_D^{25}$ = –81.4 (c = 0.5, $CHCl_3$) for an enantiomerically enriched sample of 94:6 *er*. The enantiomeric purity was established by HPLC analysis using a chiral column (Lux® Cellulose-1, 22 °C, 1 mL/min, 85:15 *n*hexane:isopropanol, 210 nm, t = 37.277 min and 43.452 min).

[a] Overlapp of 2 carbon signals (d → CH and s → Cq).
[b] Appears as triplett due to overlap of 2 carbon signals (dublett)

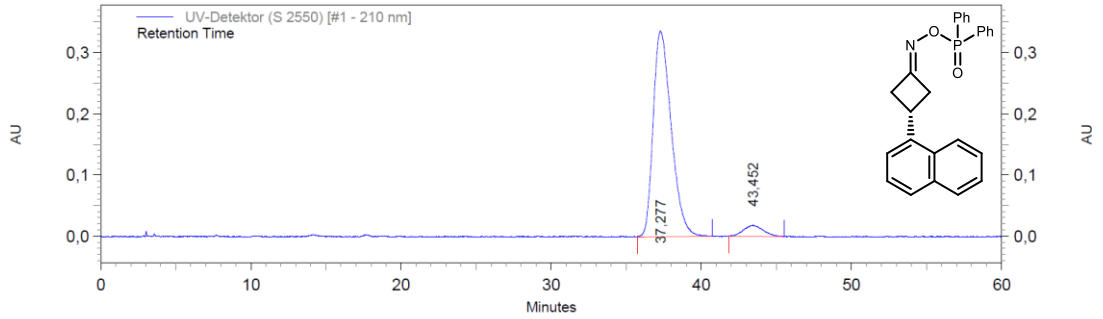

UV-Detektor (S 2550) [#1 - 210 nm] Results

Retention Time	Area	Area %
37,277	28079646	94,31
43,452	1692954	5,69

Figure 38. HPLC chromatogram for (*R*)-(((3-(naphthalen-1-yl)cyclobutylidene)amino)oxy)diphenylphosphine oxide (*R*)-3.49).

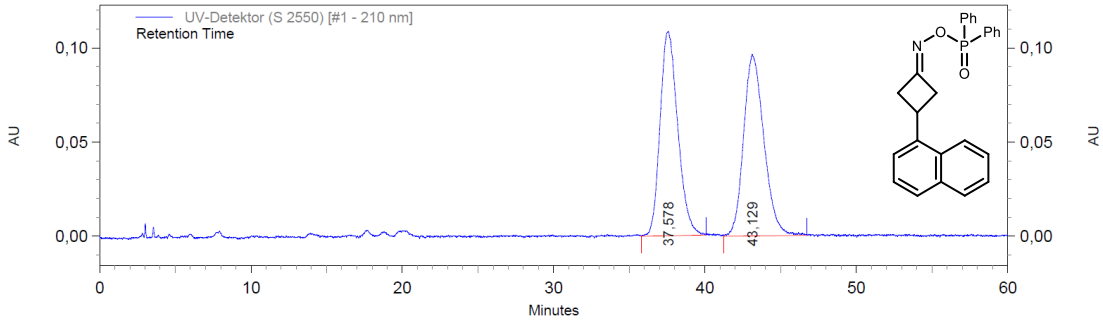

UV-Detektor (S 2550) [#1 - 210 nm] Results

Retention Time	Area	Area %
37,578	8803911	49,50
43,129	8981887	50,50

Figure 39. HPLC chromatogram for (((3-(naphthalen-1-yl)cyclobutylidene)amino)oxy)diphenylphosphine oxide (3.49).

(*R*)-(((3-(m-Tolyl)cyclobutylidene)amino)oxy)diphenylphosphine oxide ((*R*)-3.50)

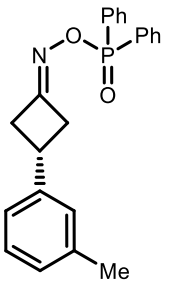

Following **GP-J** using 3-(3-methylphenyl)cyclobutan-1-one (32.0 mg, 200 µmol, 1.00 eq.), (*R*)-**3.40** (19.8 mg, 20.0 µmol, 10 mol%) and *O*-(diphenylphosphinyl)hydroxylamine **2.51** (51.3 mg, 220 µmol, 1.10 eq.) the product (*R*)-**3.50** (62.0 mg, 165 µmol, 83%) was obtained *via* automated flash column chromatography (SiO_2, Cyclohexane:EtOAc, 100:0 → 0:100, stained with $KMnO_4$) as colourless solid.

M.P.: 127 – 129 °C. **IR (neat)**: $\tilde{\nu}$ = 3057 (w), 2922 (w), 1692 (w), 1607 (w), 1591 (w), 1487 (w), 1439 (w), 1398 (w), 1311 (w), 1231 (m), 1180 (w), 1128 (m), 1112 (w), 1071 (w), 1028 (w), 999 (w), 974 (w), 872 (s), 811 (m), 785 (m), 727 (s), 695 (s), 672 (w), 645 (w), 550 (s), 534 (s), 442 (w). **^{1}H NMR (400 MHz, $CDCl_3$)**: δ = 7.93 – 7.82 (m, 4H, C$H_{arom.}$), 7.58 – 7.51 (m, 2H, C$H_{arom.}$), 7.51 – 7.42 (m, 4H, C$H_{arom.}$), 7.26 – 7.20 (m, 1H, C$H_{arom.}$), 7.09 – 7.01 (m, 3H, C$H_{arom.}$), 3.66 – 3.52 (m, 2H, C*H*, CH_2), 3.46 – 3.34 (m, 1H, CH_2), 3.25 – 3.03 (m, 2H, 2xCH_2), 2.35 (s, 3H, CH_3). **^{13}C NMR (101 MHz, $CDCl_3$)**: δ = 166.6 (d, $^3J_{C\text{-}P}$ = 12.3 Hz, *C*=N), 143.2 (C_q), 138.5 (C_q), 132.4 (d, $^4J_{C\text{-}P}$ = 2.9 Hz, *C*H), 132.2 (t, $^2J_{C\text{-}P}$ = 10.2 Hz, *C*H)[a], 130.8 (d, $^1J_{C\text{-}P}$ = 136.2 Hz, C_q), 130.7 (d, $^1J_{C\text{-}P}$ = 135.7 Hz, C_q), 128.7 (*C*H), 128.6 (d, $^3J_{C\text{-}P}$ = 13.1 Hz, *C*H), 127.7 (*C*H), 127.2 (*C*H), 123.5 (*C*H), 39.7 (*C*H_2), 39.5 (*C*H_2), 32.4 (*C*H), 21.6 (*C*H_3). **^{31}P NMR (162 MHz, $CDCl_3$)**: δ = 35.17. **HRMS (ESI):** Calculated for $C_{23}H_{22}NO_2P$ $[M+H]^+$: 376.1466, Found: 376.1464. **Optical Rotation:** $[\alpha]_D^{25}$ = –46.9 (c = 0.5, $CHCl_3$) for an enantiomerically enriched sample of 93:7 *er*. The enantiomeric purity was established by HPLC analysis using a chiral column (Lux® Cellulose-1, 22 °C, 1 mL/min, 85:15 *n*hexane:isopropanol, 210 nm, t = 13.238 min and 16.004 min).

[a] Appears as triplett due to overlap of 2 carbon signals (dublett)

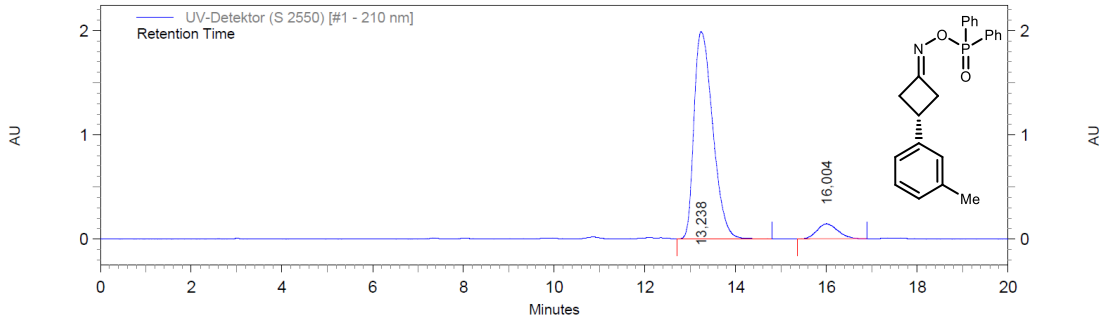

UV-Detektor (S 2550) [#1 - 210 nm] Results

Retention Time	Area	Area %
13,238	57022913	92,57
16,004	4579880	7,43

Figure 40. HPLC chromatogram for (*R*)-(((3-(*m*-tolyl)cyclobutylidene)amino)oxy)diphenylphosphine oxide ((*R*)-3.50).

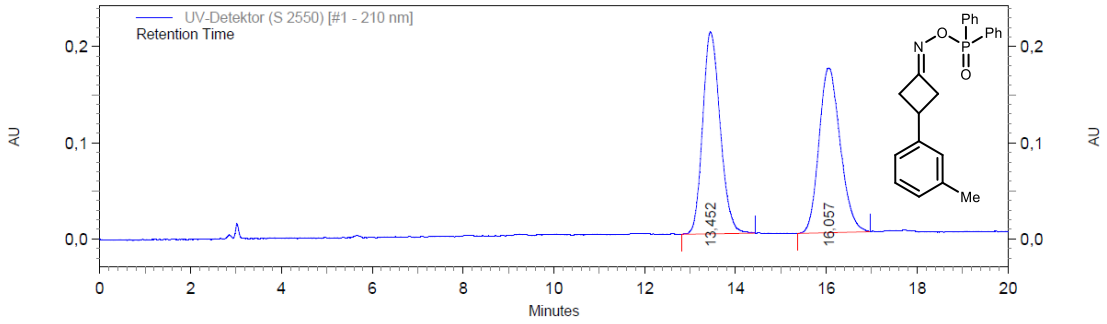

UV-Detektor (S 2550) [#1 - 210 nm] Results

Retention Time	Area	Area %
13,452	5632452	50,26
16,057	5574062	49,74

Figure 41. HPLC chromatogram for (((3-(*m*-tolyl)cyclobutylidene)amino)oxy)diphenylphosphine oxide (3.50).

(*R*)-(((3-(*o*-Tolyl)cyclobutylidene)amino)oxy)diphenylphosphine oxide ((*R*)-3.51)

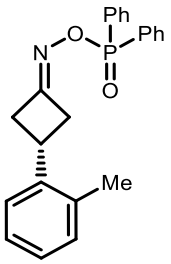

Following **GP-J** using 3-(2-methylphenyl)cyclobutanone (32.0 mg, 200 µmol, 1.00 eq.), (*R*)-**3.40** (19.8 mg, 20.0 µmol, 10 mol%) and *O*-(diphenylphosphinyl)hydroxylamine **2.51** (51.3 mg, 220 µmol, 1.10 eq.) the product (*R*)-**3.51** (67.2 mg, 179 µmol, 90%) was obtained *via* automated flash column chromatography (SiO_2, Cyclohexane:EtOAc, 100:0 → 0:100, stained with $KMnO_4$) as colourless solid.

M.P.: 137 – 138 °C. **IR (neat)**: $\tilde{\nu}$ = 3059 (w), 2926 (w), 1692 (w), 1592 (w), 1489 (w), 1460 (w), 1439 (m), 1398 (w), 1230 (m), 1182 (w), 1128 (m), 1112 (m), 1071 (w), 1027 (w), 998 (w), 872 (s), 812 (m), 726 (s), 693 (s), 667 (m), 645 (w), 548 (s), 532 (s), 441 (w). **^{1}H NMR (400 MHz, $CDCl_3$)**: δ = 7.95 – 7.82 (m, 4H, C$H_{arom.}$), 7.59 – 7.51 (m, 2H, C$H_{arom.}$), 7.51 – 7.43 (m, 4H, C$H_{arom.}$), 7.25 – 7.19 (m, 2H, C$H_{arom.}$), 7.19 – 7.14 (m, 2H, C$H_{arom.}$), 3.75 (*app*. p, J ≈ 8.4 Hz, 1H, C*H*), 3.65 – 3.53 (m, 1H, CH_2), 3.44-3.33 (m, 1H, CH_2), 3.23 – 3.05 (m, 2H, CH_2), 2.26 (s, 3H, CH_3).**^{13}C NMR (101 MHz, $CDCl_3$)**: δ = 166.3 (d, $^3J_{C\text{-}P}$ = 12.3 Hz, *C*=N), 140.3 (C_q), 136.2 (C_q), 132.4 (d, $^4J_{C\text{-}P}$ = 2.9 Hz, *C*H), 132.2 (d, $^2J_{C\text{-}P}$ = 10.0 Hz, *C*H), 132.1 (d, $^2J_{C\text{-}P}$ = 10.1 Hz, *C*H), 130.8 (d, $^1J_{C\text{-}P}$ = 136.4 Hz, C_q), 130.7 (d, $^1J_{C\text{-}P}$ = 135.7 Hz, C_q), 130.6 (*C*H), 128.6 (d, $^3J_{C\text{-}P}$ = 13.1 Hz, *C*H), 127.0 (*C*H), 126.4 (*C*H), 124.8 (*C*H), 38.3 (*C*H_2), 38.2 (*C*H_2), 30.3 (*C*H), 19.8 (*C*H_3). **^{31}P NMR (162 MHz, $CDCl_3$)**: δ = 35.18. **HRMS (ESI):** Calculated for $C_{23}H_{22}NO_2P$ $[M+H]^+$: 376.1466, Found: 376.1461. **Optical Rotation:** $[\alpha]_D^{25}$ = –53.9 (c = 0.5, $CHCl_3$) for an enantiomerically enriched sample of 95:5 *er*. The enantiomeric purity was established by HPLC analysis using a chiral column (Lux® Cellulose-1, 22 °C, 1 mL/min, 85:15 *n*hexane:isopropanol, 210 nm, t = 17.260 min and 20.956 min).

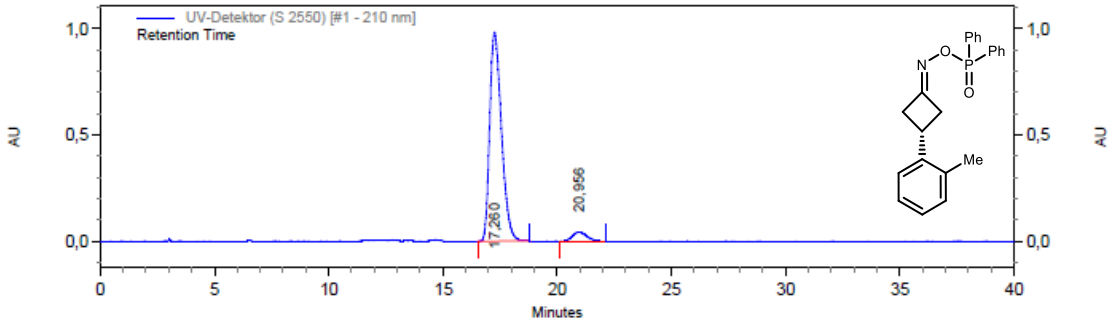

UV-Detektor (S 2550) [#1 - 210 nm] Results

Retention Time	Area	Area %
17,260	35175032	94,97
20,956	1863614	5,03

Figure 42. HPLC chromatogram for (*R*)-(((3-(*o*-tolyl)cyclobutylidene)amino)oxy)diphenylphosphine oxide ((*R*)-3.51).

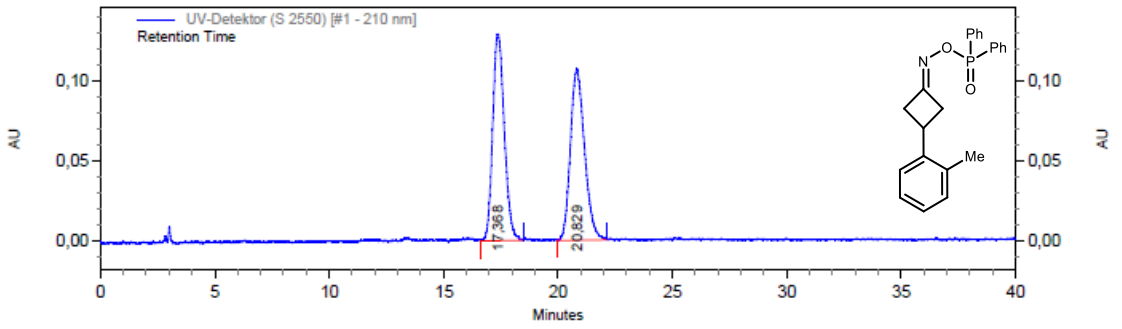

UV-Detektor (S 2550) [#1 - 210 nm] Results

Retention Time	Area	Area %
17,368	4570150	49,75
20,829	4615575	50,25

Figure 43. HPLC chromatogram for (((3-(*o*-tolyl)cyclobutylidene)amino)oxy)diphenylphosphine oxide (3.51).

(*R*)-(((3-Phenethylcyclobutylidene)amino)oxy)diphenylphosphine oxide ((*R*)-3.52)

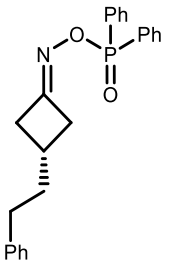

Following **GP-J** using 3-phenethylcyclobutan-1-one (34.9 mg, 200 µmol, 1.00 eq.), (*R*)-**3.40** (19.8 mg, 20.0 µmol, 10 mol%) and *O*-(diphenylphosphinyl)hydroxylamine **2.51** (51.3 mg, 220 µmol, 1.10 eq.) the product (*R*)-**3.52** (56.0 mg, 144 µmol, 72%) was obtained *via* automated flash column chromatography (SiO_2, Cyclohexane:EtOAc, 100:0 → 0:100, stained with $KMnO_4$) as colourless solid.

M.P.: 105 – 110 °C. **IR (neat)**: $\tilde{\nu}$ = 2923 (m), 2854 (w), 1496 (w), 1455 (w), 1439 (m), 1395 (w), 1237 (s), 1178 (w), 1129 (s), 1112 (m), 1072 (m), 1029 (w), 880 (s), 811 (m), 753 (m), 729 (s), 698 (s), 553 (s), 532 (s), 454 (w), 418 (w). **^{1}H NMR (400 MHz, $CDCl_3$)**: δ = 7.90 – 7.81 (m, 4H, C$H_{arom.}$), 7.57 – 7.50 (m, 2H, C$H_{arom.}$), 7.50 – 7.41 (m, 4H, C$H_{arom.}$), 7.31 – 7.26 (m, 2H, C$H_{arom.}$), 7.23 – 7.17 (m, 1H, C$H_{arom.}$), 7.16 – 7.12 (m, 2H, C$H_{arom.}$), 3.22 (*app*. ddt, J ≈ 17.6, 8.7, 3.1 Hz, 1H, CH_2), 3.05 (*app*. ddt, J ≈ 16.8, 8.6, 3.0 Hz, 1H, CH_2), 2.72 – 2.51 (m, 4H, 2xCH_2), 2.43 – 2.28 (m, 1H, C*H*), 1.84 (q, J = 7.6 Hz, 2H, CH_2). **^{13}C NMR (101 MHz, $CDCl_3$)**: δ = 167.4 (d, $^3J_{C\text{-}P}$ = 12.4 Hz, *C*=N), 141.4 (C_q), 132.3 (d, $^4J_{C\text{-}P}$ = 2.8 Hz, *C*H), 132.1 (d, $^2J_{C\text{-}P}$ = 10.2 Hz, *C*H), 132.0 (d, $^2J_{C\text{-}P}$ = 10.0 Hz, *C*H), 130.8 (d, $^1J_{C\text{-}P}$ = 136.8 Hz, C_q), 130.7 (d, $^1J_{C\text{-}P}$ = 135.8 Hz, C_q), 128.5 (d, $^3J_{C\text{-}P}$ = 13.2 Hz, *C*H), 128.5 (*C*H), 128.4 (*C*H), 126.0 (*C*H), 37.7 (*C*H$_2$), 37.4 (*C*H$_2$), 37.3 (*C*H$_2$), 33.7 (*C*H$_2$), 27.7 (*C*H). **^{31}P NMR (162 MHz, $CDCl_3$)**: δ = 34.93. **HRMS (ESI):** Calculated for $C_{24}H_{24}NO_2P$ $[M+H]^+$: 390.1623, Found: 390.1605. **Optical Rotation:** $[\alpha]_D^{25}$ = −10.5 (c = 1.0, $CHCl_3$) for an enantiomerically enriched sample of 89:11 *er*. The enantiomeric purity was established by HPLC analysis using a chiral column (Lux® Cellulose-1, 22 °C, 1 mL/min, 85:15 *n*hexane:isopropanol, 210 nm, t = 27.395 min and 35.050 min).

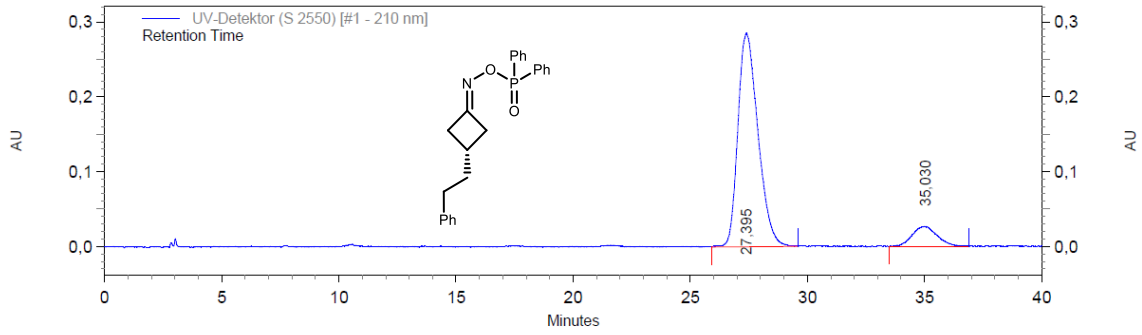

UV-Detektor (S 2550) [#1 - 210 nm] Results

Retention Time	Area	Area %
27,395	16990489	89,24
35,030	2047978	10,76

Figure 44. HPLC chromatogram for (*R*)-(((3-phenethylcyclobutylidene)amino)oxy)diphenylphosphine oxide ((*R*)-3.52).

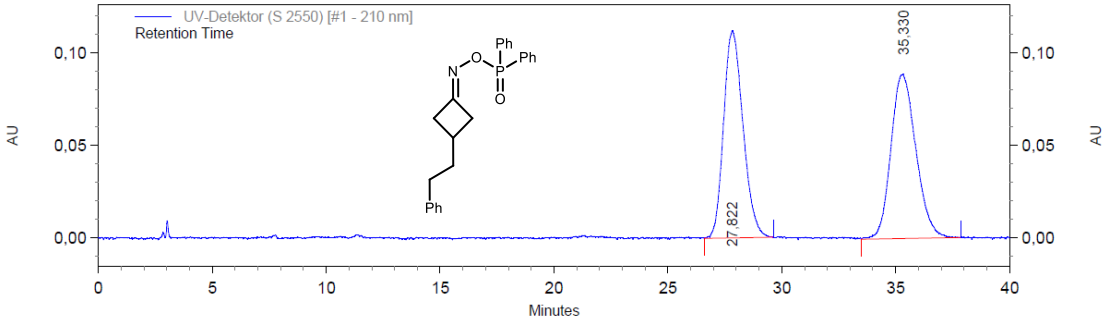

UV-Detektor (S 2550) [#1 - 210 nm] Results

Retention Time	Area	Area %
27,822	6655716	49,49
35,330	6792447	50,51

Figure 45. HPLC chromatogram for (((3-phenethylcyclobutylidene)amino)oxy)diphenylphosphine oxide (3.52).

(*R*)-(((3-Butylcyclobutylidene)amino)oxy)diphenylphosphine oxide ((R)-3.53)

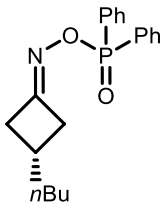

Following **GP-J** using 3-butylcyclobut-1-one (25.2 mg, 200 µmol, 1.00 eq.), (*R*)-**3.40** (19.8 mg, 20.0 µmol, 10 mol%) and *O*-(diphenylphosphinyl)hydroxylamine **2.51** (51.3 mg, 220 µmol, 1.10 eq.) the product (*R*)-**3.53** (49.0 mg, 144 µmol, 72%) was obtained *via* automated flash column chromatography (SiO_2, Cyclohexane:EtOAc, 100:0 → 0:100, stained with $KMnO_4$) as colourless solid.

M.P.: 55 – 62 °C. **IR (neat)**: $\tilde{\nu}$ = 2957 (w), 2926 (m), 2855 (w), 1694 (w), 1439 (m), 1237 (m), 1129 (s), 1113 (w), 880 (s), 809 (w), 753 (w), 729 (s), 696 (s), 553 (s), 534 (s), 444 (w). **^{1}H NMR (400 MHz, $CDCl_3$)**: δ = 7.85 (ddt, J = 12.2, 8.4, 1.6 Hz, 4H, C$H_{arom.}$), 7.60 – 7.37 (m, 6H, C$H_{arom.}$), 3.21 (ddt, J = 17.5, 8.7, 3.1 Hz, 1H, CH_2), 3.04 (ddt, J = 16.8, 8.6, 3.1 Hz, 1H, CH_2), 2.69 – 2.47 (m, 2H, CH_2), 2.41 – 2.24 (m, 1H, CH), 1.50 (q, J = 7.5 Hz, 2H, CH_2), 1.39 – 1.15 (m, 4H, CH_2), 0.89 (t, J = 7.0 Hz, 3H, CH_3). **^{13}C NMR (101 MHz, $CDCl_3$)**: δ = 168.0 (d, $^3J_{C\text{-}P}$ = 12.5 Hz, C_q), 132.3 (d, $^4J_{C\text{-}P}$ = 2.9 Hz, *C*H), 132.2 (d, $^2J_{C\text{-}P}$ = 9.9 Hz, *C*H), 132.1 (d, $^2J_{C\text{-}P}$ = 10.0 Hz, *C*H), 130.9 (d, $^1J_{C\text{-}P}$ = 136.1 Hz, C_q), 130.9 (d, $^1J_{C\text{-}P}$ = 135.8 Hz, C_q), 128.6 (d, $^3J_{C\text{-}P}$ = 13.2 Hz, *C*H), 37.6 (*C*H_2), 37.5 (*C*H_2), 35.9 (*C*H), 29.6 (*C*H_2), 28.3 (*C*H_2), 22.6 (*C*H_2), 14.2 (*C*H_3). **^{31}P NMR (162 MHz, $CDCl_3$)**: δ = 34.9. **HRMS (ESI):** Calculated for $C_{20}H_{24}NO_2P$ $[M+H]^+$: 342.1617, Found: 342.1622. **Optical Rotation:** $[\alpha]_D^{25}$ = +43.9 (c = 0.5, $CHCl_3$) for an enantiomerically enriched sample of 10:90 *er*. The enantiomeric purity was established by HPLC analysis using a chiral column (Reprosil Chiral-AMS, 22 °C, 1 mL/min, 90:10 *n*-hexane:isopropanol, 210 nm, t = 15.594 min and 19.123 min).

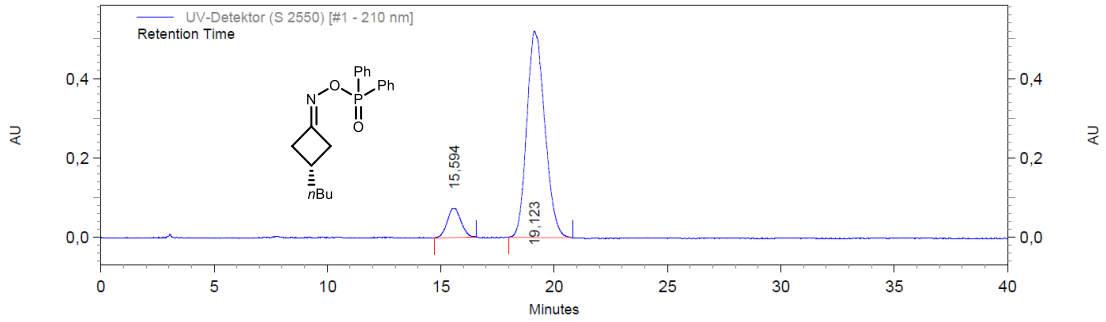

UV-Detektor (S 2550) [#1 - 210 nm] Results

Retention Time	Area	Area %
15,594	3089478	9,67
19,123	28870319	90,33

Figure 46. HPLC chromatogram for (*R*)-(((3-butylcyclobutylidene)amino)oxy)diphenylphosphine oxide ((*R*)-3.53).

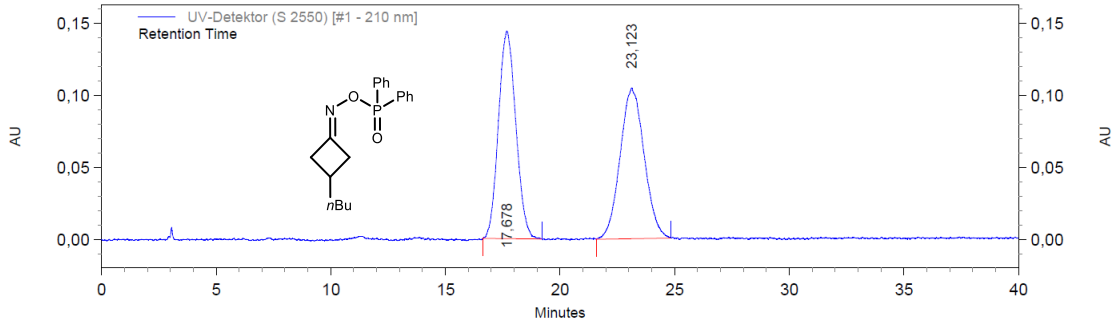

UV-Detektor (S 2550) [#1 - 210 nm] Results

Retention Time	Area	Area %
17,678	7598014	49,88
23,123	7634328	50,12

Figure 47. HPLC chromatogram for (((3-butylcyclobutylidene)amino)oxy)diphenylphosphine oxide (3.53).

(*R*)-(((3-cyclohexylcyclobutylidene)amino)oxy)diphenylphosphine oxide ((*R*)-3.54)

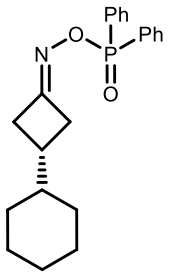

Following **GP-J** using 3-cyclohexylcyclobutanone (30.4 mg, 200 µmol, 1.00 eq.), (*R*)-**3.40** (19.8 mg, 20.0 µmol, 10 mol%) and *O*-(diphenylphosphinyl)hydroxylamine **2.51** (51.3 mg, 220 µmol, 1.10 eq.) the product (*R*)-**3.54** (40.8 mg, 111 µmol, 56%) was obtained *via* automated flash column chromatography (SiO_2, Cyclohexane:EtOAc, 100:0 → 0:100, stained with $KMnO_4$) as colourless solid.

M.P.: 116 – 119 °C. **IR (neat)**: $\tilde{\nu}$ = 2922 (s), 2850 (m), 1439 (m), 1395 (w), 1236 (s), 1179 (w), 1129 (s), 1112 (m), 1072 (w), 880 (s), 810 (w), 753 (w), 729 (s), 712 (m), 696 (s), 553 (s), 537 (m). **^{1}H NMR (400 MHz, $CDCl_3$)**: δ = 7.89 – 7.80 (m, 4H, C$H_{arom.}$), 7.56 – 7.49 (m, 2H, C$H_{arom.}$), 7.49 – 7.41 (m, 4H, C$H_{arom.}$), 3.16 (ddt, J = 17.5, 8.7, 3.2 Hz, 1H, CH_2), 2.97 (ddt, J = 16.8, 8.6, 3.2 Hz, 1H, CH_2), 2.75 – 2.54 (m, 2H, CH_2), 2.09 – 1.97 (m, 1H, C*H*), 1.78 – 1.62 (m, 4H, 2xCH_2), 1.27 – 1.07 (m, 5H, C*H*, 2xCH_2), 0.91 – 0.76 (m, 2H, CH_2). **^{13}C NMR (101 MHz, $CDCl_3$)**: δ = 167.8 (d, $^3J_{C\text{-}P}$ = 12.5 Hz, *C*=N), 132.3 (d, $^4J_{C\text{-}P}$ = 2.8 Hz, *C*H), 132.2 (d, $^2J_{C\text{-}P}$ = 10.0 Hz, *C*H), 132.1 (d, $^2J_{C\text{-}P}$ = 9.9 Hz, *C*H), 131.0 (d, $^1J_{C\text{-}P}$ = 136.3 Hz, C_q), 130.9 (d, $^1J_{C\text{-}P}$ = 135.7 Hz, C_q), 128.6 (d, $^3J_{C\text{-}P}$ = 13.2 Hz, *C*H), 43.5 (*C*H), 36.0 (*C*H$_2$), 35.9 (*C*H$_2$), 34.2 (*C*H), 30.2 (*C*H$_2$), 30.2 (*C*H$_2$), 26.4 (*C*H$_2$), 26.0 (*C*H$_2$). **^{31}P NMR (162 MHz, $CDCl_3$)**: δ = 34.79. **HRMS (ESI):** Calculated for $C_{22}H_{26}NO_2P$ $[M+H]^+$: 368.1179, Found: 368.1761. **Optical Rotation:** $[\alpha]_D^{25}$ = +11.1 (c = 0.5, $CHCl_3$) for an enantiomerically enriched sample of 82:18 *er*. The enantiomeric purity was established by HPLC analysis using a chiral column (Lux® Cellulose-1, 22 °C, 1 mL/min, 85:15 *n*hexane:isopropanol, 210 nm, t = 10.090 min and 11.546 min).

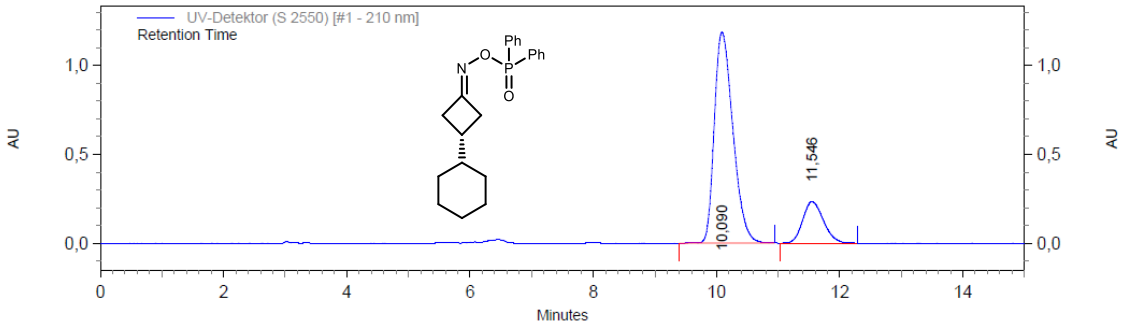

UV-Detektor (S 2550) [#1 - 210 nm] Results

Retention Time	Area	Area %
10,090	24910565	82,04
11,546	5452748	17,96

Figure 48. HPLC chromatogram for (*R*)-(((3-cyclohexylcyclobutylidene)amino)oxy)diphenylphosphine oxide ((*R*)-3.54).

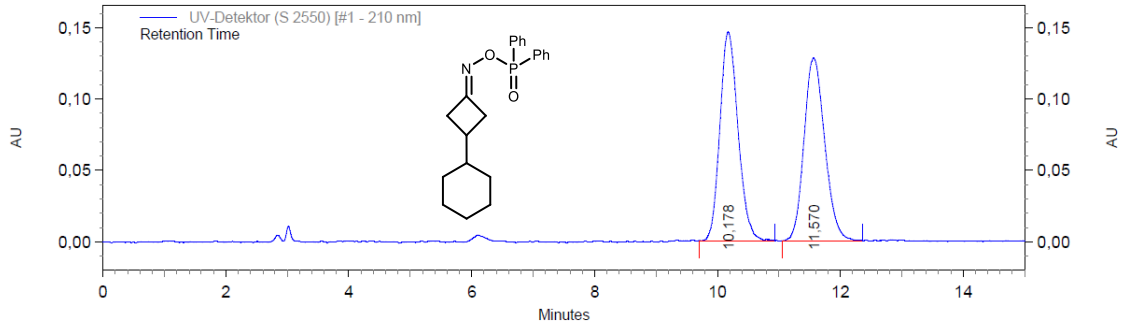

UV-Detektor (S 2550) [#1 - 210 nm] Results

Retention Time	Area	Area %
10,178	3011903	49,93
11,570	3020311	50,07

Figure 49. HPLC chromatogram for (((3-cyclohexylcyclobutylidene)amino)oxy)diphenylphosphine oxide (3.54).

(*R*)-(((3-Methyl-3-phenylcyclobutylidene)amino)oxy)diphenylphosphine oxide ((*R*)-3.55)

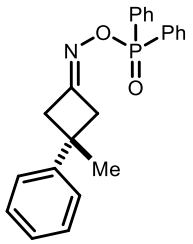

Following **GP-J** using 3-methyl-3-phenylcyclobutan-1-one (32.0 mg, 200 µmol, 1.00 eq.), (*R*)-**3.40** (19.8 mg, 20.0 µmol, 10 mol%) and *O*-(diphenylphosphinyl)hydroxylamine **2.51** (51.3 mg, 220 µmol, 1.10 eq.) the product (*R*)-**3.55** (43.0 mg, 115 µmol, 57%) was obtained *via* automated flash column chromatography (SiO_2, Cyclohexane:EtOAc, 100:0 → 0:100, stained with $KMnO_4$) as colourless solid.

M.P.: 109 – 115 °C. **IR (neat)**: $\tilde{\nu}$ = 3057 (w), 2956 (w), 2922 (w), 1695 (w), 1592 (w), 1496 (w), 1439 (m), 1398 (w), 1238 (s), 1183 (w), 1128 (s), 1112 (m), 1073 (w), 1028 (w), 874 (s), 812 (m), 745 (m), 728 (s), 697 (s), 663 (w), 554 (s), 544 (s). **^{1}H NMR (400 MHz, $CDCl_3$)**: δ = 7.92 – 7.79 (m, 4H, C$H_{arom.}$), 7.58 – 7.50 (m, 2H, C$H_{arom.}$), 7.50 – 7.42 (m, 4H, C$H_{arom.}$), 7.38 – 7.31 (m, 2H, C$H_{arom.}$), 7.25 – 7.19 (m, 3H, C$H_{arom.}$), 3.44 – 3.29 (m, 2H, CH_2), 3.25 (ddd, J = 17.0, 3.8, 2.8 Hz, 1H, CH_2), 3.04 (ddd, J = 16.3, 3.8, 2.8 Hz, 1H, CH_2), 1.53 (s, 3H, CH_3). **^{13}C NMR (101 MHz, $CDCl_3$)**: δ = 165.7 (d, $^3J_{C\text{-}P}$ = 12.5 Hz, C_q), 148.2 (C_q), 132.4 (t, $^4J_{C\text{-}P}$ = 2.6 Hz, *C*H)[a], 132.1 (t, $^2J_{C\text{-}P}$ = 10.3, *C*H)[a], 130.8 (d, $^1J_{C\text{-}P}$ = 136.3, C_q), 130.7 (d, $^1J_{C\text{-}P}$ = 136.3, C_q), 128.7 (*C*H), 128.6 (d, $^3J_{C\text{-}P}$ = 13.4 Hz, *C*H), 126.4 (*C*H), 125.2 (*C*H), 44.8 (*C*H_2), 44.8 (*C*H_2), 37.9 (C_q), 30.9 (*C*H_3). **^{31}P NMR (162 MHz, $CDCl_3$)**: δ = 35.09. **HRMS (ESI):** Calculated for $C_{23}H_{22}NO_2P$ $[M+H]^+$: 376.1461, Found: 376.1455. **Optical Rotation:** $[\alpha]_D^{25}$ = +11.5 (c = 1.0, $CHCl_3$) for an enantiomerically enriched sample of 35:65 *er*. The enantiomeric purity was established by HPLC analysis using a chiral column (Lux® Cellulose-1, 22 °C, 1 mL/min, 85:15 *n*hexane:isopropanol, 210 nm, t = 11.836 min and 13.036 min).

[a] Appears as triplett due to overlap of to signals (dublett)

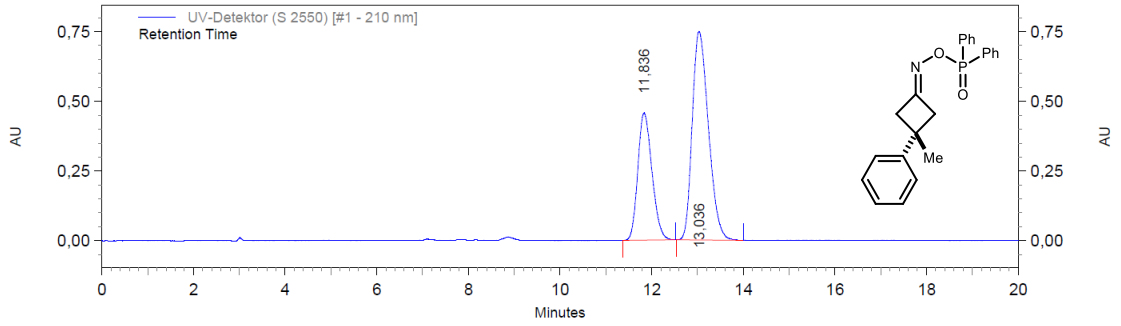

UV-Detektor (S 2550) [#1 - 210 nm] Results

Retention Time	Area	Area %
11,836	9791061	34,77
13,036	18371877	65,23

Figure 50. HPLC chromatogram for (*R*)-(((3-methyl-3-phenylcyclobutylidene)amino)oxy)diphenylphosphine ox-ide ((*R*)-3.55).

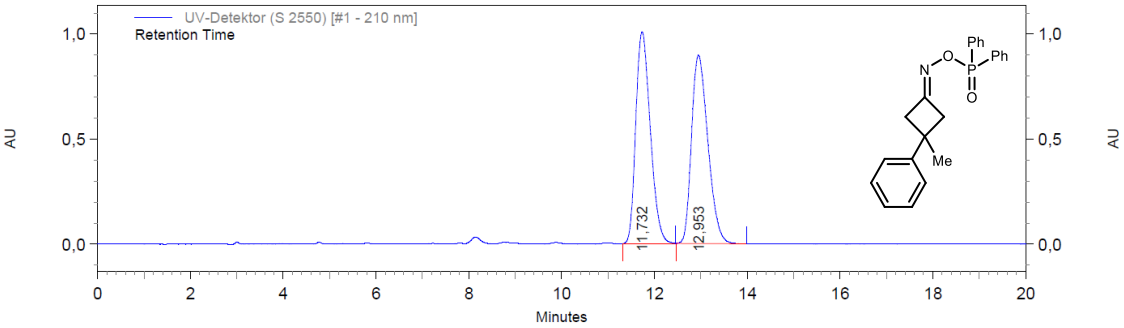

UV-Detektor (S 2550) [#1 - 210 nm] Results

Retention Time	Area	Area %
11,732	21870375	49,87
12,953	21982384	50,13

Figure 51. HPLC chromatogram for (((3-methyl-3-phenylcyclobutylidene)amino)oxy)diphenylphosphine ox-ide (3.55).

(*R*)-(((3-(4-Methoxyphenyl)-3-methylcyclobutylidene)amino)oxy)diphenyl phosphine oxide ((*R*)-3.56)

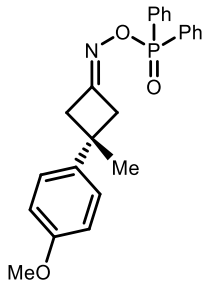

Following the **GP-J** using 3-(4-methoxyphenyl)-3-methylcyclobutan-1-one (38.1 mg, 200 µmol, 1.00 eq.), (*R*)-**3.40** (19.8 mg, 20.0 µmol, 10 mol%) and *O*-(diphenylphosphinyl)hydroxylamine **2.51** (51.3 mg, 220 µmol, 1.10 eq.) the product (*R*)-**3.56** (41.0 mg, 101 µmol, 51%) was obtained *via* flash column chromatography (SiO_2, CyHex:EtOAc, 100:0 → 0:100, stained with $KMnO_4$) as colourless solid.

IR (neat): $\tilde{\nu}$ = 3059 (w), 2955 (w), 2836 (w), 1696 (w), 1611 (w), 1514 (s), 1439 (m), 1305 (w), 1245 (s), 1181 (m), 1129 (s), 1112 (m), 1030 (m), 875 (s), 830 (m), 811 (m), 789 (m), 728 (s), 695 (s), 609 (w), 552 (s), 538 (s), 517 (m). **^{1}H NMR (400 MHz, $CDCl_3$)**: δ = 7.90 – 7.81 (m, 4H, C$H_{arom.}$), 7.58 – 7.50 (m, 2H, C$H_{arom.}$), 7.50 – 7.42 (m, 4H, C$H_{arom.}$), 7.17 – 7.11 (m, 2H, C$H_{arom.}$), 6.91 – 6.84 (m, 2H, C$H_{arom.}$), 3.80 (s, 3H, CH_3), 3.39 – 3.25 (m, 2H, CH_2), 3.25 – 3.17 (m, 1H, CH_2), 3.05 – 2.97 (m, 1H, CH_2), 1.51 (s, 3H, CH_3). **^{13}C NMR (101 MHz, $CDCl_3$)**: δ = 165.8 (d, $^3J_{C\text{-}P}$ = 12.4 Hz, C_q), 158.1 (C_q), 140.2 (C_q), 132.4 (d, $^4J_{C\text{-}P}$ = 2.6 Hz, *C*H), 132.2 (t, $^2J_{C\text{-}P}$ = 9.8, *C*H)[a], 130.8 (d, $^1J_{C\text{-}P}$ = 136.2, C_q), 130.7 (d, $^1J_{C\text{-}P}$ = 135.9, C_q), 128.6 (d, $^3J_{C\text{-}P}$ = 13.4 Hz, *C*H), 126.3 (*C*H), 114.0 (*C*H), 55.4 (*C*H_3), 45.0 (*C*H_2), 45.0 (*C*H_2), 37.2 (C_q), 30.9 (*C*H_3). **^{31}P NMR (162 MHz, $CDCl_3$)**: δ = 35.0. **HRMS (ESI):** Calculated for $C_{24}H_{24}NO_3P$ $[M+H]^+$: 406.1567, Found: 406.1561. **Optical Rotation:** $[\alpha]_D^{25}$ = +7.9 (c = 1.0, $CHCl_3$) for an enantiomerically enriched sample of 34:66 *er*. The enantiomeric purity was established by HPLC analysis using a chiral column (iAmylose-3, 22 °C, 1 mL/min, 85:15 *n*hexane:isopropanol, 210 nm, t = 32.996 min and 37.305 min).

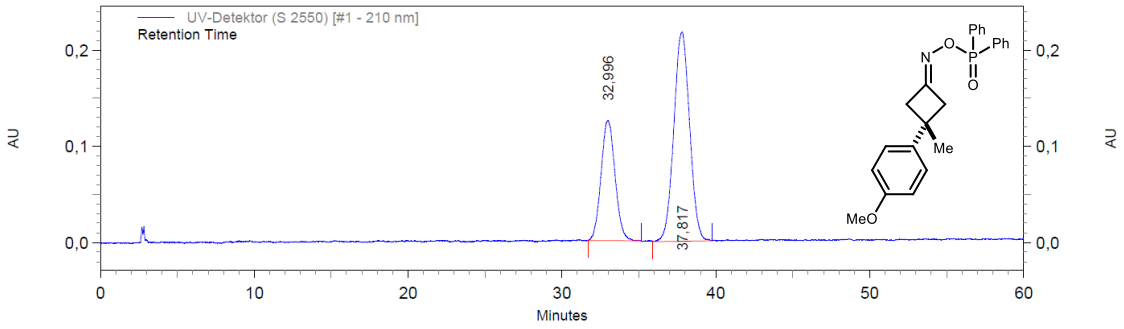

UV-Detektor (S 2550) [#1 - 210 nm] Results

Retention Time	Area	Area %
32,996	7919053	33,79
37,817	15519456	66,21

Figure 52. HPLC chromatogram for (*R*)-(((3-(4-Methoxyphenyl)-3-methylcyclobutylidene)amino)oxy)diphenyl phosphine oxide ((*R*)-3.56).

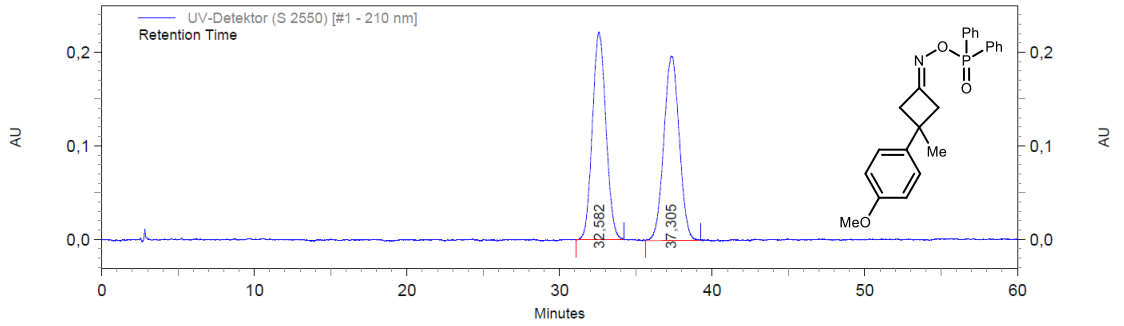

UV-Detektor (S 2550) [#1 - 210 nm] Results

Retention Time	Area	Area %
32,582	13775254	49,82
37,305	13876995	50,18

Figure 53. HPLC chromatogram for (((3-(4-Methoxyphenyl)-3-methylcyclobutylidene)amino)oxy)diphenyl phosphine oxide (3.56).

(*R*)-(((3-((Benzyloxy)methyl)cyclobutylidene)amino)oxy)diphenylphosphine oxide ((*R*)-3.57)

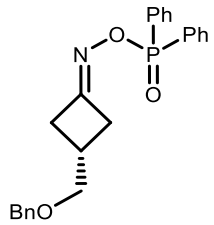

Following the general procedure **GP-J** using 3-(phenylmethoxymethyl)cyclobutan-1-one (38.1 mg, 200 µmol, 1.00 eq.), (*R*)-**3.40** (19.8 mg, 20.0 µmol, 10 mol%) and *O*-(diphenylphosphinyl)hydroxylamine **2.51** (51.3 mg, 220 µmol, 1.10 eq.) the product (*R*)-**3.57** (78.0 mg, 192 µmol, 96%) was obtained *via* flash column chromatography (SiO_2, CyHex:EtOAc, 100:0 → 0:100, stained with $KMnO_4$) as colourless solid.

M.P.: 84 – 89 °C. **IR (neat)**: $\tilde{\nu}$ = 2922 (m), 2851 (m), 1782 (s), 1449 (w), 1377 (w), 1237 (w), 1206 (w), 1106 (m), 985 (w), 884 (w), 495 (w). **^{1}H NMR (400 MHz, $CDCl_3$)**: δ = 7.89 – 7.79 (m, 4H, C$H_{arom.}$), 7.58 – 7.49 (m, 2H, C$H_{arom.}$), 7.49 – 7.40 (m, 4H, C$H_{arom.}$), 7.39 – 7.27 (m, 5H, C$H_{arom.}$), 4.53 (s, 2H, CH_2), 3.51 (d, J = 6.2 Hz, 2H, CH_2), 3.18 (ddt, J = 17.8, 8.9, 2.9 Hz, 2H, CH_2), 3.04 (ddt, J = 17.0, 8.8, 2.9 Hz, 1H, CH_2), 2.96 – 2.72 (m, 2H, CH_2), 2.67 (*app*. tt, J ≈ 8.8, 6.1 Hz, 1H, C*H*). **^{13}C NMR (101 MHz, $CDCl_3$)**: δ = 167.3 (d, $^3J_{C\text{-}P}$ = 12.4 Hz, *C*=N), 138.2 (C_q), 132.4 (d, $^4J_{C\text{-}P}$ = 2.8 Hz, *C*H), 132.2 (d, $^2J_{C\text{-}P}$ = 10.0 Hz, *C*H), 132.1 (d, $^2J_{C\text{-}P}$ = 10.0 Hz, *C*H), 130.8 (d, $^1J_{C\text{-}P}$ = 136.1 Hz, C_q), 130.8 (d, $^1J_{C\text{-}P}$ = 135.8 Hz, C_q), 128.6 (d, $^3J_{C\text{-}P}$ = 13.2 Hz, *C*H), 128.6 (*C*H), 127.9 (*C*H), 127.8 (*C*H), 73.4 (*C*H$_2$), 72.7 (*C*H$_2$), 34.9 (*C*H$_2$), 34.8 (*C*H$_2$), 27.9 (*C*H). **^{31}P NMR (162 MHz, $CDCl_3$)**: δ = 35.0. **HRMS (ESI):** Calculated for $C_{22}H_{26}NO_2P$ $[M+H]^+$: 406.1572, Found: 406.1558. **Optical Rotation:** $[\alpha]_D^{25}$ = −21.5 (c = 0.5, $CHCl_3$) for an enantiomerically enriched sample of 26:74 *er*. The enantiomeric purity was established by HPLC analysis using a chiral column (Lux® Cellulose-1, 22 °C, 1 mL/min, 85:15 *n*hexane:isopropanol, 210 nm, t = 23.873 min and 24.145 min).

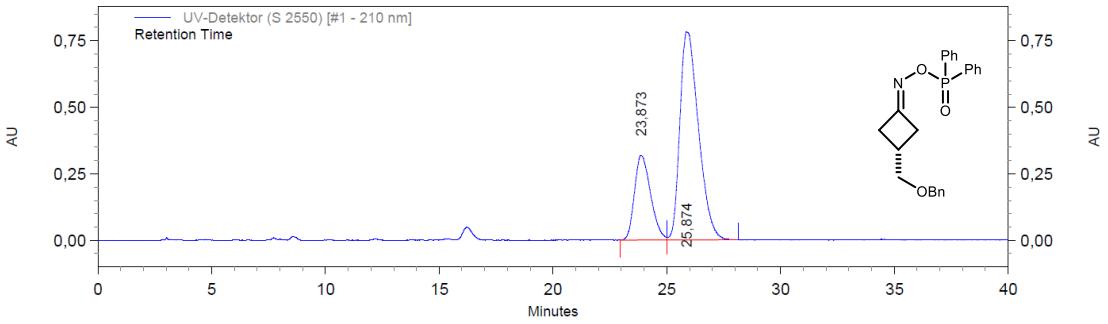

UV-Detektor (S 2550) [#1 - 210 nm] Results

Retention Time	Area	Area %
23,873	15676296	26,01
25,874	44601660	73,99

Figure 54. HPLC chromatogram for (*R*)-(((3-((Benzyloxy)methyl)cyclobutylidene)amino)oxy)diphenylphosphine oxide ((*R*)-3.57).

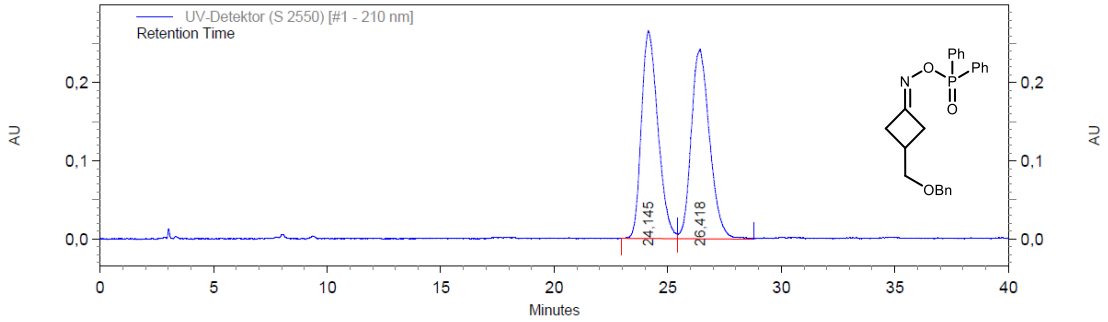

UV-Detektor (S 2550) [#1 - 210 nm] Results

Retention Time	Area	Area %
24,145	13425281	49,55
26,418	13669382	50,45

Figure 55. HPLC chromatogram for (((3-((Benzyloxy)methyl)cyclobutylidene)amino)oxy)diphenylphosphine oxide (3.57).

(*R*)-((((3-(Benzyloxy)cyclobutylidene)amino)oxy)diphenylphosphine oxide ((*R*)-3.58)

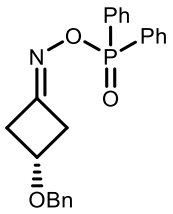

Following the general procedure **GP-J** using 3-(benzoyloxy)cyclobutan-1-one (35.2 mg, 200 µmol, 1.00 eq.), (*R*)-**3.40** (19.8 mg, 20.0 µmol, 10 mol%) and *O*-(diphenylphosphinyl)hydroxylamine **2.51** (51.3 mg, 220 µmol, 1.10 eq.) the product (*R*)-**3.58** (33.0 mg, 84 µmol, 42%) was obtained *via* flash column chromatography (SiO_2, CyHex:EtOAc, 100:0 → 0:100, stained with $KMnO_4$) as colourless solid.

M.P.: 105 – 108 °C. **^{1}H NMR (400 MHz, $CDCl_3$)**: δ = 7.89 – 7.79 (m, 4H, C$H_{arom.}$), 7.57 – 7.50 (m, 2H, C$H_{arom.}$), 7.50 – 7.42 (m, 4H, C$H_{arom.}$), 7.40 – 7.28 (m, 5H, C$H_{arom.}$), 4.47 (s, 2H, CH_2), 4.22 (*app*. tt, J ≈ 6.7, 5.3 Hz, 1H, C*H*), 3.40 (dddd, J = 17.6, 7.1, 4.7, 2.8 Hz, 1H, CH_2), 3.20 (dddd, J = 17.0, 7.2, 4.7, 2.8 Hz, 1H, CH_2), 3.10 – 2.94 (m, 2H, C$H_{arom.}$). **^{13}C NMR (101 MHz, $CDCl_3$)**: δ = 163.5 (d, $^3J_{C\text{-}P}$ = 12.7 Hz, C_q), 137.3 (C_q), 132.5 (d, $^4J_{C\text{-}P}$ = 2.9 Hz, *C*H), 132.3 (d, $^3J_{C\text{-}P}$ = 10.0 Hz, *C*H), 132.1 (d, $^3J_{C\text{-}P}$ = 9.9 Hz, *C*H), 130.7 (d, $^1J_{C\text{-}P}$ = 136.6 Hz, C_q), 130.6 (d, $^1J_{C\text{-}P}$ = 135.6 Hz, C_q), 128.7 (*C*H), 128.6 (d, $^2J_{C\text{-}P}$ = 13.4, *C*H), 128.2 (*C*H), 128.0 (*C*H), 71.2 (*C*H_2), 66.7 (*C*H), 40.5 (*C*H_2), 40.4 (*C*H_2). **^{31}P NMR (162 MHz, $CDCl_3$)**: δ = 35.4. **Optical Rotation:** $[\alpha]_D^{25}$ = +8.2 (c = 0.5, $CHCl_3$) for an enantiomerically enriched sample of 55:45 *er*. The enantiomeric purity was established by HPLC analysis using a chiral column (Lux® Cellulose-1, 22 °C, 1 mL/min, 85:15 *n*hexane:isopropanol, 210 nm, t = 22.225 min and 25.051 min).

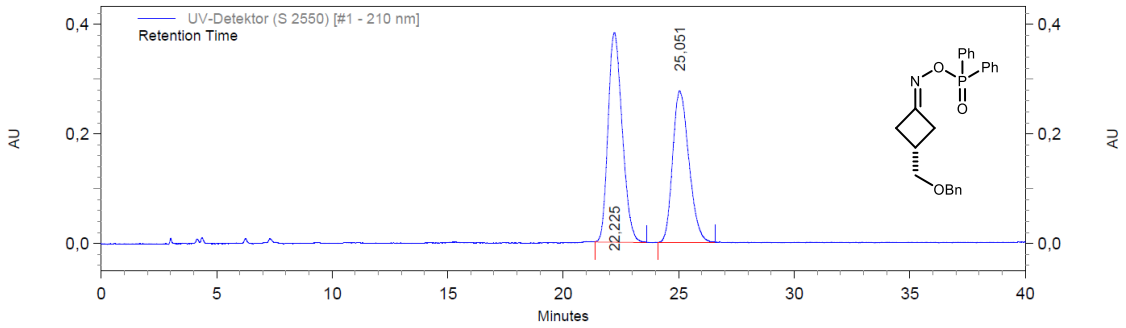

UV-Detektor (S 2550) [#1 - 210 nm] Results

Retention Time	Area	Area %
22,225	16266485	54,62
25,051	13513619	45,38

Figure 56. HPLC chromatogram for (*R*)-((((3-(Benzyloxy)cyclobutylidene)amino)oxy)diphenylphosphine ox-ide ((*R*)-3.58)

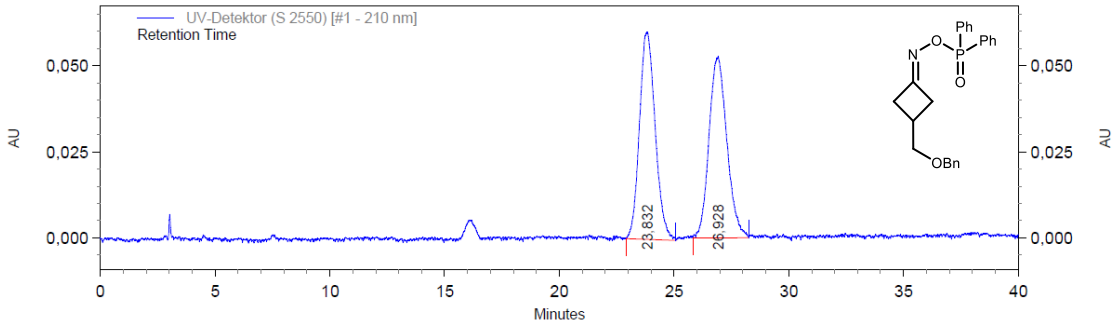

UV-Detektor (S 2550) [#1 - 210 nm] Results

Retention Time	Area	Area %
23,832	2868074	50,19
26,928	2846268	49,81

Figure 57. HPLC chromatogram for ((((3-(Benzyloxy)cyclobutylidene)amino)oxy)diphenylphosphine ox-ide (3.58)

(*R*)-3-(((Diphenylphosphoryl)oxy)imino)cyclobutane-1- methyl carboxylate ((*R*)-3.59)

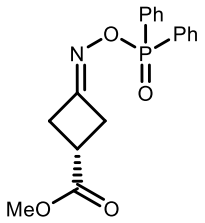

Following the general procedure **GP-J** using methyl 3-oxocyclobutan-1-one (25.6 mg, 200 µmol, 1.00 eq.), (*R*)-**3.40** (19.8 mg, 20.0 µmol, 10 mol%) and *O*-(diphenylphosphinyl)hydroxylamine **2.51** (51.3 mg, 220 µmol, 1.10 eq.) the product (*R*)-**3.59** (27.0 mg, 79 µmol, 39%) was obtained *via* flash column chromatography (SiO_2, CyHex:EtOAc, 100:0 → 0:100, stained with $KMnO_4$) as colourless solid.

M.P.: 136 – 141 °C. **^{1}H NMR (600 MHz, $CDCl_3$)**: δ = 7.89 – 7.80 (m, 4H, C*H*$_{arom.}$), 7.57 – 7.51 (m, 2H, C*H*$_{arom.}$), 7.49 – 7.44 (m, 4H, C*H*$_{arom.}$), 3.73 (s, 3H, C*H*$_3$), 3.36 (dd, J = 6.7, 2.0 Hz, 2H, C*H*$_2$), 3.30 – 3.17 (m, 3H, C*H*, C*H*$_2$). **^{13}C NMR (151 MHz, $CDCl_3$)**: δ = 173.9 (*C*$_q$), 164.7 (d, $^3J_{C\text{-}P}$ = 12.6 Hz, *C*$_q$), 132.5 (d, $^4J_{C\text{-}P}$ = 2.8 Hz, *C*H), 132.3 (d, $^3J_{C\text{-}P}$ = 10.1 Hz, *C*H), 132.1 (d, $^3J_{C\text{-}P}$ = 10.0 Hz, *C*H), 130.5 (d, $^1J_{C\text{-}P}$ = 136.5 Hz, *C*$_q$), 130.4 (d, $^1J_{C\text{-}P}$ = 135.4 Hz, *C*$_q$), 128.7 (d, $^2J_{C\text{-}P}$ = 13.2, *C*H), 128.6 (d, $^2J_{C\text{-}P}$ = 13.2, *C*H), 52.5 (*C*H$_3$), 35.9 (*C*H$_2$), 35.7 (*C*H$_2$), 30.8 (*C*H). **^{31}P NMR (162 MHz, $CDCl_3$)**: δ = 35.6. **Optical Rotation:** $[\alpha]_D^{25}$ = −10.9 (c = 0.5, $CHCl_3$) for an enantiomerically enriched sample of 68:32 *er*. The enantiomeric purity was established by HPLC analysis using a chiral column (Lux® Cellulose-1, 22 °C, 1 mL/min, 90:10 *n*hexane:isopropanol, 210 nm, t = 12.749 min and 14.367 min).

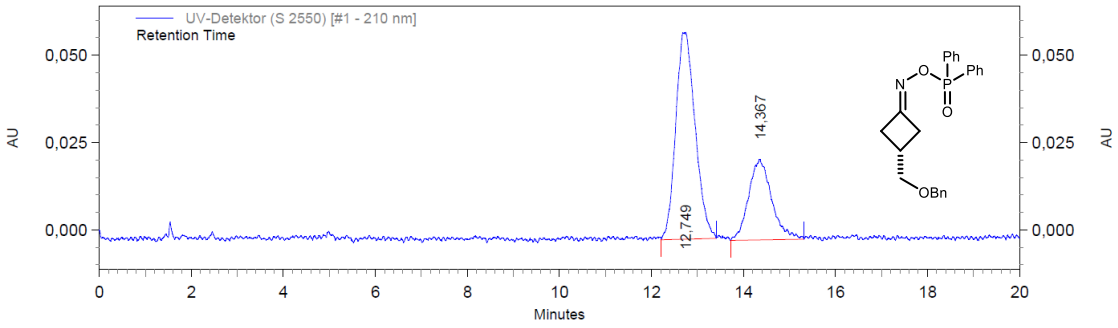

UV-Detektor (S 2550) [#1 - 210 nm] Results

Retention Time	Area	Area %
12,749	1733109	68,31
14,367	804057	31,69

Figure 58. HPLC chromatogram for (*R*)-3-(((Diphenylphosphoryl)oxy)imino)cyclobutane-1- methyl carbox-ylate ((*R*)-3.59).

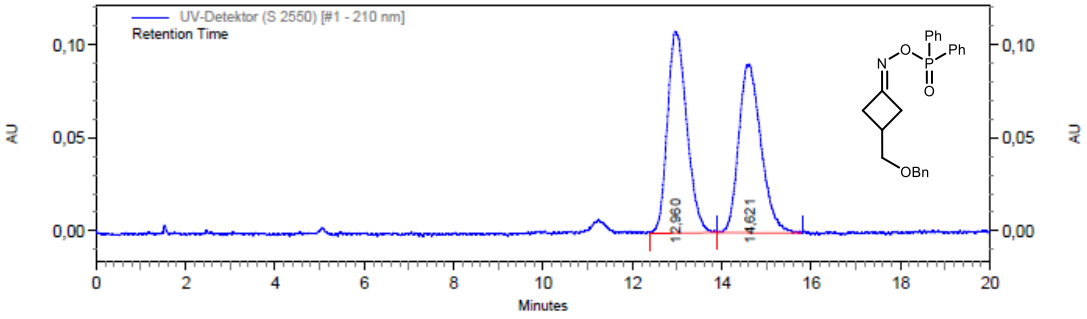

UV-Detektor (S 2550) [#1 - 210 nm] Results

Retention Time	Area	Area %
12,960	3265952	50,89
14,621	3151698	49,11

Figure 59. HPLC chromatogram for 3-(((Diphenylphosphoryl)oxy)imino)cyclobutane-1- methyl carbox-ylate (3.59).

((((3*R*,4*S*)-3,4-Diphenylcyclopentylidene)amino)oxy)diphenylphosphine oxide ((2*R,4S*)-2.63)

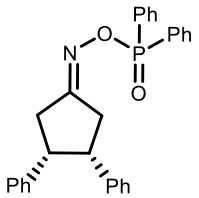

Following **GP-J** using *cis*-3,4-diphenylcyclopentan-1-one **2.46** (47.3 mg, 200 µmol, 1.00 eq.), (*R*)-**3.40** (19.8 mg, 20.0 µmol, 10 mol%) and *O*-(diphenylphosphinyl)hydroxylamine **2.51** (51.3 mg, 220 µmol, 1.10 eq.) the product (79.0 mg, 175 µmol, 87%) was obtained *via* automated flash column chromatography (SiO_2, Cyclohexane:EtOAc, 100:0 → 0:100, stained with $KMnO_4$) as colourless solid.

^{1}H NMR (400 MHz, $CDCl_3$): δ = 7.99 – 7.84 (m, 4H, CH_{arom}), 7.60 – 7.54 (m, 2H, CH_{arom}), 7.54 – 7.44 (m, 4H, CH_{arom}), 7.14 – 7.03 (m, 6H, CH_{arom}), 6.70 (ddt, J = 11.1, 6.2, 1.9 Hz, 4H, CH_{arom}), 3.79 – 3.59 (m, 2H, 2xC*H*), 3.27 – 3.10 (m, 2H, CH_2), 2.97 (qd, J = 17.7, 6.6 Hz, 2H, CH_2). **^{13}C NMR (101 MHz, $CDCl_3$)**: δ = 175.4 (d, $^3J_{C\text{-}P}$ = 12.5 Hz, C_q), 139.4 (C_q), 139.3 (C_q), 132.5 (t, 3.1 Hz, $^4J_{C\text{-}P}$ = 2.6 Hz, *C*H), 132.3 (d, $^2J_{C\text{-}P}$ = 10.0 Hz, *C*H), 132.3 (d, $^2J_{C\text{-}P}$ = 10.0 Hz, *C*H), 131.0 (d, $^1J_{C\text{-}P}$ = 136.3, C_q), 131.0 (d, $^1J_{C\text{-}P}$ = 135.6, C_q) 128.7 (d, $^3J_{C\text{-}P}$ = 13.2 Hz, *C*H), 128.7 (d, $^3J_{C\text{-}P}$ = 13.2 Hz, *C*H), 128.2 (*C*H), 128.2 (*C*H), 128.0 (*C*H), 126.8 (*C*H), 126.8 (*C*H), 49.0 (*C*H), 48.6 (*C*H), 35.5 (*C*H$_2$), 34.4 (*C*H$_2$). **^{31}P NMR (162 MHz, $CDCl_3$)**: δ = 34.73. **Optical Rotation:** $[\alpha]_D^{25}$ = −73.5° (c = 1.0, $CHCl_3$) for an enantiomerically enriched sample of 1:99 *er*. The enantiomeric purity was established by HPLC analysis using a chiral column (Lux® Amylose-1, 40 °C, 1 mL/min, 85:15 *n*hexane:isopropanol, 214 nm, t = 25.841 min and 28.484 min).

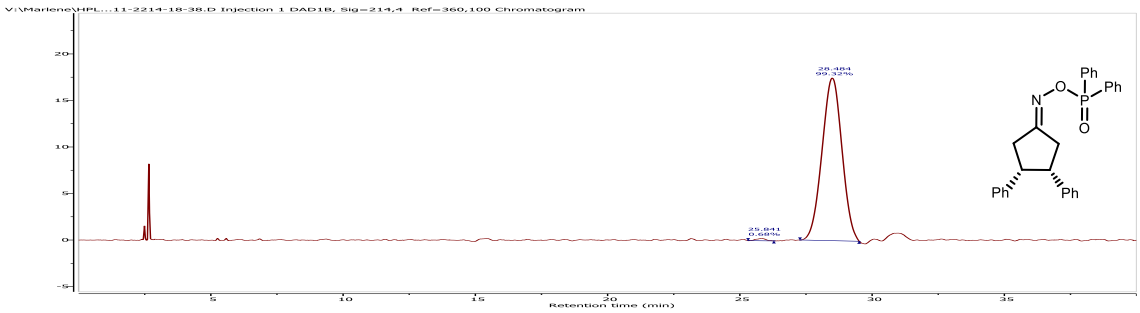

Retention Time	Area%
25.841	0.68
28.484	99.32

Figure 60. HPLC chromatogram for ((((3*R*,4*S*)-3,4-Diphenylcyclopentylidene)amino)oxy)diphenylphosphine oxide ((2*R*,*4S*)-2.63).

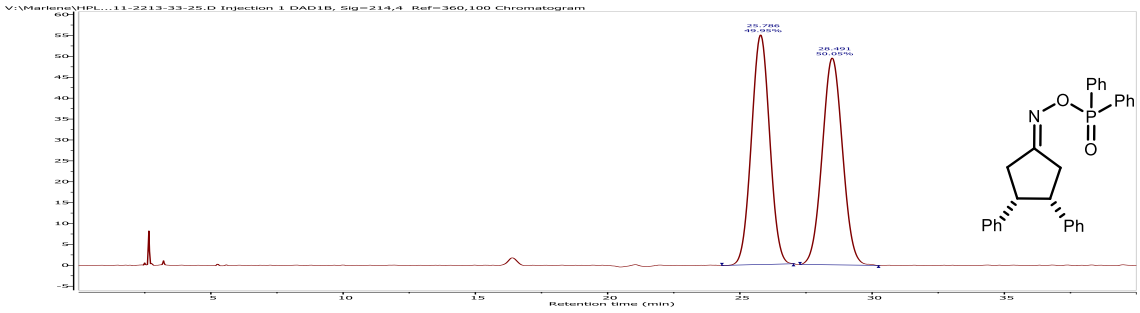

Retention Time	Area%
25.786	49.95
28.491	50.05

Figure 61. HPLC chromatogram for (((3,4-Diphenylcyclopentylidene)amino)oxy)diphenylphosphine oxide (2.63).

(*R*)-(((4-Phenylcyclohexylidene)amino)oxy)diphenylphosphine oxide ((*R*)-3.60)

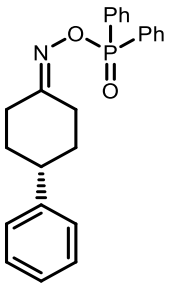

Following the general procedure **GP-J** using 3-(4-fluorophenyl)cyclobutan-1-one (32.8 mg, 200 µmol, 1.00 eq.), (*R*)-**3.40** (19.8 mg, 20.0 µmol, 10 mol%) and *O*-(diphenylphosphinyl)hydroxylamine **2.51** (51.3 mg, 220 µmol, 1.10 eq.) the product (*R*)-**3.60** (71.0 mg, 187 µmol, 94%) was obtained *via* flash column chromatography (SiO_2, CyHex:EtOAc, 100:0 → 0:100, stained with $KMnO_4$) as colourless solid.

IR (neat): $\tilde{\nu}$ = 3056 (w), 2928 (w), 2863 (w), 1593 (w), 1493 (w), 1439 (m), 1235 (s), 1129 (m), 1113 (w), 888 (s), 826 (m), 813 (m), 771 (m), 753 (m), 728 (s), 698 (s), 553 (s), 541 (s), 498 (w), 443 (w), 420 (w). **^{1}H NMR (400 MHz, $CDCl_3$)**: δ = 7.92 – 7.82 (m, 4H, C$H_{arom.}$), 7.58 – 7.51 (m, 2H, C$H_{arom.}$), 7.51 – 7.43 (m, 4H, C$H_{arom.}$), 7.31 (dd, J = 7.3, 6.7 Hz, 2H, C$H_{arom.}$), 7.24 – 7.15 (m, 2H, C$H_{arom.}$), 3.57 (ddd, J = 12.2, 4.3, 2.1 Hz, 1H, CH_2), 2.79 (tt, J = 12.3, 3.3 Hz, 1H, C*H*), 2.64 (ddt, J = 14.2, 4.5, 2.5 Hz, 1H, CH_2), 2.26 (td, J = 13.8, 4.9 Hz, 1H, CH_2), 2.16 – 2.00 (m, 3H, 2xCH_2), 1.77 – 1.63 (m, 2H, CH_2). **^{13}C NMR (101 MHz, $CDCl_3$)**: δ = 168.5 (d, $^3J_{C\text{-}P}$ = 11.3 Hz, C_q), 145.2 (C_q), 132.3 (t, $^4J_{C\text{-}P}$ = 2.7 Hz, *C*H)[a], 132.2 (d, $^2J_{C\text{-}P}$ = 10.0, *C*H), 131.1 (d, $^1J_{C\text{-}P}$ = 136.4, C_q), 131.0 (d, $^1J_{C\text{-}P}$ = 136.5, C_q), 128.7 (*C*H), 128.6 (d, $^3J_{C\text{-}P}$ = 13.2 Hz, *C*H), 126.8 (*C*H), 126.7 (*C*H), 43.5 (*C*H), 33.8 (*C*H$_2$), 32.9 (*C*H$_2$), 31.9 (*C*H$_2$), 26.4 (*C*H$_2$). **^{31}P NMR (162 MHz, $CDCl_3$)**: δ = 34.8. **HRMS (ESI):** Calculated for $C_{24}H_{24}NO_2P$ $[M+H]^+$: 390.1617, Found: 390.1612. **Optical Rotation:** $[\alpha]_D^{25}$ = –9.3 (c = 0.5, $CHCl_3$) for an enantiomerically enriched sample of 34:66 *er*. The enantiomeric purity was established by HPLC analysis using a chiral column (Reprosil Chiral-AMS, 22 °C, 1 mL/min, 85:15 *n*hexane:isopropanol, 210 nm, t = 16.605 min and 21.863 min).

[a] Looks like triplett due to overlap of to signals (dublett)

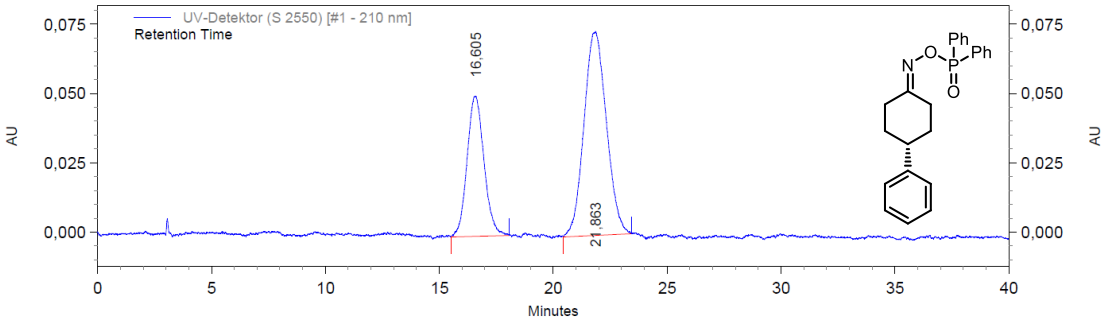

UV-Detektor (S 2550) [#1 - 210 nm] Results

Retention Time	Area	Area %
16,605	2619928	34,26
21,863	5027244	65,74

Figure 62. HPLC chromatogram for (*R*)-(((4-Phenylcyclohexylidene)amino)oxy)diphenylphosphine oxide ((*R*)-3.60).

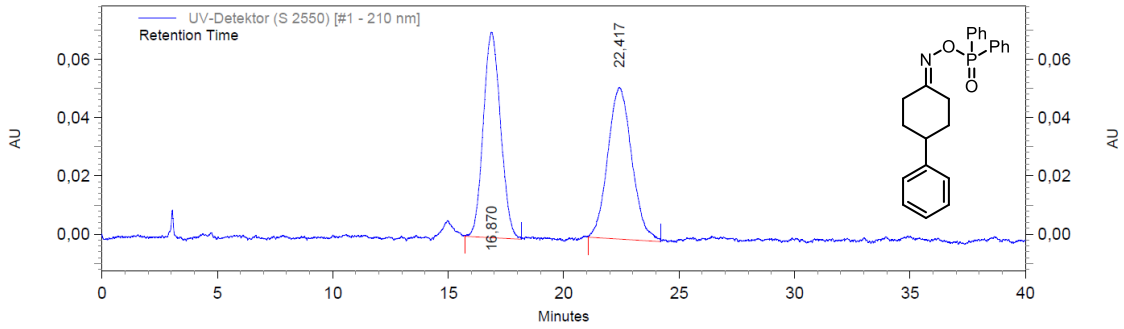

UV-Detektor (S 2550) [#1 - 210 nm] Results

Retention Time	Area	Area %
16,870	3677245	49,42
22,417	3763025	50,58

Figure 63. HPLC chromatogram for (((4-Phenylcyclohexylidene)amino)oxy)diphenylphosphine oxide (3.60).

5.4 Transformations of cyclobutanone oxime esters

5.4.1 Ring-expansion of cyclobutanone oxime esters

General procedure K (GP-K) for ring-expansion reaction of cyclobutanone oxime esters

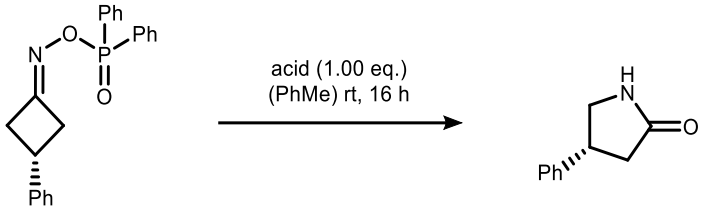

In a Schlenk flask, cyclobutanone oxime ester (50.0 µmol, 1.00 eq.) was dissolved in dry toluene (0.05 M) under N_2-atmosphere and the solution was cooled to −20 °C. Acid (50.0 µmol, 1.00 eq.) was added, and the reaction mixture was stirred at −20 °C for 16 h. A sat. aq. $NaHCO_3$-solution (2.0 mL) was added, and the aqueous phase was extracted with CH_2Cl_2 (5x10 mL). The combined organic phases were dried over $MgSO_4$, filtered and concentrated under reduced pressure. Crude NMR yield was determined with CH_2Br_2 as internal standard.

The reaction was performed in similar fashion with other acids and temperatures (*cf.* chapter 4.2.1).

General procedure L (GP-L) for one-pot reaction dual catalysis:

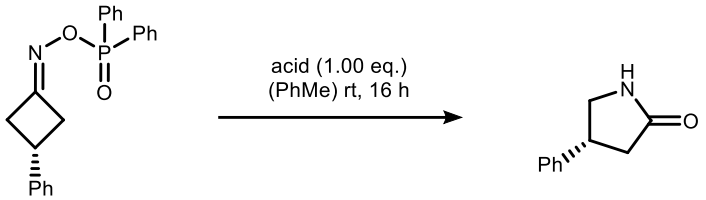

In a Schlenk flask, (*R*)-TCYP (5.00 µmol 10 mol%) and cyclobutanone (50.0 µmol, 1.00 eq.) was dissolved in dry toluene (0.05 M) under N_2-atmosphere. Acid (10.0 µmol, 0.200 eq.) was added and the solution was cooled to −20 °C. *O*-Diphenylphosphinylhydroxylamine (55.0 µmol, 1.10 eq.) was added and the reaction mixture was stirred at −20 °C for 24 h. A sat. aq. $NaHCO_3$-solution (2.0 mL) was added and the aqueous phase was extracted with CH_2Cl_2 (5x10 mL). The combined organic phases were dried over $MgSO_4$, filtered and concentrated under reduced pressure. Crude NMR yield was determined with CH_2Br_2 as internal standard. The lactam was obtained *via* column chromatography (SiO_2, EtOAc:MeOH 100:0 → 90:10).

The reaction was performed in similar fashion with other acids (*cf.* chapter 4.2.1).

General procedure M (GP-M) for sequential one pot reaction:

In a Schlenk flask, (*R*)-TCYP (10 mol%) and cyclobutanone (50.0 µmol, 1.00 eq.) was dissolved in dry toluene (0.05 M) under N_2-atmosphere. 4 Å MS was added and the mixture was cooled to –20 °C. *O*-Diphenylphosphinylhydroxylamine (55.0 µmol, 1.10 eq.) was added, and the reaction mixture was stirred at –20 °C for 24 h. Acid (50.0 µmol, 1.00 eq.) was added, and the solution was stirred at –20 °C for 16 h. A sat. aq. $NaHCO_3$-solution (2.0 mL) was added, and the aqueous phase was extracted with CH_2Cl_2 (5x10 mL). The combined organic phases were dried over $MgSO_4$, filtered and concentrated under reduced pressure. Crude NMR yield was determined with CH_2Br_2 as internal standard. The lactam was obtained *via* column chromatography (SiO_2, EtOAc:MeOH 100:0 → 90:10).

The reaction was performed in similar fashion with other stoichiometries and additives (*cf*. chapter 4.2.1).

(*R*)-4-Phenylpyrrolidin-2-one ((*R*)-2.49)

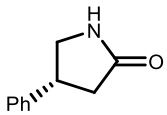

Following the general procedure **GP-K** using 3-phenyl cyclobutanone oxime ester (R)-**3.32** (18.1 mg, 50 µmol, 1.00 eq.) and $BF_3{\cdot}OEt_2$ (7.1 mg, 50 µmol, 1.00 eq.) the product (*R*)-**3.49** (7.8 mg, 48 µmol, 97%) was obtained *via* flash column chromatography (SiO_2, EtOAc:MeOH, 100:0 → 90:10, stained with $KMnO_4$) as colourless solid.

^{1}H NMR (400 MHz, $CDCl_3$): δ = 7.39 – 7.29 (m, 2H), 7.29 – 7.22 (m, 3H), 6.70 (br s, 1H), 3.82 – 3.74 (m, 1H), 3.74 – 3.62 (m, 1H), 3.41 (dd, J = 9.3, 7.2 Hz, 1H), 2.73 (dd, J = 16.9, 8.8 Hz, 1H), 2.51 (dd, J = 16.9, 8.8 Hz, 1H). **^{13}C NMR (101 MHz, $CDCl_3$)** δ = 177.9, 142.2, 129.0, 127.2, 126.9, 49.7, 40.4, 38.1. The spectroscopic data was in agreement to those previously reported.[162]
HPLC: The enantiomeric ratio of 92:8 *er* was established by HPLC analysis using a chiral column (*i*Amylose-3, 40 °C, 1 mL/min, 90:10 *n*hexane:isopropanol, 214 nm, t = 13.994 min and 15.499 min).

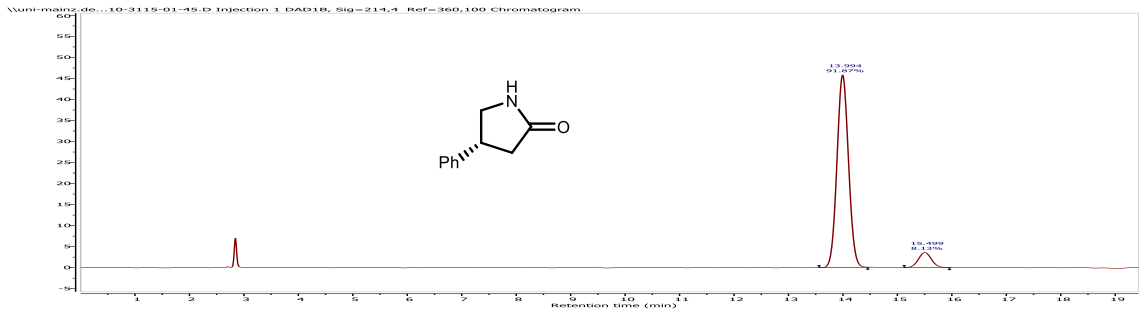

Retention Time	Area%
13.994	91.87
15.499	8.12

Figure 64. HPLC chromatogram of (*R*)-4-phenylpyrrolidin-2-one ((*R*)-2.49) prepared with enantioenriched starting material.

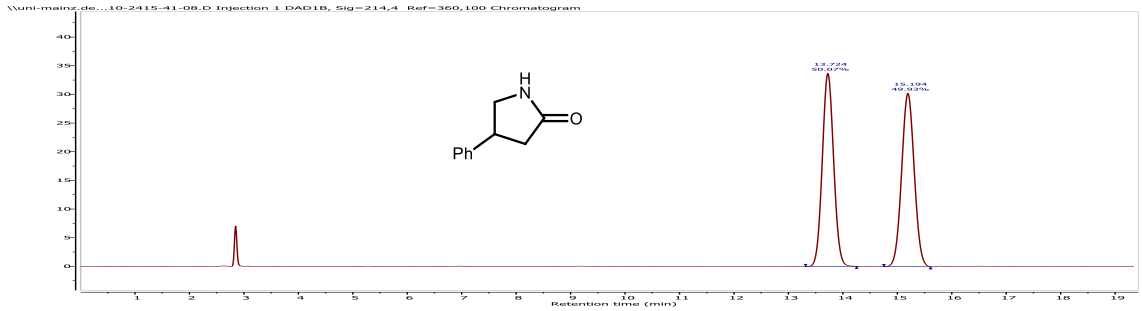

Retention Time	Area%
13.724	50.07
15.194	49.93

Figure 65. HPLC chromatogram of 4-phenylpyrrolidin-2-one (2.49) prepared with racemic starting material.

5.4.2 Ring-opening of cyclocbutanone oxime esters

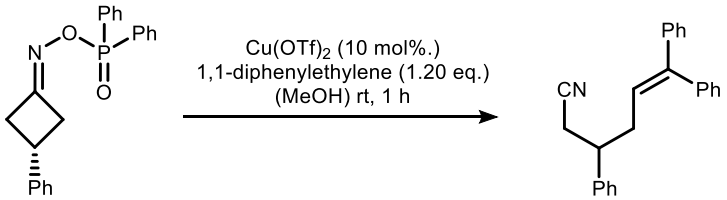

Following a procedure by Zhao *et al.*[123], an oven dried Schlenk tube was charged with copper(II) trifluoromethanesulfonate (3.62 mg, 10.0 µmol, 10 mol%) and oxime ester (*R*)-**3.32** (36.1 mg, 100 µmol, 1.00 eq.) under N_2 atmosphere. Dry 1,4-dioxane (500 µL), $PhCF_3$ (500 µL) and 1-phenylethenylbenzene (21.6 mg, 21.2 µL, 120 µmol, 1.20 eq.) was added. The resulting reaction mixture was stirred at 90 °C for 16 h. The solvent was removed under reduced pressure and the crude product was purified *via* automated flash column chromatography (95:5 pent:EtOAc) to obtain the title compound (25.6 mg, 79.2 µmol, 79%) as yellow oil.

^{1}H NMR (400 MHz, $CDCl_3$): δ = 7.41 – 7.30 (m, 5H), 7.30 – 7.17 (m, 4H), 7.17 – 7.02 (m, 6H), 5.91 (t, *J* = 7.3 Hz, 1H), 3.10 (ddd, *J* = 14.6, 8.1, 6.5 Hz, 1H), 2.69 – 2.49 (m, 4H). **^{13}C NMR (101 MHz, $CDCl_3$)** δ = 144.4, 142.2, 141.2, 139.7, 129.8, 129.0, 128.5, 128.3, 127.7, 127.4, 127.4, 127.3, 125.5, 118.6, 42.9, 35.4, 24.5. The spectroscopic data was in agreement to those previously reported.[123]

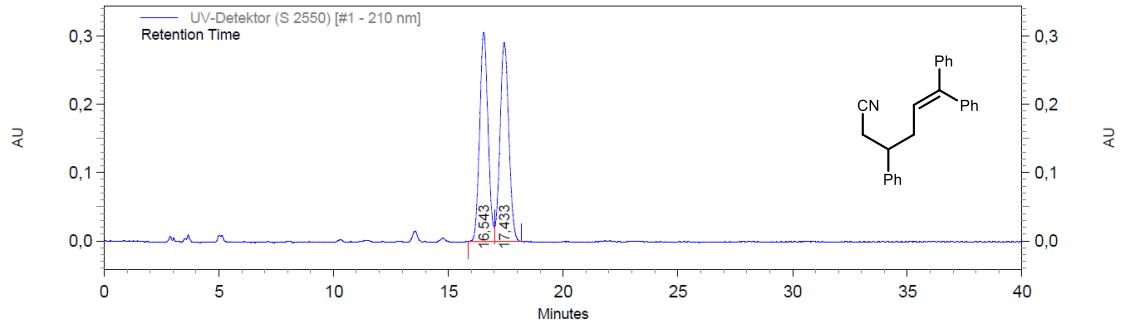

UV-Detektor (S 2550) [#1 - 210 nm] Results

Retention Time	Area	Area %
16,543	7750779	49,99
17,433	7753267	50,01

Figure 66. HPLC chromatogram for 3,6,6-triphenylhex-5-enenitrile (4.41) prepared with enantioenriched starting material.

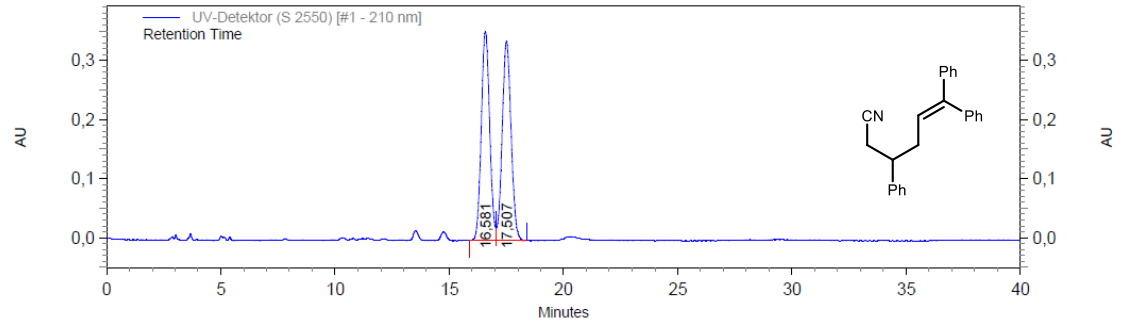

UV-Detektor (S 2550) [#1 - 210 nm] Results

Retention Time	Area	Area %
16,581	8968441	49,72
17,507	9069205	50,28

Figure 67. HPLC chromatogram for 3,6,6-triphenylhex-5-enenitrile (4.41) prepared with enantioenriched starting material.

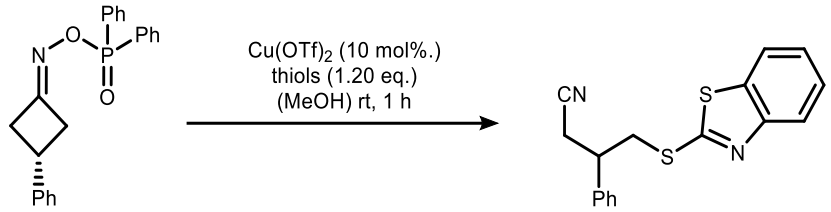

Following a procedure by He *et al.*[131], an oven dried Schlenk tube was charged with copper(II) trifluoromethanesulfonate (1.0 mg, 5.0 µmol, 10 mol%), oxime ester (*R*)-**3.32** (18.1 mg, 50 µmol, 1.00 eq.), 1,3-benzothiazole-2-thione (4.20 mg, 25.0 µmol, 1.20 eq.) and 1,8-diazabicyclo[5.4.0]undec-7-en (45.7 mg, 300.0 µmol, 12.0 eq.) under N_2 atmosphere. EtOAc (500 µL) was added and the the resulting reaction mixture was stirred at room temperature for 16 h. The solvent was removed under reduced pressure and the crude product was purified *via* automated flash column chromatography (95:5 pent:EtOAc) to obtain the title compound (4.00 mg, 12.9 µmol, 79%) as yellow oil.

^{1}H NMR (400 MHz, $CDCl_3$): δ = 7.90 (d, *J* = 8.1 Hz, 1H), 7.76 (d, *J* = 8.0 Hz, 1H), 7.50 – 7.29 (m, 7H), 3.75 (dd, *J* = 7.3, 1.7 Hz, 2H), 3.64 – 3.52 (m, 1H), 2.96 – 2.86 (m, 2H). **^{13}C NMR (101 MHz, $CDCl_3$)** δ = 165.2, 152.9, 139.7, 135.3, 129.1, 128.2, 127.3, 126.2, 124.5, 121.6, 121.1, 118.0, 41.7, 37.7, 23.3. 144.4, 142.2, 141.2, 139.7, 129.8, 129.0, 128.5, 128.3, 127.7, 127.4, 127.4, 127.3, 125.5, 118.6, 42.9, 35.4, 24.5. The spectroscopic data was in agreement to those previously reported. [131]

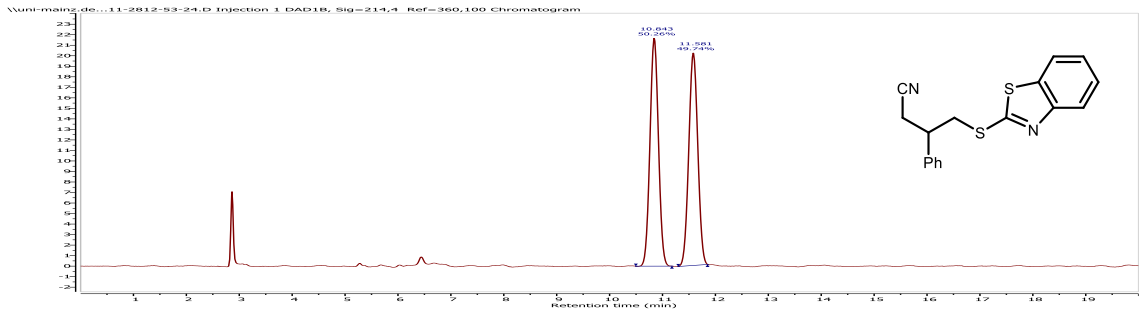

Retention Time	Area%
10.843	50.26
11.581	49.74

Figure 68. HPLC chromatogram of 4-(benzo[d]thiazol-2-ylthio)-3-phenylbutanenitrile (4.43) prepared with enantioenriched starting material.

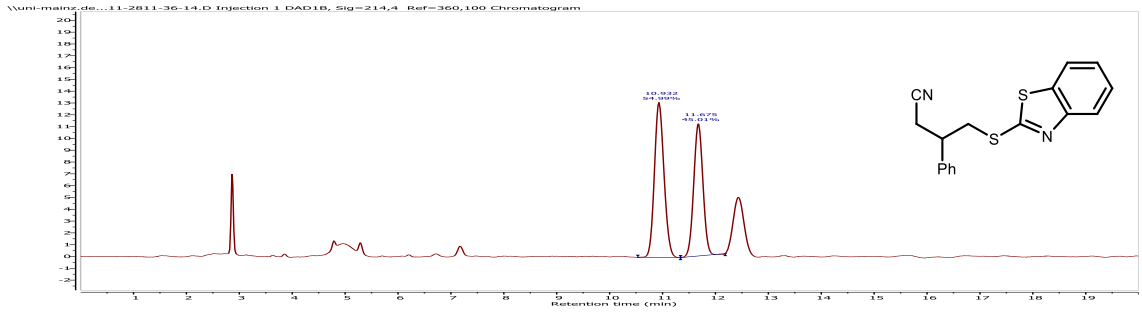

Retention Time	Area%
10.939	50.09
11.675	49.01

Figure 69. HPLC chromatogram of 4-(benzo[d]thiazol-2-ylthio)-3-phenylbutanenitrile (4.43) prepared with enantioenriched starting material.

5.4.3 Ring-contraction of cyclobutanone oxime esters

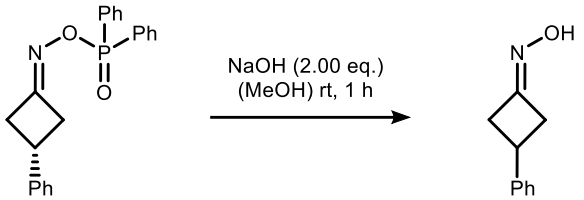

In a round bottom flask, oxime ester (*R*)-**3.32** (36.1 mg, 100 µmol, 1.00 eq.) was dissolved in a solution of NaOH (8.00 mg, 200 µmol, 2.00 eq.) in MeOH (2.0 mL). The reaction mixture was stirred at room temperature for 16 h. Water was added and the mixture was diluted with CH_2Cl_2. The phases were separated and the aqueous phase was extracted (5 x 10 mL) with CH_2Cl_2. The combined organic phases were dried over $MgSO_4$, filtered and concentrated under reduced pressure. The product **4.45** (13.4 mg, 83.1 µmol, 83%) was obtained *via* automated column chromatography (SiO_2, cyclohexane:EtOAc, 50:50, stained with $KMnO_4$).

^{1}H NMR (400 MHz, $CDCl_3$): δ = 7.46 – 7.16 (m, 5H), 3.62 (ddd, J = 16.2, 9.4, 7.6 Hz, 1H), 3.51 – 3.42 (m, 1H), 3.36 (ddt, J = 16.5, 9.0, 3.1 Hz, 1H), 3.05 (dddd, J = 16.4, 7.3, 3.1, 1.5 Hz, 2H).**^{13}C NMR (101 MHz, $CDCl_3$)** δ = 156.9, 144.1, 128.8, 126.8, 126.6, 39.5, 38.3, 32.9. The spectroscopic data was in agreement to those previously reported.[139,163]

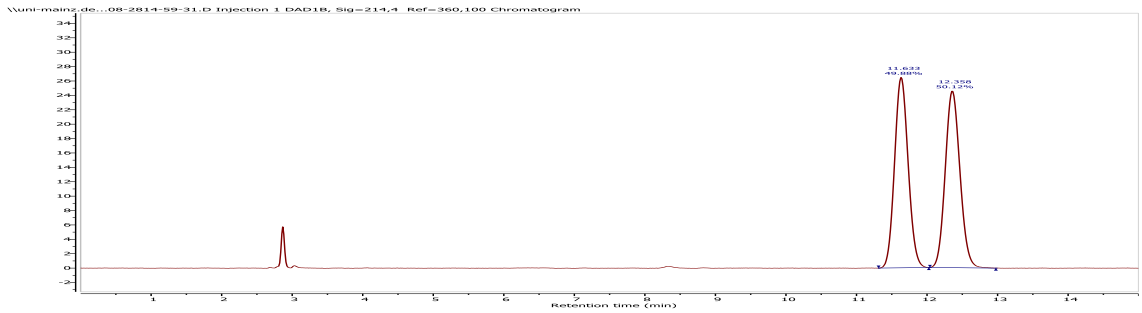

Retention Time	Area%
11.633	49.88
12.358	50.12

Figure 70. HPLC chromatogram for 3-phenylcyclobutanone oxime (4.45) prepared with enantioenriched starting material.

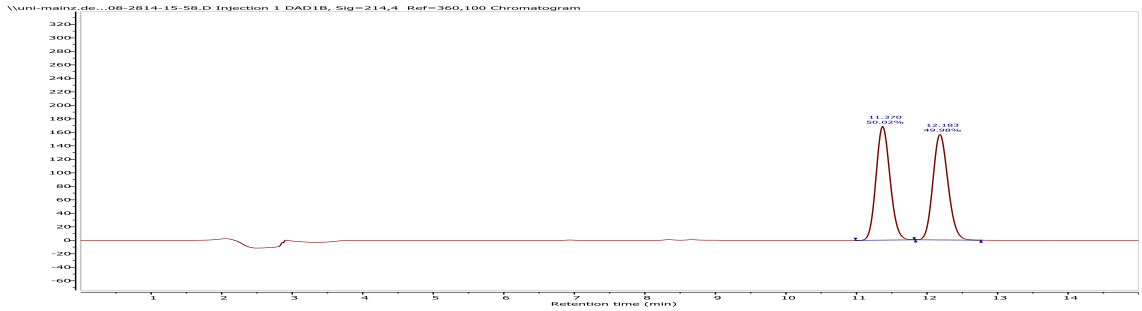

Retention Time	Area%
11.370	50.03
12.182	49.97

Figure 71. HPLC chromatogram for 3-phenylcyclobutanone oxime (4.45) prepared with racemic starting material.

Optimisation of reaction conditions

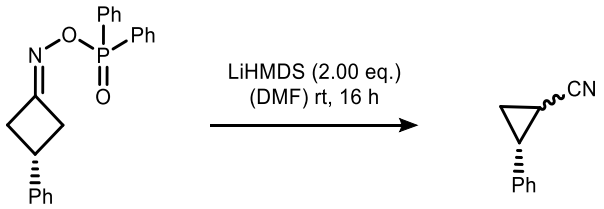

Following a modified procedure by Shuai *et al.*[136], in a round bottom flask, oxime ester (*R*)-**3.32** (36.1 mg, 100 µmol, 1.00 eq.) was dissolved in dry DMF (2.0 mL). LiHMDS in THF (1.0 M, 0.20 mL, 200 µmol, 2.00 eq.) was added and the reaction mixture was stirred at room temperature for 16 h. A sat. aqu. NH_4Cl solution was added and the mixture was diluted with EtOAc. The phases were separated and the organic phase was dried over $MgSO_4$, filtered and concentrated under reduced pressure. The diastereomeric ratio (62:38 dr, trans:cis) was determined *via* crude ^1H NMR analysis using CH_2Br_2 as internal standard. The crude mixture was purified *via* column chromatography (SiO_2, pentane:EtOAc, 100:0 → 90:10, stained with CAM) to obtain **4.48** (4.0 mg, 27.9 µmol, 28%), and **4.49** (2.5 mg, 17.5 µmol, 17%).

The reaction was performed in similar fashion with other bases and solvents (*cf.* chapter 4.4.1).

***Trans*-diastereomer** (**4.48**): **^{1}H NMR (400 MHz, $CDCl_3$)** δ = 7.35 – 7.29 (m, 2H), 7.29 – 7.23 (m, 1H), 7.14 – 7.08 (m, 2H), 2.63 (ddd, J = 9.2, 6.7, 4.7 Hz, 1H), 1.62 (*app.* dt, J ≈ 9.1, 5.2 Hz, 1H), 1.55 (ddd, J = 8.6, 5.4, 4.8 Hz, 1H), 1.45 (ddd, J = 8.6, 6.7, 5.0 Hz, 1H). **^{13}C NMR (101 MHz, $CDCl_3$)** δ = 137.7, 128.9, 127.5, 126.4, 121.2, 25.0, 15.3, 6.7. Spectroscopic data was in agreement to those previously reported.[164] Enantiomerically enriched sample of 73:27 *er*. The enantiomeric purity was established by HPLC analysis using a chiral column (Lux® Cellulose-1, 40 °C, 1 mL/min, 95:05 *n*hexane:isopropanol, 210 nm, t = 12.559 min and 13.604 min).
***Cis*-diastereomer** (**4.49**): **^{1}H NMR (400 MHz, $CDCl_3$)** δ = 7.40 – 7.34 (m, 2H), 7.33 – 7.26 (m, 3H), 2.54 (td, J = 8.4, 7.1 Hz, 1H), 1.84 (ddd, J = 8.9, 8.3, 5.7 Hz, 1H), 1.60 – 1.48 (m, 2H).**^{13}C NMR (101 MHz, $CDCl_3$)** δ = 135.2, 128.6, 128.1, 127.7, 119.5, 23.2, 12.9, 6.4. Spectroscopic data was in agreement to those previously reported.[165] Enantiomerically enriched sample of 73:27 *er*. The enantiomeric purity was established by HPLC analysis using a chiral column (Lux® Cellulose-1, 40 °C, 1 mL/min, 95:05 *n*hexane:isopropanol, 210 nm, t = 12.559 min and 13.604 min).

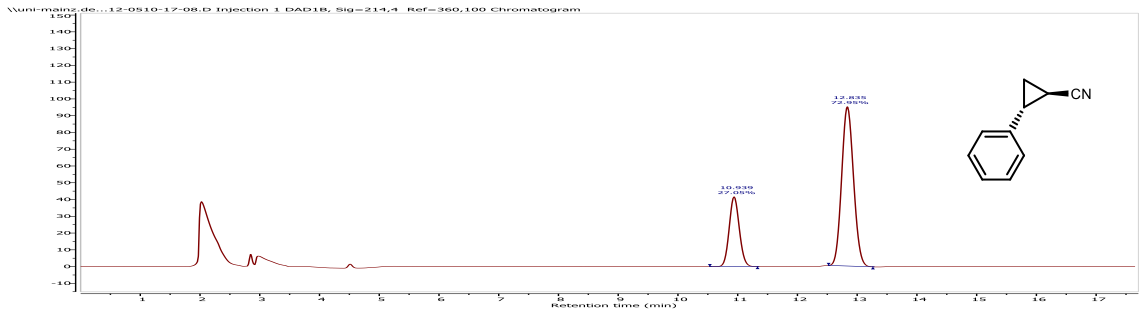

Retention Time	Area%
10.939	27.05
12.825	72.95

Figure 72. HPLC chromatogram for 2-phenylcyclopropane-1-carbonitrile (4.48) prepared with enantioenriched starting material.

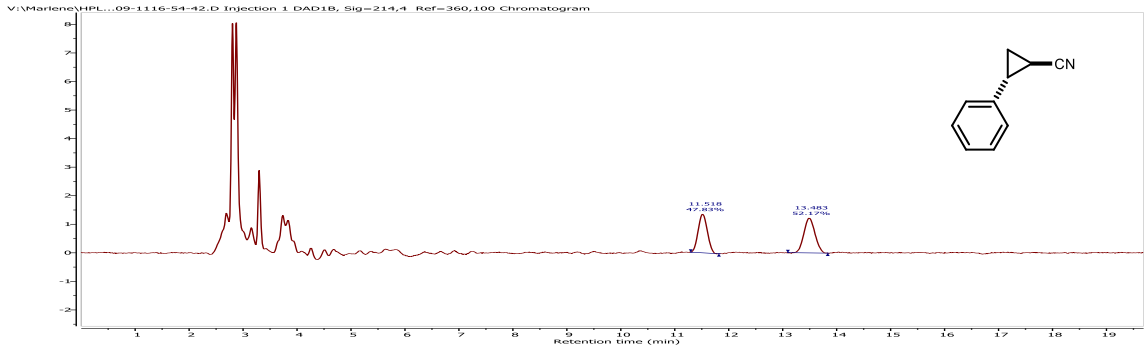

Retention Time	Area%
11.518	47.83
13.483	52.17

Figure 73. HPLC chromatogram for 2-phenylcyclopropane-1-carbonitrile (4.48) prepared with racemic starting material.

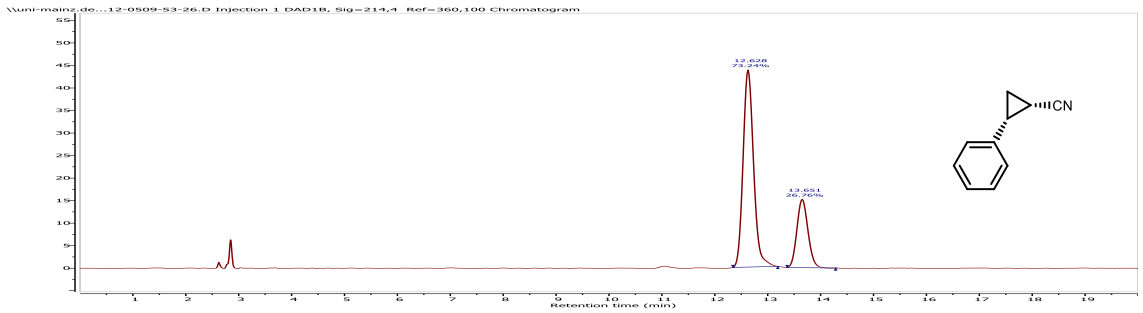

Retention Time	Area%
12.628	73.24
13.651	26.76

Figure 74. Figure 75. HPLC chromatogram for 2-phenylcyclopropane-1-carbonitrile (4.49) prepared with enantioenriched starting material.

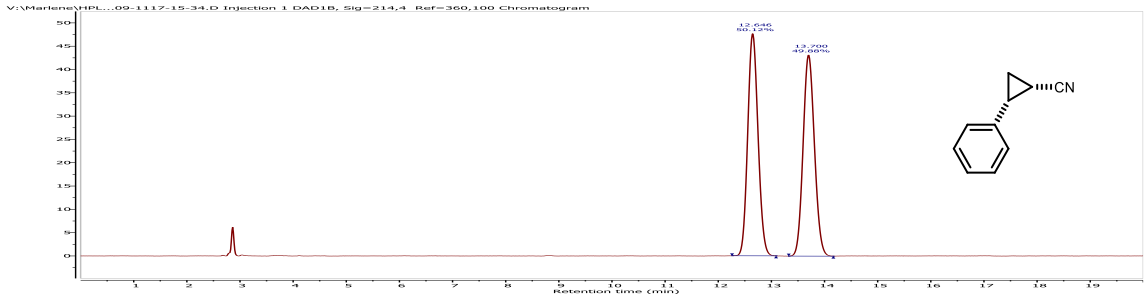

Retention Time	Area%
12.646	50.12
13.700	49.88

Figure 76. Figure 77. HPLC chromatogram for 2-phenylcyclopropane-1-carbonitrile (4.48) prepared with racemic starting material.

Mechanistic experiments

In a Schlenk flask, diphenyl(((4-phenylcyclohexylidene)amino)oxy)phosphine oxide (38.9 mg, 0.10 mmol, 1.00 eq.) was dissolved in dry toluene (1.0 mL) under N_2-atmosphere. 4 Å Molecular sieves was added and the mixture was cooled to –78 °C. LiHMDS in THF (1.0 M, 0.15 mmol, 1.5 eq.) was added and the solution was stirred for 1 h. The mixture was directly purified *via* column chromatography, to obtain 2,7-diphenyl-1,2,3,4,6,7,8,9-octahydrophenazine (13.0 mg, 0.38 mmol, 38%) as a slightly yellow solid.

M.P.: 232 – 238 °C. **IR (neat)**: $\tilde{\nu}$ = 2925 (m), 2853 (w), 1725 (w), 1494 (m), 1454 (m), 1434 (m), 1397 (s), 1158 (m), 759 (m), 700 (s), 532 (w). **^{1}H NMR (400 MHz, $CDCl_3$)** δ = 7.41 – 7.33 (m, 5H, C$H_{arom.}$), 7.32 – 7.22 (m, 5H, C$H_{arom.}$), 3.34 – 2.96 (m, 10H, CH_2, CH), 2.34 – 2.21 (m, 2H, CH_2), 2.12 – 1.97 (m, 2H, CH_2). **^{13}C NMR (101 MHz, $CDCl_3$)** δ = 149.2 (C_q), 145.1 (C_q), 128.8 (*C*H), 126.9 (*C*H), 126.7 (*C*H), 40.1 (*C*H), 39.1 (*C*H_2), 31.4 (*C*H_2), 30.2 (*C*H_2). **HRMS (ESI):** Calculated for $C_{24}H_{25}N_2$ $[M+H]^+$: 342.2012, Found: 342.2009.

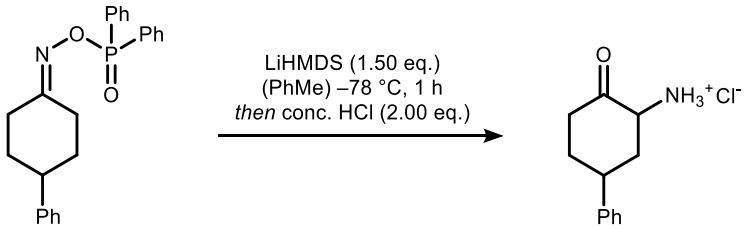

In a Schlenk flask, diphenyl(((4-phenylcyclohexylidene)amino)oxy)phosphine oxide (38.9 mg, 100 µmol, 1.00 eq.) was dissolved in dry toluene (1.0 mL) under N_2-atmosphere. 4 Å Molecular sieves was added and the mixture was cooled to –78 °C. LiHMDS in THF (1.0 M, 150 µmol, 1.50 eq.) was added and the solution was stirred for 1 h. Conc. HCl (6.8 µL, 200 µmol, 2.00 eq.) was added and the reaction mixture was stirred for 30 minutes. Water was added and the phases were separated. The aqueous phase was concentrated under reduced pressure. The crude material was analyzed by HRMS (ESI) (Calculated for $C_{12}H_{16}NO$ $[M]^+$: 190.1226, Found: 190.1221).

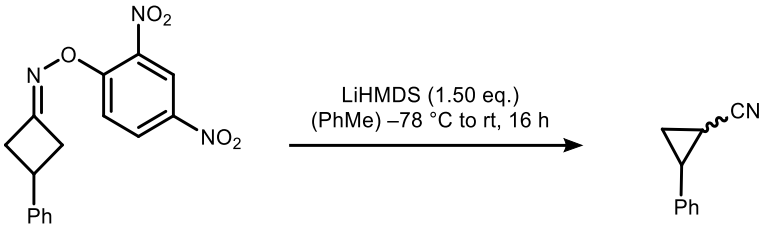

In a Schlenk flask, 3-phenylcyclobutan-1-one *O*-(2,4-dinitrophenyl) oxime (32.7 mg, 100 µmol, 1.00 eq.) was dissolved in dry toluene (1.0 mL) under N_2-atmosphere. 4 Å Molecular sieves was added and the mixture was cooled to –78 °C. LiHMDS in THF (1.0 M, 150 µmol, 1.50 eq.) was added and the solution was allowed to warm to room temperature over night. The mixture was filtered over a short plug of silica and the solvent was removed under reduced pressure. By ^{1}H NMR analysis of the crude reaction mixture trans and cis cyclopropane formation (32%) were observed with a diastereomeric ratio of (72:28 trans:cis).

Substrate Scope

The racemic products were prepared according to the following procedures:

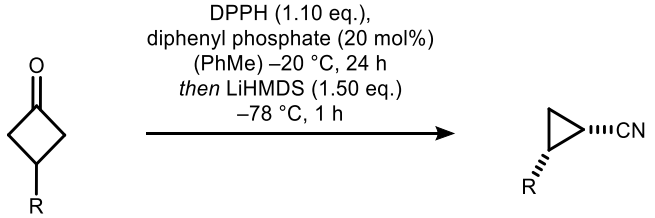

In a round bottom flask, diphenyl phosphate (20 mol%) and cyclobutanone (200 µmol, 1.00 eq.) was dissolved in toluene (0.05 M). The mixture was cooled to 0 °C. *O*-Diphenylphosphinylhydroxylamine (220 µmol, 1.10 eq.) was added, and the reaction mixture was allowed to warm to room temperature over night. After cooling to –78 °C, LiHMDS in THF (1.0 M, 300 µmol, 1.50 eq.) was added and the solution was stirred for 1 h. The mixture was directly purified *via* column chromatography with the conditions given in the corresponding entry.

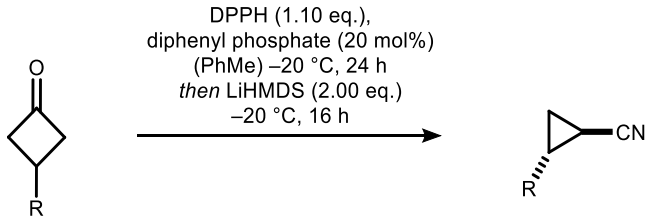

In a round bottom flask, diphenyl phosphate (20 mol%) and cyclobutanone (200 µmol, 1.00 eq.) was dissolved in toluene (0.05 M). The mixture was cooled to 0 °C. *O*-Diphenylphosphinylhydroxylamine (220 µmol, 1.10 eq.) was added, and the reaction mixture was allowed to warm to room temperature over night. After cooling to –20 °C, LiHMDS in THF (1.0 M, 400 µmol, 2.00 eq.) was added

and the solution was stirred for 16 h. The mixture was directly purified *via* column chromatography with the conditions given in the corresponding entry.

General procedure N (GP-N) for the one pot synthesis of *cis* cyclopropanes

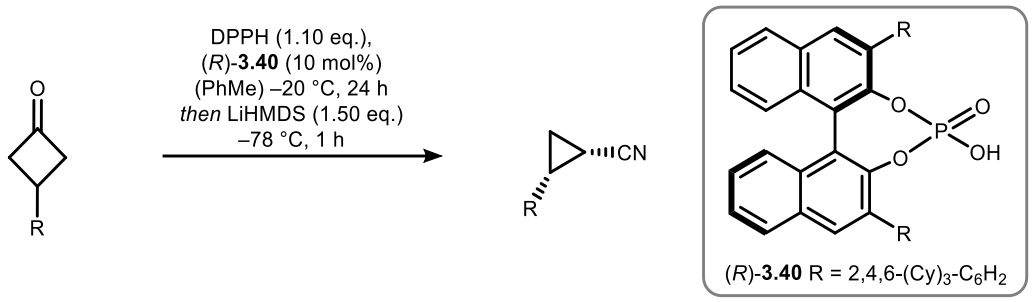

In a Schlenk flask, (*R*)-TCYP (10 mol%) and cyclobutanone (200 µmol, 1.00 eq.) was dissolved in dry toluene (0.05 M) under N_2-atmosphere. Activated 4 Å molecular sieves was added and the mixture was cooled to –20 °C. *O*-Diphenylphosphinylhydroxylamine (220 µmol, 1.10 eq.) was added, and the reaction mixture was stirred at –20 °C for 24 h. After cooling to –78 °C, LiHMDS in THF (1.0 M, 300 µmol, 1.50 eq.) was added and the solution was stirred for 1 h. The mixture was directly purified *via* column chromatography with the conditions given in the corresponding entry.

General procedure O (GP-O) for the one pot synthesis of *trans* cyclopropanes

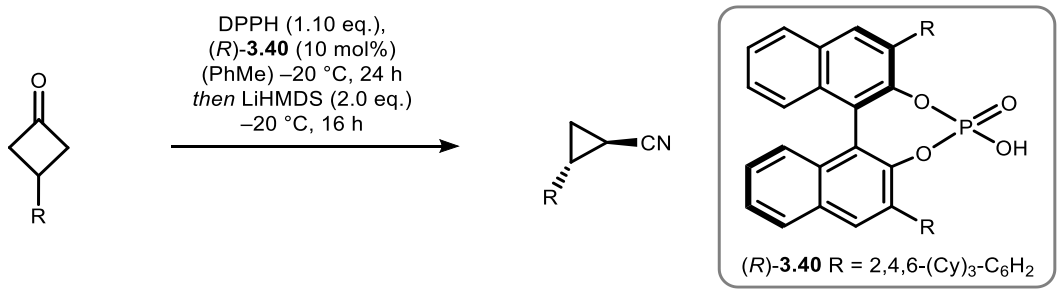

In a Schlenk falsk, (*R*)-**3.40** (10 mol%) and cyclobutanone (200 µmol, 1.00 eq.) was dissolved in dry toluene (0.05 M) under N_2-atmosphere. 4 Å molecular sieves was added and the mixture was cooled to –20 °C. *O*-Diphenylphosphinylhydroxylamine (220 µmol, 1.10 eq.) was added, and the reaction mixture was stirred at –20 °C for 24 h. LiHMDS in THF (1.0 M, 400 µmol, 2.00 eq.) was added and the solution was stirred for 16 h. The mixture was directly purified *via* column chromatography with the conditions given in the corresponding entry.

(1*R*,2*R*)-2-Phenylcyclopropane-1-carbonitrile ((1*R*,2*R*)-4.48)

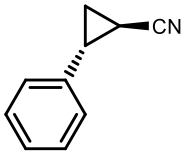

Following **GP-O** using 3-phenylcyclobutanone (29.2 mg, 200 µmol, 1.00 eq.), (*R*)-**3.40** (19.9 mg, 20 µmol, 10 mol%) and LiHMDS (1.0 M in THF, 0.4 mL, 400 µmol, 2.00 eq.) the product (13.8 mg, 96 µmol, 48%) was obtained *via* flash column chromatography (SiO_2, n-hexane:EtOAc, 100:0 → 90:10, stained with CAM) as colourless solid.

^{1}H NMR (400 MHz, $CDCl_3$) δ = 7.35 – 7.29 (m, 2H), 7.29 – 7.23 (m, 1H), 7.14 – 7.08 (m, 2H), 2.63 (ddd, J = 9.2, 6.7, 4.7 Hz, 1H), 1.62 (*app*. dt, J ≈ 9.1, 5.2 Hz, 1H), 1.55 (ddd, J = 8.6, 5.4, 4.8 Hz, 1H), 1.45 (ddd, J = 8.6, 6.7, 5.0 Hz, 1H). **^{13}C NMR (101 MHz, $CDCl_3$)** δ = 137.7, 128.9, 127.5, 126.4, 121.2, 25.0, 15.3, 6.7. Spectroscopic data was in agreement to those previously reported.[164] **Optical Rotation:** $[\alpha]_D^{25}$ = –223.5 (c = 0.5, $CHCl_3$) for an enantiomerically enriched sample of 10:90 *er*. The enantiomeric purity was established by HPLC analysis using a chiral column (Lux® Cellulose-1, 40 °C, 1 mL/min, 95:05 *n*hexane:isopropanol, 214 nm, t = 10.869 min and 12.470 min).

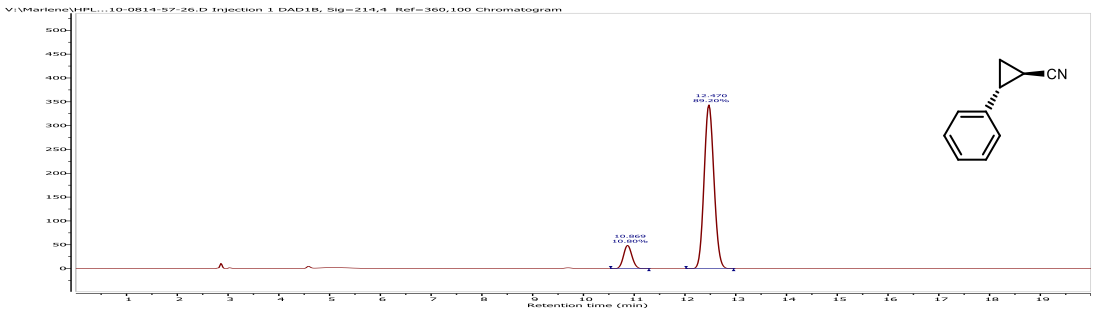

Retention Time	Area%
10.869	10.08
12.470	89.02

Figure 78. HPLC chromatogram of (1*R*,2*R*)-2-phenylcyclopropane-1-carbonitrile ((1*R*,2*R*)-4.48).

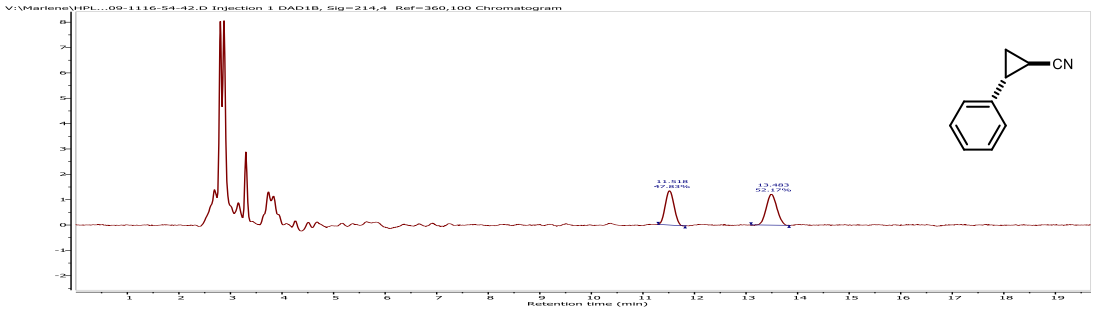

Retention Time	Area%
11.518	47.83
13.483	52.17

Figure 79. HPLC chromatogram of 2-phenylcyclopropane-1-carbonitrile (4.48).

(1*S*,2*S*)-2-Phenylcyclopropane-1-carbonitrile ((1*S*,2*S*)-4.48).

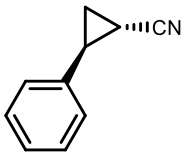

Following **GP-O** using 3-phenylcyclobutanone (29.2 mg, 200 µmol, 1.00 eq.), (*S*)-**3.40** (19.9 mg, 20 µmol, 10 mol%) and LiHMDS (1.0 M in THF, 0.4 mL, 400 µmol, 2.00 eq.) the product (12.5 mg, 88 µmol, 44%) was obtained *via* flash column chromatography (SiO_2, n-hexane:EtOAc, 100:0 → 90:10, stained with CAM) as colourless solid.

^{1}H NMR (400 MHz, $CDCl_3$) δ = 7.35 – 7.29 (m, 2H), 7.29 – 7.23 (m, 1H), 7.14 – 7.08 (m, 2H), 2.63 (ddd, J = 9.2, 6.7, 4.7 Hz, 1H), 1.62 (*app*. dt, $J \approx 9.1$, 5.2 Hz, 1H), 1.55 (ddd, J = 8.6, 5.4, 4.8 Hz, 1H), 1.45 (ddd, J = 8.6, 6.7, 5.0 Hz, 1H). **^{13}C NMR (101 MHz, $CDCl_3$)** δ = 137.7, 128.9, 127.5, 126.4, 121.2, 25.0, 15.3, 6.7. Spectroscopic data was in agreement to those previously reported.[164] **Optical Rotation:** $[\alpha]_D^{25}$ = +252.9 (c = 0.5, $CHCl_3$) for an enantiomerically enriched sample of 95:5 *er*. The enantiomeric purity was established by HPLC analysis using a chiral column (Lux® Cellulose-1, 40 °C, 1 mL/min, 95:05 *n*hexane:isopropanol, 214 nm, t = 11.187 min and 13.035 min).

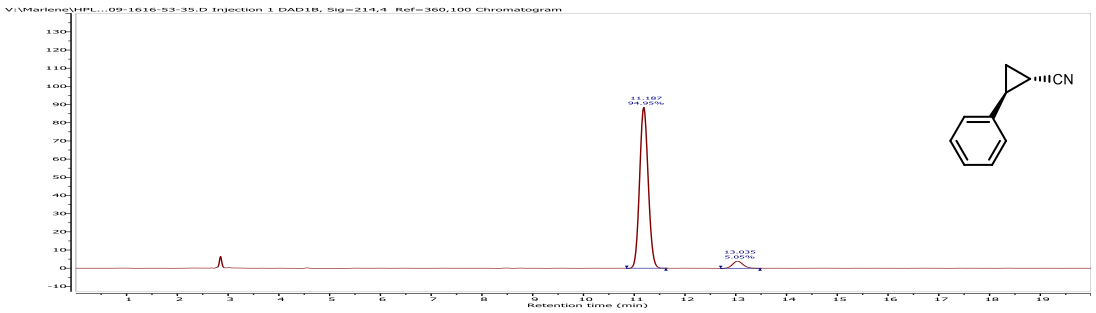

Retention Time	Area%
11.187	94.95
13.035	5.05

Figure 80. HPLC chromatogram of (1*S*,2*S*)-2-phenylcyclopropane-1-carbonitrile ((1*S*,2*S*)-4.48).

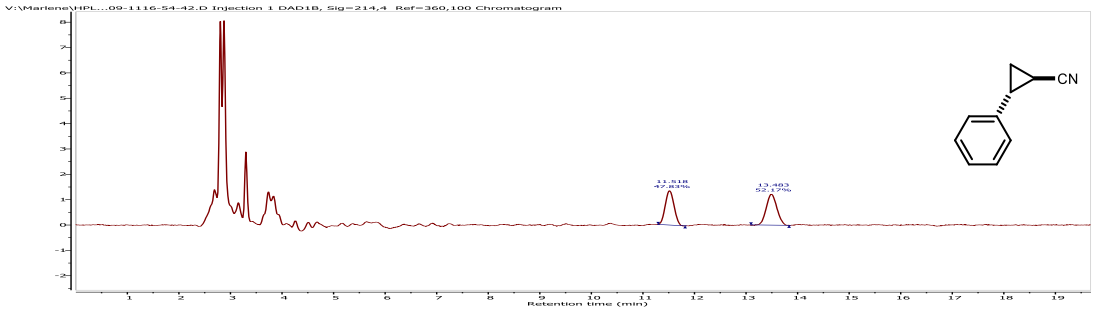

Retention Time	Area%
11.518	47.83
13.483	52.17

Figure 81. HPLC chromatogram of 2-phenylcyclopropane-1-carbonitrile (4.48).

(1*S*,2*R*)-2-Phenylcyclopropane-1-carbonitrile ((1*S*,2*R*)-4.49)

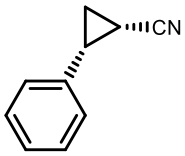

Following **GP-N** using 3-phenylcyclobutanone (29.2 mg, 200 µmol, 1.00 eq.), (*R*)-**3.40** (19.9 mg, 20 µmol, 10 mol%) and LiHMDS (1.0 M in THF, 0.3 mL, 300 µmol, 2.00 eq.) the product (16.0 mg, 112 µmol, 56%) was obtained *via* flash column chromatography (SiO_2, pentane:EtOAc, 100:0 → 90:10, stained with CAM) as colourless solid.

^{1}H NMR (400 MHz, $CDCl_3$) δ = 7.40 – 7.34 (m, 2H), 7.33 – 7.26 (m, 3H), 2.54 (td, J = 8.4, 7.1 Hz, 1H), 1.84 (ddd, J = 8.9, 8.3, 5.7 Hz, 1H), 1.60 – 1.48 (m, 2H).**^{13}C NMR (101 MHz, $CDCl_3$)** δ = 135.2, 128.6, 128.1, 127.7, 119.5, 23.2, 12.9, 6.4. Spectroscopic data was in agreement to those previously reported.[165]
Optical Rotation: $[\alpha]_D^{25}$ = +15.2 (c = 0.5, $CHCl_3$) for an enantiomerically enriched sample of 90:10 *er*. The enantiomeric purity was established by HPLC analysis using a chiral column (Lux® Cellulose-1, 40 °C, 1 mL/min, 95:05 *n*hexane:isopropanol, 214 nm, t = 12.559 min and 13.604 min).

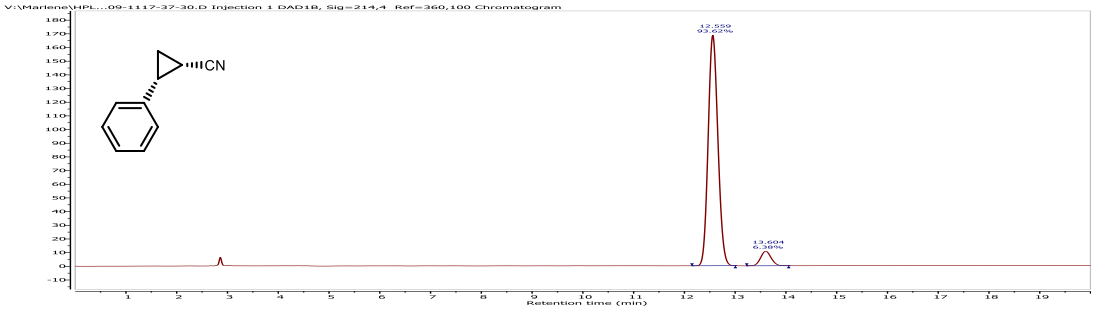

Retention Time	Area%
12.559	90.06
13.604	9.94

Figure 82. HPLC chromatogram of (1*S*,2*R*)-2-phenylcyclopropane-1-carbonitrile ((1*S*,2*R*)-4.49).

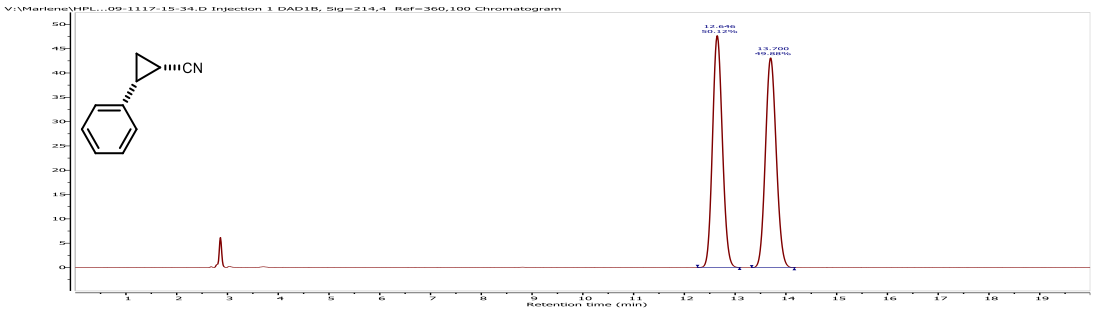

Retention Time	Area%
12.646	50.12
13.700	49.88

Figure 83. HPLC chromatogram of 2-phenylcyclopropane-1-carbonitrile (4.49).

(1*R*,2*S*)-2-Phenylcyclopropane-1-carbonitrile ((1*R*,2*S*)-4.49)

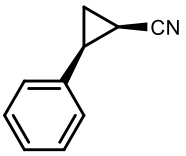

Following **GP-N** using 3-phenylcyclobutanone (29.2 mg, 200 µmol, 1.00 eq.), (*S*)-**3.40** (19.9 mg, 20 µmol, 10 mol%) and LiHMDS (1.0 M in THF, 0.3 mL, 300 µmol, 2.00 eq.) the product (16.0 mg, 112 µmol, 56%) was obtained *via* flash column chromatography (SiO_2, pentane:EtOAc, 100:0 → 90:10, stained with CAM) as colourless solid.

^{1}H NMR (400 MHz, $CDCl_3$) δ = 7.40 – 7.34 (m, 2H), 7.33 – 7.26 (m, 3H), 2.54 (td, J = 8.4, 7.1 Hz, 1H), 1.84 (ddd, J = 8.9, 8.3, 5.7 Hz, 1H), 1.60 – 1.48 (m, 2H).**^{13}C NMR (101 MHz, $CDCl_3$)** δ = 135.2, 128.6, 128.1, 127.7, 119.5, 23.2, 12.9, 6.4. Spectroscopic data was in agreement to those previously reported.[165]
Optical Rotation: $[\alpha]_D^{25}$ = –7.1 (c = 0.5, $CHCl_3$) for an enantiomerically enriched sample of 11:89 *er*. The enantiomeric purity was established by HPLC analysis using a chiral column (Lux® Cellulose-1, 40 °C, 1 mL/min, 95:05 *n*hexane:isopropanol, 214 nm, t = 12.318 min and 13.306 min).

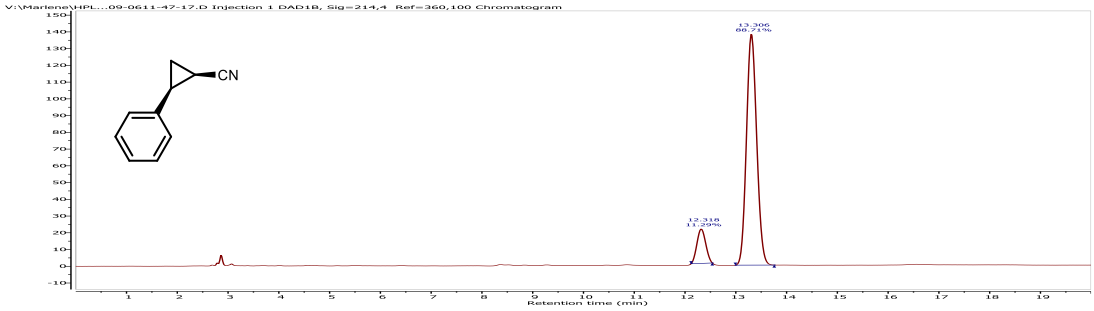

Retention Time	Area%
12.318	10.64
13.306	89.36

Figure 84. HPLC chromatogram of (1*R*,2*S*)-2-phenylcyclopropane-1-carbonitrile ((1*S*,2*R*)-4.49).

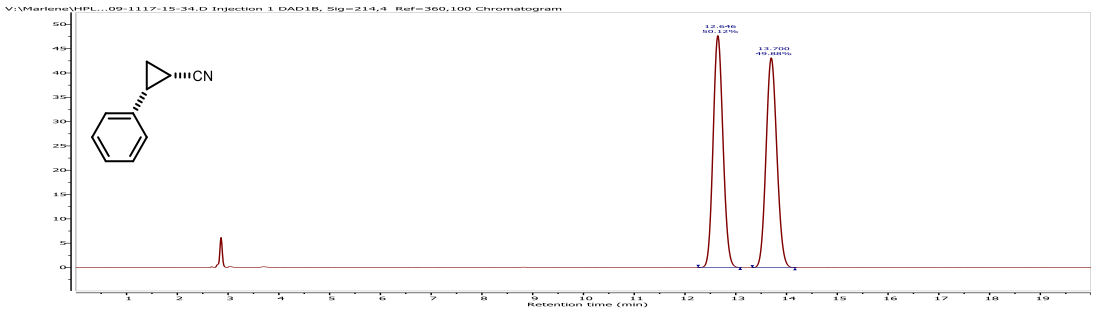

Retention Time	Area%
12.646	50.12
13.700	49.88

Figure 85. HPLC chromatogram of 2-phenylcyclopropane-1-carbonitrile (4.49).

(1*S*,2*R*)-2-(4-Fluorophenyl)cyclopropane-1-carbonitrile ((1*S*,2*R*)-4.62)

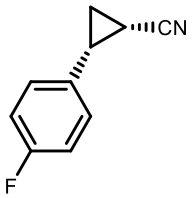

Following **GP-N** using 3-(4-fluorophenyl)cyclobutan-1-one (32.8 mg, 200 µmol, 1.00 eq.), (*R*)-**3.40** (19.9 mg, 20 µmol, 10 mol%) and LiHMDS (1.0 M in THF, 0.3 mL, 300 µmol, 1.50 eq.) the product (1*S*,2*R*)-**4.62** (17.3 mg, 106 µmol, 53%) was obtained *via* flash column chromatography (SiO_2, pentane:EtOAc, 100:0 → 90:10, stained with CAM) as colourless solid.

IR (neat): $\tilde{\nu}$ = 2924 (w), 2854 (w), 2238 (w), 1606 (w), 1513 (s), 1451 (w), 1230 (m), 1160 (w), 1103 (w), 1015 (w), 964 (w), 836 (m), 811 (m), 765 (w), 731 (w), 614 (w), 513 (w), 483 (w). **^{1}H NMR (400 MHz, $CDCl_3$)** δ = 7.29 – 7.21 (m, 2H, C*H*$_{arom.}$), 7.09 – 7.01 (m, 2H, C*H*$_{arom.}$), 2.53 (q, J = 8.0 Hz, 1H, C*H*), 1.84 (td, J = 8.4, 6.0 Hz, 1H, C*H*), 1.58 – 1.47 (m, 2H, CH_2). **^{13}C NMR (101 MHz, $CDCl_3$)** δ = 162.4 (d, $^1J_{C\text{-}F}$ = 246.4 Hz, C_q), 131.1 (d, $^4J_{C\text{-}F}$ = 3.3 Hz, C_q), 129.9 (d, $^3J_{C\text{-}F}$ = 8.1 Hz, *C*H), 119.5 (*C*N), 115.7 (d, $^2J_{C\text{-}F}$ = 21.7 Hz, *C*H), 22.6 (*C*H), 13.2 (*C*H_2), 6.40 (*C*H). ^{19}F NMR (376 MHz, $CDCl_3$) δ = –114.47 (tt, *J* = 8.3, 5.0 Hz). Spectroscopic data was in agreement to those previously reported.[166] **Optical Rotation:** $[\alpha]_D^{25}$ = +12.6 (c = 0.5, $CHCl_3$) for an enantiomerically enriched sample of 88:12 *er*. The enantiomeric purity was established by HPLC analysis using a chiral column (Lux® Cellulose-1, 22 °C, 1 mL/min, 95:05 *n*hexane:isopropanol, 210 nm, t = 17.769 min and 19.106 min).

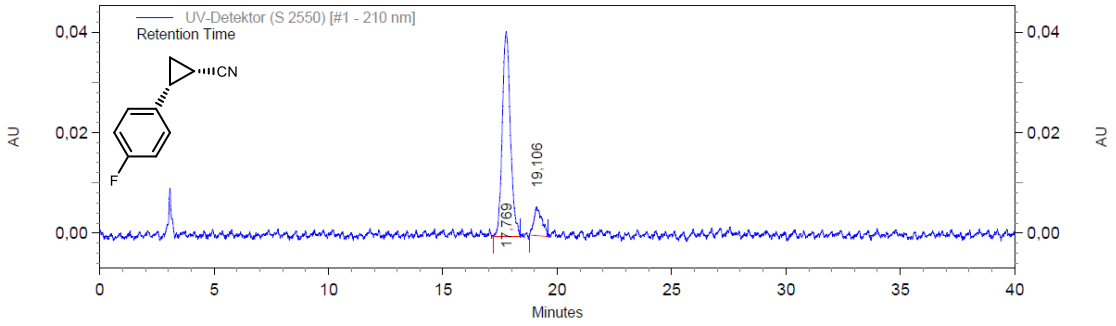

UV-Detektor (S 2550) [#1 - 210 nm] Results

Retention Time	Area	Area %
17,769	998878	87,71
19,106	140021	12,29

Figure 86. HPLC chromatogram of (1*S*,2*R*)-2-(4-fluorophenyl)cyclopropane-1-carbonitrile ((1*S*,2*R*)-4.62).

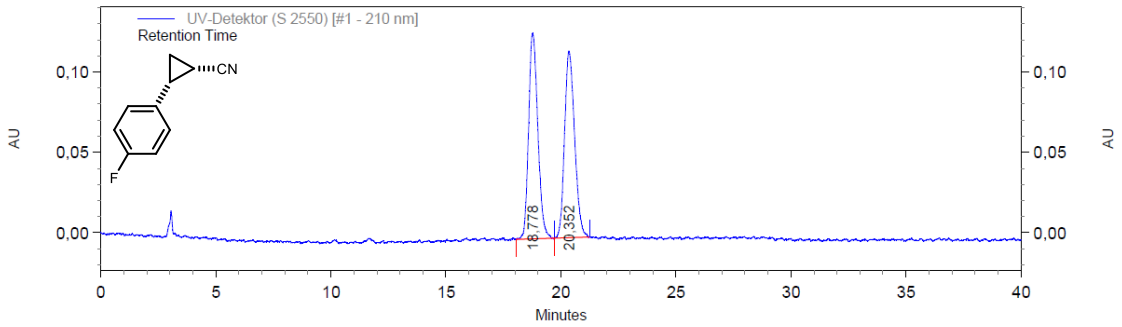

UV-Detektor (S 2550) [#1 - 210 nm] Results

Retention Time	Area	Area %
18,778	3553159	50,28
20,352	3513609	49,72

Figure 87. HPLC chromatogram of 2-(4-fluorophenyl)cyclopropane-1-carbonitrile (4.62).

(1*S*,2*R*)-2-(4-(Trifluoromethyl)phenyl)cyclopropane-1-carbonitrile ((1*S*,2*R*)-4.63)

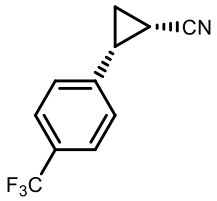

Following **GP-N** using 3-(4-(trifluoromethyl)phenyl)cyclobutan-1-one (42.8 mg, 200 µmol, 1.00 eq.), (*R*)-**3.40** (19.9 mg, 20 µmol, 10 mol%) and LiHMDS (1.0 M in THF, 0.3 mL, 300 µmol, 1.50 eq.) the product (1*S*,2*R*)-**4.63** (22.1 mg, 92 µmol, 46%) was obtained *via* flash column chromatography (SiO_2, pentane:EtOAc, 100:0 → 90:10, stained with CAM) as colourless solid.

IR (neat): $\tilde{\nu}$ = 3692 (w), 2925 (s), 2855 (m), 2363 (w), 2011 (m), 1960 (w), 1750 (m), 1326 (s), 1225 (m), 1164 (s), 1125 (s), 1069 (s), 670 (m), 650 (m), 596 (m), 582 (m), 555 (s), 527 (s), 515 (s), 504 (s), 493 (s), 482 (s), 464 (s), 446 (s), 433 (s), 413 (s). **^{1}H NMR (400 MHz, $CDCl_3$)** δ = 7.67 – 7.59 (m, 2H, C$H_{arom.}$), 7.43 – 7.36 (m, 2H, C$H_{arom.}$), 2.59 (*app.* q, $J \approx$ 8.1 Hz, 1H, C*H*), 1.93 (td, J = 8.3, 6.6 Hz, 1H, C*H*), 1.67 – 1.57 (m, 2H, CH_2). **^{13}C NMR (101 MHz, $CDCl_3$)** δ = 139.4 (C_q), 130.1 (q, $^2J_{C\text{-}F}$ = 32.5 Hz, C_q), 128.5 (*C*H), 125.7 (q, $^3J_{C\text{-}F}$ = 3.8 Hz, *C*H), 124.2 (q, $^1J_{C\text{-}F}$ = 272.0 Hz, C_q) 119.0 (C_q), 23.0 (*C*H), 13.3 (*C*H$_2$), 6.9 (*C*H). **^{19}F NMR (376 MHz, $CDCl_3$)** δ = –62.53. **HRMS (APCI):** Calculated for $C_{11}H_7F_3N$ [M-H]$^-$: 210.0536, Found: 210.0529. **Optical Rotation:** $[\alpha]_D^{25}$ = +43.0 (c = 0.5, $CHCl_3$) for an enantiomerically enriched sample of 13:87 *er*. The enantiomeric purity was established by HPLC analysis using a chiral column (Lux® Whelk-OI, 22 °C, 1 mL/min, 95:05 *n*hexane:isopropanol, 210 nm, t = 23.304 min and 30.989 min).

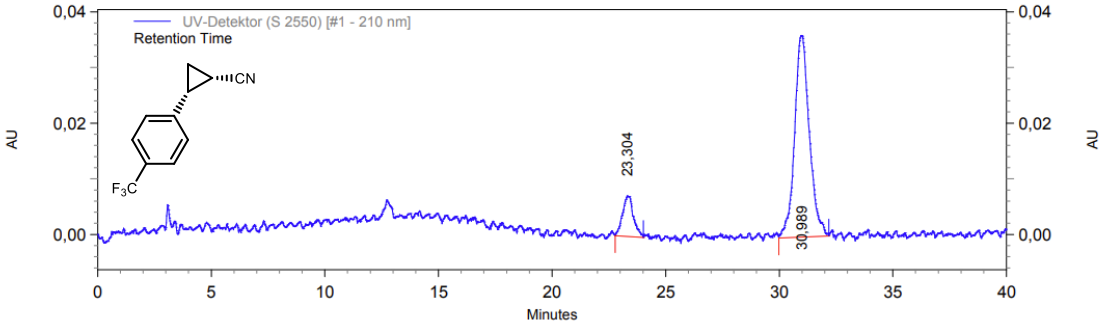

UV-Detektor (S 2550) [#1 - 210 nm] Results

Retention Time	Area	Area %
23,304	241609	12,89
30,989	1633116	87,11

Figure 88. HPLC chromatogram of (1*S*,2*R*)-2-(4-(trifluoromethyl)phenyl)cyclopropane-1-carbonitrile ((1*S*,2*R*)-4.63).

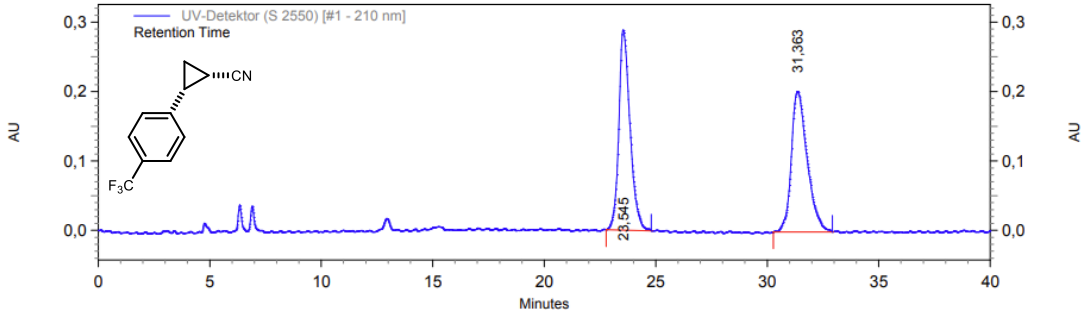

UV-Detektor (S 2550) [#1 - 210 nm] Results

Retention Time	Area	Area %
23,545	10100908	50,19
31,363	10023513	49,81

Figure 89. HPLC chromatogram of (1*S*,2*R*)-2-(4-(trifluoromethyl)phenyl)cyclopropane-1-carbonitrile ((1*S*,2*R*)-4.63).

(1*S*,2*R*)-2-(4-Methoxyphenyl)cyclopropane-1-carbonitrile ((1*S*,2*R*)-4.64)

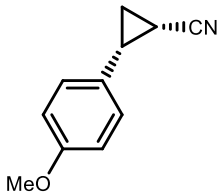

Following **GP-N** using 3-(4-methoxyphenyl)cyclobutan-1-one (35.2 mg, 200 µmol, 1.00 eq.), (*R*)-**3.40** (19.9 mg, 20 µmol, 10 mol%) and LiHMDS (1.0 M in THF, 0.3 mL, 300 µmol, 2.00 eq.) the product (1*S*,2*R*)-**4.64** (16.2 mg, 94.1 µmol, 47%) was obtained *via* flash column chromatography (SiO_2, pentane:EtOAc, 100:0 → 90:10, stained with CAM) as colourless solid.

^{1}H NMR (400 MHz, $CDCl_3$) δ = 7.23 – 7.17 (m, 2H), 6.93 – 6.86 (m, 2H), 3.80 (s, 3H), 2.50 (q, J = 8.1 Hz, 1H), 1.79 (td, J = 8.0, 6.6 Hz, 1H), 1.53 – 1.46 (m, 2H). **^{13}C NMR (101 MHz, $CDCl_3$)** δ = 159.2, 129.4, 127.3, 119.8, 114.2, 55.4, 22.7, 13.0, 6.27. Spectroscopic data was in agreement to those previously reported.[166] **Optical Rotation:** $[\alpha]_D^{25}$ = +12.7 (c = 0.5, $CHCl_3$) for an enantiomerically enriched sample of 88:12 *er*. The enantiomeric purity was established by HPLC analysis using a chiral column (Lux® Cellulose-1, 40 °C, 1 mL/min, 95:05 *n*hexane:isopropanol, 214 nm, t = 15.468 min and 16.439 min).

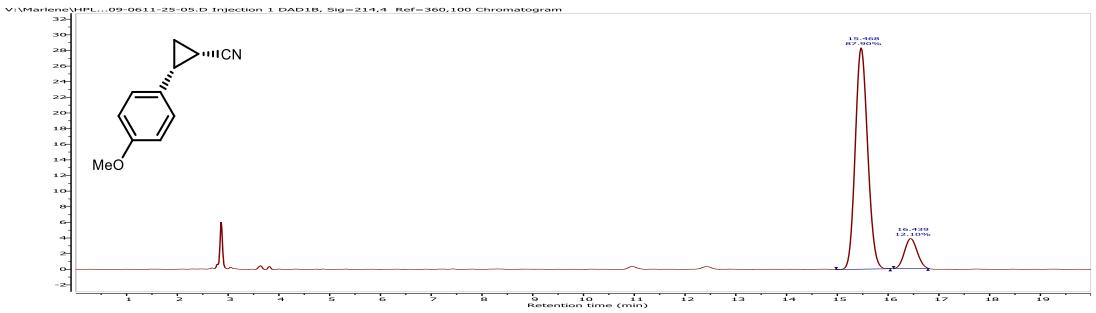

Retention Time	Area%
15.468	87.56
16.441	12.44

Figure 90. HPLC chromatogram of (1*S*,2*R*)-2-(4-methoxyphenyl)cyclopropane-1-carbonitrile ((1*S*,2*R*)-4.64).

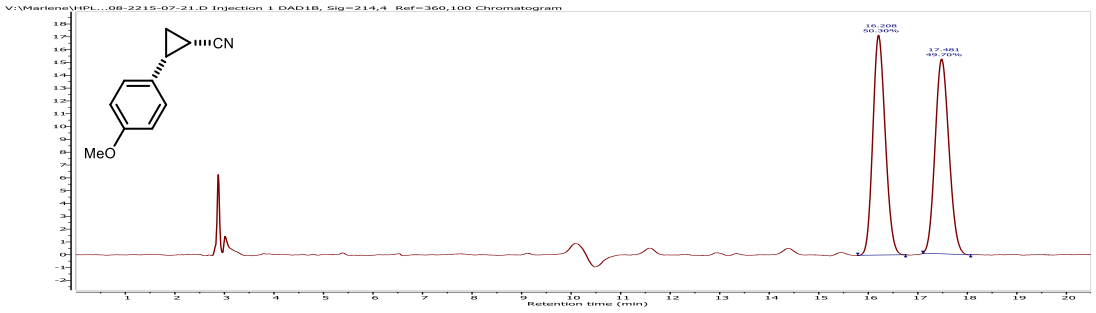

Retention Time	Area%
16.208	50.30
17.481	49.70

Figure 91. HPLC chromatogram of 2-(4-methoxyphenyl)cyclopropane-1-carbonitrile (4.64).

(1*S*,2*R*)-2-(*o*-Tolyl)cyclopropane-1-carbonitrile ((1*S*,2*R*)-4.65)

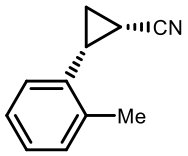

Following **GP-N** using 3-(2-methylphenyl)cyclobutanone (32.0 mg, 200 µmol, 1.00 eq.), (*R*)-**3.40** (19.9 mg, 20 µmol, 10 mol%) and LiHMDS (1 M in THF, 0.3 mL, 300 µmol, 1.50 eq.) the product (1*S*,2*R*)-**4.65** (15.4 mg, 95.4 µmol, 48%) was obtained *via* flash column chromatography (SiO_2, pentane:EtOAc, 100:0 → 90:10, stained with CAM) as colourless solid.

IR (neat): $\tilde{\nu}$ = 2953 (w), 2922 (w), 2851 (w), 2237 (m), 1492 (w), 1460 (w), 1107 (w), 1048 (w), 1034 (w), 962 (w), 839 (w), 799 (w), 768 (s), 731 (s), 637 (w), 442 (m). **^{1}H NMR (400 MHz, $CDCl_3$)** δ = 7.26 – 7.14 (m, 4H, C$H_{arom.}$), 2.48 (*app.* q, J ≈ 8.1 Hz, 1H, C*H*), 2.44 (s, 3H, CH_3), 1.90 (ddd, J = 8.8, 8.3, 5.4 Hz, 1H, C*H*), 1.61 (dt, J = 7.3, 5.4 Hz, 1H, CH_2), 1.53 (td, J = 8.6, 5.5 Hz, 1H, CH_2). **^{13}C NMR (101 MHz, $CDCl_3$)** δ = 138.6 (C_q), 133.6 (C_q), 130.4 (C$H_{arom.}$), 128.0 (C$H_{arom.}$), 127.8 (C$H_{arom.}$), 126.2 (C$H_{arom.}$), 119.6 (*C*N), 22.0 (*C*H), 19.6 (*C*H_3), 12.4 (*C*H_2), 5.4 (*C*H). **HRMS (ESI):** Calculated for $C_{11}H_{15}N_2$ $[M+NH_4]^+$: 175.1235, Found: 175.1233. **Optical Rotation:** $[\alpha]_D^{25}$ = +27.4 (c = 0.5, $CHCl_3$) for an enantiomerically enriched sample of 88:12 *er*. The enantiomeric purity was established by HPLC analysis using a chiral column (Lux® Cellulose-1, 22 °C, 1 mL/min, 95:05 *n*hexane:isopropanol, 210 nm, t = 13.480 min and 14.254 min).

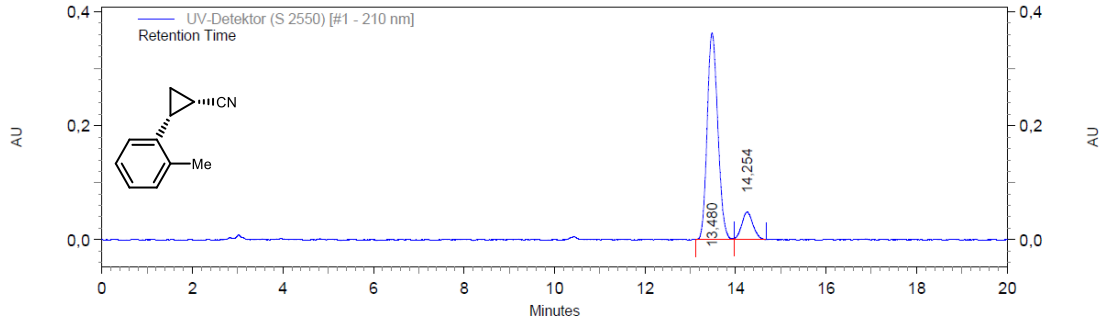

UV-Detektor (S 2550) [#1 - 210 nm] Results

Retention Time	Area	Area %
13,480	5927355	87,66
14,254	834649	12,34

Figure 92. HPLC chromatogram of (1*S*,2*R*)-2-(*o*-tolyl)cyclopropane-1-carbonitrile ((1*S*,2*R*)-4.65).

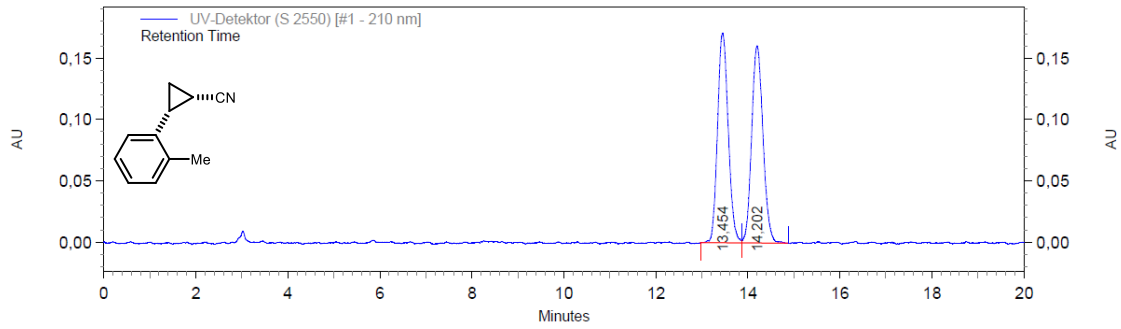

UV-Detektor (S 2550) [#1 - 210 nm] Results

Retention Time	Area	Area %
13,454	2753872	50,01
14,202	2752623	49,99

Figure 93. HPLC chromatogram of 2-(*o*-tolyl)cyclopropane-1-carbonitrile (4.65).

(1*S*,2*R*)-2-(*m*-Tolyl)cyclopropane-1-carbonitrile ((1*S*,2*R*)-4.66)

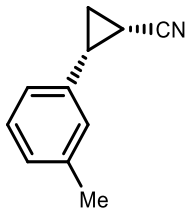

Following **GP-N** using 3-(3-methylphenyl)cyclobutan-1-one (32.0 mg, 200 µmol, 1.00 eq.), (*R*)-**3.40** (19.9 mg, 20 µmol, 10 mol%) and LiHMDS (1.0 M in THF, 0.3 mL, 300 µmol, 1.50 eq.) the product (1*S*,2*R*)-**4.66** (17.2 mg, 109 µmol, 53%) was obtained *via* flash column chromatography (SiO_2, pentane:EtOAc, 100:0 → 90:10, stained with CAM) as colourless solid.

^{1}H NMR (400 MHz, $CDCl_3$) δ = 7.29 – 7.22 (m, 1H), 7.14 – 7.05 (m, 3H), 2.51 (q, J = 8.3 Hz, 1H), 2.37 (s, 3H, CH_3), 1.82 (ddd, J = 8.9, 8.3, 5.7 Hz, 1H), 1.59 – 1.46 (m, 2H). **^{13}C NMR (101 MHz, $CDCl_3$)** δ = 138.3, 135.2, 129.0, 128.6, 128.6, 125.1, 119.6, 23.2, 21.6, 12.9, 6.4. Spectroscopic data was in agreement with those previously reported.[167] **Optical Rotation:** $[\alpha]_D^{25}$ = +13.8 (c = 0.5, $CHCl_3$) for an enantiomerically enriched sample of 90:10 *er*. The enantiomeric purity was established by HPLC analysis using a chiral column (Lux® Cellulose-1, 22 °C, 1 mL/min, 95:05 *n*hexane:isopropanol, 210 nm, t = 10.936 min and 12.133 min).

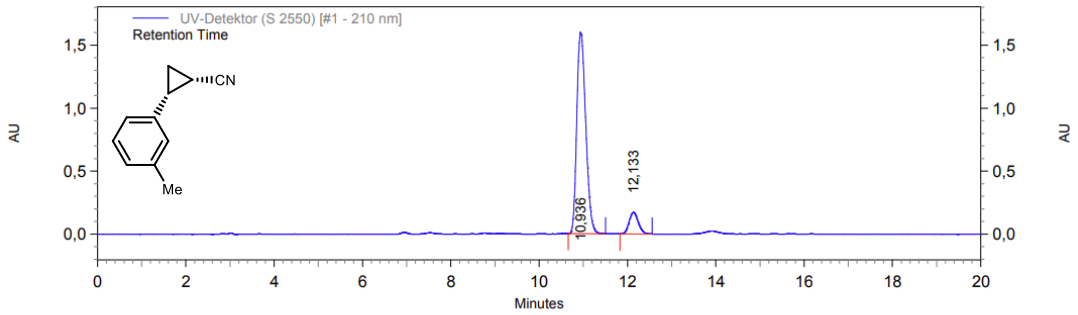

UV-Detektor (S 2550) [#1 - 210 nm] Results

Retention Time	Area	Area %
10,936	22497692	90,11
12,133	2467996	9,89

Figure 94. HPLC chromatrogram of (1*S*,2*R*)-2-(*m*-tolyl)cyclopropane-1-carbonitrile ((1*S*,2*R*)-4.66).

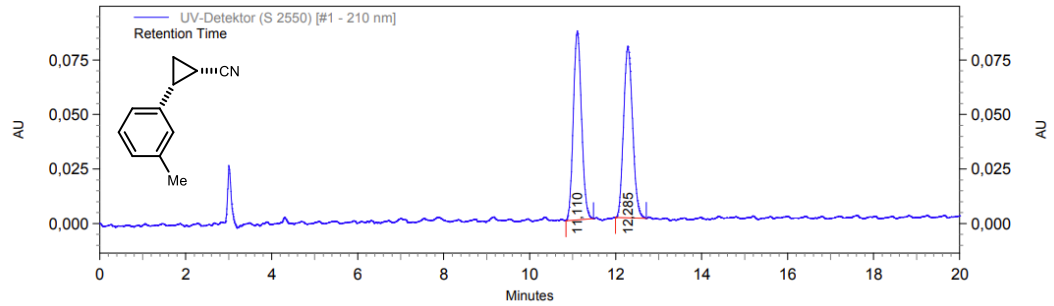

UV-Detektor (S 2550) [#1 - 210 nm] Results

Retention Time	Area	Area %
11,110	1152930	50,20
12,285	1143939	49,80

Figure 95. HPLC chromatrogram of 2-(*m*-tolyl)cyclopropane-1-carbonitrile (4.66).

(1*S*,2*R*)-2-Phenethylcyclopropane-1-carbonitrile ((1*S*,2*R*)-4.67)

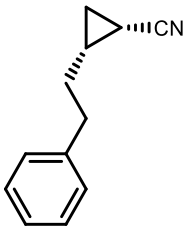

Following **GP-N** using 3-phenethylcyclobutan-1-one (34.9 mg, 200 µmol, 1.00 eq.), (*R*)-**3.40** (19.9 mg, 20 µmol, 10 mol%) and LiHMDS (1.0 M in THF, 0.3 mL, 300 µmol, 1.50 eq.) the product (1*S*,2*R*)-**4.67** (16.1 mg, 94 µmol, 47%) was obtained *via* flash column chromatography (SiO_2, pentane:EtOAc, 100:0 → 90:10, stained with CAM) as colourless solid.

^{1}H NMR (400 MHz, $CDCl_3$) δ = 7.33 – 7.27 (m, 2H, C$H_{arom.}$), 7.25 – 7.16 (m, 3H, C$H_{arom.}$), 2.92 – 2.72 (m, 2H, CH_2), 1.86 (dtd, J = 8.3, 7.0, 3.1 Hz, 2H, CH_2), 1.45 (ddd, J = 8.5, 8.0, 5.3 Hz, 1H, C*H*), 1.25 (ddt, J = 14.8, 7.9, 6.8 Hz, 1H, C*H*), 1.14 (td, J = 8.4, 5.0 Hz, 1H, CH_2), 0.79 (dt, J = 6.7, 5.1 Hz, 1H, CH_2). **^{13}C NMR (101 MHz, $CDCl_3$)** δ = 141.2 (C_q), 128.7 (*C*H), 128.6 (*C*H), 126.2 (*C*H), 120.7 (C_q), 35.0 (*C*H_2), 32.7 (*C*H_2), 18.2 (*C*H), 13.91 (*C*H_2), 2.7 (*C*H). Spectroscopic data was in agreement with those previously reported.[167] **Optical Rotation:** $[\alpha]_D^{25}$ = −12.8 (c = 0.5, $CHCl_3$) for an enantiomerically enriched sample of 21:79 *er*. The enantiomeric purity was established by HPLC analysis using a chiral column (Lux® iAmylose-3, 40 °C, 1 mL/min, 95:05 *n*hexane:isopropanol, 214 nm, t = 7.403 min and 7.965 min).

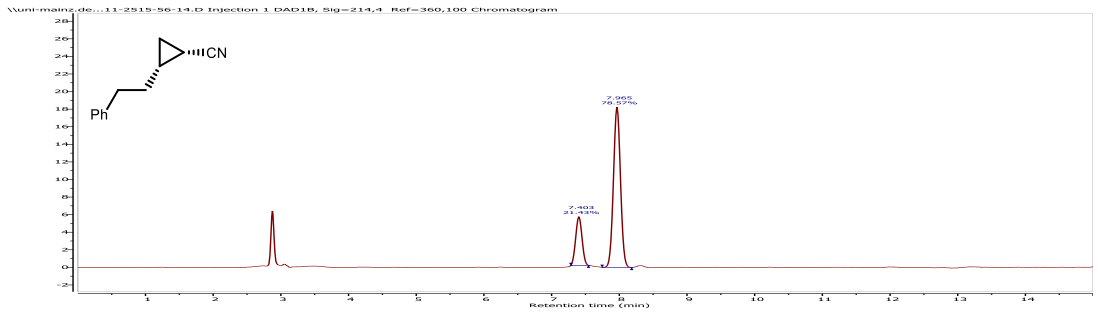

Retention Time	Area%
7.402	21.43
7.965	78.57

Figure 96. HPLC chromatogram of (1*S*,2*R*)-2-phenethylcyclopropane-1-carbonitrile ((1*S*,2*R*)-4.67).

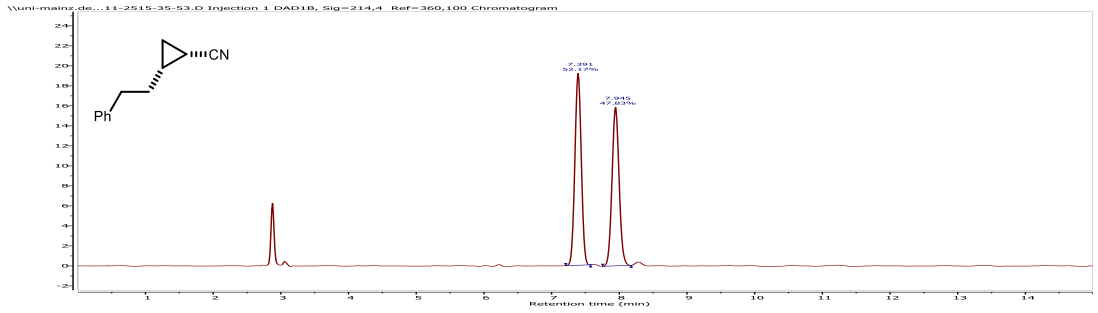

Retention Time	Area%
7.291	52.17
7.945	47.83

Figure 97. HPLC chromatogram of 2-phenethylcyclopropane-1-carbonitrile (4.67).

Formal Synthesis of Tasimelteon

4-Chloro-2,3-dihydrobenzofuran (5.13)

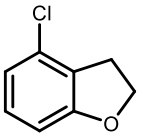

Following a procedure by *Zhu et al.*[168], 2,6-dichlorophenyl ethanol (3.44 g, 18.0 mmol, 1.00 eq.) was dissolved in dry toluene (70 mL) in a Schlenk flask. Sodium hydride (864 mg, 21.6 mmol, 1.20 eq.) was added and the reaction mixture was stirred at 40 °C for 15 minutes. After cooling to room temperature, CuCl (89.1 mg, 5.0 mol%) and EtOAc (0.1 mL) was added. The resulting mixture was heated under reflux for 24 h. After cooling to room temperature, water was added (25 mL) and the phases were separated. The aqueous layer was extracted with EtOAc (3 × 25 mL) and the combined organic phase was washed with HCl (1.0 M, 20 mL), aq. sat. $NaHCO_3$ solution (20 mL) and brine (20 mL). The organic phase was dried over $MgSO_4$, filtered and concentrated under reduced pressure. 4-Chloro-2,3-dihydrobenzofuran (2.10 g, 13.6 mmol, 75%) was isolated *via* automated flash column chromatography (SiO_2, cyclohexane:EtOAc, 95:5, stained with $KMnO_4$) as a yellow oil.

^{1}H NMR (400 MHz, $CDCl_3$): δ = 7.04 (*app.* tt, J ≈ 8.0, 0.8 Hz, 1H), 6.83 (dd, J = 8.1, 0.8 Hz, 1H), 6.67 (dd, J = 7.9, 0.7 Hz, 1H), 4.61 (t, J = 8.8 Hz, 2H), 3.29 – 3.21 (m, 2H). **^{13}C NMR (101 MHz, $CDCl_3$)**: δ = 161.1, 130.8, 129.3, 126.1, 120.6, 107.8, 71.2, 29.6. The spectroscopic data was in agreement to those previously reported.[168]

3-(2,3-Dihydrobenzofuran-4-yl)cyclobutan-1-one (4.71)

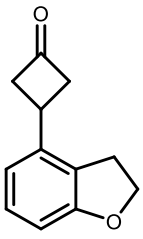

Following a procedure by *Littke et al.*[169], $Pd_2(dba)_3$ (147 mg, 0.160 mmol, 1.5 mol%) and tri-*tert*-butlyphosphine (121 mg, 0.146 mL, 0.600 mmol, 6.0 mol%) were dissolved in dry 1,4-dioxane (5 mL) under N_2 atmosphere. A solution of 4-chloro-2,3-dihydro-1-benzofuran (1.55 g, 10.0 mmol, 1.00 eq.) in dry 1,4-dioxane (5 mL) and cesium fluoride (3.34 g, 2.20 mmol, 2.20 eq.) were added. Tributyl(ethenyl)stannane (3.33 g, 3.07 mL, 1.05 mmol, 1.05 eq.) was added and the reaction mixture was stirred at 100 °C for 24 h. After cooling to room temperature, water (20 mL) was added, and the aqueous phase was extracted with Et_2O

(3 × 20 mL). The combined organic phase was washed with water (3 × 20 mL), aq. sat. NH_4Cl solution (3 × 20 mL) and brine (3 × 20 mL), dried over $MgSO_4$ and concentrated under reduced pressure. The mixture was filtered through a short silica plug (SiO_2, cyclohexane:EtOAc, 95:5, stained with $KMnO_4$) and used without further purification.

The dichlorinated cyclobutanone was prepared following an adapted literature protocol by Lu *et al.*[88]. To an oven dried Schlenk flask Zn powder (2.00 eq.) was suspended in anhydrous Et_2O (1.3 M) under inert atmosphere. 4-Vinyl-2,3-dihydrobenzofuran (375 mg, 2.57 mmol, 1.00 eq.) was added and the flask was placed into a sonication bath. The mixture was irradiated with ultrasound, while a solution of trichloroacetyl chloride (1.50 eq.) in Et_2O (2.0 M) was added dropwise over a period of 40 min. The sonication bath was cooled by adding ice to maintain a temperature of <25 °C. Once the addition was completed, the mixture was kept under sonication. The progress of the reaction was monitored by TLC. The mixture was diluted with Et_2O (20 mL) and the solids were filtered off through a pad of Celite® and washed with Et_2O. The filtrate was washed with water (2 × 50 mL), an sat. aq. $NaHCO_3$ solution (4 × 50 mL) and brine. The organic phase was dried over $MgSO_4$, filtered and concentrated under reduced pressure. The crude reaction mixture was used without further purification.

In a round bottom flask, the crude reaction mixture of the first step was dissolved in glacial acetic acid (20 mL). The solution was cooled with a water bath and Zn dust (4.00 eq.) was slowly added. The reaction mixture was heated to 80 °C for 16 h. After cooling to room temperature, the mixture was filtered through a pad of Celite® and washed with CH_2Cl_2. The solvent was removed under reduced pressure. The residue was redissolved in Et_2O (20 mL), and the organic layer was washed with water (3 × 20 mL), sat. aq. $NaHCO_3$ solution (3 × 20 mL) and brine (3 × 20 mL). The organic phase was dried over $MgSO_4$, filtered and the solvent was removed under reduced pressure. The product **4.71** (173 mg, 910 µmol, 35%) was obtained *via* automated flash column chromatography (SiO_2, cyclohexane:EtOAc, 97:3, stained with KMnO4) as a yellow solid.

M.P. 80 – 82 °C. **IR (neat)**: $\tilde{\nu}$ = 2922 (w), 1782 (s), 1588 (m), 1478 (w), 1454 (m), 1379 (w), 1235 (m), 1166 (w), 1107 (w), 1035 (w), 985 (m), 946 (w), 839 (w), 777 (m), 718 (w), 445 (w). **^{1}H NMR (600 MHz, $CDCl_3$)**: δ = 7.15 (t, J = 7.9 Hz, 1H, CH_{arom}), 6.80 (d, J = 8.0 Hz, 1H, CH_{arom}), 6.72 (d, J = 8.0 Hz, 1H, CH_{arom}), 4.60 (t, J = 8.7 Hz, 2H, CH_2), 3.64 (*app.* p, J ≈ 8.2 Hz, 1H, C*H*), 3.49 – 3.42 (m, 2H, CH_2), 3.32 – 3.25 (m, 2H, CH_2), 3.17 (t, J = 8.7 Hz, 2H, CH_2). **^{13}C NMR (151 MHz, $CDCl_3$)**: δ = 206.6 (C_q), 160.3 (C_q), 139.9 (C_q), 128.7 (*C*H), 125.4 (C_q), 116.9 (*C*H), 108.0 (*C*H), 71.1 (*C*H_2), 53.5 (2x*C*H_2), 28.9 (*C*H_2), 26.6 (*C*H).

(1*R*,2*R*)-2-(2,3-dihydrobenzofuran-4-yl)cyclopropane-1-carbonitrile ((1*R*,2*R*)-4.73)

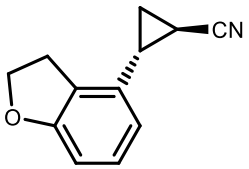

Following **GP-O** using 3-(2,3-dihydrobenzofuran-4-yl)cyclobutan-1-one (37.6 mg, 200 µmol, 1.00 eq.) (*R*)-**3.40** (19.9 mg, 20 µmol, 10 mol%) and LiHMDS (1.0 M in THF, 0.4 mL, 400 µmol, 2.00 eq.) the product (1*R*,2*R*)-**4.73** (20.6 mg, 112 µmol, 56%) was obtained *via* flash column chromatography (SiO_2, pentane:EtOAc, 100:0 → 90:10, stained with CAM) as colourless solid.

^{1}H NMR (400 MHz, $CDCl_3$) δ = 7.10 – 7.01 (m, 1H, C$H_{arom.}$), 6.70 (d, J = 7.9 Hz, 1H, C$H_{arom.}$), 6.38 (d, J = 7.8 Hz, 1H, C$H_{arom.}$), 4.63 (t, J = 8.7 Hz, 2H, CH_2), 3.34 – 3.25 (m, 2H, CH_2), 2.53 (ddd, J = 9.2, 6.8, 4.9 Hz, 1H, C*H*), 1.62 (dt, J = 9.1, 5.1 Hz, 1H, CH_2), 1.54 (dt, J = 8.6, 5.0 Hz, 1H, C*H*), 1.46 (ddd, J = 8.6, 6.8, 4.9 Hz, 1H, CH_2). **^{13}C NMR (101 MHz, $CDCl_3$)** δ = 160.3 (C_q), 134.3 (C_q), 128.8 (*C*H), 127.1 (C_q), 121.2 (C_q), 116.2 (*C*H), 108.7 (*C*H), 71.3 (*C*H_2), 28.7 (*C*H_2), 23.0 (*C*H), 14.6 (*C*H_2), 5.73 (*C*H). Spectroscopic data was in agreement with those previously reported.[170] **Optical Rotation:** $[\alpha]_D^{25}$ = –61.0 (c = 0.5, $CHCl_3$) for an enantiomerically enriched sample of 12:88 *er*. The enantiomeric purity was established by HPLC analysis using a chiral column (Lux® AMS, 40 °C, 1 mL/min, 95:05 *n*hexane:isopropanol, 214 nm, t = 17.147 min and 20.378 min).

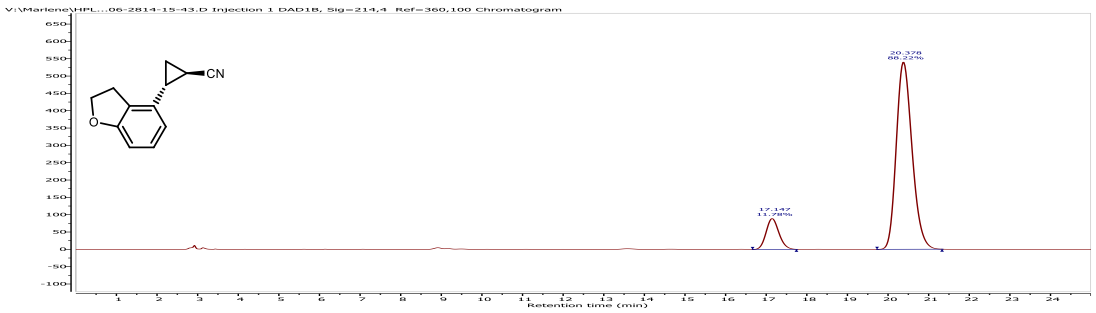

Retention Time	Area%
17.147	11.78
20.378	88.22

Figure 98. HPLC chromatogram of (1*R*,2*R*)-2-(2,3-dihydrobenzofuran-4-yl)cyclopropane-1-carbonitrile ((1*R*,2*R*)-4.73).

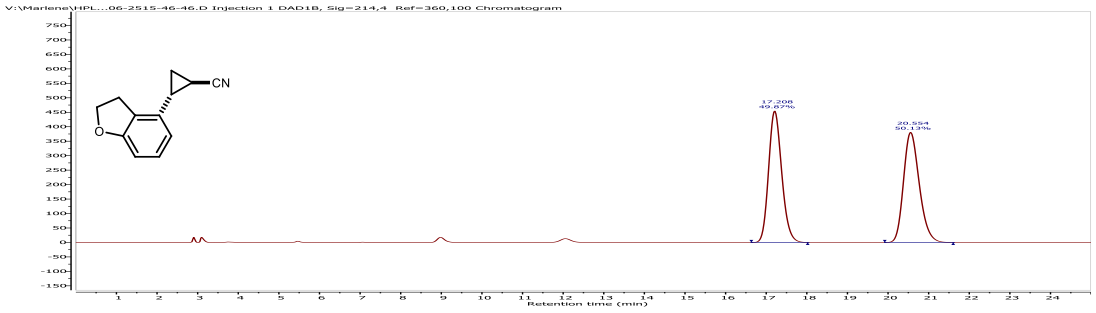

Retention Time	Area%
17.208	49.87
20.554	50.13

Figure 99. HPLC chromatogram of 2-(2,3-dihydrobenzofuran-4-yl)cyclopropane-1-carbonitrile (4.73).

5.5 Crystallographic Data

All X-ray measurements and structure refinements were performed by [redacted].

X-ray crystal structure analysis of 3.41 (MAR648)

A colourless needle like specimen of $C_{22}H_{19}ClNO_2P$, approximately dimensions 0.060 x 0.080 x 0.690 mm^3, was used for the X-ray crystallographic analysis. The X-ray intensity data were measured on a STOE STADIVARI Diffractometer system.

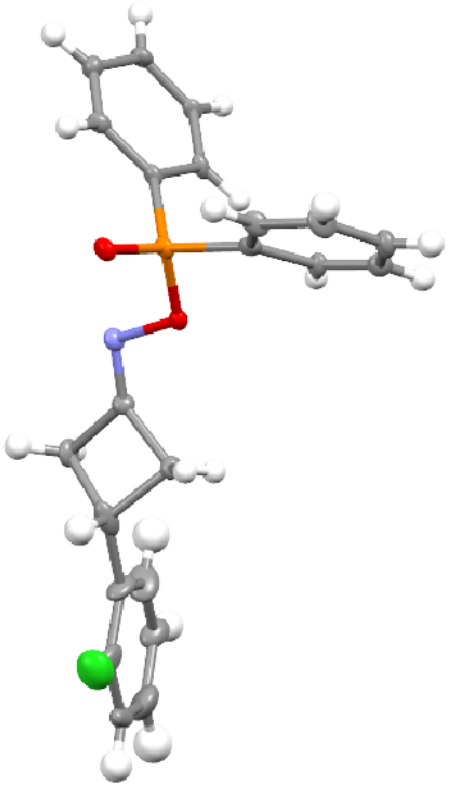

Figure 100. Graphical representation of the X-ray structure of (*R*)-3.41.

Table 19. Crystal data and structure refinement for (*R*)-3.41 (mar648)

Identification code	Mar648
Empirical formula	$C_{22}H_{19}ClNO_2P$
Moiety formula	$C_{22}H_{19}ClNO_2P$
Formula weight	395.80
Temperature	120(2) K
Wavelength, radiation type	1.54186Å, CuK*α*
Diffractometer	STOE STADIVARI
Crystal type	Monoclinic
Space group name, number	$P2_1$, (4)
Unit cell dimensions	a = 17.7846(13) Ă α = 90° b = 8.5371(4) Å β = 106.358(6)° c = 26.505(2) Å γ = 90°
Volume	3861.3(5) Å^3
Number of reflections	18838
And range used for lattice	2.59° <=Θ<= 69.30°
Parameters	
Z	8
Density (calculated)	1.362 Mg/m^3
Absorption coefficient	2.671 mm^{-1}
Absorption correction	integration
Max. and min. transmission	0.7735 and 0.4134
F(000)	1648
Crystal size, color and form	0.060 x 0.080 x 0.690 mm^3, colourless needle
Theta range for data collection	2.589 to 69.932°
Index ranges	-21<=h<=19, -10<=k=10, -31=l<=32
Number of reflections:	
Collected	37837
Independent	13674 [R_{int}= 0.1130]
Observed [I>2sigma(l)]	6363
Completeness of theta = 25.2°	99.1%
Refinement method	Full-matrix least-squares on F^2
Data / restraints / parameters	13674 / 49 / 973
Goodness-of-fit on F^2	1.166
Final R indices [I>2sigma(l)]	R1 = 0.1450, wR2 = 0.3428
R indices (all data)	R1 = 0.2361, wR2 = 0.3989
Absolute structure parameter	-0.01(6)
Largest diff. peak and hole	0.930 and -0.510 eĂ$^{-3}$
Comment	Crystal contains four distinct molecules

X-ray crystal structure analysis of 3.42 (mar647)

A colourless plate like specimen of $C_{22}H_{19}ClNO_2P$, approximately dimensions 0.030 x 0.190 x 0.290 mm^3, was used for the X-ray crystallographic analysis. The X-ray intensity data were measured on a STOE IPDS 2T Diffractometer system.

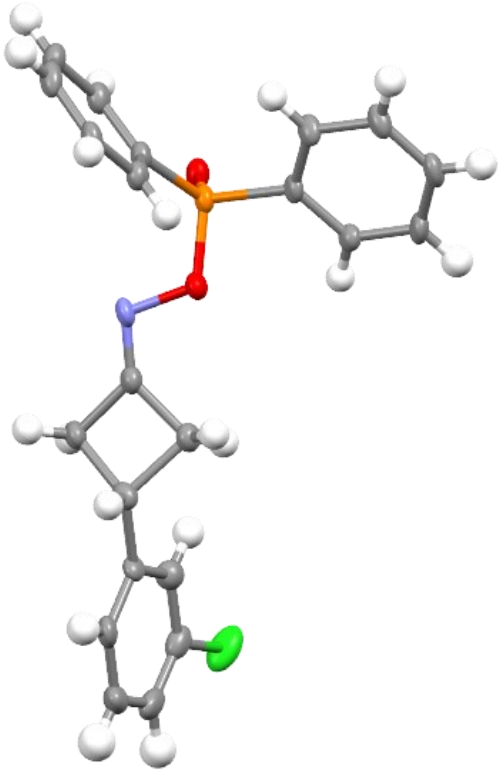

Figure 101. Graphical representation of the X-ray structure of (*R*)-3.42.

Table 20. Crystal data and structure refinement for (*R*)-3.42 (mar647)

Identification code	mar647
Empirical formula	$C_{22}H_{19}ClNO_2P$
Moiety formula	$C_{22}H_{19}ClNO_2P$
Formula weight	395.80
Temperature	120(2) K
Wavelength, radiation type	0.71073Å, MoKα
Diffractometer	STOE IPDS 2T
Crystal type	Triclinic
Space group name, number	P 1, (1)
Unit cell dimensions	a = 8.2954(5)(3) Ă α = 73.851(5)° b = 9.0584(5) Å β = 85.864(5)° c = 13.3668(8) Å γ = 79.040(4)°
Volume	946.99(10) Ă^3
Number of reflections	34553
And range used for lattice Parameters	2.50°<=Θ<=28.48°
Z	2
Density (calculated)	1.388 Mg/m^3
Absorption coefficient	0.304 mm^{-1}
Absorption correction	integration
Max. and min. transmission	0.9886 and 0.9288
F(000)	412
Crystal size, color and form	0.030 x 0.190 x 0.290 mm^3, colourless plate
Theta range for data collection	2.935 to 28.409°
Index ranges	-10<=h<=11, -12<=k=12, -17=l<=17
Number of reflections:	
Collected	22786
Independent	8806 [R_{int}=0.0470]
Observed [I>2sigma(l)]	6632
Completeness of theta = 25.2°	99.9%
Refinement method	Full-matrix least-squares on F^2
Data / restraints / parameters	8806 / 48 / 545
Goodness-of-fit on F^2	1.066
Final R indices [I>2sigma(l)]	R1 = 0.0657, wR2 = 0.1267
R indices (all data)	R1 = 0.1022, wR2 = 0.1479
Absolute structure parameter	-0.07(9)
Largest diff. peak and hole	0.310 and -0.376 eĂ$^{-3}$
comment	Structure contains 2 distinct molecules, with enantiomeric ratio of 91:9

X-ray crystal structure analysis of (1*S*,2*R*)-4.49 (488f2)

A colourless block like specimen of $C_{10}H_9N$, approximately dimensions 0.060 x 0.270 x 0.530 mm^3, was used for the X-ray crystallographic analysis. The x-ray intensity data were measured on a STOE STADIVARI Diffractometer system. CCDC number: 2419831

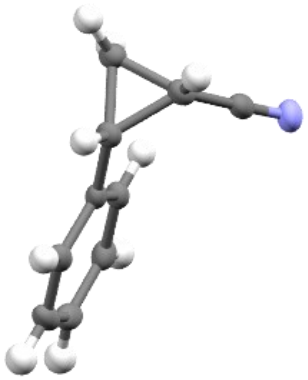

Figure 102. Graphical representation of the X-ray structure of (1*S*,2*R*)-4.49.

Table 21. Crystal data and structure refinement for (1*S*,2*R*)-4.49 (468f2)

Identification code	468f2
Empirical formula	$C_{10}H_9N$
Moiety formula	$C_{10}H_9N$
Formula weight	143.18
Temperature	120(2) K
Wavelength, radiation type	1.54178Å, CuKα
Diffractometer	STOE STADIVARI
Crystal type	Monoclinic
Space group name, number	$P2_1$, (4)
Unit cell dimensions	a = 5.8962(3) Ă α = 90°
	b = 8.0964(4) Å β = 106.756(5)°
	c = 8.5292(5) Å γ = 90°
Volume	389.88(4) Ă^3
Number of reflections	6656
And range used for lattice	5.42°<=Θ<=68.91°
Parameters	
Z	2
Density (calculated)	1.220 Mg/m^3
Absorption coefficient	0.553 mm^{-1}
Absorption correction	integration
Max. and min. transmission	0.9645 and 0.8243
F(000)	152
Crystal size, color and form	0.060 x 0.270 x 0.530 mm^3, colorless block
Theta range for data collection	5.416 to 68.227°
Index ranges	-6<=h<=7, -9<=k=9, -10<=l<=10
Number of reflections:	
Collected	3124
Independent	1345 [R_{int}=0.0159]
Observed [I>2sigma(l)]	1314
Completeness of theta = 25.2°	99.3%
Refinement method	Full-matrix least-squares on F^2
Data / restraints / parameters	1345 / 1 / 100
Goodness-of-fit on F^2	1.061
Final R indices [I>2sigma(l)]	R1 = 0.0269, wR2 = 0.0705
R indices (all data)	R1 = 0.0275, wR2 = 0.0710
Absolute structure parameter	0.1(3)
Largest diff. peak and hole	0.099 and -0.150 eĂ$^{-3}$

References

[1] P. Ball, *Nature* **2015**, *528*, 327.

[2] a) S. L. Schreiber, *Proc. Natl. Acad. Sci. U. S. A.* **2011**, *108*, 6699; b) B. Lu, A. Atala, *Drug discovery today* **2014**, *19*, 801; c) L. Zhong, Y. Li, L. Xiong, W. Wang, M. Wu, T. Yuan, W. Yang, C. Tian, Z. Miao, T. Wang et al., *Signal Transduction Targeted Ther.* **2021**, *6*, 201.

[3] a) K. R. Campos, P. J. Coleman, J. C. Alvarez, S. D. Dreher, R. M. Garbaccio, N. K. Terrett, R. D. Tillyer, M. D. Truppo, E. R. Parmee, *Science* **2019**, *363*; b) D. C. Blakemore, L. Castro, I. Churcher, D. C. Rees, A. W. Thomas, D. M. Wilson, A. Wood, *Nat. Chem.* **2018**, *10*, 383.

[4] a) K. Wu, E. Karapetyan, J. Schloss, J. Vadgama, Y. Wu, *Drug discovery today* **2023**, *28*, 103730; b) F. D. Makurvet, *Med. Drug Discovery* **2021**, *9*, 100075.

[5] a) J.-L. Reymond, L. Ruddigkeit, L. Blum, R. van Deursen, *WIREs Comput. Mol. Sci.* **2012**, *2*, 717; b) C. J. Gerry, S. L. Schreiber, *Nat. Rev. Drug Discovery* **2018**, *17*, 333; c) D. G. Brown, J. Boström, *J. Med. Chem.* **2016**, *59*, 4443.

[6] P. Arora, V. Arora, H. S. Lamba, D. Wadhwa, *Int. J. Pharm. Sci. Res.* **2012**, *3*, 2947.

[7] a) P. Das, M. D. Delost, M. H. Qureshi, D. T. Smith, J. T. Njardarson, *J. Med. Chem.* **2019**, *62*, 4265; b) C. M. Marshall, J. G. Federice, C. N. Bell, P. B. Cox, J. T. Njardarson, *J. Med. Chem.* **2024**, *67*, 11622.

[8] a) V. H. Masand, S. Al-Hussain, A. Y. Alzahrani, N. N. E. El-Sayed, C. I. Yeo, Y. S. Tan, M. E. A. Zaki, *Expert. Opin. Drug Discovery* **2024**, *19*, 111; b) E. Vitaku, D. T. Smith, J. T. Njardarson, *J. Med. Chem.* **2014**, *57*, 10257.

[9] a) Y. Ozkay, I. Işikdağ, Z. Incesu, G. Akalin, *Eur. J. Med. Chem.* **2010**, *45*, 3320; b) M. M. Heravi, V. Zadsirjan, *RSC Adv.* **2020**, *10*, 44247; c) N. Kerru, L. Gummidi, S. Maddila, K. K. Gangu, S. B. Jonnalagadda, *Molecules* **2020**, *25*.

[10] L. D. Pennington, D. T. Moustakas, *J. Med. Chem.* **2017**, *60*, 3552.

[11] D. R. Lide, W. M. Haynes (Eds.) *CRC handbook of chemistry and physics. A ready-reference book of chemical and physical data*, CRC Press, Boca Raton, Florida, **2009**.

[12] a) C. Bissantz, B. Kuhn, M. Stahl, *J. Med. Chem.* **2010**, *53*, 5061; b) B. D. Cons, D. G. Twigg, R. Kumar, G. Chessari, *J. Med. Chem.* **2022**, *65*, 7476.

[13] a) E. M. Gordon, R. W. Barrett, W. J. Dower, S. P. Fodor, M. A. Gallop, *J. Med. Chem.* **1994**, *37*, 1385; b) Z. Hosseinzadeh, A. Ramazani, N. Razzaghi-Asl, *Curr. Org. Chem.* **2018**, *22*, 2256; c) O. Ebenezer, M. A. Jordaan, G. Carena, T. Bono, M. Shapi, J. A. Tuszynski, *Int. J. Mol. Sci.* **2022**, *23*; d) L. D. Pennington, P. N. Collier, E. Comer, *Med. Chem. Res.* **2023**, *32*, 1278.

[14] a) Y. Park, Y. Kim, S. Chang, *Chem. Rev.* **2017**, *117*, 9247; b) J. Bariwal, E. van der Eycken, *Chem. Soc. Rev.* **2013**, *42*, 9283; c) F. Ullmann, *Ber. Dtsch. Chem. Ges.* **1903**, *36*, 2382; d) I. Goldberg, *Ber. Dtsch. Chem. Ges.* **1906**, *39*, 1691; e) A. S. Guram, S. L. Buchwald, *J. Am. Chem. Soc.* **1994**, *116*, 7901; f) F. Paul, J. Patt, J. F. Hartwig, *J. Am. Chem. Soc.* **1994**, *116*, 5969; g) D. M. Chan, K. L. Monaco, R.-P. Wang, M. P. Winters, *Tetrahedron Lett.* **1998**, *39*, 2933; h) P. Y. Lam, C. G. Clark, S. Saubern, J. Adams, M. P. Winters, D. M. Chan, A. Combs, *Tetrahedron Lett.* **1998**, *39*, 2941; i) A. F. Abdel-Magid, K. G. Carson, B. D. Harris, C. A. Maryanoff, R. D. Shah, *J. Org. Chem.* **1996**, *61*, 3849; j) O. I. Afanasyev, E. Kuchuk, D. L. Usanov, D. Chusov, *Chem. Rev.* **2019**, *119*, 11857; k) M. Corpet, C. Gosmini, *Synthesis* **2014**, *46*, 2258; l) R. Dorel, C. P. Grugel, A. M. Haydl, *Angew. Chem. Int. Ed.* **2019**, *58*, 17118; m) R. Tripathi, S. Verma, J. Pandey, V. Tiwari, *Curr. Org. Chem.* **2008**, *12*, 1093; n) Z. Zhou, L. Kürti, *Synlett* **2019**, *30*, 1525.

[15] a) M. Kienle, S. Reddy Dubbaka, K. Brade, P. Knochel, *Eur. J. Org. Chem.* **2007**, *2007*, 4166; b) N. Jiao, *Nitrogenation Strategy for the Synthesis of N-containing Compounds*, Springer, Singapore, **2017**.

[16] a) J. Börgel, T. Ritter, *Chem* **2020**, *6*, 1877; b) T. Cernak, K. D. Dykstra, S. Tyagarajan, P. Vachal, S. W. Krska, *Chem. Soc. Rev.* **2016**, *45*, 546; c) L. Guillemard, N. Kaplaneris, L. Ackermann, M. J. Johansson, *Nat. Rev. Chem.* **2021**, *5*, 522; d) L. Zhang, T. Ritter, *J. Am. Chem. Soc.* **2022**, *144*, 2399; e) J. Jurczyk, J. Woo, S. F. Kim, B. D. Dherange, R. Sarpong, M. D. Levin, *Nat. Synth.* **2022**, *1*, 352.

[17] a) J. M. Lopchuk, K. Fjelbye, Y. Kawamata, L. R. Malins, C.-M. Pan, R. Gianatassio, J. Wang, L. Prieto, J. Bradow, T. A. Brandt et al., *J. Am. Chem. Soc.* **2017**, *139*, 3209; b) Y.-F. Liang, M. Bilal, L.-Y. Tang, T.-Z. Wang, Y.-Q. Guan, Z. Cheng, M. Zhu, J. Wei, N. Jiao, *Chem. Rev.* **2023**, *123*, 12313; c) C. Hui, L. Craggs, A. P. Antonchick, *Chem. Soc. Rev.* **2022**, *51*, 8652; d) R. Gianatassio, J. M. Lopchuk, J. Wang, C.-M. Pan, L. R. Malins, L. Prieto, T. A. Brandt, M. R. Collins, G. M. Gallego, N. W. Sach et al., *Science* **2016**, *351*, 241; e) J. Turkowska, J. Durka, D. Gryko, *Chem. Commun.* **2020**, *56*, 5718.

[18] M. Murakami, N. Ishida, *Chem. Rev.* **2021**, *121*, 264.

[19] J. Sietmann, J. M. Wahl, *Angew. Chem. Int. Ed.* **2020**, *59*, 6964.

[20] a) A. D. McNaught, A. Wilkinson, *Compendium of chemical terminology*, Blackwell Science, Oxford, **1997**; b) V. Gold, A. McNaught, *The IUPAC Compendium of Chemical Terminology*, International Union of Pure and Applied Chemistry (IUPAC), Research Triangle Park, NC, **2025**.

[21] T. Dudev, C. Lim, *J. Am. Chem. Soc.* **1998**, *120*, 4450.

[22] R. D. Bach, O. Dmitrenko, *J. Am. Chem. Soc.* **2006**, *128*, 4598.

[23] P. R. Khoury, J. D. Goddard, W. Tam, *Tetrahedron* **2004**, *60*, 8103.

[24] A. Baeyer, *Ber. Dtsch. Chem. Ges.* **1885**, *18*, 2269.

[25] A. Bauzá, D. Quiñonero, P. M. Deyà, A. Frontera, *Chem. Phys. Lett.* **2012**, *536*, 165.

[26] a) E. V. Anslyn, D. A. Dougherty, *Modern Physical Organic Chemistry*, University Science Books, Mill Valley, California, **2006**; b) J. F. Liebman, A. Greenberg, *Chem. Rev.* **1976**, *76*, 311; c) K. B. Wiberg, *Angew. Chem. Int. Ed.* **1986**, *25*, 312.

[27] a) X. Hu, *Tetrahedron* **2004**, *60*, 2701; b) P. Lu, *Tetrahedron* **2010**, *66*, 2549; c) D. R. Mishra, N. P. Mishra, *Org. Biomol. Chem.* **2025**; d) S. Sabir, G. Kumar, V. P. Verma, J. L. Jat, *ChemistrySelect* **2018**, *3*, 3702; e) C. Schneider, *Angew. Chem. Int. Ed.* **2009**, *48*, 2082.

[28] a) F. Couty, G. Evano, *Synlett* **2009**, *2009*, 3053; b) H. Mughal, M. Szostak, *Org. Biomol. Chem.* **2021**, *19*, 3274; c) G. Rousseau, S. Robin in *Modern Heterocyclic Chemistry* (Eds.: J. Alvarez-Builla, J. J. Vaquero, J. Barluenga), Wiley, Weinheim, **2011**, pp. 163–268.

[29] Z. Wang, F. K. Sheong, H. H. Y. Sung, I. D. Williams, Z. Lin, J. Sun, *J. Am. Chem. Soc.* **2015**, *137*, 5895.

[30] Y. Peng, G. Wang, H. F. T. Klare, M. Oestreich, *Angew. Chem. Int. Ed.* **2024**, *136*.

[31] A. Sandvoß, J. M. Wahl, *Org. Lett.* **2023**, *25*, 5795.

[32] N. E. Allen, D. B. Boyd, J. B. Campbell, J. B. Deeter, T. K. Elzey, B. J. Foster, L. D. Hatfield, J. N. Hobbs, W. J. Hornback, D. C. Hunden et al., *Tetrahedron* **1989**, *45*, 1905.

[33] a) Z. Wang, G.-Q. Li, H.-T. Zhang, *Chem. Biodiversity* **2024**, *21*, e202400939; b) J. Li, Y. Wang, K. Solanki, R. Atre, M. Lavrijsen, Q. Pan, M. S. Baig, P. Li, *Antivital Res.* **2023**, *211*, 105555; c) P. Li, Y. Wang, M. Lavrijsen, M. M. Lamers, A. C. de Vries, R. J. Rottier, M. J. Bruno, M. P. Peppelenbosch, B. L. Haagmans, Q. Pan, *Cell Res.* **2022**, *32*, 322.

[34] a) M. Wang, S. Yu, S. Qi, B. Zhang, K. Song, T. Liu, H. Gao, *J. Nat. Prod.* **2021**, *84*, 2175; b) A. Hernández-Guadarrama, M. A. Díaz-Román, I. Linzaga-Elizalde, B. E. Domínguez-Mendoza, A. B. Aguilar-Guadarrama, *Molecules* **2024**, *29*.

[35] a) A. Albrecht, J. F. Koszuk, J. Modranka, M. Rózalski, U. Krajewska, A. Janecka, K. Studzian, T. Janecki, *Bioorg. Med. Chem.* **2008**, *16*, 4872; b) X. Del Corte, A. López-Francés, A. Maestro, I. Villate-Beitia, M. Sainz-Ramos, E. Martínez de Marigorta, J. L. Pedraz, F. Palacios, J. Vicario, *Pharmaceuticals* **2021**, *14*.

[36] A. Janecka, A. Wyrębska, K. Gach, J. Fichna, T. Janecki, *Drug discovery today* **2012**, *17*, 561.

[37] a) J. Caruano, G. G. Muccioli, R. Robiette, *Org. Biomol. Chem.* **2016**, *14*, 10134; b) F. I. Saldívar-González, E. Lenci, A. Trabocchi, J. L. Medina-Franco, *RSC Adv.* **2019**, *9*, 27105.

[38] X. Armoiry, G. Aulagner, T. Facon, *J. Clin. Pharm. Ther.* **2008**, *33*, 219.
[39] E. Russo, R. Citraro, M. Mula, *Expert. Opin. Drug Discovery* **2017**, *12*, 1169.
[40] a) D. R. Owen, C. M. N. Allerton, A. S. Anderson, L. Aschenbrenner, M. Avery, S. Berritt, B. Boras, R. D. Cardin, A. Carlo, K. J. Coffman et al., *Science* **2021**, *374*, 1586; b) R. S. P. Singh, S. S. Toussi, F. Hackman, P. L. Chan, R. Rao, R. Allen, L. van Eyck, S. Pawlak, E. P. Kadar, F. Clark et al., *Clin. Pharmacol. Ther. Pediatr. Perspect.* **2022**, *112*, 101.
[41] a) A. G. M. Barrett, J. Head, M. L. Smith, N. S. Stock, A. J. P. White, D. J. Williams, *J. Org. Chem.* **1999**, *64*, 6005; b) J. M. Andrés, N. de Elena, R. Pedrosa, A. Pérez-Encabo, *Tetrahedron: Asymmetry* **2001**, *12*, 1503; c) K. Shimamoto, M. Ishida, H. Shinozaki, Y. Ohfune, *J. Org. Chem.* **1991**, *56*, 4167.
[42] a) H. Ikuta, H. Shirota, S. Kobayashi, Y. Yamagishi, K. Yamada, I. Yamatsu, K. Katayama, *J. Med. Chem.* **1987**, *30*, 1995; b) J. F. Kadow, D. M. Vyas, T. W. Doyle, *Tetrahedron Lett.* **1989**, *30*, 3299.
[43] S. Y. Hong, Y. Park, Y. Hwang, Y. B. Kim, M.-H. Baik, S. Chang, *Science* **2018**, *359*, 1016.
[44] a) L.-W. Ye, C. Shu, F. Gagosz, *Org. Biomol. Chem.* **2014**, *12*, 1833; b) C. H. Yoon, A. Nagle, C. Chen, D. Gandhi, K. W. Jung, *Org. Lett.* **2003**, *5*, 2259; c) D. Craig, C. J. T. Hyland, S. E. Ward, *Chem. Commun.* **2005**, 3439.
[45] E. Beckmann, *Ber. Dtsch. Chem. Ges.* **1886**, *19*, 988.
[46] K. F. Schmidt, *Ber. dtsch. Chem. Ges.* **1924**, *57*, 704.
[47] P. A. S. Smith, *J. Am. Chem. Soc.* **1948**, *70*, 320.
[48] a) J. C. Eck, Marvel C. S., *Org. Synth.* **1939**, *19*, 20; b) J. Ritz, H. Fuchs, H. Kieczka, W. C. Moran in *Ullmann's Encyclopedia of Industrial Chemistry* (Ed.: F. Ullmann), Wiley, Weinheim, **2003**.
[49] P. W. Jeffs, G. Molina, N. A. Cortese, P. R. Hauck, J. Wolfram, *J. Org. Chem.* **1982**, *47*, 3876.
[50] Y. Yamamoto, H. Hasegawa, H. Yamataka, *J. Org. Chem.* **2011**, *76*, 4652.
[51] R. E. Gawley in *Organic Reactions* (Ed.: S. E. Denmark), Wiley, Weinheim, **2004**, pp. 1–420.
[52] S. Yamabe, N. Tsuchida, S. Yamazaki, *J. Org. Chem.* **2005**, *70*, 10638.
[53] a) O. Wallach, *Justus Liebigs Ann. Chem.* **1890**, *259*, 309; b) O. Wallach, *Justus Liebigs Ann. Chem.* **1899**, *309*, 1.
[54] a) M. T. Nguyen, G. Raspoet, L. G. Vanquickenborne, *J. Am. Chem. Soc.* **1997**, *119*, 2552; b) R. F. Brown, N. M. van Gulick, G. H. Schmid, *J. Am. Chem. Soc.* **1955**, *77*, 1094.
[55] C. Ramalingan, Y.-T. Park, *Synthesis* **2008**, *2008*, 1351.
[56] a) J. H. Boyer, J. Hamer, *J. Am. Chem. Soc.* **1955**, *77*, 951; b) V. Gracias, K. E. Frank, G. L. Milligan, J. Aubé, *Tetrahedron* **1997**, *53*, 16241; c) J. Aube, G. L. Milligan, *J. Am. Chem. Soc.* **1991**, *113*, 8965.

[57] J. Aube, G. L. Milligan, C. J. Mossman, *J. Org. Chem.* **1992**, *57*, 1635.
[58] S. E. Denmark (Ed.) *Organic Reactions*, Wiley, Weinheim, **2004**.
[59] L. H. Briggs, G. C. de Ath, S. R. Ellis, *J. Chem. Soc.* **1942**, 61.
[60] a) R. Akimoto, T. Tokugawa, Y. Yamamoto, H. Yamataka, *J. Org. Chem.* **2012**, *77*, 4073; b) T. Katori, S. Itoh, M. Sato, H. Yamataka, *J. Am. Chem. Soc.* **2010**, *132*, 3413.
[61] a) D. H. R. Barton, M. J. Day, R. H. Hesse, M. M. Pechet, *J. Chem. Soc. D* **1971**, 945; b) D. H. R. Barton, M. J. Day, R. H. Hesse, M. M. Pechet, *J. Chem. Soc., Perkin Trans. 1* **1975**, 1764.
[62] a) Tamura Y., J. Miamikawa, M. Ikeda, *Synthesis* **1977**, *1977*, 1; b) Tamura Y., H. Fuijwara, K. Sumoto, M. Ikeda, Y. Kita, *Synthesis* **1973**, *1973*, 215; c) R. V. Hoffman, J. M. Salvador, *Tetrahedron Lett.* **1989**, *30*, 4207.
[63] M. Lachia, F. Richard, R. Bigler, A. Kolleth-Krieger, M. Dieckmann, A. Lumbroso, U. Karadeniz, S. Catak, A. de Mesmaeker, *Tetrahedron Lett.* **2018**, *59*, 1896.
[64] M. Renz, B. Meunier, *Eur. J. Org. Chem.* **1999**, *1999*, 737.
[65] A. Baeyer, V. Villiger, *Ber. Dtsch. Chem. Ges.* **1899**, *32*, 3625.
[66] G. R. Krow in *Organic Reactions* (Ed.: S. E. Denmark), Wiley, Weinheim, **2004**, pp. 251–798.
[67] S. S. Canan Koch, A. R. Chamberlin, *Synth. Commun.* **1989**, *19*, 829.
[68] a) W. v. E. Doering, E. Dorfman, *J. Am. Chem. Soc.* **1953**, *75*, 5595; b) R. Criegee, *Justus Liebigs Ann. Chem.* **1948**, *560*, 127.
[69] W. v. E. Doering, L. Speers, *J. Am. Chem. Soc.* **1950**, *72*, 5515.
[70] a) C. M. Crudden, A. C. Chen, L. A. Calhoun, *Angew. Chem. Int. Ed.* **2000**, *39*, 2851; b) P. Deslongchamps, *Stereoelectronic Effects in Organic Chemistry*, Elsevier Science & Technology Books, Amsterdam, **1983**.
[71] a) R. Noyori, T. Sato, H. Kobayashi, *Tetrahedron Lett.* **1980**, *21*, 2569; b) R. Noyori, H. Kobayashi, T. Sato, *Tetrahedron Lett.* **1980**, *21*, 2573.
[72] a) N. Chida, T. Tobe, S. Ogawa, *Tetrahedron Lett.* **1994**, *35*, 7249; b) E. Butkus, S. Stončius, *J. Chem. Soc., Perkin Trans. 1* **2001**, 1885.
[73] S. L. Friess, A. H. Soloway, *J. Am. Chem. Soc.* **1951**, *73*, 3968.
[74] M. Lachia, H. C. Wolf, P. J. M. Jung, C. Screpanti, A. de Mesmaeker, *Bioorg. Med. Chem. Lett.* **2015**, *25*, 2184.
[75] Y. Zhou, C. Rao, Q. Song, *Org. Lett.* **2016**, *18*, 4000.
[76] Y. Yang, M. Li, H. Cao, X. Zhang, L. Yu, *Mol. Catal.* **2019**, *474*, 110450.
[77] J. Xia, G. Yang, R. Zhuge, Y. Liu, W. Zhang, *Chemistry* **2016**, *22*, 18354.
[78] Y. Liu, G. Yang, D. Yao, F. Tian, W. Zhang, *Sci. China Chem.* **2011**, *54*, 87.
[79] F. Tian, D. Yao, Y. J. Zhang, W. Zhang, *Tetrahedron* **2009**, *65*, 9609.
[80] J. Xia, Y. Nie, G. Yang, Y. Liu, I. D. Gridnev, W. Zhang, *Chin. J. Chem.* **2018**, *36*, 612.

[81] E. V. Anslyn, D. A. Dougherty, *Modern Physical Organic Chemistry*, University Science Books, Mill Valley, California, **2006**.

[82] a) D. A. Bak, W. T. Brady, *J. Org. Chem.* **1979**, *44*, 107; b) W. T. Brady, H. G. Liddell, W. L. Vaughn, *J. Org. Chem.* **1966**, *31*, 626.

[83] L. R. Krepski, A. Hassner, *J. Org. Chem.* **1978**, *43*, 2879.

[84] J.-B. Falmagne, J. Escudero, S. Taleb-Sahraoui, L. Ghosez, *Angew. Chem. Int. Ed.* **1981**, *20*, 879.

[85] a) J. Marchand-Brynaert, L. Ghosez, *J. Am. Chem. Soc.* **1972**, *94*, 2870; b) I. Marko, B. Ronsmans, A. M. Hesbain-Frisque, S. Dumas, L. Ghosez, B. Ernst, H. Greuter, *J. Am. Chem. Soc.* **1985**, *107*, 2192; c) A. Sidani, J. Marchand-Brynaert, L. Ghosez, *Angew. Chem. Int. Ed.* **1974**, *13*, 267.

[86] a) A. B. Charette, M. Grenon, *Can. J. Chem.* **2001**, *79*, 1694; b) M. Ramirez, W. Li, Y.-H. Lam, L. Ghosez, K. N. Houk, *J. Org. Chem.* **2020**, *85*, 2597.

[87] M. Lachia, P. M. Jung, A. de Mesmaeker, *Tetrahedron Lett.* **2012**, *53*, 4514.

[88] X. Zhao, L. Ji, Y. Gao, T. Sun, J. Qiao, A. Li, K. Lu, *J. Org. Chem.* **2021**, *86*, 11399.

[89] G. Mehta, H. S. P. Rao, *Synth. Commun.* **1985**, *15*, 991.

[90] a) A. Hassner, J. L. Dillon, *J. Org. Chem.* **1983**, *48*, 3382; b) Z. Du, M. J. Haglund, L. A. Pratt, K. L. Erickson, *J. Org. Chem.* **1998**, *63*, 8880.

[91] S. Müller, M. J. Webber, B. List, *J. Am. Chem. Soc.* **2011**, *133*, 18534.

[92] M. Ong, *Dissertation*, Johannes Gutenberg-University, Mainz, **2024**.

[93] a) L. A. Nguyen, H. He, C. Pham-Huy, *Int. J. Biomed. Sci.* **2006**, *2*, 85; b) R. D. Taylor, M. MacCoss, A. D. G. Lawson, *J. Med. Chem.* **2014**, *57*, 5845; c) J. H. Kim, A. R. Scialli, *Toxicol. Sci.* **2011**, *122*, 1.

[94] a) W. H. Brooks, W. C. Guida, K. G. Daniel, *Curr. Top. Med. Chem.* **2011**, *11*, 760; b) G.-Q. Lin, Q.-D. You, J.-F. Cheng, *Chiral Drugs*, Wiley, Weinheim, **2011**; c) N. R. Srinivas, R. H. Barbhaiya, K. K. Midha, *J. Pharm. Sci.* **2001**, *90*, 1205.

[95] a) M. Christmann, S. Bräse, *Asymmetric Synthesis*, Wiley Online Library, Weinheim, **2007**; b) R. E. Gawley, J. Aubé, *Principles of asymmetric synthesis*, Elsevier, Amsterdam, **2012**; c) G.-Q. Lin, Y.-M. Li, A. S. C. Chan, *Principles and applications of asymmetric synthesis*, John Wiley & Sons, Hoboken, New Jersey, **2001**.

[96] a) T. Akiyama, I. Ojima, *Catalytic asymmetric synthesis*, John Wiley & Sons, Hoboken, New Jersey, **2022**; b) J. Halpern, B. M. Trost, *Proc. Natl. Acad. Sci. U. S. A.* **2004**, *101*, 5347; c) R. Noyori, *Angew. Chem. Int. Ed.* **2002**, *41*, 2008; d) B. M. Trost, *Proc. Natl. Acad. Sci. U. S. A.* **2004**, *101*, 5348; e) P. J. Walsh, M. C. Kozlowski, *Fundamentals of asymmetric catalysis*, University Science Books, **2009**.

[97] a) M. Wang, M. Feng, B. Tang, X. Jiang, *Tetrahedron Lett.* **2014**, *55*, 7147; b) J. Merad, M. Candy, J.-M. Pons, C. Bressy, *Synthesis* **2017**, *49*, 1938; c) M. C. Willis, *J. Chem. Soc., Perkin Trans. 1* **1999**, 1765; d) A. Borissov, T. Q. Davies, S. R. Ellis, T. A. Fleming, M. S. W. Richardson, D. J. Dixon, *Chem. Soc. Rev.* **2016**, *45*, 5474; e) X.-P. Zeng, Z.-Y. Cao, Y.-H. Wang, F. Zhou, J. Zhou, *Chem. Rev.* **2016**, *116*, 7330.

[98] a) M. Lopp, A. Paju, T. Kanger, T. Pehk, *Tetrahedron Lett.* **1996**, *37*, 7583; b) C. Bolm, T. Khanh Luong, G. Schlingloff, *Synlett* **1997**, *1997*, 1151; c) H. Kotsuki, T. Shinohara, S. Fujioka, *Heterocycles* **2001**, *55*, 237; d) A. Cavarzan, G. Bianchini, P. Sgarbossa, L. Lefort, S. Gladiali, A. Scarso, G. Strukul, *Chemistry* **2009**, *15*, 7930; e) A. Drożdż, M. Foreiter, A. Chrobok, *Synlett* **2014**, *25*, 559; f) S. Fatima, A. F. Zahoor, S. G. Khan, S. A. R. Naqvi, S. M. Hussain, U. Nazeer, A. Mansha, H. Ahmad, A. R. Chaudhry, A. Irfan, *RSC Adv.* **2024**, *14*, 23423; g) A. V. Malkov, F. Friscourt, M. Bell, M. E. Swarbrick, P. Kocovský, *J. Org. Chem.* **2008**, *73*, 3996; h) S.-I. Murahashi, S. Ono, Y. Imada, *Angew. Chem. Int. Ed.* **2002**, *41*, 2366; i) K. S. Petersen, B. M. Stoltz, *Tetrahedron* **2011**, *67*, 4352; j) P. P. Poudel, K. Arimitsu, K. Yamamoto, *Chem. Commun.* **2016**, *52*, 4163; k) A. Riebel, M. J. Fink, M. D. Mihovilovic, M. W. Fraaije, *ChemCatChem* **2014**, *6*, 1112; l) S. Xu, Z. Wang, Y. Li, X. Zhang, H. Wang, K. Ding, *Chemistry* **2010**, *16*, 3021; m) L. Zhou, X. Liu, J. Ji, Y. Zhang, X. Hu, L. Lin, X. Feng, *J. Am. Chem. Soc.* **2012**, *134*, 17023.

[99] S. Xu, Z. Wang, X. Zhang, X. Zhang, K. Ding, *Angew. Chem. Int. Ed.* **2008**, *47*, 2840.

[100] K. Sahasrabudhe, V. Gracias, K. Furness, B. T. Smith, C. E. Katz, D. S. Reddy, J. Aubé, *J. Am. Chem. Soc.* **2003**, *125*, 7914.

[101] K. Furness, J. Aubé, *Org. Lett.* **1999**, *1*, 495.

[102] J. Sietmann, M. Ong, C. Mück-Lichtenfeld, C. G. Daniliuc, J. M. Wahl, *Angew. Chem. Int. Ed.* **2021**, *60*, 9719.

[103] S. K. Nimmagadda, S. C. Mallojjala, L. Woztas, S. E. Wheeler, J. C. Antilla, *Angew. Chem. Int. Ed.* **2017**, *56*, 2454.

[104] S.-J. He, S. Zhu, S.-Q. Qiu, W.-Y. Ding, J. K. Cheng, S.-H. Xiang, B. Tan, *Angew. Chem. Int. Ed.* **2023**, *62*, e202213914.

[105] M. Terada, *Synthesis* **2010**, *2010*, 1929.

[106] Y. Sun, N. Cramer, *Angew. Chem. Int. Ed.* **2017**, *56*, 364.

[107] M. J. P. Harger, *J. Chem. Soc., Chem. Commun.* **1979**, 768.

[108] M. J. P. Harger, *J. Chem. Soc., Perkin Trans. 1* **1981**, 3284.

[109] P. Jin, P.-J. Liu, Y. Chong, S. Pruksawan, L. Li, Y. Wen, H. Wei, F. Wang, *Computational and Theoretical Chemistry* **2024**, *1237*, 114635.

[110] T. D. Heim, *Bachelor Thesis*, Johannes Gutenberg-University, Mainz, **2022**.

[111] a) J.-H. Li, X.-K. Li, J. Feng, W. Yao, H. Zhang, C.-J. Lu, R.-R. Liu, *Angew. Chem. Int. Ed.* **2024**, *136*; b) B.-R. Shao, B.-H. Ren, W.-F. Jiang, L. Shi, *Org. Lett.* **2024**, *26*, 2646.

[112] K. A. Rykaczewski, E. R. Wearing, D. E. Blackmun, C. S. Schindler, *Nat. Synth.* **2022**, *1*, 24.

[113] a) Z. Rappoport (Ed.) *The chemistry of the cyano group*, Interscience Publishers, London, **1970**; b) S. H. Wilen, *Stereochemistry of organic compounds*, Wiley, Weinheim, **1994**; c) J.-Y. Le Questel, M. Berthelot, C. Laurence, *J. Phys. Org. Chem.* **2000**, *13*, 347; d) T. Steiner, G. Koellner, *J. Mol. Biol.* **2001**, *305*, 535; e) N. Teno, T. Miyake, T. Ehara, O. Irie, J. Sakaki, O. Ohmori, H. Gunji, N. Matsuura, K. Masuya, Y. Hitomi et al., *Bioorg. Med. Chem. Lett.* **2007**, *17*, 6096; f) C. Laurence, K. A. Brameld, J. Graton, J.-Y. Le Questel, E. Renault, *J. Med. Chem.* **2009**, *52*, 4073.

[114] F. F. Fleming, L. Yao, P. C. Ravikumar, L. Funk, B. C. Shook, *J. Med. Chem.* **2010**, *53*, 7902.

[115] a) X. Wang, Y. Wang, X. Li, Z. Yu, C. Song, Y. Du, *RSC Med. Chem.* **2021**, *12*, 1650; b) V. Bonatto, R. F. Lameiro, F. R. Rocho, J. Lameira, A. Leitão, C. A. Montanari, *RSC Med. Chem.* **2023**, *14*, 201.

[116] a) A. W. Patterson, W. J. L. Wood, M. Hornsby, S. Lesley, G. Spraggon, J. A. Ellman, *J. Med. Chem.* **2006**, *49*, 6298; b) M. J. Boyd, S. N. Crane, J. Robichaud, J. Scheigetz, W. C. Black, N. Chauret, Q. Wang, F. Massé, R. M. Oballa, *Bioorg. Med. Chem. Lett.* **2009**, *19*, 675; c) P. D. Singh, J. R. Jackson, S. P. James, *Biochem. Pharmacol.* **1985**, *34*, 2207.

[117] Y. Xia, H. Jiang, W. Wu, *Eur. J. Org. Chem.* **2021**, *2021*, 6658.

[118] M. B. Smith, *March's advanced organic chemistry: reactions, mechanisms, and structure*, John Wiley & Sons, Hoboken, New Jersey, **2020**.

[119] a) U. Todorović, R. Martin Romero, L. Anthore-Dalion, *Eur. J. Org. Chem.* **2023**, *26*; b) M. Kitamura, K. Narasaka, *Chem. Rec.* **2002**, *2*, 268; c) K. Narasaka, M. Kitamura, *Eur. J. Org. Chem.* **2005**, *2005*, 4505.

[120] a) C. Pratley, S. Fenner, J. A. Murphy, *Chem. Rev.* **2022**, *122*, 8181; b) T. Xiao, H. Huang, D. Anand, L. Zhou, *Synthesis* **2020**, *52*, 1585.

[121] a) J. Boivin, E. Fouquet, S. Z. Zard, *Tetrahedron Lett.* **1991**, *32*, 4299; b) J. Boivin, E. Fouquet, S. Z. Zard, *J. Am. Chem. Soc.* **1991**, *113*, 1055; c) J. Boivin, A.-M. Schiano, S. Z. Zard, *Tetrahedron Lett.* **1992**, *33*, 7849; d) J. Boivin, A.-M. Schiano, S. Z. Zard, *Tetrahedron Lett.* **1994**, *35*, 249; e) J. Boivin, A.-C. Callier-Dublanchet, B. Quiclet-Sire, A.-M. Schiano, S. Z. Zard, *Tetrahedron* **1995**, *51*, 6517; f) J. Boivin, E. Fouquet, A.-M. Schiano, S. Z. Zard, *Tetrahedron* **1994**, *50*, 1769; g) J. Boivin, E. Fouquet, S. Z. Zard, *Tetrahedron* **1994**, *50*, 1757.

[122] a) C. K. Prier, D. A. Rankic, D. W. C. MacMillan, *Chem. Rev.* **2013**, *113*, 5322; b) L. Zhou, M. Lokman Hossain, T. Xiao, *Chem. Rec.* **2016**, *16*, 319.

[123] B. Zhao, Z. Shi, *Angew. Chem. Int. Ed.* **2017**, *56*, 12727.

[124] Y.-R. Gu, X.-H. Duan, L. Yang, L.-N. Guo, *Org. Lett.* **2017**, *19*, 5908.
[125] H.-B. Yang, N. Selander, *Chemistry* **2017**, *23*, 1779.
[126] T. Nishimura, T. Yoshinaka, Y. Nishiguchi, Y. Maeda, S. Uemura, *Org. Lett.* **2005**, *7*, 2425.
[127] X.-Y. Yu, J.-R. Chen, P.-Z. Wang, M.-N. Yang, D. Liang, W.-J. Xiao, *Angew. Chem. Int. Ed.* **2018**, *57*, 738.
[128] E. M. Dauncey, S. U. Dighe, J. J. Douglas, D. Leonori, *Chem. Sci.* **2019**, *10*, 7728.
[129] W. Ai, Y. Liu, Q. Wang, Z. Lu, Q. Liu, *Org. Lett.* **2018**, *20*, 409.
[130] L. Tian, S. Gao, R. Wang, Y. Li, C. Tang, L. Shi, J. Fu, *Chem. Commun.* **2019**, *55*, 5347.
[131] M. He, Z. Yan, F. Zhu, S. Lin, *J. Org. Chem.* **2018**, *83*, 15438.
[132] J.-J. Zhang, X.-H. Duan, Y. Wu, J.-C. Yang, L.-N. Guo, *Chem. Sci.* **2019**, *10*, 161.
[133] E. M. Dauncey, S. P. Morcillo, J. J. Douglas, N. S. Sheikh, D. Leonori, *Angew. Chem. Int. Ed.* **2018**, *57*, 744.
[134] T. Nishimura, S. Uemura, *J. Am. Chem. Soc.* **2000**, *122*, 12049.
[135] T. Nishimura, Y. Nishiguchi, Y. Maeda, S. Uemura, *J. Org. Chem.* **2004**, *69*, 5342.
[136] B. Shuai, P. Fang, T.-S. Mei, *Synlett* **2021**, *32*, 1637.
[137] Y. Wu, M. Inoue, S. Sakakura, K. Hyodo, *Org. Biomol. Chem.* **2024**, *22*, 4364.
[138] B. Zhao, H. Tan, C. Chen, N. Jiao, Z. Shi, *Chin. J. Chem.* **2018**, *36*, 995.
[139] M. Ong, M. Arnold, A. W. Walz, J. M. Wahl, *Org. Lett.* **2022**, *24*, 6171.
[140] M. Liu, N. Le, C. Uyeda, *Angew. Chem. Int. Ed.* **2023**, *62*, e202308913.
[141] a) B. Y. Kimura, T. L. Brown, *J. Organomet. Chem.* **1971**, *26*, 57; b) J. F. Remenar, B. L. Lucht, D. B. Collum, *J. Am. Chem. Soc.* **1997**, *119*, 5567; c) B. L. Lucht, D. B. Collum, *J. Am. Chem. Soc.* **1996**, *118*, 2217.
[142] a) C. S. Beshara, A. Hall, R. L. Jenkins, T. C. Jones, R. T. Parry, S. P. Thomas, N. C. O. Tomkinson, *Chem. Commun.* **2005**, 1478; b) C. S. Beshara, A. Hall, R. L. Jenkins, K. L. Jones, T. C. Jones, N. M. Killeen, P. H. Taylor, S. P. Thomas, N. C. O. Tomkinson, *Org. Lett.* **2005**, *7*, 5729; c) O. R. S. John, N. M. Killeen, D. A. Knowles, S. C. Yau, M. C. Bagley, N. C. O. Tomkinson, *Org. Lett.* **2007**, *9*, 4009.
[143] S. M. Rajaratnam, M. H. Polymeropoulos, D. M. Fisher, T. Roth, C. Scott, G. Birznieks, E. B. Klerman, *Lancet* **2009**, *373*, 482.
[144] a) J. Hammes, *Research Report*, Johannes Gutenberg-University, Mainz, **2024**; b) M. Rodinger, *Bachelor Thesis*, Johannes Gutenberg-University, Mainz, **2024**.
[145] W. Wang, X. Meng, J. Zhu, X. Zhang, *Synth. Commun.* **2019**, *49*, 129.

[146] C. P. Rosenau, B. J. Jelier, A. D. Gossert, A. Togni, *Angew. Chem. Int. Ed.* **2018**, *57*, 9528.
[147] T. Nordvik, U. H. Brinker, *J. Org. Chem.* **2003**, *68*, 9394.
[148] J. A. Dabrowski, D. C. Moebius, A. J. Wommack, A. F. Kornahrens, J. S. Kingsbury, *Org. Lett.* **2010**, *12*, 3598.
[149] J. M. O'Brien, J. S. Kingsbury, *J. Org. Chem.* **2011**, *76*, 1662.
[150] M. D. Lachia, A. De Mesmaeker, H. Alain, H. C. Wolf, P. J. M. Jung, WO2012/080115 A1, **2012**.
[151] H.-J. Xu, F.-F. Zhu, Y.-Y. Shen, X. Wan, Y.-S. Feng, *Tetrahedron* **2012**, *68*, 4145.
[152] a) L. Wu, Z. Zhang, J. Liao, J. Li, W. Wu, H. Jiang, *Chem. Commun.* **2016**, *52*, 2628; b) Le Guo, X. Ma, H. Fang, X. Jia, Z. Huang, *Angew. Chem. Int. Ed.* **2015**, *54*, 4023.
[153] Z. Sun, B. Tang, K. K.-C. Liu, H. Y. Zhu, *Chem. Commun.* **2020**, *56*, 1294.
[154] D. C. Behenna, Y. Liu, T. Yurino, J. Kim, D. E. White, S. C. Virgil, B. M. Stoltz, *Nat. Chem.* **2011**, *4*, 130.
[155] H. Wang, Y. Park, Z. Bai, S. Chang, G. He, G. Chen, *J. Am. Chem. Soc.* **2019**, *141*, 7194.
[156] L. Angelini, J. Davies, M. Simonetti, L. Malet Sanz, N. S. Sheikh, D. Leonori, *Angew. Chem. Int. Ed.* **2019**, *58*, 5003.
[157] Y. Hwang, H. Jung, E. Lee, D. Kim, S. Chang, *J. Am. Chem. Soc.* **2020**, *142*, 8880.
[158] J. A. Smulik, E. Vedejs, *Org Lett* **2003**, *5*, 4187.
[159] C. A. Busacca, J. C. Lorenz, N. Grinberg, N. Haddad, M. Hrapchak, B. Latli, H. Lee, P. Sabila, A. Saha, M. Sarvestani et al., *Org Lett* **2005**, *7*, 4277.
[160] M. Klussmann, L. Ratjen, S. Hoffmann, V. Wakchaure, R. Goddard, B. List, *Synlett* **2010**, *2010*, 2189.
[161] V. Rauniyar, Z. J. Wang, H. E. Burks, F. D. Toste, *J. Am. Chem. Soc.* **2011**, *133*, 8486.
[162] J. P. Hilton-Proctor, O. Ilyichova, Z. Zheng, I. G. Jennings, R. W. Johnstone, J. Shortt, S. J. Mountford, M. J. Scanlon, P. E. Thompson, *Eur. J. Med. Chem.* **2020**, *191*, 112120.
[163] E. Horáková, P. Drabina, L. Brůčková, Š. Štěpánková, K. Vorčáková, M. Sedlák, *Monatsh. Chem.* **2017**, *148*, 2143.
[164] A. L. Chandgude, R. Fasan, *Angew. Chem. Int. Ed.* **2018**, *57*, 15852.
[165] L. An, F.-F. Tong, S. Zhang, X. Zhang, *J. Am. Chem. Soc.* **2020**, *142*, 11884.
[166] M.-X. Wang, G.-Q. Feng, *New J. Chem.* **2002**, *26*, 1575.
[167] H. Saitoh, T. Watanabe, T. Kimura, Y. Kato, T. Satoh, *Tetrahedron* **2012**, *68*, 2481.

[168] J. Zhu, B. A. Price, S. X. Zhao, P. M. Skonezny, *Tetrahedron Lett.* **2000**, *41*, 4011.
[169] A. F. Littke, G. C. Fu, *Angew. Chem. Int. Ed.* **1999**, *38*, 2411.
[170] X.-A. Li, L. Yue, J. Zhu, H. Ren, H. Zhang, D. Hu, G. Han, J. Feng, Z. Nan, *Tetrahedron Lett.* **2019**, *60*, 1986.

Declaration of academic integrity

I hereby confirm that this thesis, entitled “Novel Strategies for the Synthesis and Transformation of Nitrogen-Containing Molecules” was prepared independently and no sources or aids other than the ones stated were used. All passages in my thesis for which other sources, including electronic media, have been used, be it direct quotes or content references, have been acknowledged as such and the sources cited. I assure, that any ideas taken over, verbatim or in spirit, have been clearly stated.

Place, Date Marlene Arnold

Curriculum Vitae

Personal data

Name:	Marlene Arnold
Date of Birth:	[redacted]
Address:	[redacted]
E-Mail:	[redacted]

Education

[redacted]

Publications

Stereospecific nitrogen insertion using amino diphenylphosphinates: an Aza-Baeyer–Villiger rearrangement

M. Ong, M. Arnold, A. W. Walz, J. M. Wahl,*
Org. Lett. **2022**, *24*, 6171–6175.
*corresponding author

Synthesis of 4-phenylpyrrolidin-2-one *via* an Aza-Baeyer-Villiger rearrangement

M. Arnold,# M. Ong,# J. M. Wahl,*
Org. Synth. **2023**, *100*, 347-360.
#authors contributed equally to this work
*corresponding author

Nitrogen insertion *via* asymmetric condensation and chirality transfer: a stereodivergent entry to cyanocyclopropanes

M. Arnold, J. Hammes, M. Ong, C. Mück-Lichtenfeld, J. M. Wahl,*
manuscript submitted.
*corresponding author

Presentations on Scientific Conferences

05/2024	Thinking out of the ring. Present and future of small cyclic compounds; Lorentz Center Leiden, The Netherlands Poster presantation about the topic: "*Synthesis and application of axially chiral cyclobutanone oxime esters*"
09/2022	Hochschule trifft Industries, Stein, Switzerland Oral presenatition about the topic: "*Synthesis and application of axially chiral cyclobutanone oxime esters for the preparation of chiral cyclopropanes*"

Scholarships

[redacted]